**Universidad de Cantabria**

**Escuela Técnica Superior de Ingenieros Industriales y de Telecomunicación**

Departamento de Ingenierías Química y Biomolecular

# "Separación de dióxido de carbono utilizando membranas soportadas con líquidos iónicos"

**"Carbon dioxide separation by means of supported ionic liquid membranes"**

Memoria de Tesis Doctoral presentada para optar al título de Doctora por la Universidad de Cantabria

Programa Oficial de Doctorado en Ingeniería Química y de Procesos
(BOE núm. 36, de 10 de febrero de 2010. RUCT: 5311209)
con Mención hacia la Excelencia
(BOE núm. 253, de 20 de Octubre de 2011. Referencia: MEE2011-0031)

**Esther Santos Santamaría**

Directores de Tesis:

Prof. Dr. Ángel Irabien Gulías
Dr. Jonathan Albo Sánchez

Santander, enero 2014

La Tesis Doctoral se presenta como un resumen de trabajos previamente publicados o aceptados para su publicación en revistas científicas incluidas en el *Journal of Citation Reports-Science Edition (JCR),* cumpliendo con la normativa existente en la Universidad de Cantabria y en el Departamento de Ingenierías Química y Biomolecular referente a la elaboración de Tesis Doctorales por compendio de artículos. Durante la elaboración de la Tesis Doctoral se ha realizado una estancia predoctoral de tres meses de duración (enero-abril 2012) en la *Faculdade de Ciências e Tecnologia* de la *Universidade Nova de Lisboa*, bajo la supervisión del Prof. Dr. João G. Crespo.

A continuación se listan las publicaciones que forman parte de la presente Tesis:

Compendio de artículos publicados/aceptados:

1. Santos E., Albo J., Daniel C.I., Portugal C.A.M., Crespo J.G., Irabien A. Permeability modulation of Supported Magnetic Ionic Liquid Membranes (SMILMs) by an external magnetic field*. J. Membr. Sci.* **2013**, 430:56- 61.

2. Santos E., Albo J., Rosatella A., Afonso C.A.M., Irabien A. Synthesis and characterization of Magnetic Ionic Liquids (MILs) for $CO_2$ separation. *J. Chem. Technol. Biotechnol.* Accepted.

3. Santos E., Albo J., Irabien A. Acetate based Supported Ionic Liquid Membranes (SILMs) for $CO_2$ separation: Influence of the temperature. *J. Membr. Sci.* **2014**, 452: 277-283.

4. Albo J., Santos E., Neves L.A., Simeonov S.P., Afonso C.A.M., Crespo J.G., Irabien A. Separation performance of $CO_2$ through Supported Magnetic Ionic Liquid Membranes (SMILMs). *Sep. Purif. Technol.* **2012**, 97:26-33.

5. Daniel C.I., Albo J., Santos E., Portugal C.A.M., Crespo J.G., Irabien A. A group contribution method for the influence of the temperature in the viscosity of magnetic ionic liquids*. Fluid Phase Equilib.* **2013**, 360:29-35.

Este trabajo ha sido financiado por el Ministerio de Educación y Ciencia y el Ministerio de Economía y Competitividad a través de los proyectos CTM2006-00317 *"Sostenibilidad de la Producción: Intensificación e integración de procesos en la industria química y transformadora"*, CTQ2008-00690 *"Investigación y desarrollo de separaciones reactivas. Contribución al desarrollo tecnológico sostenible"*, CTQ2008-04990-E *"Sostenibilidad de procesos y productos químicos"*, EUI2008-03857 *"Proyecto MIL: Nuevas Membranas estímulo-respuesta para procesos de separación innovadores*", ENE2010-14828 *"Desarrollo de un proceso de captura y reciclado de $CO_2$"* y CTQ2012-31229 *"Nuevas membranas selectivas para la separación de $CO_2$"*.

Durante la ejecución del presente trabajo, su autora, Esther Santos Santamaría, ha disfrutado de una beca ERASMUS para la realización de una estancia breve de investigación de tres meses de duración en la Universidade Nova de Lisboa (Caparica, Portugal).

Por todo ello, expresamos nuestro más sincero agradecimiento hacia dichas instituciones.

A mi familia,

por darme todo su apoyo,

ayudarme a perseguir mis sueños,

y quererme sobre todas las cosas.

## Agradecimientos

Me gustaría que estas líneas sirvieran para expresar mi más profundo y sincero agradecimiento a todas aquellas personas que con su ayuda han colaborado en la realización del presente trabajo.

En primer lugar, me gustaría expresar mi más sincera gratitud al Prof. Ángel Irabien por la confianza depositada en mí dándome la oportunidad de unirme a su grupo de investigación para realizar esta tesis doctoral bajo su dirección. Su apoyo y confianza en mí y su capacidad para guiar mi trabajo de manera rigurosa ha sido un aporte incalculable, no solamente en el desarrollo de esta tesis, sino también en mi formación como investigadora.

Al Dr. Jonathan Albo por la orientación, el seguimiento y la supervisión continua del trabajo, pero sobre todo por la motivación y el apoyo recibido a lo largo de estos años.

A la Dra. Clara Casado por el trabajo conjunto y sus buenos consejos durante esta última parte de mi tesis.

A todos los profesores del Departamento de Ingenierías Química y Biomolecular por la formación recibida.

A los técnicos de laboratorio y al Personal de Administración y Servicios del Departamento por facilitarme las labores técnicas y de gestión del día a día.

Gostaria de agradecer ao Prof. João G. Crespo, Dra. Carla A.M. Portugal, Prof. Carlos A.M. Afonso e Dra. Andreia Rosatella da Universidade Nova de Lisboa e Instituto Superior Técnico a oportunidade de trabalhar com vocês no âmbito do projecto ERANET. Agradeço-lhes ainda terem-me recebido no seu laboratório durante três meses. O meu agradecimento pelo apoio científico e também humano.

A minha querida colega e amiga PhD Carla Daniel pela ajuda sempre que foi preciso. Sempre fortíssima!

Por último, um agradecimento muito especial os meus amigos Luisa Neves e Ignacio Lázaro por ser minha família em Portugal.

Muito obrigada!

A TODOS mis compañeros de doctorado, a los que están y a los que pasaron por aquí dejando su huella, gracias por hacerme más agradable el día a día. Es un placer haber coincidido con vosotros. Sois una gran familia para mí.

Quisiera agradecer de manera especial a Pablo, Germán, Lucía, Isa, Gabi, Sara, Mariana, Andrés y Carolina por su amistad, por hacerme desconectar y sacarme siempre una sonrisa.

A mis compañeros de despacho Antonio y Enrique porque trabajar en un ambiente cómodo y distendido es un lujo al alcance de muy pocos y a Beatriz por los buenos momentos compartidos.

Un agradecimiento muy especial merece la comprensión, paciencia y el apoyo incondicional que recibo día a día de mi familia. No existen palabras que puedan agradeceros todo lo que habéis hecho por mí. Os quiero.

A todos y cada uno de vosotros, MUCHAS GRACIAS, porque parte de este trabajo es también vuestro!

# Índice

«La paciencia es la fortaleza del débil y

la impaciencia la debilidad del fuerte»

Immanuel Kant (1724-1804)

Filósofo alemán

**Índice**

# Resumen

# Abstract

# Sumário

«Para investigar la verdad es preciso dudar,
en cuanto sea posible, de todas las cosas»

René Descartes (1596 - 1650)

Filósofo y matemático francés

## Resumen

Las últimas décadas han puesto de manifiesto la imposibilidad de trasladar la intensidad del consumo energético del mundo desarrollado a la totalidad del planeta y en consecuencia, la necesidad de un cambio global hacia una economía baja en carbono y por tanto a un modelo energético más eficiente y sostenible. Por consiguiente, se requiere de un esfuerzo tecnológico dirigido a la reducción de las emisiones de gases de efecto invernadero, lo que implica necesariamente el desarrollo de tecnologías para capturar y almacenar o valorizar dióxido de carbono ($CO_2$). Uno de los problemas técnicos fundamentales asociados a los procesos de captura es la separación de $CO_2$ de las corrientes de gases de post-combustión.

En este contexto, la presente Tesis Doctoral estudia el desarrollo de nuevas membranas soportadas con líquidos iónicos para separación de $CO_2$ a través de un doble enfoque: desarrollo de membranas estímulo-respuesta basadas en líquidos iónicos magnéticos que presenten respuesta ante la aplicación de un campo magnético externo y membranas soportadas con líquidos iónicos basados en el anión acetato con una elevada solubilidad de $CO_2$, que pueden alcanzar mejores prestaciones en la separación/concentración.

En la primera parte de la Tesis, se inmoviliza un grupo de líquidos iónicos magnéticos conteniendo diferentes aniones metálicos en su estructura en soportes porosos poliméricos para el estudio de la separación de $CO_2$. Se lleva a cabo la caracterización de los líquidos iónicos magnéticos mediante la medida de la susceptibilidad magnética, densidad, viscosidad, propiedades térmicas y solubilidad de $CO_2$. Se desarrolla un modelo de contribución de grupos basado en la ecuación de Orrick-Erbar para la estimación de la viscosidad de los líquidos iónicos magnéticos a diferentes temperaturas evaluando la influencia del anión y catión en la viscosidad. Finalmente, se evalúa experimentalmente la posibilidad de modular la permeabilidad y/o selectividad de $CO_2$ a través de membranas soportadas con líquidos iónicos magnéticos en presencia de una fuerza externa producida por un campo magnético.

En la segunda parte de la Tesis, se caracteriza la separación $CO_2/N_2$. Se lleva a cabo un estudio de permeabilidad a través de membranas soportadas con líquidos iónicos basados en el anión acetato donde, de acuerdo con la bibliografía, se pretenden obtener los mejores resultados. La influencia de la temperatura en la permeabilidad se describe mediante una ecuación tipo Arrhenius con una energía de activación que permite describir la influencia de la temperatura en la permeabilidad a través de su influencia en la difusividad y solubilidad.

Los resultados presentados en esta Tesis identifican un nuevo tipo de membranas soportadas utilizando líquidos iónicos magnéticos describiendo la influencia del campo magnético en la permeabilidad del $CO_2$. Así mismo, se caracteriza los sistemas de membranas soportadas para la separación de $CO_2$ basados en líquidos iónicos con el anión acetato.

## *Abstract*

The last decades have shown the impossibility of transferring the energy intensity of the developed world to the entire planet and thus, the need for a global shift towards a low carbon economy and therefore, to a more efficient and sustainable energy model. Consequently, a technological effort is required aimed at reducing greenhouse gas emissions, which necessarily involves the development of carbon dioxide ($CO_2$) capture and storage or valorization technologies. One of the main technical problems associated with the capture processes is the $CO_2$ separation from post-combustion gas streams.

In this context, this Thesis studies the development of new supported ionic liquid membranes for $CO_2$ separation aiming for a dual approach: development of novel stimuli-responsive magnetic ionic liquids based membranes showing a response to the application of an external magnetic field and acetate based supported ionic liquid membranes with a high $CO_2$ solubility, which can achieve a better performance in its separation/concentration.

In the first part of this PhD Thesis, a group of magnetic ionic liquids containing different magnetic anions in their structure are immobilized on porous polymeric supports for $CO_2$ separation evaluation. Magnetic ionic liquids characterization is performed by measuring the magnetic susceptibility, density, viscosity, thermal properties and $CO_2$ solubility. A group contribution method based on the Orrick–Erbar equation is developed for the estimation of magnetic ionic liquids viscosity at different temperatures by evaluating the influence of the anion and the cation in the viscosity. Finally, the possibility to modulate the $CO_2$ permeability and/or selectivity is experimentally evaluated through supported magnetic ionic liquid membranes at the presence of an external force produced by a magnetic field is evaluated.

In the second part of this Thesis, it is characterized the $CO_2/N_2$ separation. Gas permeability studies through acetate based supported ionic liquid membranes are carried out, where, based on the literature, the best results are expected. The influence of the temperature in the permeability is described by an Arrhenius type equation, with activation energy for describing the influence of temperature on the permeability through its influence on the diffusivity and solubility.

The results presented in this Thesis identify a new type of supported membranes using magnetic ionic liquids describing the influence of magnetic field on the $CO_2$ permeability. Furthermore, it is characterized supported membrane systems for $CO_2$ separation based on ionic liquids including the acetate anion.

## *Sumário*

As últimas décadas têm demonstrado a impossibilidade de transferir a intensidade energética do mundo desenvolvido para todo o planeta e, portanto, a necessidade de uma transição para uma economia de baixo carbono e, assim, a um modelo energético mais eficiente e sustentável. Portanto, é necessário um esforço tecnológico para reduzir as emissões de gases de efeito estufa, o que implica, necessariamente, o desenvolvimento de tecnologias para a captura e armazenamento ou conversão de dióxido de carbono ($CO_2$). Um dos problemas técnicos fundamentais associados com o processo de captura é a separação de $CO_2$ do gás de pós-combustão.

Neste contexto, nesta Tese de Doutoramento foi estudado o desenvolvimento das membranas suportadas com novos líquidos iónicos, a fim de avaliar o seu potencial para a utilização em processos de separação do $CO_2$, tendo em vista duas vertentes: o desenvolvimento de membranas estímulo-resposta baseadas em líquidos iónicos magnéticos que apresentam uma resposta perante a aplicação de um campo magnético externo, e o desenvolvimento de membranas suportadas com líquidos iónicos, baseados no anião acetato, com um elevado grau de solubilidade de $CO_2$, que possibilitam a obtenção de um melhor desempenho na separação/concentração.

Na primeira parte do trabalho desenvolvido neste projecto de Doutoramento, foram imobilizados numa estrutura porosa de membranas poliméricas um número de líquidos iónicos magnéticos contendo diferentes aniões de metais na sua estrutura para o estudo da separação do $CO_2$. A caracterização dos líquidos iónicos magnéticos foi efectuada pela medição da susceptibilidade magnética, densidade, viscosidade, propriedades térmicas e solubilidade de $CO_2$. Foi ainda desenvolvido um modelo de contribuição de grupos utilizando a equação Orrick-Erbar para estimar a viscosidade dos líquidos iónicos magnéticos a diferentes temperaturas, a fim de avaliar a influência do anião e catião na viscosidade. Finalmente, avalia-se a possibilidade de modular a permeabilidade e / ou selectividade do $CO_2$ através de membranas suportadas com líquidos iónicos magnéticos na presença de uma força externa produzida por um campo magnético.

Na segunda parte do trabalho desenvolvido nesta Tese, foi efectuada a caracterização da separação $CO_2/N_2$. Estudos de permeabilidade foram realizados através de membranas suportadas com líquidos iónicos baseados no anião acetato, o qual, com base na literatura, destina-se a produzir os melhores resultados. A influência da temperatura sobre a permeabilidade é descrita pela equação de Arrhenius, com uma energia de activação que permite descrever a influência da temperatura na permeabilidade através de sua influência na difusividade e solubilidade.

Os resultados apresentados nesta Tese de Doutoramento identificam um novo tipo de membranas suportadas usando líquidos iónicos magnéticos descrevendo a influência do campo magnético na permeabilidade de $CO_2$. Da mesma forma, caracteriza-se os sistemas de membranas suportadas com líquidos iónicos baseados no anião acetato para separação de $CO_2$.

# 1 Planteamiento

«Investigar es ver lo que todo el mundo ha visto,

y pensar lo que nadie ha pensado»

Albert Szent-Györgi (1893 -1986)

Fisiólogo húngaro

# CAPÍTULO 1. PLANTEAMIENTO

## 1.1. Justificación y antecedentes

La concentración de $CO_2$ en la atmósfera se ha incrementado de manera significativa desde la era pre-industrial debido fundamentalmente a la quema de combustibles fósiles para la generación de electricidad y calor (NOAA, IEA 2011). Las predicciones indican que la demanda mundial de energía seguirá siendo dependiente de los combustibles fósiles (Toftegaard et al., 2010). Por lo tanto, se requiere de un cambio hacia una economía menos intensiva en carbono que permita reducir las emisiones de $CO_2$ y mitigar el cambio climático.

Se están considerando diferentes estrategias para la reducción de las emisiones de $CO_2$, donde la captura y almacenamiento de $CO_2$ (CAC) es una solución reciente con un enfoque a corto plazo que pretende lograr reducciones significativas de las emisiones de $CO_2$ (Olajire, 2010; MacDowell et al., 2010). Por otro lado, el desarrollo de procesos innovadores para el reciclado del $CO_2$ capturado aparece como una opción atractiva que permitiría la valorización de $CO_2$ mediante su conversión en productos útiles y valiosos como combustibles o hidrocarburos derivados (Álvarez-Guerra et al., 2012).

Las tres principales vías actuales de captura de $CO_2$ son (Ghoniem, 2011):

- *Post-combustión:* es la vía más utilizada tanto para plantas de nuevo diseño como para plantas existentes. El combustible se quema completamente en exceso de aire, creándose una corriente de gas a elevada temperatura y presión atmosférica con una concentración de $CO_2$ entre el 3-15% diluida principalmente en $N_2$ (Olajire, 2010). Actualmente la mejor tecnología disponible para la captura de $CO_2$ se basa en la absorción química con aminas, generalmente monoetanolamina (MEA), con una eficiencia de en torno al 90% (Steeneveldt et al., 2006). Entre las principales desventajas de este método, destaca el elevado consumo energético asociado a la etapa de regeneración así como evaporación de disolvente debido al contacto directo entre las fases gas y líquida (Rao y Rubin, 2002).

Dentro de las tecnologías emergentes en este campo a medio y largo plazo destacan los procesos de separación con membranas (Figueroa et al., 2008) y la absorción utilizando líquidos iónicos (Wappel et al., 2010; Albo et al., 2011).

- *Pre-combustión:* busca capturar el $CO_2$ antes de la etapa de combustión. El combustible es gasificado o reformado (en función de que el combustible utilizado sea carbón o gas natural) para dar gas de síntesis (CO e $H_2$). Se hace reaccionar el CO con vapor de agua para producir $CO_2$ e $H_2$, resultando una corriente con un contenido de $CO_2$ entre 15-40% a elevada presión y temperatura (Page et al., 2009). El $CO_2$ es separado del $H_2$ y enviado a la unidad de compresión para su posterior transporte. La pre-combustión se beneficia de la elevada presión de la

corriente de salida reduciendo los costes asociados a la presurización, lo que permite la aplicación de tecnologías de separación energéticamente menos intensivas. Uno de los inconvenientes de esta vía es su exclusiva utilización en plantas de nuevo diseño, no siendo posible su implementación en plantas ya existentes. La tecnología convencional para la separación $CO_2/H_2$ es la absorción física utilizando disolventes orgánicos como Selexol, Purisol o Rectisol con una eficiencia entre 85-90% (Olajire, 2010).

Dentro de las tecnologías de separación emergentes en la pre-combustión destaca la tecnología de membranas debido a que es energéticamente menos intensiva y a su facilidad de operación (Zhao et al., 2010a) y la adsorción con sólidos.

- *Oxi-combustión:* en el proceso de oxi-combustión el combustible es quemado en presencia de oxígeno de elevada pureza (mayor del 95%) dando como resultado una corriente compuesta principalmente por $CO_2$ (≈75%) y $H_2O$. El $CO_2$ es recuperado fácilmente mediante la condensación del vapor de agua (Brunetti et al., 2010).

La tecnología convencional para la separación $O_2/N_2$ es la destilación criogénica (Darde et al., 2009). La eficiencia del proceso se sitúa en torno al 90-98%. La utilización de membranas se perfila como la tecnología más prometedora a medio plazo utilizando tanto materiales poliméricos como cerámicos (Ion Transport Membranes (ITM)), mientras que otras nuevas tecnologías como el Chemical Looping o la recuperación cerámica autotérmica (CAR) aparecen como opciones interesantes a largo plazo (Adanez et al., 2012).

La Figura 1.1 muestra un resumen de las diferentes tecnologías en los procesos de separación de $CO_2$.

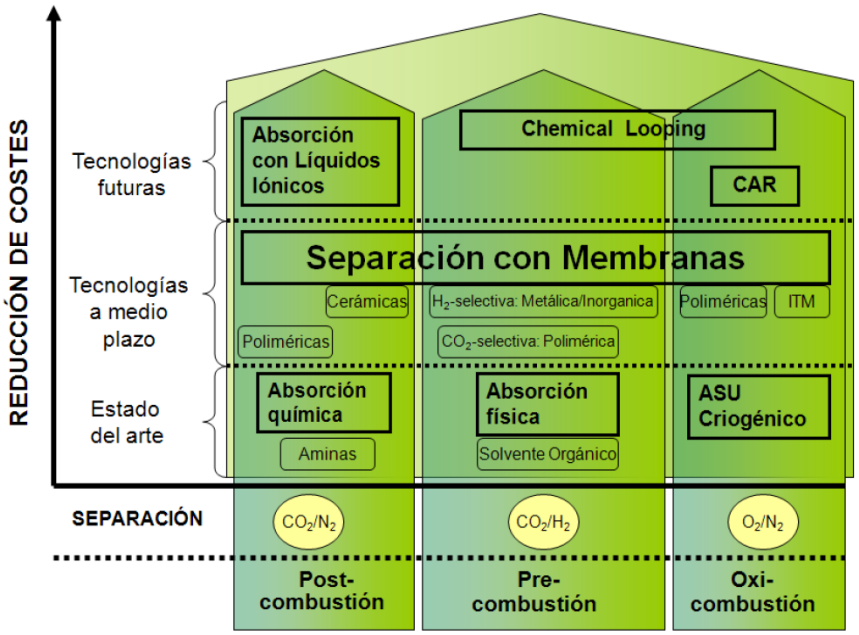


**Figura 1.1.** Tecnologías para la separación de $CO_2$ (Cristóbal J., 2013).

## 1.2. La tecnología de membranas en la separación de $CO_2$ en post-combustión

La tecnología de membranas representa una alternativa prometedora para la separación $CO_2/N_2$ en procesos industriales (Baker, 2002; Favre, 2007). El interés de la industria en las membranas para la separación de mezclas gaseosas se ha visto incrementado desde su introducción comercial en la década de 1980 debido a la simplicidad y modularidad del proceso y el potencial ahorro energético en comparación con otros métodos de separación convencionales (Luis et al., 2012). La tecnología de membranas utiliza entre 70-75 kWh/Ton$CO_2$ recuperado, siendo sensiblemente inferior a otras tecnologías tales como la adsorción (160-180 kWh), destilación criogénica (600-800 kWh) o absorción con aminas (330-340 kWh) haciendo de la tecnología de membranas una alternativa más atractiva (Khoo y Tan, 2006). En lo referente a los costes, los sistemas convencionales de absorción con aminas llevan asociados unos costes de 40-100$/Ton$CO_2$ capturado, mientras que en los sistemas de nuevas membranas comerciales (ej. Membrana Polaris$^{TM}$) se estiman unos costes de captura en torno a 23$/Ton$CO_2$ capturado (Merkel et al., 2010).

La separación de $CO_2$ de corrientes de gas de combustión es una aplicación difícil para cualquier tecnología de separación. Los principales problemas asociados son la baja concentración de $CO_2$ y la baja presión parcial de la corriente de alimentación junto con el elevado caudal de gas a tratar. Además, la corriente de gas contiene una amplia variedad de contaminantes incluyendo cenizas volantes, $SO_2$, $NO_x$, agua y trazas de metales (Merkel et al., 2010). La combinación de estos factores hace de la separación de $CO_2$ una operación costosa con las tecnologías existentes.

Hasta la fecha, han sido estudiados diferentes tipos de membranas para la separación de $CO_2$ incluyendo membranas poliméricas (Powell y Qiao, 2006), inorgánicas (Bredesen et al., 2004) y de transporte facilitado (Luis et al., 2009). Desde el punto de vista comercial, los polímeros son los materiales empleados mayoritariamente en la fabricación de membranas debido a la flexibilidad de procesamiento que permite la obtención de equipos más compactos y eficientes (Hägg M.-B., 2009). Además, presentan bajo coste, buenas propiedades mecánicas y buena reproducibilidad.

Las moléculas son transportadas a través de membranas poliméricas de acuerdo con el modelo de solución-difusión:

$$P = D.S \tag{1.1}$$

donde $P$ es el coeficiente de permeabilidad habitualmente expresado en barrer ($10^{-10}$ $cm^3(STP).cm^{-2}.s^{-1}.cmHg^{-1}$); $D$ el coeficiente de difusividad en $cm^2.s^{-1}$ y $S$ el coeficiente de solubilidad $cm^3(STP).cmHg^{-1}$.

Experimentalmente la permeabilidad es obtenida de acuerdo a la expresión:

$$\frac{P}{l} = \frac{Q}{A\Delta p} \tag{1.2}$$

donde $l$ representa el espesor efectivo de membrana; $Q$ la velocidad de permeación a través de la membrana; $A$ el área superficial de membrana e $\Delta p$ la diferencia de presión a través de la membrana.

La selectividad ideal de un gas A sobre otro gas B, $\alpha$ , se define como:

$$\alpha = \frac{P_A}{P_B} \tag{1.3}$$

Las membranas utilizadas en la separación $CO_2/N_2$ deben presentar tanto valores de permeabilidad como selectividad altos: un valor elevado de permeabilidad hace que disminuya el área de membrana requerida para tratar un caudal de gas dado, mientras que una selectividad alta implica mayor pureza del gas permeable en la corriente de salida. Es posible obtener membranas con elevada permeabilidad y selectividad; sin embargo, el mayor inconveniente en la separación $CO_2/N_2$ con membranas es el escalado del proceso y la necesidad de equipos de compresión de gran tamaño y con un elevado consumo energético (Hägg M.-B., 2009; Merkel et al., 2010).

Los límites de operación de las membranas poliméricas fueron establecidos por Robeson (Robeson, 2008). Desde entonces, el *upper bound* o *límite máximo* definido por Robeson es el método para comparar el rendimiento en la separación gaseosa de materiales de membrana. Existe un compromiso entre la permeabilidad y selectividad de tal modo que una membrana altamente selectiva tiende a tener una permeabilidad baja y viceversa, tal y como se muestra en la Figura 1.2. Algunos de los materiales próximos a este límite máximo son Polidimetilsiloxano (PDMS), Poly(1-trimetil silil propino) (PTMSP), Polifosfaceno (PPZ), PEBAX® o polímeros de porosidad intrínseca (PIM). El desarrollo de nuevos materiales que superen dicho límite es, por tanto, de vital importancia en los procesos de separación de $CO_2$.

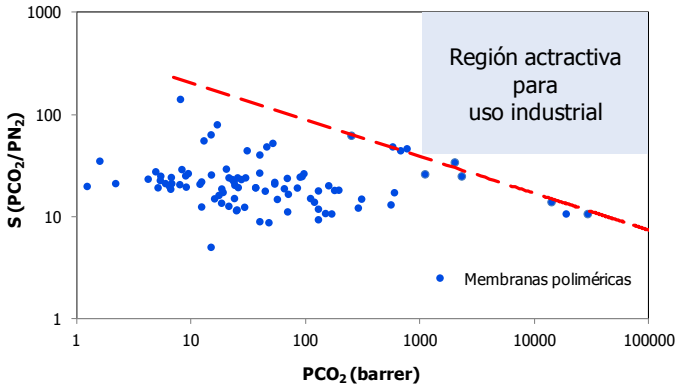


**Figura 1.2.** Diagrama de Robeson para la separación $CO_2/N_2$. Datos obtenidos de (Powell y Qiao, 2006).

El uso de membranas líquidas soportadas para la separación gaseosa ha sido ampliamente estudiado durante las dos últimas décadas (Lozano et al., 2011) debido a sus numerosas ventajas tales como un menor coste de inversión y de operación, menor consumo energético y simplicidad de operación (De Gyves y Rodriguez de San Miguel, 1999). El mecanismo consiste en la impregnación de los poros de la membrana con un disolvente seleccionado y el posterior transporte de especies a través de la membrana de acuerdo al mecanismo de solución-difusión. La molécula de soluto se disuelve en la interfase entre la fase gaseosa de alimentación y la membrana, difunde a través de la membrana y desorbe en la superficie opuesta, tal y como muestra la Figura 1.3. La mayoría de los sistemas de membranas líquidas soportadas tienen configuración plana, utilizando soportes poliméricos puesto que los soportes inorgánicos tienen un mayor espesor limitando la viabilidad técnica de la membrana. Diferentes disolventes orgánicos tales como Monoetanolamina (MEA), Dietanolamina (DEA), Diisopropilamina (DIPA), Etilendiamina (EDA), Diglicolamina (DGA) o Polietilenglicol (PEG) han sido inmovilizados en soportes poliméricos para llevar a cabo la separación de $CO_2$ (Park et al., 2000; Matsumiya et al., 2005; Francisco et al., 2010). El mayor reto técnico de estos sistemas es la estabilidad de la membrana puesto que el disolvente retenido en los poros puede evaporarse tras un cierto tiempo de operación. La viscosidad es otro parámetro clave en el diseño de sistemas de membranas líquidas soportadas; una viscosidad del líquido baja está asociada en general con permeabilidades de $CO_2$ elevadas debido a que el gas difunde más fácilmente a través de la membrana (Gorji y Kaghazchi, 2008).

A pesar de que la tecnología de membranas pueda resultar atractiva para la separación gaseosa, su aplicación en la industria sigue estando limitada por los problemas de estabilidad y de rendimiento a largo plazo considerados el cuello de botella de esta tecnología.

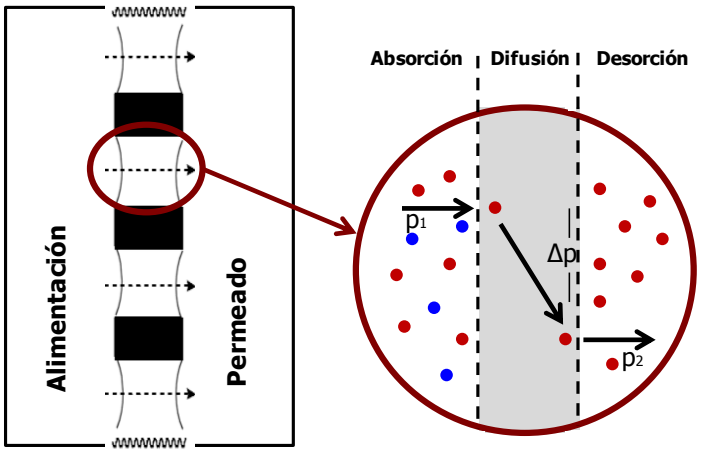


**Figura 1.3**. Mecanismo de solución-difusión (Albo J., 2012).

## 1.3. Desarrollo y progreso de los líquidos iónicos en la separación de $CO_2$

Una de las estrategias más interesantes para mejorar la estabilidad de las membranas líquidas soportadas es el empleo de líquidos iónicos (LIs) como fase inmovilizada en los poros de la membrana, debido a que estos compuestos presentan una presión de vapor despreciable. Esta característica elimina el problema de la evaporación de disolvente presente en las membranas líquidas soportadas consiguiéndose una mayor estabilidad (Fortunato et al., 2005; Hernández-Fernández et al., 2009). Los LIs son compuestos constituidos por cationes orgánicos voluminosos y aniones orgánicos o inorgánicos y tienen la especial característica de ser líquidos a temperatura ambiente. A diferencia de los electrolitos convencionales en los que los iones disueltos son solvatados por las moléculas de disolvente, los líquidos iónicos están compuestos en su totalidad por iones tal y como muestra la Figura 1.4.

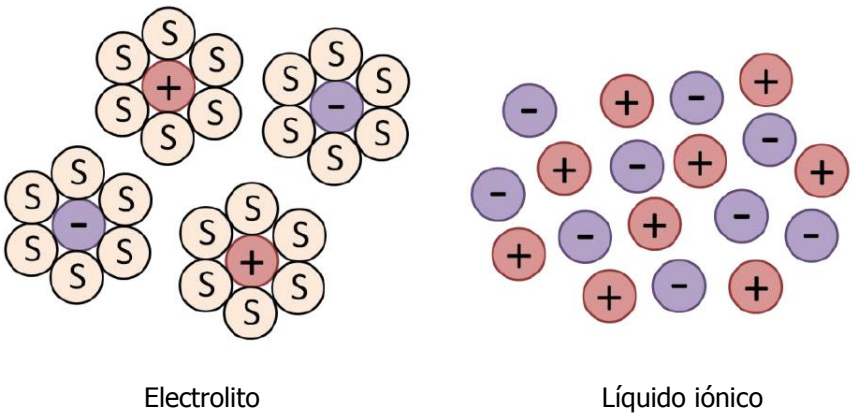


**Figura 1.4.** Definición esquemática de los líquidos iónicos y comparación con electrolitos convencionales.

Algunos ejemplos de los cationes y aniones más utilizados se muestran en la Figura 1.5.

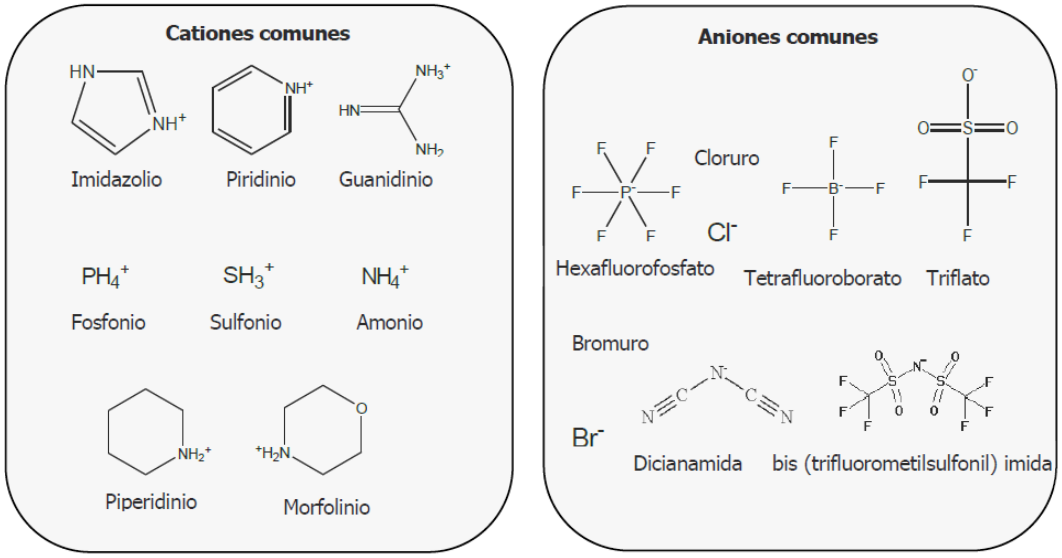


**Figura 1.5.** Cationes y aniones más utilizados.

Los LIs presentan una gran variedad de propiedades tales como una presión de vapor despreciable o una elevada estabilidad térmica y mecánica. Sin embargo, la propiedad más importante de los LIs es su estructura modular catión-anión que permite ajustar sus propiedades físico-químicas y optimizarlas para una aplicación específica. Por esta razón se han considerado como "disolventes de diseño" (Seddon, 1997; Freemantle, 1998; Stark y Seddon, 2007). Una de las limitaciones de aplicación de los LIs a gran escala es su precio. Los precios actuales de los LIs (a escala de laboratorio) oscilan sobre los 1000 $/kg. Sin embargo, según BASF, aplicando una economía de escala, el precio del LI para un proceso a gran escala caería por debajo de los 40 $/kg, situándolos aún con un precio de 10 a 20 veces superior a los disolventes convencionales (Ramdin et al., 2012).

Debido a sus interesantes características, el desarrollo e implementación de los LIs se ha extendido a diferentes campos de aplicación tales como la química analítica (Berthod et al., 2008), catálisis (Sheldon, 2001; Parvulescu y Hardacre, 2007), electroquímica (Galinski et al., 2006; Wang et al., 2003), uso biológico (Tan y Macfarlane, 2009) y procesos de separación (Blanchard y Brennecke, 2001; Buzzeo et al., 2005; Han y Armstrong, 2007). Existe un gran interés en el uso de los LIs para separación de $CO_2$ de corrientes de gases de post-combustión (Bates et al., 2002; Baltus et al., 2005).

Existen diversos trabajos en la bibliografía donde se estudia la utilización de membranas soportadas con líquidos iónicos (MSLIs) para la separación $CO_2/N_2$ (Lozano et al., 2011; Ramdin et al., 2012). Se ha estudiado el empleo de MSLIs basadas en [Emim][$Tf_2N$], [Emim][$CF_3SO_3$], [Emim][Dca] y [Thtdp][Cl] sobre un soporte poroso hidrofílico de polietersulfona (PES)

obteniéndose permeabilidades entre 350 y 920 barrers (1 barrer = $10^{-10}$ $cm^3(STP).cm^{-2}.s^{-1}.cmHg^{-1}$) y selectividades ideales $CO_2/N_2$ entre 15-61 (Scovazzo et al., 2004). Se ha estudiado el comportamiento de MSLIs conteniendo el grupo fluoroalquilo encontrándose permeabilidades entre 210-320 barrers y selectividades $CO_2/N_2$ 16-26 (Bara et al., 2009). También se han evaluado MSLIs basadas en el catión 1-n-alquil-3-metilimidazolio y diferentes aniones utilizando dos soportes porosos de diferente hidrofobicidad con selectividades ideales $CO_2/N_2$ comprendidas entre 22 y 39 (Neves et al., 2010). Se ha investigado el uso de MSLIs preparadas con doce tipos diferentes de LIs inmobilizados sobre un soporte poroso hidrofílico de fluoruro de polivinilideno (PVDF). Las permeabilidades de $CO_2$ oscilan en el rango 94-750 barrers mientras las selectividades ideales $CO_2/N_2$ varían de 10 a 52 (Cserjési et al., 2010). Además, se ha estudiado la permeabilidad de $CO_2$ a través de MSLIs utilizando LIs basados en el catión imidazolio soportadas en un soporte poroso de PVDF. Se reportaron permeabilidades entre 120 y 445 barrers y selectividades $CO_2/N_2$ de 42 a 86 (Jindaratsamee et al., 2011).

La configuración plana es el enfoque más común para los experimentos a escala de laboratorio; sin embargo, un valor de área por unidad de volumen superior (ej. el que se puede conseguir mediante enrollado en espiral o módulos de fibras huecas) es requerido para su aplicación a escala industrial (Lozano et al., 2011). La utilización de LIs elimina el problema de la evaporación de disolvente que ocurre en membranas líquidas soportadas lo que pretende mejorar la estabilidad de las membranas. Sin embargo, la estabilidad de las membranas sigue siendo un asunto pendiente; se observa un comportamiento diferente en términos de estabilidad dependiendo del tipo de LI utilizado y de la naturaleza de la membrana (hidrofóbica o hidrofílica) (Luis et al., 2012). Se ha reportado una pérdida de peso importante (11-13%) a 1 bar de diferencia de presión utilizando membranas hidrofílicas con LIs basados en el catión imidazolio (Neves et al., 2010). Además, el contenido en humedad es una variable decisiva en la permeabilidad y selectividad de $CO_2$. Un contenido de agua bajo puede tener un efecto positivo en la permeabilidad y selectividad de $CO_2$ al disminuir la viscosidad incrementándose la difusividad de $CO_2$ (Zhao et al., 2010b). Sin embargo, la formación de micro-dominios dentro de los LIs mejora la difusión de los componentes disminuyendo la selectividad (Neves et al., 2010; Luis et al., 2012).

### *a. Líquidos iónicos de elevada solubilidad*

Los LIs han recibido un interés creciente en aplicaciones relacionadas con la separación de $CO_2$ debido a que el $CO_2$ presenta una elevada solubilidad en ciertos LIs. De entre la gran variedad de LIs existentes, se espera que aquellos basados en el catión imidazolio presenten una mayor solubilidad de $CO_2$ (Neves et al, 2010). El anión juega un papel importante en la solubilidad del gas debido a la formación de complejos con el $CO_2$ (Anthony et al, 2005). Los LIs

conteniendo el anión de acetato, particularmente los LIs comerciales 1-etil-3-metilimidazolio acetato [Emim][Ac] y 1-butil-3-metilimidazolio acetato [Bmim][Ac], han sido muy estudiados en la bibliografía mostrando una elevada solubilidad de $CO_2$.

Maginn et al. (Maginn et al., 2005) reportaron por primera vez la elevada solubilidad de $CO_2$ en el LI [Bmim][Ac] a través de un mecanismo que consiste en la extracción de protones por parte del anión acetato de la posición C2 del anillo imidazolio lo que supondría la obtención de ácido acético en el proceso. En una etapa posterior, el $CO_2$ reacciona formando bicarbonato. Chinn et al. (Chinn et al., 2005) propusieron el sistema $CO_2$/[Bmim][Ac]/agua para la captura de $CO_2$ a través de un mecanismo donde el grupo acetato interactúa con el agua y el $CO_2$ es capturado como grupo bicarbonato. Partiendo de una disolución de [Bmim][Ac] en agua al 14% peso se demostró que la absorción de $CO_2$ en este sistema presentaba un comportamiento típico de complejación química. La capacidad de absorción volumétrica del LI basado en acetato (~ 25 $m^3/m^3$) presenta un valor intermedio entre las aminas (~ 65 $m^3/m^3$ para una disolución acuosa de MEA al 30% peso) y los LIs con absorción física (~ 3 $m^3/m^3$). Del mismo modo, la entalpía de reacción del $CO_2$ en el LI de acetato es de -40 kJ/mol, que también es un valor intermedio entre una disolución al 30% de MEA (-85 kJ/mol) y LIs con absorción física (-15 kJ/mol) (Ramdin et al., 2012). Por lo tanto, la etapa de regeneración requiere un aporte de energético mucho menor que el proceso de absorción convencional con MEA.

Shifflet et al. (Shifflet et al., 2008) llevaron a cabo un estudio experimental del sistema $CO_2$+[Bmim][Ac] tanto en presencia como en ausencia de agua observando fuertes interacciones intermoleculares y la formación de complejos. Se llevó a cabo una evaluación económica del proceso que demostraba que el empleo del sistema $CO_2$+[Bmim][Ac] podría reducir las pérdidas energéticas en un 16% comparado con el proceso convencional con MEA. Por otra parte, se estima una inversión alrededor de un 11% menor en el proceso con este LI y un 12% de reducción en la huella de los equipos en relación con el proceso convencional con MEA (Shifflet et al., 2010).

Shifflet y Yokozeki (Shifflet y Yokozeki, 2009) investigaron la solubilidad de $CO_2$ en los LIs [Emim][Ac], [Emim][$F_3$Ac], y mezclas de ambos LIs. El [Emim][Ac] absorbe el $CO_2$ a través de una absorción química, mientras que el [Emim][$F_3$Ac] mostró comportamiento de absorción física. La mezcla de ambos líquidos iónicos mostró una combinación de absorción física y química.

Más recientemente, se ha estudiado la separación $CO_2/H_2$ en el LI [Emim][Ac] (Shi et al., 2012). Además, se ha modelado la interacción de $CO_2$ con el anión acetato como ejemplo prototipo de un anión que se une fuertemente al $CO_2$ (Carvalho et al., 2009; Kim et al., 2011; Shi et al., 2012; Steckel, 2012).

*b. Líquidos iónicos polimerizables*

Es posible la polimerización de algunos LIs formándose polímeros iónicos con capacidades de absorción de $CO_2$ mayores que las de sus LIs precursores debido a mayores velocidades de absorción y desorción (Supasitmongkol et al., 2010). Los polímeros iónicos han sido extensamente estudiados por Noble y colaboradores como posibles materiales de membrana para la separación de $CO_2$ (Bara et al., 2008a; Bara et al., 2008b; Bara et al., 2010).

El catión de los polímeros iónicos juega un papel importante en la absorción de $CO_2$. Los cationes tipo amonio muestran una elevada solubilidad por el $CO_2$ como por ejemplo poli(vinilbenzil trimetil amonio tetrafluoroborato), p[Vbtma][$BF_4$], frente a los basados en imidazolio (ej. poli(1-p-vinilbenzil-3-metil imidazolio tetrafluoroborato), p[Vbmi][$BF_4$], (Blasig et al., 2007)). Además, se ha demostrado que los polímeros iónicos basados en el catión p[Vbtma] con diferentes aniones ($PF_6$, $BF_4$ y $Tf_2N$) exhiben diferentes capacidades de absorción de $CO_2$ (Tang et al., 2005; Supasitmongkol et al., 2010; Bhavsar et al., 2012).

*c. Líquidos iónicos magnéticos*

El comportamiento de los líquidos iónicos magnéticos (LIMs) está siendo recientemente estudiado en bibliografía debido a la combinación única de las propiedades de los LIs con las propiedades magnéticas asociadas a la incorporación de un ión metálico en su estructura. Los LIMs están empezando a atraer un gran interés en diferentes campos de aplicación tales como catálisis (Valkenberg et al., 2001; Tilve et al., 2004; Nguyen et al., 2008; Wang et al., 2010a; Misuka et al., 2011), dispositivos electrónicos o baterías (Branco et al., 2011; Arora y Zhang, 2004) y procesos selectivos de separación (Jiang et al., 2006; Lee et al., 2007; Deng et al., 2011; Wang et al., 2010b; Wang et al., 2012).

Los LIMs 1-butil-3-metilimidazolio tetracloroferrato [Bmim][$FeCl_4$] y 1-butironitrilo-3-metilimidazolio tetracloroferrato [n-Bmim][$FeCl_4$] fueron los primeros en los que se observó respuesta magnética ante la aplicación de un campo magnético externo de neodimio de 0,55 Tesla (Hayashi y Hagamuchi, 2004; Hayashi et al., 2006). Este comportamiento ante un campo magnético externo es el que explica la Figura 1.6. Posteriormente, fueron sintetizados LIMs basados en diferentes metales de transición tales como hierro, cobalto, manganeso o gadolinio (Del Sesto et al., 2008). Se observaron propiedades magnéticas con aplicaciones potenciales como interruptores magnético y electrocrómico. Okuno y Hamaguchi (Okuno y Hamaguchi, 2006) demostraron por primera la vez la posibilidad de conseguir el transporte de un gas en presencia de un campo magnético externo, mediante la modificación de la trayectoria de las burbujas de $N_2$ en presencia de un campo magnético tal y como muestra la Figura 1.7. De forma más reciente, han sido reportadas dos aplicaciones en el campo de los procesos de

separación: mejora de la extracción de compuestos orgánicos en presencia de un campo magnético externo (Deng et al., 2011) y el empleo de LIMs como agente extractante de fracciones de asfalto de los residuos de la licuefacción del carbón (Wang et al., 2012).

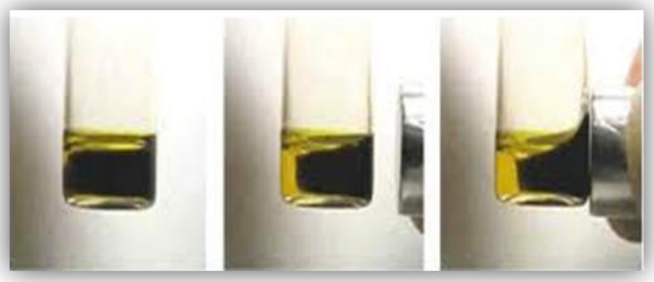

**Figura 1.6.** Respuesta de [Bmim][$FeCl_4$] ante un pequeño imán de neodimio (0,55 T). Se añade agua para mostrar claramente el desplazamiento. Cuando no se aplica campo magnético se observan dos fases claramente diferenciadas (agua en la parte superior y [Bmim][$FeCl_4$] en la inferior), mientras que al aplicar campo magnético se observa una distorsión del LIM en forma cóncava (Hayashi y Hamaguchi, 2004; Hayashi et al., 2006).

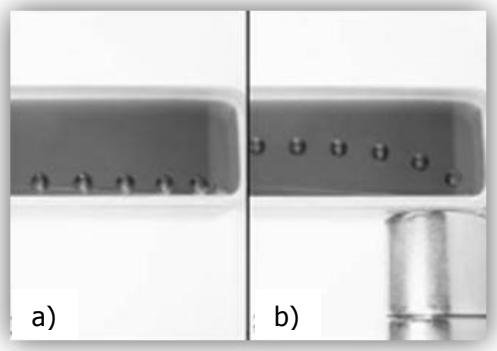


**Figura 1.7.** Cambio de la trayectoria de las burbujas de $N_2$ a) en ausencia y b) en presencia campo magnético (Okuno y Hamaguchi, 2006).

Algunas de las propiedades de los LIMs tales como la solubilidad, la viscosidad o la tensión superficial pueden verse afectadas por la aplicación de un campo magnético externo (Hayashi et al., 2006; Lee et al., 2007; De Pedro et al., 2010). Se ha observado la posibilidad de modular la solubilidad de benceno en [Bmim][$FeCl_4$] en función del campo magnético aplicado (Jiang et al., 2006). Del mismo modo, se ha encontrado una dependencia entre la concentración de mezclas binarias LIM/agua y la intensidad del campo magnético aplicado (Lee et al., 2007) observándose un incremento de la solubilidad del LIM en el medio acuoso.

Estos nuevos LIs con propiedades magnéticas permitirían el desarrollo de nuevos procesos de separación basados en membranas estímulo-respuesta tal y como se explica en la Figura 1.8.

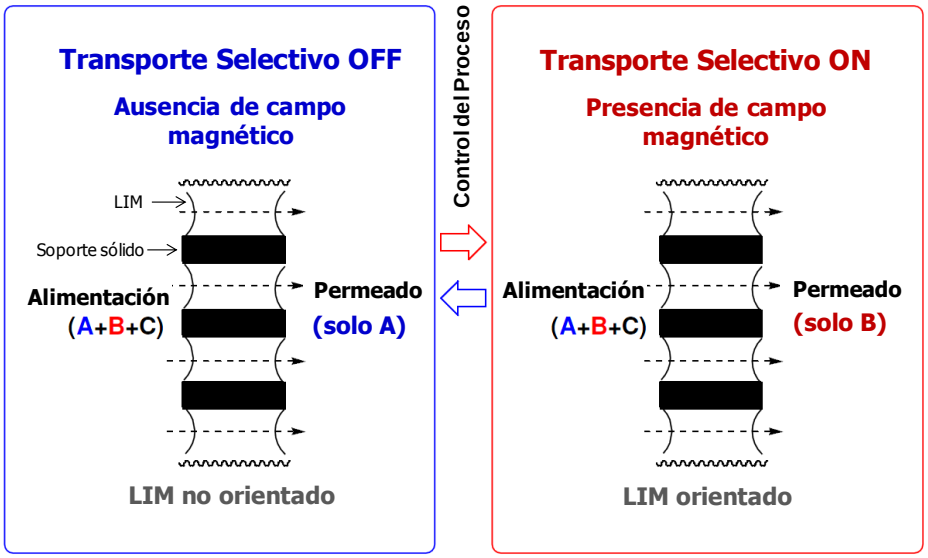


**Figura 1.8**. Transporte selectivo de un componente A (en ausencia de campo magnético) y transporte selectivo de un componente B (en presencia de campo magnético).

### 1.4. Objetivos y estructura de la tesis

La presente Tesis se ha desarrollado en el marco del proyecto ENE2010-14828 *"Desarrollo de un proceso de captura y reciclado de $CO_2$"* y en el marco del proyecto europeo ERANET EUI2008-03857 *"Development of Novel Stimuli-Responsive Membranes Integrating Magnetic Ionic Liquids for Innovative Separation Processes (MIL-Project)"* en colaboración con la Universidade Nova de Lisboa y el Instituto Superior Técnico (Portugal). El objetivo general es el desarrollo de nuevos procesos de separación basados en la utilización de membranas y líquidos iónicos magnéticos para el transporte selectivo de gases y especies bioactivas aplicando un campo magnético externo.

La separación de $CO_2$ de una corriente de gases de combustión es uno de los problemas fundamentales en los procesos de captura de $CO_2$. En este contexto, **el objetivo general de esta Tesis Doctoral consiste en el desarrollo de nuevas membranas soportadas utilizando líquidos iónicos para la separación de $CO_2$.** Esta Tesis supone una contribución innovadora en una doble vertiente: por un lado mediante el desarrollo de nuevas membranas basadas en líquidos iónicos magnéticos que permitan modular la permeabilidad y selectividad $CO_2/N_2$ en presencia de un campo magnético externo, y por otro, a través de membranas

soportadas con líquidos iónicos basados en el anión acetato donde se pretenden obtener los mejores resultados.

Para alcanzar este objetivo general es necesario abordar los siguientes objetivos específicos:

- Caracterización de líquidos iónicos magnéticos para separación de $CO_2$.
- Desarrollo y aplicación de un método de contribución de grupos para estimar la viscosidad de los líquidos iónicos magnéticos a diferentes temperaturas.
- Estudio de la permeabilidad y selectividad de $CO_2$ a través de membranas soportadas con líquidos iónicos magnéticos en ausencia/presencia de campo magnético.
- Estudio de la permeabilidad, solubilidad y difusividad en membranas soportadas con líquidos iónicos de alta solubilidad basados en el anión acetato.

De acuerdo con estos objetivos específicos, y considerando la normativa de Tesis basada en compendio de artículos, el trabajo se desarrolla en cuatro capítulos de la siguiente forma: el Capítulo 1 incluye el planteamiento de la Tesis. El Capítulo 2 incluye una descripción detallada de los procedimientos y materiales empleados para la realización de la Tesis, así como un resumen global de los resultados y la discusión de los mismos. El Capítulo 3 resume las conclusiones generales obtenidas y el progreso de la investigación. Y finalmente el Capítulo 4 supone el núcleo central de la Tesis, incluyendo copia de los artículos que la sustentan.

## 1.5. Referencias del Capítulo 1

Adanez J., Abad A., García-Labiano F., Gayan P., de Diego L.F. Progress in chemical-looping combustion and reforming technologies. *Prog. Energy Combust. Sci.* **2012**, 38, 215-282.

Albo J., Luis P., Irabien A. Absorption of coal combustion flue gases in ionic liquids using different membrane contactors. *Desalin. Water Treat.* **2011**, 27, 54-59.

Albo J. Desarrollo de una tecnología innovadora para la mitigación del cambio climático: Absorción no dispersiva con líquidos iónicos, Tesis Doctoral, Universidad de Cantabria, Santander, **2012**.

Alvarez-Guerra M., Quintanilla S., Irabien A. Conversion of carbon dioxide into formate using a continuous electrochemical reduction process in a lead cathode. *Chem. Eng. J.* **2012**, 207, 278-284.

Anthony J.L., Anderson J.L., Maginn E.J., Brennecke F. Anion effects on gas solubility in ionic liquids. *J. Phys. Chem. B* **2005**, 109, 6366-6374.

Arora P. y Zhang Z. Battery separators. *Chem. Rev.* **2004**, 104, 4419-4462.

Baker R.W. Future directions of membrane gas separation technology. *Ind. Eng. Chem. Res.* **2002**, 41, 1393-1411.

Baltus R., Counce R.M., Culbertson B.H., Luo H.M., DePaoli D.W., Dai S., Duckworth D.C. Examination of the potential of ionic liquids for gas separations. *Sep. Sci. Technol.* **2005**, 40, 525-541.

Bara J.E., Gin D.L., Noble R.D. Effect of anion on gas separation performance of polymer−room-temperature ionic liquid composite membranes. *Ind. Eng. Chem. Res*. **2008a**, 47, 9919-9924.

Bara J.E., Hatakeyama E.S., Gin D.L., Noble R.D. Improving $CO_2$ permeability in polymerized room-temperature ionic liquid gas separation membranes through the formation of a solid composite with a room-temperature ionic liquid. *Polym. Adv. Technol.* **2008b**, 19, 1415-1420.

Bara J.E., Carlisle T.K., Gabriel C.J., Camper D., Finotello A., Gin D.L., Noble R.D. Guide to $CO_2$ separations in imidazolium-based room-temperature ionic liquids. *Ind. Eng. Chem. Res.* **2009,** 48, 2739-2751.

Bara J.E., Camper D.E., Gin D.L., Noble R.D. Room-temperature ionic liquids and composite materials: platform technologies for $CO_2$ capture. *Accounts Chem. Res*. **2010**, 43, 152-159.

Bates E.D., Mayton R.D., Ntai I., Davis J.H. $CO_2$ capture by a task-specific ionic liquid. *J. Am. Chem. Soc.* **2002**, 124, 926-927.

Berthod A., Ruiz-Angel M.J., Carda-Broch S. Ionic liquids in separation techniques. *J. Chromatogr. A* **2008**, 1184, 6-18.

Bhavsar R.S., Kumbharkar S.C., Kharul U.K. Polymeric ionic liquids (PILs): effect of anion variation on their $CO_2$ sorption. *J. Membr. Sci.* **2012**, 389, 305-315.

Blanchard L.A. y Brennecke J.F. Recovery of organic products from ionic liquids using supercritical carbon dioxide. *Ind. Eng. Chem. Res.* **2001**, 40, 287-292.

Blasig A., Tang J., Hu X., Tan S.P., Shen Y., Radosz M. Carbon dioxide solubility in polymerized ionic liquids containing ammonium and imidazolium cations from magnetic suspension balance: P[VBTMA][$BF_4$] and P[VBMI][$BF_4$]. *Ind. Eng. Chem. Res.* **2007**, 46, 5542–5547.

Branco A., Branco L.C., Pina F. Electrochromic and magnetic ionic liquids. *Chem. Commun.* **2011**, 47, 2300-2302.

Bredesen R., Jordal K., Bolland O. High-temperature membranes in power generation with $CO_2$ capture. *Chem. Eng. Process.* **2004**, 43, 1129-1158.

Brunetti A., Scura F., Barbieri G., Drioli E. Membrane technologies for $CO_2$ separation. *J. Membr. Sci.* **2010**, 359, 115-125.

Buzzeo M.C., Evans R.G., Compton R.G. Examination of the potential of ionic liquids for gas separations. *Sep. Sci. Technol*. **2005**, 40, 525-541.

Carvalho P.J., Álvarez V.H., Schröder B., Gil A.M., Marrucho I.M., Aznar M., Santos L.M.N.B.F., Coutinho J.A.P. Specific solvation interactions of $CO_2$ on acetate and trifluoroacetate imidazolium based ionic liquids at high pressures *J. Phys. Chem. B* **2009**, 113, 6803-6812.

Chinn D., Vu D. Q., Driver M.S., Boudreau L.C. $CO_2$ removal from gas using ionic liquid absorbents, US Patent US20,060,251,558A1 (2006), November 9; US20,050,129,598A1 (**2005**), June 16.

Cristóbal J., Optimización multi-objetivo para la evaluación de la sostenibilidad de tecnologías de generación de electricidad a partir de carbón, Tesis Doctoral, Universidad de Cantabria, Santander, **2013**.

Cserjési P., Nemestóthy N., Bélafi-Bakó K. Gas separation properties of supported liquid membranes prepared with unconventional ionic liquids. *J. Membr. Sci.* **2010**, 349, 6-11.

Darde A., Prabhakar R., Tranier J.P., Perrin N. Air separation and the flue gas compression and purification units for oxy-coal combustion systems. *Energy Procedia* **2009**, 1, 527-534.

De Gyves J. y Rodriguez de San Miguel E. Metal ion separation by supported liquid membrane. *Ind. Eng. Chem. Res.* **1999**, 38, 2182-2202.

De Pedro I., Rojas D.P., Albo J., Luis P., Irabien A., Blanco J., Rodriguez J. Long-range magnetic ordering in magnetic ionic liquid: emim[$FeCl_4$]. *J. Phys. Condens. Matter.* **2010**, 22, 296-306.

Del Sesto R.E., McCleskey T.M., Burrel A.K., Baker G.A., Thompson J.D., Scott B.L., Wilkes J.S., Williams P. Structure and magnetic behaviour of transition metal based ionic liquids. *Chem. Commun.* **2008**, 447-449.

Deng N., Lin M., Zhao L., Liu C., de Rooy S., Warner I.M. Highly efficient extraction of phenolic compounds by use of magnetic room temperature ionic liquids for environmental remediation. *J. Hazard. Mater.* **2011**, 192, 1350-1357.

Favre E. Carbon dioxide recovery from post-combustion processes: Can gas permeation membranes compete with absorption? *J. Membr. Sci*. **2007**, 294, 50–59.

Figueroa J.D., Fout T., Plasynski S., McIlvried H., Srivastava R.D. Advances in $CO_2$ capture technology – The U.S. Department of Energy's Carbon Sequestration Program. *Int. J. Greenh. Gas Control* **2008**, 2, 9-20.

Fortunato R., Afonso C.A.M., Benavente J., Rodriguez-Castellon E., Crespo J.G. Stability of supported ionic liquid membranes as studied by X-ray photoelectron spectroscopy. *J. Membr. Sci*. **2005**, 256, 216-223.

Francisco G.J., Chakma A., Feng X. Separation of carbon dioxide from nitrogen using diethanolamine-impregnated poly(vinyl alcohol) membranes. *Sep. Purif. Technol.* **2010**, 71, 205-213.

Freemantle M. Designer solvents. *Chem. Eng. News* **1998**, 76, 32-37.

Galinski M., Lewandowski A., Stepniak I. Ionic liquids as electrolytes. *Electrochim. Acta* **2006**, 51, 5567-5580.

Ghoniem A.F. Needs, resources and climate change: clean and efficient conversion technologies. *Prog. Energy Combust. Sci.* **2011**, 37, 15-51.

Gorji A.H. y Kaghazchi T. $CO_2/H_2$ separation by facilitated transport membranes immobilized with aqueous single and mixed amine solutions: experimental and modeling study. *J. Membr. Sci.* **2008**, 325, 40-49.

Hägg M.-B., Membranes in gas separations, en: Handbook of membrane separations (Eds.: Pabby A. K., Rizvi S. S. H., Sastre A.M.) CRC Press, Taylor & Francis: NW, USA, 65-105, **2009**.

Han X. y Armstrong D. W. Ionic liquids in separations. *Acc. Chem. Res.* **2007**, 40, 1079-1086.

Hayashi S. y Hamaguchi H.A. Discovery of a magnetic ionic liquid bmim [$FeCl_4$]. *Chem. Lett.* **2004**, 33, 1590-1591.

Hayashi S., Saha S., Hamaguchi H.A. A new class of magnetic fluids: bmim[$FeCl_4$] n-bmim[FeCl4] ionicliquids. *IEEE Trans. Magn.* **2006**, 42, 12-14.

Hernández-Fernández F.J., de los Ríos A.P., Tomás-Alonso F., Palacios J.M., Víllora G. Preparation of supported ionic liquid membranes: Influence of the ionic liquid immobilization method on their operational stability. *J. Membr. Sci.* **2009**, 341, 172-177.

IEA – International Energy Agency, $CO_2$ emissions from fuel combustion: Highlights. **2011**.

Jiang Y., Gou C., Liu H. Magnetically rotational reactor for absorbing benzene emissions by ionic liquids. *China Particuology* **2006**, 5, 130-133.

Jindaratsamee P., Shimoyama Y., Morizaki H., Ito A. Effects of temperature and anion species on $CO_2$ permeability and $CO_2/N_2$ separation coefficient through ionic liquid membranes. *J. Chem. Thermodyn.* **2011**, 43, 311-314.

Khoo H.H. y Tan R.B.H. Life cycle investigation of $CO_2$ recovery and sequestration. *Environ. Sci. Technol.* **2006**, 40, 4016-4024.

Kim N., Jeong S.K., Yoon S., Park G. Ab-initio study on the interaction of $CO_2$ to the acetate. Bull. *Korean Chem. Soc.* **2011**, 32, 4441-4444.

Lee S.H., Ha S.H., Jin H.B., You C.Y., Koo Y. Magnetic behaviour of mixture of magnetic ionic liquid [bmim][$FeCl_4$] and water. *J. Appl. Phys.* **2007**, 101, 09J102.

Lozano L.J., Godinez C., de los Rios A.P., Hernandez- Fernandez F.J., Sanchez-Segado S., Alguacil F.J. Recent advances in supported ionic liquid membrane technology. *J. Membr. Sci.* **2011**, 376, 1-14.

Luis P., Neves L.A., Afonso C.A.M., Coelhoso I.M., Crespo J.G., Garea A., Irabien A. Facilitated transport of $CO_2$ and $SO_2$ through Supported Ionic Liquid Membranes (SILMs). *Desalination*, **2009**, 245, 485-493.

Luis P., Van Gerven T., Van der Bruggen B. Recent developments in membrane-based technologies for $CO_2$ capture. *Prog. Energy Combust. Sci.* **2012**, 38, 419-448.

MacDowell N., Florin N., Buchard A., Hallett J., Galindo A., Jackson G., Adjiman C.S., Williams C.K., Shah N., Fennell P. An overview of $CO_2$ capture technologies. *Energy Environ. Sci.* **2010**, 3, 1645-1669.

Maginn E.J. Design and evaluation of ionic liquids as novel $CO_2$ absorbents. http://www.netl.doe.gov/technologies/coalpower/ewr/$CO_2$/pubs (accessed Jan 24.01.13)

Matsumiya N. Teramoto M., Kitada S., Matsuyama H. Evaluation of energy consumption for separation of $CO_2$ in flue gas by hollow fiber facilitated transport membrane module with permeation of amine solution. *Sep. Purif. Technol*. **2005**, 46, 26-32.

Merkel T.C., Lin H., Wei X., Baker R. Power plant post-combustion carbon dioxide capture: An opportunity for membranes. *J. Membr. Sci.* **2010**, 359, 126-139.

Misuka V., Breuch D., Löwe H. Paramagnetic ionic liquids as "liquid fixed-bed" cataysts in flow applications. *Chem. Eng. J.* **2011**, 173, 536-540.

National Oceanic and Atmospheric Administration (NOAA), United States Department of Commerce, http://www.noaa.gov/ (accessed Nov 19.11.13)

Neves L.A., Crespo J.G., Coelhoso I.M. Gas permeation studies in supported ionic liquid membranes. *J. Membr. Sci.* **2010**, 357, 160-170.

Nguyen M.D., Nguyen L.V., Jeon E.H., Kim J.H., Cheong M., Kim H.S., Lee J.S. Fe containing ionic liquids as catalysts for the dimerization of bicyclo [2.2.1] hepta-2,5- diene. *J. Catal.* **2008**, 258, 5-13.

Okuno M., Hamaguchi H., Hayashi S. Magnetic manipulation of materials in a magnetic ionic liquid. *Appl. Phys. Lett.* **2006**, 89, 132506-132508.

Olajire A.A. $CO_2$ capture and separation technologies for end-of-pipe applications – a review, *Energy* **2010**, 35, 2610-2628.

Page S.C., Williamson A.G., Mason I.G. Carbon capture and storage: fundamental thermodynamics and current technology. *Energy Policy* **2009**, 37, 3314-3324.

Park S.W., Heo N.H., Kim G.W., Sohn I.J., Kumazawa H. Facilitated transportof carbon dioxide through an immobilized liquid membrane of aqueous carbonate solution with additives. *Sep. Sci. Technol.* **2000**, 35, 2497-24512.

Parvulescu V. I. y Hardacre C. Catalysis in ionic liquids. *Chem. Rev.* **2007**, 107, 2615-2665.

Powell C.E. y Qiao G. Polymeric $CO_2/N_2$ gas separation membranes for the capture of carbon dioxide from power plant flue gases. *J. Membr. Sci.* **2006**, 279, 1-49.

Ramdin M., de Loos T.W., Vlugt T.J.H. State-of-the-art of $CO_2$ capture with ionic liquids. *Ind. Eng. Chem. Res.*, **2012**, 51, 8149-8177.

Rao A.B. y Rubin E.S. A technical, economic, and environmental assessment of amine-based $CO_2$ capture technology for power plant greenhouse gas control, *Environ. Sci. Technol*. **2002**, 36, 4467-4475.

Robeson L.M. The upper bound revisited. *J. Membr. Sci.* **2008,** 320, 390-400.

Scovazzo P., Kieft J., Finan D.A., Koval C., DuBois D., Noble R. Gas separations using non-hexafluorophosphate $[PF_6]^-$ anion supported ionic liquid membranes. *J. Membr. Sci.* **2004**, 238 57-63.

Seddon K.R. Ionic liquids for clean technology. *J. Chem. Tech. Biotechnol.* **1997**, 68, 351-356.

Sheldon R. Catalytic reactions in ionic liquids. *Chem. Commun.* **2001**, 23, 2399-2407.

Shi W., Myers C.R., Luebke D.R., Steckel J.A., Sorescu D.C. Theoretical and experimental studies of $CO_2$ and $H_2$ separation using the 1-ethyl-3 methylimidazolium acetate ([emim][$CH_3COO$]) ionic liquid. *J. Phys. Chem. B* **2012**, 116, 283-295.

Shiflett M.B., Kasprzak D.J., Junk C.P., Yokozeki A. Phase behavior of {carbon dioxide + [bmim][Ac]} mixtures, *J. Chem. Thermodyn*. **2008**, 40, 25-31.

Shiflett M.B., Yokozeki A. Phase Behavior of carbon dioxide in ionic liquids: [emim][Acetate], [emim][trifluoroacetate], and [emim][Acetate] + [emim][trifluoroacetate] mixtures. *J. Chem. Eng. Data* **2009**, 54, 108-114.

Shiflett M.B., Drew D.W., Cantini R.A., Yokozeki A. Carbon dioxide capture using ionic liquid 1-butyl-3-methylimidazolium acetate. *Energy Fuels* **2010**, 24, 5781-578.

Stark A. y Seddon K.R. Ionic liquids, en: Kirk-Othmer Encyclopedia of Chemical Technology, John Wiley & Sons, Inc., Vol. 26. **2007**, pp. 836-920.

Steckel J.A. Ab-initio calculations of the interaction between $CO_2$ and the acetate ion, *J. Phys. Chem. A* **2012,** 116, 11643-11650.

Steeneveldt R., Berger B., Torp T.A. $CO_2$ capture and storage: closing the knowing –doing gap. *Chem. Eng. Res. Des.* **2006**, 84, 739-763.

Supasitmongkol S., Styrring P. High $CO_2$ solubility in ionic liquids and a tetraalkylammonium-based poly(ionic liquid). *Energy Environ. Sci.* **2010**, 3, 1961-1972.

Tan S.S.Y., Macfarlane D.R. Ionic liquids in biomass processing. *Top. Curr. Chem.* **2009**, 290, 311-339.

Tang J., Tang H., Sun W., Plancher H., Radosz M., Shen Y. Poly(ionic liquid)s: a new material with enhanced and fast $CO_2$ absorption. *Chem. Commun.* **2005**, 332, 3325-3327.

Tilve R.D., Alexander M.V., Khandekar A.C., Samant S.D., Kanetkar V.R. Synthesis of 2, 3-unsaturated glycopyranosides by Ferrier rearrangement in $FeCl_3$ based ionic liquid. *J. Mol. Catal. A* **2004**, 223, 237-240.

Toftegaard M.B., Brix J., Jensen P.A., Glarborg P., Jensen A.D. Oxy-fuel combustion of solid fuels. *Prog. Energy Combust. Sci.* **2010,** 36, 581-625.

Valkenberg M.H., De Castro C., Hölderich W.F. Friedel-Crafts acylation of aromatics catalysed by supported ionic liquids. *Appl. Catal. A* **2001**, 215, 185-190.

Wang P., Zakeeruddin S. M., Moser J.-E., Gratzel M. A new ionic liquid electrolyte enhances the conversion efficiency of dye-sensitized solar cells. *J. Phys. Chem. B* **2003**, 107, 13280-13285.

Wang H., Yan R., Li Z., Zhang X., Zhang S. Fe-containing magnetic ionic liquid as an effective catalyst for the glycolysis of poly (ethylene terephthalate). *Catal. Commun.* **2010a**, 11, 763-767.

Wang M., Li B., Zhao C., Qian X., Xu Y., Chen G. Recovery of $[BMIM]FeCl_4$ from homogeneous mixture using a simple chemical method. *Korean J. Chem. Eng.* **2010b**, 27, 1275-1277.

Wang J., Yao H., Nie Y., Bai L., Zhang X., Li J. Application of iron-containing magnetic ionic liquids in extraction process of coal direct liquefaction residues. *Ind. Eng. Chem. Res.* **2012**, 51, 3776-3782.

Wappel D., Gronald G., Kalb R., Draxler J. Ionic liquids for post-combustion $CO_2$ absorption. *Int. J. Greenh. Gas Control* **2010**, 4, 486-494.

Yokozeki A., Shiflett M.B., Grieco L.M., Foo T. Physical and chemical absorptions of carbon dioxide in room-temperature ionic liquids. *J. Phys. Chem. B* **2008**, 112, 16654-16663.

Zhao L., Riensche E., Blum L., Stolten D. Multi-stage gas separation membrane processes used in post-combustion capture: energetic and economic analyses. *J. Membr. Sci.* **2010a**, 359, 160-172.

Zhao W., He G., Zhang L., Ju J., Dou H., Nie F. Effect of water in ionic liquid on the separation performance of supported ionic liquid membrane for $CO_2/N_2$. *J. Membr. Sci.* **2010b**, 350, 279-285.

# 2 Desarrollo

«Es de importancia para quien desee alcanzar una certeza en su investigación, el saber dudar a tiempo»

Aristóteles (384 AC-322 AC)

Filósofo griego

# CAPÍTULO 2. DESARROLLO

## 2.1. Líquidos iónicos magnéticos para la separación de $CO_2$

El comportamiento de los líquidos iónicos magnéticos (LIMs) es objeto de estudios recientes en la bibliografía. La combinación de las propiedades generales que presentan los líquidos iónicos (LIs) (ej. elevada estabilidad térmica y química, carácter no volátil y no inflamable) junto a las nuevas propiedades asociadas a la incorporación de un ión metálico en su estructura, ha abierto un nuevo área de investigación que está empezando a atraer gran interés. En particular, los LIMs están empezando a captar la atención en el campo de los procesos de separación (Wang et al., 2010; Deng et al., 2011; Wang et al., 2012). Debido a la etapa inicial de desarrollo en la que se encuentran, es necesario el estudio de sus propiedades fundamentales para permitir el desarrollo de nuevas aplicaciones.

En este contexto, se ha sintetizado una serie de LIMs basados en el catión trihexil (tetradecil) fosfonio y en aniones conteniendo metales con diferente respuesta al campo magnético (Del Sesto et al., 2008) para el estudio de la separación de $CO_2$ cuando estos LIMs son inmovilizados en soportes porosos poliméricos. Los nuevos LIMs han sido caracterizados mediante la medida de la susceptibilidad magnética, densidad, viscosidad, propiedades térmicas y solubilidad de $CO_2$ (Santos et al., 2013b). La síntesis de los LIMs utilizados se ha llevado a cabo en la *Faculdade de Farmácia, Universidade de Lisboa (Portugal)*, bajo la supervisión del profesor Carlos A.M. Afonso. Sus principales características están recogidas en la Tabla 2.1.

### 2.1.1. Caracterización de líquidos iónicos magnéticos

*a. Susceptibilidad magnética*

Las medidas de susceptibilidad magnética de los LIMs han sido suministradas por el grupo de *Magnetismo de la Materia, CITIMAC, de la Universidad de Cantabria*. El procedimiento de medida (De Pedro et al., 2010) consiste básicamente en la introducción de una cápsula que contiene el LIM en un magnetómetro (Quantum Design MPMS, SQUID, EEUU) a 300 K y un campo magnético de entre -85 y 85 kOe. Además, se ha estudiado la dependencia de la susceptibilidad magnética con la temperatura de 2 a 300 K bajo la aplicación de un campo magnético externo de 1 kOe.

La Figura 2.1 muestra la dependencia lineal del momento magnético de los LIMs con el campo magnético aplicado a una temperatura constante de 300 K, lo que indica un comportamiento paramagnético de los LIMs estudiados. La susceptibilidad magnética de los cuatro LIMs se obtiene de la pendiente del ajuste lineal de los datos y está recogida en la Tabla 2.2.

**Tabla 2.1.** Propiedades de los LIMs sintetizados.

| *Nombre* | *Abreviatura* | *Apariencia* | *Peso Molecular* *(g.mol$^{-1}$)* | *Estructura* |
|---|---|---|---|---|
| Trihexil (tetradecil) fosfonio tetraclorocobalto | $[P_{66614}][CoCl_4]$ |  | 1112 | 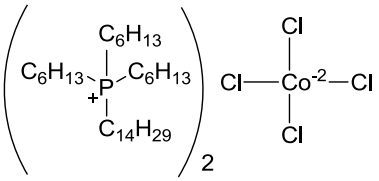 |
| Trihexil (tetradecil) fosfonio tetracloroferrato | $[P_{66614}][FeCl_4]$ |  | 681,51 | 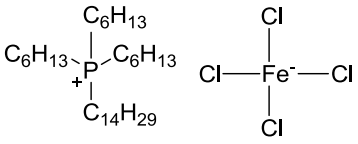 |
| Trihexil (tetradecil) fosfonio tetracloromanganeso | $[P_{66614}][MnCl_4]$ | 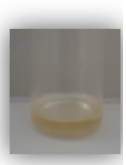 | 1103 | 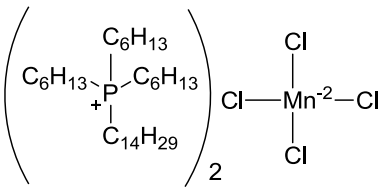 |
| Trihexil (tetradecil) fosfonio hexaclorogadolinio | $[P_{66614}][GdCl_6]$ | 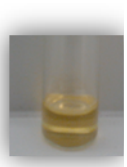 | 1821,54 | 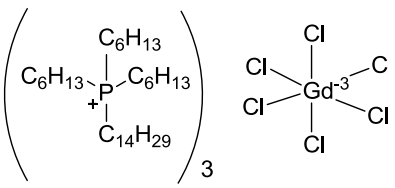 |

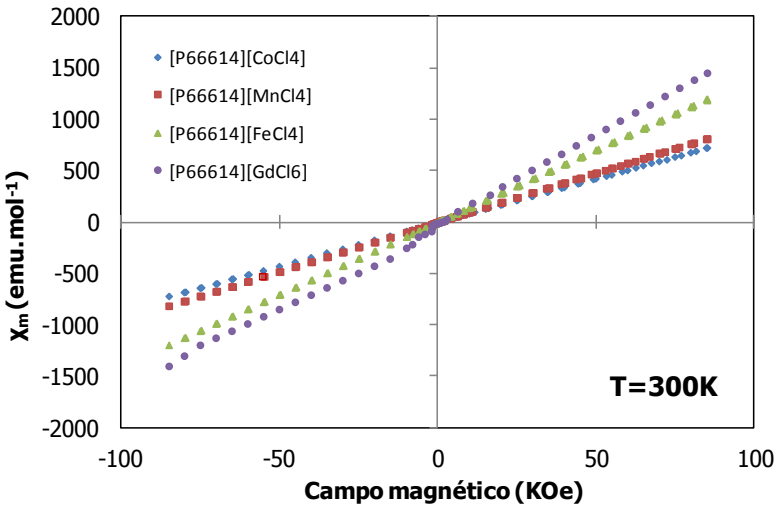


**Figura 2.1.** Momento magnético en función del campo magnético aplicado a 300 K.

**Tabla 2.2.** Susceptibilidad magnética, χmT, de los LIMs estudiados.

| *Anión* | *Catión* | *χmT (emu.K.mol$^{-1}$)* | *Referencia* |
|---|---|---|---|
| $[CoCl_4]$ | $[P_{66614}]$ | 2,10 | Santos et al., 2013b |
| | $[PR_4]$ | 2,48 | Del Sesto et al., 2008 |
| $[Co(NCS)_4]$ | $[PR_4]$ | 2,06 | Del Sesto et al., 2008 |
| $[MnCl_4]$ | $[P_{66614}]$ | 4,23 | Santos et al., 2013b |
| | $[PR_4]$ | 4,22 | Del Sesto et al.,2008 |
| $[FeCl_4]$ | $[P_{66614}]$ | 4,29 | Santos et al., 2013b |
| | [Bmim] | 4,11 | Hayashi et al., 2006 |
| | $[C_{10}mim]$ | 4,01 | Del Sesto et al., 2008 |
| | $[PR_4]$ | 4,34 | Del Sesto et al., 2008 |
| | [Nbmim] | 4,34 | Hayashi et al., 2006 |
| $[GdCl_6]$ | $[P_{66614}]$ | 6,51 | Santos et al., 2013b |
| | $[PR_4]$ | 7,72 | Del Sesto et al., 2008 |

Los momentos magnéticos obtenidos están en concordancia con los resultados mostrados en la bibliografía para los aniones $[CoCl_4]$ (2,06-2,48 emu.K.mol$^{-1}$), $[FeCl_4]$ (4,01-4,34 emu.K.mol$^{-1}$), $[MnCl_4]$ (4,22 emu.K.mol$^{-1}$) y $[GdCl_6]$ (7,72 emu.K.mol$^{-1}$) (Hayashi et al., 2006; Del Sesto et al., 2008).

La dependencia del momento magnético con la temperatura bajo un campo magnético aplicado constante de 1 kOe muestra que todos los LIMs estudiados siguen la ley de Curie-Weiss tal y como se muestra en la Figura 2.2.

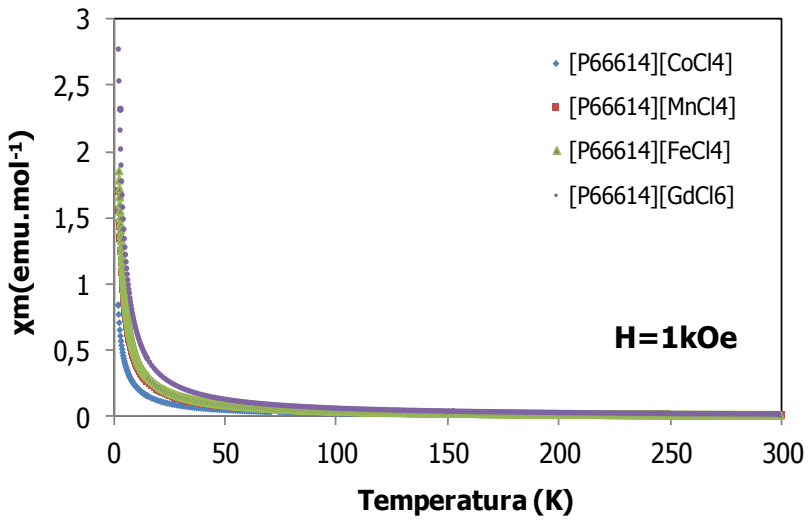


**Figura 2.2.** Momento magnético en función de la temperatura bajo la aplicación de un campo magnético de 1kOe.

*b. Densidad y viscosidad*

Se ha estudiado la dependencia de la densidad y la viscosidad con la temperatura de 293 a 373 K. La densidad de los LIMs ha sido medida gravimétricamente utilizando un picnómetro de 10 mL, mientras que las medidas de viscosidad se han realizado en el *Instituto Superior de Agronomia (ISA), Universidade Técnica Lisboa* utilizando un reómetro (Haake RS75, Alemania). La Tabla 2.3 muestra los datos experimentales de densidad y viscosidad a diferentes temperaturas.

**Tabla 2.3.** Medidas de densidad y viscosidad a diferentes temperaturas.

| *T (K)* | *$[P_{66614}][CoCl_4]$* | | *$[P_{66614}][FeCl_4]$* | | *$[P_{66614}][MnCl_4]$* | | *$[P_{66614}][GdCl_6]$* | |
|---|---|---|---|---|---|---|---|---|
| | *ρ (g.cm$^{-3}$)* | *μ (cP)* | *ρ (g.cm$^{-3}$)* | *μ (cP)* | *ρ (g.cm$^{-3}$)* | *μ (cP)* | *ρ (g.cm$^{-3}$)* | *μ (cP)* |
| 293,15 | 0,965 | 123500 | 1,012 | 790 | 0,956 | 112300 | 0,983 | 28230 |
| 298,15 | 0,962 | 83450 | 1,008 | 650 | 0,949 | 75230 | 0,981 | 18390 |
| 303,15 | 0,959 | 40250 | 1,004 | 520 | 0,943 | 41560 | 0,979 | 13010 |
| 323,15 | - | 15360 | - | 230 | - | 13970 | - | 2890 |
| 373,15 | - | 11050 | - | 44 | - | 920 | - | 290 |

La dependencia de la densidad con la temperatura se describe de acuerdo a la siguiente ecuación (Gardas y Coutinho, 2008):

$$\rho = \frac{M}{NV\left(a + bT + cP\right)} \tag{2.1}$$

donde $\rho$ es la densidad (g.cm$^{-3}$); $M$ la masa molecular (g.mol$^{-1}$); $N$ la constante de Avogadro (mol$^{-1}$); $V$ el volumen molecular (Å$^3$); $T$ la temperatura (K); $P$ la presión (MPa) y $a$, $b$ y $c$ los coeficientes a estimar mediante el ajuste.

Todos los experimentos se han llevado a cabo a presión constante por lo que la ecuación 2.1 puede simplificarse de acuerdo a la expresión:

$$\rho = \frac{1}{\alpha + \beta T} \tag{2.2}$$

donde $\alpha = \frac{NV}{M}\left(a + cP\right)$ (Å$^3$.kg$^{-1}$.Mpa$^{-1}$) y $\rho = \frac{NVb}{M}$ ( Å$^3$.K$^{-1}$.kg$^{-1}$)

Los parámetros $\alpha$ y $\beta$ estimados con un intervalo de confianza del 95% mediante el software Fitteia se muestran en la Tabla 2.4. El porcentaje de desviación global (MPD) de un 0,22% es consistente con el 0,29% obtenido de la bibliografía para un estudio similar (Gardas y Coutinho, 2008).

**Tabla 2.4.** Parámetros de ajuste para la correlación densidad-temperatura.

| *LIMs* | $\alpha$ | $\beta$ | *MPD (%)* |
|---|---|---|---|
| $[P_{66614}][GdCl_6]$ | 9,3x10$^{-4}$ | 3,1x10$^{-7}$ | 0,25 |
| $[P_{66614}][MnCl_4]$ | 5,8x10$^{-4}$ | 1,6x10$^{-6}$ | 0,28 |
| $[P_{66614}][FeCl_4]$ | 7,6x10$^{-4}$ | 7,7 x10$^{-7}$ | 0,21 |
| $[P_{66614}][CoCl_4]$ | 8,2x10$^{-4}$ | 7,4x10$^{-7}$ | 0,14 |
| MPD global | | | 0,22 |

La viscosidad a diferentes temperaturas ha sido estimada utilizando la ecuación de Orrick–Erbar (Gardas y Coutinho, 2008):

$$\ln\left(\frac{\mu}{\rho.M}\right) = A + \frac{B}{T} \qquad (2.3)$$

donde $\mu$ es la viscosdiad (cP); $\rho$ la densidad (g.cm$^{-3}$); $M$ el peso molecular (g.mol$^{-1}$); $T$ la temperatura (K) y $A$ *y* $B$ los parámetros característicos de la ecuación Orrick-Erbar.

Los parámetros A y B estimados con un intervalo de confianza del 95% utilizando el software Fitteia se muestran en la Tabla 2.5. El porcentaje de desviación global (MPD) es del 7,64%, consistente con el 7,78% obtenido de la bibliografía para un estudio similar (Gardas y Coutinho, 2008).

**Tabla 2.5.** Parámetros de ajuste para la correlación viscosidad-temperatura.

| *LIMs* | *A* | *B* | *MPD (%)* |
|---|---|---|---|
| $[P_{66614}][GdCl_6]$ | -18,39 | 6172,05 | 8,13 |
| $[P_{66614}][MnCl_4]$ | -16,98 | 6328,50 | 4,04 |
| $[P_{66614}][FeCl_4]$ | -12,78 | 3745,09 | 1,47 |
| $[P_{66614}][CoCl_4]$ | -4,58 | 2530,10 | 16,93 |
| MPD global | | | 7,64 |

*c. Análisis termogravimétrico*

Los análisis termogravimétricos se han llevado a cabo utilizando la termobalanza TG-DTA 60H Shimadzu (Japón) en una atmósfera de nitrógeno en un rango de temperaturas desde temperatura ambiente hasta 873 K con una velocidad de calentamiento de 5 K·min$^{-1}$. Para llevar a cabo el análisis de calorimetría diferencial de barrido (DSC) se ha utilizado el DSC SETARAM Setsys Evolution cubriendo un rango de temperaturas de 300 a 3123 K con una velocidad de calentamiento de 5 K·min$^{-1}$ en una atmósfera de nitrógeno.

La Figura 2.3 muestra el análisis termogravimétrico de los LIMs estudiados. Se ha calculado la temperatura de inicio de la descomposición ($T_{onset}$) como la intersección de la línea de base del peso desde el inicio del experimento con la tangente de la curva de peso frente a temperatura, los resultados se recogen en la Tabla 2.6. Los LIMs presentan una buena estabilidad térmica siendo térmicamente estables hasta 619 K y estando en concordancia con la bibliografía (Anderson et al., 2010; Bäcker et al., 2011; Deng et al., 2011). Del estudio de la

calorimetría diferencial de barrido (DSC) se observa una pérdida inicial de agua alrededor de los 300 K para $[P_{66614}][CoCl_4]$ y $[P_{66614}][GdCl_6]$. Para el caso del $[P_{66614}][FeCl_4]$ se detecta un pico exotérmico por encima de los 600 K (a diferencia de los picos endotérmicos observados para el resto de LIMs) posiblemente debido a la formación de compuestos clorados.

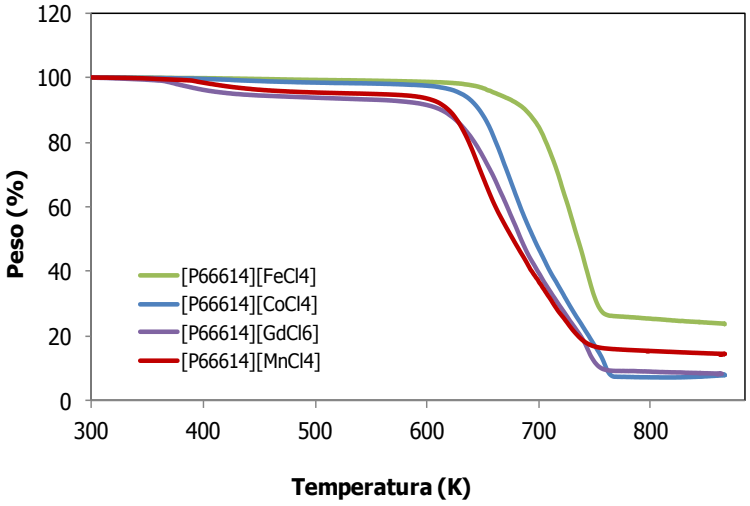


**Figura 2.3**. Análisis termogravimétrico de los LIMs.

**Tabla 2.6.** Temperaturas de descomposicion de los LIMs.

| *LIMs* | $T_{onset}$ *(K)* | *Referencia* |
|---|---|---|
| $[P_{66614}][CoCl_4]$ | 646 | Santos et al., 2013b |
| $[P_{66614}][FeCl_4]$ | 655 | Santos et al., 2013b |
| $Fe((OHCH_2CH_2)_2NH)_6(CF_3SO_3)_3$ | 533 | Anderson et al., 2010 |
| $[3C_6PC1_4][FeCl_4]$ | 623 | Deng et al., 2011 |
| $[C_2mim][FeCl_4]$ | 623 | Bäcker et al., 2011 |
| $[P_{66614}][MnCl_4]$ | 619 | Santos et al., 2013b |
| $[P_{66614}][GdCl_6]$ | 625 | Santos et al., 2013b |

*d. Solubilidad de $CO_2$*

El estudio de la solubilidad de $CO_2$ en los LIMs se realiza por métodos termogravimétricos utilizando la termobalanza TG-DTA 60H Shimadzu (Japón). La temperatura de la muestra se mide con una precisión de ± 0,1 K, mientras que la sensibilidad de la TG está en torno a 1 µg. Las condiciones de operación han sido: caudal de gas de 50 $mL.min^{-1}$, temperatura ambiente y presión atmosférica. Se ha utilizado un volumen de muestra de 30 µl en un crisol de alúmina durante 180 minutos por experimento.

La solubilidad, $S_{CO_2}$, es calculada a través de la expresión:

$$S_{CO2} = \left( \frac{p_f - pi}{p_f} \right) \cdot 100 \qquad (2.4)$$

donde $p_f$ y $p_i$ son el peso final e inicial de la muestra. Se determina el contenido de agua en la muestra mediante método de valoración Karl-Fisher, salvo en el caso del LIM $[P_{66614}][FeCl_4]$ en el cual se determina gravimétricamente pesando 1 mL antes y después de 48 horas de aplicación de vacío y calor (333 K) dando lugar a valores entre 0,0005 y 1,02 % (Albo et al., 2012).

Los resultados de solubilidad de $CO_2$ en LIMs se muestran en la Tabla 2.7. Se trata de valores de solubilidad bajos si se comparan con los publicados en bibliografía para otros LIs bajo las mismas condiciones de operación (T=298 K, P=1atm) (Shiflett et al., 2008; Shiflett et al., 2009); sin embargo, se espera que el valor de la solubilidad pueda verse modificado bajo la aplicación de un campo magnético externo.

**Tabla 2.7.** Solubilidad de $CO_2$ a 298 K.

| *LIMS* | *Solubilidad $CO_2$ (% peso)* |
|---|---|
| $[P_{66614}][CoCl_4]$ | 0,40 |
| $[P_{66614}][FeCl_4]$ | 0,50 |
| $[P_{66614}][MnCl_4]$ | 0,36 |
| $[P_{66614}][GdCl_6]$ | 0,25 |

El estudio de las propiedades fundamentales de los LIMs ha permitido obtener un conocimiento básico de los mismos (Santos et al., 2013b). En este sentido, la predicción de las propiedades físicoquímicas supone una estrategia que permitiría profundizar de una manera más amplia en su comportamiento para el desarrollo de nuevas aplicaciones. Una de las propiedades físicas más importantes de los LIs es la viscosidad, más elevada en la mayor parte de los LIs que en los disolventes orgánicos convencionales. Además, esta propiedad puede ajustarse mediante la selección de la combinación catión-anión apropiada pudiéndose obtener LIs con mayor o menor viscosidad dependiendo de los requerimientos del proceso.

## 2.2. Desarrollo y aplicación de un método de contribución de grupos para estimar la viscosidad de los líquidos iónicos magnéticos a diferentes temperaturas

La utilización de métodos de contribución de grupos es habitual en la estimación de la viscosidad en moléculas complejas (Reid et al., 1987; Gastonbonhomme et al., 1994; Sastry et al., 2000) asumiendo que las propiedades fisicoquímicas de las moléculas son el sumatorio de la contribución de sus átomos y/o fragmentos (Luis et al., 2007). Los modelos que estiman la influencia de la temperatura en la viscosidad de los LIs son muy diversos. Dentro de los más utilizados destacan: Arrhenius (Andrade, 1934), Vogel-Fulcher-Tamman (VFT) (Vogel, 1921; Fulcher, 1925), ecuación de Litovitz (Litovitz, 1952) y ecuación de Orrick-Erbar (Reid et al., 1987).

### 2.2.1. Metodología

La estimación de la viscosidad de los LIMs a diferentes temperaturas se ha llevado a cabo utilizando la ecuación de Orrick–Erbar (Gardas y Coutinho, 2008) a través del método de contribución de grupos considerando el catión trihexil (tetradecil) fosfonio, [$P_{66614}$], con diferentes longitudes de cadena y los aniones metálicos: tetraclorocobalto [$CoCl_4$], tetracloroferrato [$FeCl_4$], tetracloromanganeso [$MnCl_4$] y hexaclorogadolinio [$GdCl_6$] (Daniel et al., 2013). Los datos experimentales de partida de densidad y viscosidad a diferentes temperaturas se recogen en la Tabla 2.3 de la sección 2.1.1.

Se aplica un método de contribución de grupos tanto para el anión como el catión partiendo de la ecuación de Orrick–Erbar:

$$\ln\left(\frac{\mu}{\rho.M}\right) = n\left(A^{+} + \frac{B^{+}}{T}\right) + \left(A^{-} + \frac{B^{-}}{T}\right) \tag{2.5}$$

donde $\mu$ es la viscosidad (cP); $\rho$ la densidad (g.cm$^{-3}$); $M$ el peso molecular (g.mol$^{-1}$); $T$ la temperatura absoluta (K); $A$ y $B$ los parámetros de la ecuación de Orrick-Erbar; $n$ representa la longitud de cadena del catión; $A^{+}$ y $B^{+}$ los parámetros de contribución del catión y $A^{-}$ y $B^{-}$ los parámetros de contribución del anión.

El catión es común para todos los LIMs, pero cada uno de ellos tendrá una longitud de cadena y un anión metálico diferentes. Por lo tanto, la ecuación global 2.5 puede reescribirse como se indica:

$$\ln\left(\frac{\mu}{\rho.M}\right) = n_i\left(A + B\frac{1}{T}\right) + \sum_i\left(A_i + B_i\frac{1}{T}\right) \tag{2.6}$$

donde $n_i$ es la longitud de cadena de cada catión; *A y B* son los parámetros de contribución del catión y $A_i$ *y* $B_i$ son los parámetros de contribución del anión.

Tal y como se indica en la ecuación 2.6, la variable dependiente $\ln\left(\frac{\mu}{\rho.M}\right)$ incluye el término de la densidad. La dependencia de la densidad con la temperatura ha sido descrita en la ecuación 2.2 de la sección 2.1.1.

Se han utilizado variables normalizadas con el objetivo de evitar la influencia de los valores absolutos en la estimación de los parámetros tal y como se indica en las ecuaciones 2.7 y 2.8:

$$Y^* = \frac{-Y + \left(\left(Y_{\max} + Y_{\min}\right)/2\right)}{\left(\left(Y_{\max} - Y_{\min}\right)/2\right)} \tag{2.7}$$

$$X^* = \frac{-X + \left(\left(X_{\max} + X_{\min}\right)/2\right)}{\left(\left(X_{\max} - X_{\min}\right)/2\right)} \tag{2.8}$$

donde *X* e Y** representan la inversa de la temperatura y la viscosidad adimensional respectivamente y toman valores entre +1 y -1. $Y_{max}$ y $X_{max}$ representan los valores máximos de $\ln\left(\frac{\mu}{\rho.M}\right)$ y 1/T e $Y_{min}$ y $X_{min}$ los valores mínimos. Estos valores están recogidos en la Tabla 2.8.

**Tabla 2.8.** Variables absolutas y normalizadas para viscosidad y temperatura de los LIMs.

| *LIMs* | *T(K)* | *1/T(K$^{-1}$)* | $\ln\left(\frac{\mu}{\rho.M}\right)$ | *1/T Normalizado* | $\ln\left(\frac{\mu}{\rho.M}\right)$ *Normalizado* |
|---|---|---|---|---|---|
| | 293,15 | 0,00341 | 2,76 | -1,00 | -0,48 |
| | 298,15 | 0,00335 | 2,33 | -0,84 | -0,37 |
| $[P_{66614}][GdCl_6]$ | 303,15 | 0,00330 | 1,99 | -0,69 | -0,28 |
| | 323,15 | 0,00309 | 0,52 | -0,13 | 0,11 |
| | 373,15 | 0,00268 | -1,79 | 1,00 | 0,72 |
| | 293,15 | 0,00341 | 4,67 | -1,00 | -0,98 |
| | 298,15 | 0,00335 | 4,28 | -0,84 | -0,88 |
| $[P_{66614}][MnCl_4]$ | 303,15 | 0,00330 | 3,69 | -0,69 | -0,72 |
| | 323,15 | 0,00309 | 2,63 | -0,13 | -0,44 |
| | 373,15 | 0,00268 | -0,02 | 1,00 | 0,25 |
| | 293,15 | 0,00341 | -0,01 | -1,00 | 0,25 |
| | 298,15 | 0,00335 | -0,21 | -0,84 | 0,30 |
| $[P_{66614}][FeCl_4]$ | 303,15 | 0,00330 | -0,43 | -0,69 | 0,36 |
| | 323,15 | 0,00309 | -1,24 | -0,13 | 0,57 |
| | 373,15 | 0,00268 | -2,87 | 1,00 | 1,00 |
| | 293,15 | 0,00341 | 4,75 | -1,00 | -1,00 |
| | 298,15 | 0,00335 | 4,36 | -0,84 | -0,90 |
| $[P_{66614}][CoCl_4]$ | 303,15 | 0,00330 | 3,63 | -0,69 | -0,71 |
| | 323,15 | 0,00309 | 2,68 | -0,13 | -0,46 |
| | 373,15 | 0,00268 | 2,39 | 1,00 | -0,38 |

Las Tablas 2.9 y 2.10 definen los descriptores de los LIMs y determinan la dependencia de la contribución de cada grupo (anión y catión) en la estimación de la viscosidad.

**Tabla 2.9.** Contribución de grupos a la viscosidad adimensional.

| *Grupo* | *Descriptor molecular* |
|---|---|
| Catión | |
| *n* | Influencia del número de cadenas (1, 2 o 3) |
| *A** y *B** | Influencia del catión [$P_{66614}$]: 1 si existe y 0 si no existe |
| Anión | |
| $A_1$* y $B_1$* | Influencia del anión [$GdCl_6$]: 1 si existe y 0 si no existe |
| $A_2$* y $B_2$* | Influencia del anión [$MnCl_4$]: 1 si existe y 0 si no existe |
| $A_3$* y $B_3$* | Influencia del anión [$FeCl_4$]: 1 si existe y 0 si no existe |
| $A_4$* y $B_4$* | Influencia del anión [$CoCl_4$]: 1 si existe y 0 si no existe |
| Número de descriptores | 11 |

La viscosidad adimensional puede ser calculada siguiendo el modelo de contribución de grupos si se reescribe la ecuación 2.5 para este caso particular como sigue:

$$Y^* = n_i.\left(A^* + B^*.X^*\right) + \sum_i \left(A_i^* + B_i^*.X^*\right) \qquad (2.9)$$

**Tabla 2.10.** Viscosidad, viscosidad adimensional y descriptores de contribución de grupos.

| *LIMs* | *1/T(K$^{-1}$)* | $\ln\left(\frac{\mu}{\rho.M}\right)$ | *Y** | *n* | *A** | *B** | *A$_1$** | *A$_2$** | *A$_3$** | *A$_4$** | *B$_1$** | *B$_2$** | *B$_3$** | *B$_4$** |
|---|---|---|---|---|---|---|---|---|---|---|---|---|---|---|
| $[P_{66614}][GdCl_6]$ | | | | 3 | 1 | 1 | 1 | 0 | 0 | 0 | 1 | 0 | 0 | 0 |
| | 0,00341 | 2,76 | -0,48 | | | | | | | | | | | |
| | 0,00335 | 2,33 | -0,37 | | | | | | | | | | | |
| | 0,00330 | 1,99 | -0,28 | | | | | | | | | | | |
| | 0,00309 | 0,52 | 0,11 | | | | | | | | | | | |
| | 0,00268 | -1,79 | 0,72 | | | | | | | | | | | |
| $[P_{66614}][MnCl_4]$ | | | | 2 | 1 | 1 | 0 | 1 | 0 | 0 | 0 | 1 | 0 | 0 |
| | 0,00341 | 4,67 | -0,98 | | | | | | | | | | | |
| | 0,00335 | 4,28 | -0,88 | | | | | | | | | | | |
| | 0,00330 | 3,69 | -0,72 | | | | | | | | | | | |
| | 0,00309 | 2,63 | -0,44 | | | | | | | | | | | |
| | 0,00268 | -0,02 | 0,25 | | | | | | | | | | | |
| $[P_{66614}][FeCl_4]$ | | | | 1 | 1 | 1 | 0 | 0 | 1 | 0 | 0 | 0 | 1 | 0 |
| | 0,00341 | -0,01 | 0,25 | | | | | | | | | | | |
| | 0,00335 | -0,21 | 0,30 | | | | | | | | | | | |
| | 0,00330 | -0,43 | 0,36 | | | | | | | | | | | |
| | 0,00309 | -1,24 | 0,57 | | | | | | | | | | | |
| | 0,00268 | -2,87 | 1,00 | | | | | | | | | | | |
| $[P_{66614}][CoCl_4]$ | | | | 2 | 1 | 1 | 0 | 0 | 0 | 1 | 0 | 0 | 0 | 1 |
| | 0,00341 | 4,75 | -1,00 | | | | | | | | | | | |
| | 0,00335 | 4,36 | -0,90 | | | | | | | | | | | |
| | 0,00330 | 3,63 | -0,71 | | | | | | | | | | | |
| | 0,00309 | 2,68 | -0,46 | | | | | | | | | | | |
| | 0,00268 | 2,39 | -0,38 | | | | | | | | | | | |

### 2.2.2. Resultados

Los resultados del ajuste a la ecuación 2.9 se muestran en la Figura 2.4 y Tabla 2.11. Se observa una contribución negativa del anión en la viscosidad contrarrestándose con el efecto positivo del catión en dicha variable. En términos absolutos, existe una contribución mayor por parte del anión que del catión. Con respecto a la influencia de la temperatura, puede concluirse que la influencia del catión en la viscosidad es menor que la observada en el anión tal y como se observa en los valores A* y B* (Daniel et al., 2013).

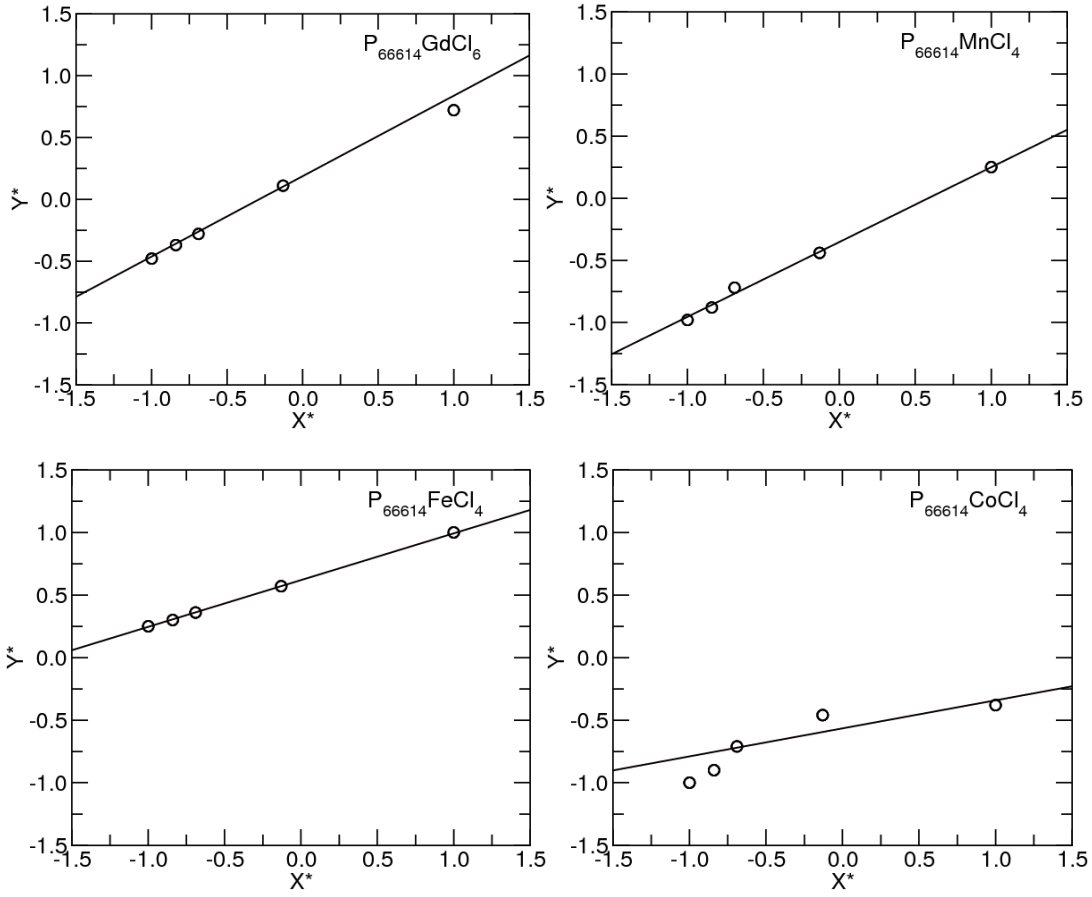


**Figura 2.4.** Ajuste de la viscosidad normalizada a la ecuación Orrick-Erbar utilizando el software Fitteia.

**Tabla 2.11.** Parámetros de contribución de grupos ajustados utilizando el modelo de Orrick-Erbar.

| *LIMs* | $A^*$ | $B^*(K)$ | $\chi^2$ |
|---|---|---|---|
| Catión | | | 28,8 |
| $[P_{66614}]$ | 0,8±0,03 | 0,07±0,06 | |
| Anión | | | |
| $[GdCl_6]$ | -2,3±0,09 | 0,45±0,19 | |
| $[MnCl_4]$ | -2,0±0,06 | 0,47±0,13 | |
| $[FeCl_4]$ | -0,21±0,07 | 0,31±0,07 | |
| $[CoCl_4]$ | -2,2±0,06 | 0,088±0,05 | |

La Figura 2.5 muestra el gráfico de paridad de la viscosidad experimental y calculada. Se obtiene un buen ajuste de los datos con un $R^2$=0,98. La Tabla 2.12 resume los parámetros estadísticos de la base de datos utilizada en el ajuste.

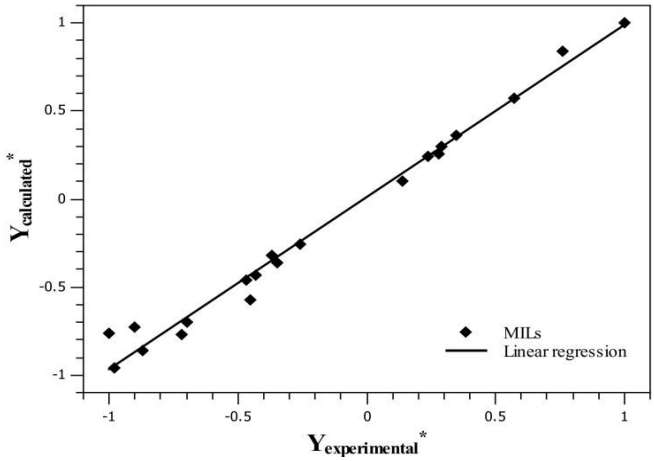


**Figura 2.5.** Viscosidad adimensional experiemental y calculada utilizando el software Fitteia.

**Tabla 2.12.** Parámetros estadísticos de la base de datos.

| | |
|---|---|
| Número de datos | 20 |
| Valor máximo (Y) | 4,75 |
| Valor mínimo (Y) | -2,87 |
| Promedio (Y) | 1,71 |
| Mediana | 2,36 |
| Desviación estándar | 2,30 |

### 2.2.3. Comparación bibliográfica

Con el objetivo de comparar los parámetros de contribución de grupos con los descritos en la bibliografía, se calculan los parámetros absolutos A y B que son recgidos en la Tabla 2.13.

**Tabla 2.13.** Valores absolutos de los parámetros de la ecuación Orrick-Erbar para la estimación de la viscosidad de los LIMs.

| *LIMs* | *A* | *B(K)* | $\chi^2$ |
|---|---|---|---|
| Catión | | | 18,3 |
| $[P_{66614}]$ | 1,48±0,08 | 975±2,7 | |
| Anión | | | |
| $[GdCl_6]$ | -22,9±0,4 | 3426±129,3 | |
| $[MnCl_4]$ | -19,8±0,02 | 4333±7,9 | |
| $[FeCl_4]$ | -14,3±0,01 | 2772±3,2 | |
| $[CoCl_4]$ | -7,56±0,95 | 581±312,2 | |

La Tabla 2.14 compara la contribución del catión de este trabajo con la bibliografía (Gardas y Coutinho, 2008). El catión fosfonio estudiado en el presente trabajo presenta una contribución inferior que los cationes imidazolio, piridinio o pirrolidinio tal y como refleja los valores del parámetro A, mientras que la inlfuencia en la temperatura (valores del parámetro B) es inferior para el catión fosfonio que para el resto.

**Tabla 2.14.** Comparación bibliográfica de los parámetros absolutos A y B de la ecuación Orrick-Erbar para el catión.

| *Catión* | *A* | *B(K)* |
|---|---|---|
| Fosfonio[a] | 1,48 | 975 |
| Imidazolio[b] | 6,56 | 1757 |
| Piridinio[b] | 6,87 | 1704 |
| Pirrolidinio[b] | 5,43 | 2233 |

[a]Daniel et al., 2013

[b]Gardas y Coutinho, 2008

La Tabla 2.15 compara la contribución del anión de este trabajo con la bibliografía. Los valores del parámetro A para [$FeCl_4$] y [$CoCl_4$] muestran la contribución más baja, mientras que el parámetro de temperatura B presenta una influencia más baja para los aniones [$CoCl_4$] y [$Tf_2N$] y una mayor influencia en los aniones [$MnCl_4$] y [Cl]. Estos resultados confirman el interés de este modelo para estimar la viscosidad y la influencia de la temperatura, pudiendo ser extendido para otras combinaciones catión-anión, así como a otras aplicaciones.

**Tabla 2.15.** Comparación bibliográfica de los parámetros absolutos A y B de la ecuación Orrick-Erbar para el anión.

| *Anión* | *A* | *B(K)* |
|---|---|---|
| [$GdCl_6$][a] | -22,9 | 3426 |
| [$MnCl_4$][a] | -19,8 | 4333 |
| [$FeCl_4$][a] | -14,3 | 2772 |
| [$CoCl_4$][a] | -7,56 | 581 |
| [$PF_6$][b] | -20,49 | 2099 |
| [$BF_4$][b] | -18,1 | 1192 |
| [$Tf_2N$][b] | -17,4 | 510 |
| [Cl][b] | -27,6 | 5458 |
| [$CH_3COO$][b] | -21,3 | 2742 |
| [$MeSO_4$][b] | -19,5 | 1733 |
| [$EtSO_4$][b] | -19,1 | 1587 |
| [$CF_3SO_3$][b] | -17,7 | 906 |

[a]Daniel et al., 2013

[b]Gardas y Coutinho, 2008

Algunas de las propiedades de los LIMs, tales como la solubilidad, la viscosidad o la tensión superficial, pueden verse afectadas por la aplicación de un campo magnético externo (Hayashi et al., 2006; Lee et al., 2007; De Pedro et al., 2010). Algunos trabajos previos mencionan la posibilidad de modular la solubilidad de benceno en el LIM [Bmim][$FeCl_4$] en función del campo magnético aplicado (Jiang et al., 2006). Del mismo modo, se ha observado una dependencia entre la concentración de mezclas binarias LIM/agua y la intensidad del campo (Lee et al., 2007) dando lugar a un incremento de la solubilidad del LIM en el medio acuoso.

En este sentido, en este trabajo se plantea evaluar la influencia de la aplicación de un campo magnético externo sobre la viscosidad de los LIMs y la permeabilidad y selectividad de gas a través de membranas soportadas con líquidos iónicos magnéticos.

## 2.3. Separación de $CO_2$ a través de membranas soportadas con líquidos iónicos magnéticos bajo la aplicación de un campo magnético externo

En una Tesis previa (Albo, 2012), se evaluó por primera vez la estabilidad, permeabilidad y selectividad de $CO_2$ a través de membranas soportadas con LIMs incluyendo metales magnéticos en su anión (MSLIMs). A partir de aquellos resultados, se plantea evaluar el comportamiento de estas nuevas membranas en presencia de una fuerza externa producida por un campo magnético. El carácter innovador de esta Tesis radica en la combinación por primera vez de membranas que incorporan LIMs basados en diferentes aniones magnéticos para el transporte selectivo de gases con la aplicación de un campo magnético externo, lo que permite el desarrollo de una nueva generación de membranas estímulo-respuesta para procesos de separación.

### 2.3.1. Estudio experimental

El estudio de la viabilidad técnica de la separación de $CO_2$ a través de MSLIMs bajo la aplicación de un campo magnético externo ha sido realizado en el Laboratorio de Ingeniería de Membranas del Departamento de Química en la *Faculdade de Ciências e Tecnología de la Universidade Nova de Lisboa (Portugal)*, bajo la supervisión del profesor João G. Crespo.

#### *a. Preparación de MSLIMs*

Las MSLIMs se han preparado utilizando un soporte polimérico comercial (Millipore Corporation). Se trata de un soporte hidrófobo de fluoruro de polivinilideno (PVDF) con un tamaño de poro de 0,22 µm y un espesor promedio de 125 µm. El material de soporte ha sido seleccionado debido a la elevada resistencia química y por su estabilidad en combinación con LIs (Neves et al., 2010). El procedimiento experimental de preparación ha sido descrito previamente (Albo et al., 2012; Santos et al., 2013a). Básicamente, se introduce el soporte microporoso a vacío durante una hora con el objetivo de eliminar el aire y/o agua que pudiesen contener los poros, facilitando así el posterior mojado del soporte. A continuación, se extienden gotas de líquido iónico sobre la superficie de la membrana, utilizando una jeringa, manteniendo en todo momento el vacío en el interior del compartimento. Finalmente, se elimina el exceso de líquido sobre la superficie de la membrana. El incremento en peso y espesor de la membrana se mide antes y después del proceso de inmovilización mostrando un incremento del 52,2-54,3% y

6,9-11,1% de peso y espesor respectivamente después de la inmovilización, dependiendo de la combinación de membrana microporosa-LIM estudiada (Albo et al., 2012). Los estudios de estabilidad llevados a cabo en una celda de filtración frontal (Amicon 8010) hasta 2 bares de presión, confirman que las membranas son estables hasta 1,5 bares, lo que asegura su operación en los valores de presión del proceso (Albo et al., 2012).

### *b. Sistema de permeación de gases*

El esquema del sistema experimental para el estudio de permeabilidad de gases a través de MSLIMs se muestra en la Figura 2.6. Este sistema está compuesto por una celda de PVDF (Micrux Technologies, España) con dos compartimentos idénticos separados por la membrana líquida soportada. El área efectiva de membrana es de 12,6 $cm^2$. El gas de alimentación ($CO_2$, $N_2$ o aire) es introducido en ambos compartimentos (alimentación y permeado) y después de la apertura de la salida del compartimento de permeado se establece una fuerza impulsora de 0,45 bar, lo que se traduce en un flujo a través de la membrana. Los cambios de presión en ambos compartimentos con el tiempo son registrados mediante transductores de presión (Omega, Reino Unido). En el Apéndice A se recoge un esquema detallado del diseño de la celda para realizar los experimentos de permeación en presencia de campo magnético.

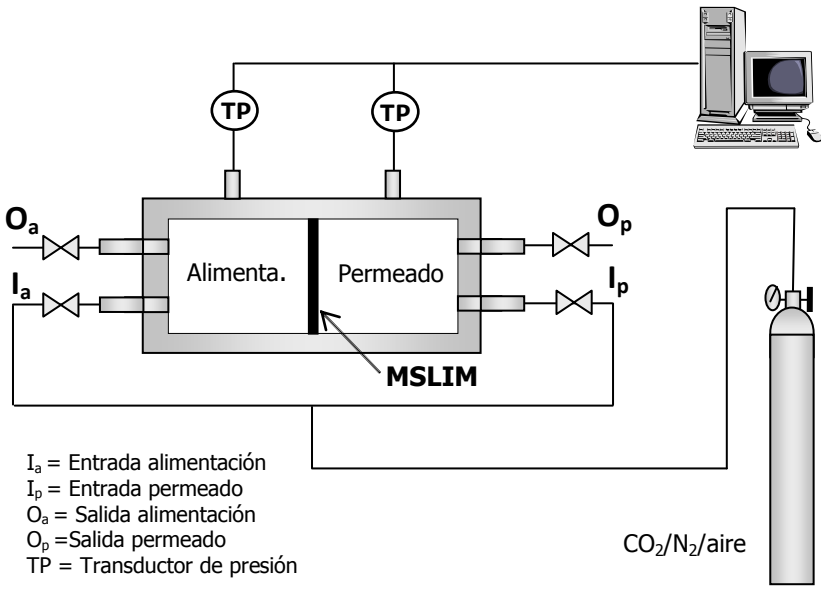


**Figura 2.6.** Sistema experimental para el estudio de permeación de gases.

La influencia de aplicación de un campo magnético externo en la separación de $CO_2$ se ha llevado a cabo utilizando un electroimán GMW Dipole Electromagnet (Modelo 3473-70,EEUU), que proporciona un campo magnetico de hasta 2,5 Tesla con una distancia entre los polos de 0 a 100 mm. Los experimentos de permeación se llevaron a cabo utilizando la celda en posición vertical con los poros de la membrana situados perpendicularmente a los polos del electroimán, aplicándose un campo magnético uniforme sobre toda la superficie de la membrana (Santos et al., 2013a).

En la Figura 2.7 se muestra una fotografía de la instalación experimental construida en el *Departamento de Química, Faculdade de Ciências e Tecnologia, Universidade Nova de Lisboa*.

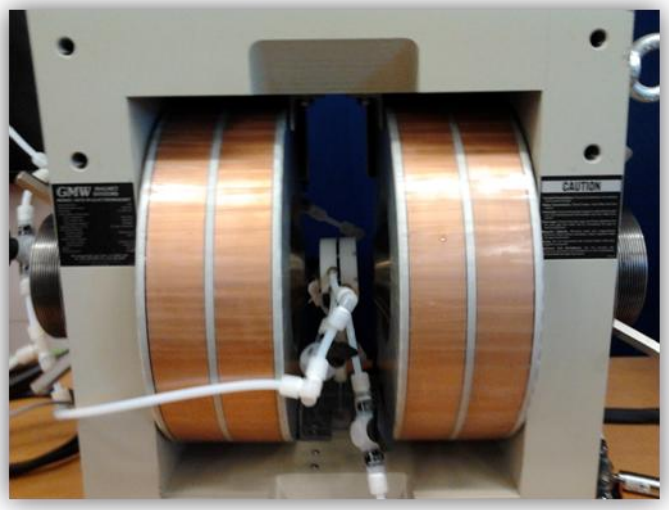


**Figura 2.7.** Imagen de la instalación experimental.

La permeabilidad del gas a través de la membrana se calcula a través de la presión registrada en los compartimentos de alimentación y permeado, según la ecuación (Cussler, 1997):

$$ln\left(\frac{\left[p_{alim}-p_{perm}\right]_0}{\left[p_{alim}-p_{perm}\right]}\right)=ln\left(\frac{\Delta p_0}{\Delta p}\right)=\frac{D\cdot H\cdot\beta}{\delta}\cdot t \qquad (2.10)$$

donde $p_{alim}$ y $p_{perm}$ son las presiones en los compartimentos de alimentación y permeado (Pa), respectivamente; $D$ la difusividad ($m^2.s^{-1}$); $H$ el coeficiente de partición (-); $\beta$ el factor geométrico que toma un valor de 118,96 $m^{-1}$; $t$ el tiempo (s); y $\delta$ el espesor de la membrana (m). Los valores de presión pueden ser representados como $\ln(\Delta p_0.\Delta p^{-1})$, frente $t$, y la permeabilidad del gas se obtiene de la pendiente mientras que la selectividad ideal se calcula como la relación de permeabilidades de dos gases puros.

### 2.3.2. Resultados

Se ha evaluado la influencia de la aplicación de un campo magnético externo sobre la permeabilidad y selectividad de $CO_2/N_2$. Los experimentos han sido realizados en un rango de intensidad de campo magnético de 0 a 1,5 Tesla a una temperatura constante de 298 K siendo la permeabilidad calculada de acuerdo a la ecuación 2.10. La aplicación de un campo magnético externo incrementa ligeramente la permeabilidad (4,1-21,6%) sin mostrar ningún tipo de influencia en la selectividad $CO_2/N_2$ y $CO_2$/aire. La Tabla 2.16 muestra el máximo incremento de permeabilidad alcanzado a 1,5 Tesla (Santos et al., 2013a).

**Tabla 2.16.** Máximo incremento de la permeabilidad a 1,5 Tesla.

| *MSLIMs* | *Gas* | *P(barrers)* | | *ΔP* | $P_{CO2}/P_{N2}$ | | $P_{CO2}/P_{aire}$ | |
|---|---|---|---|---|---|---|---|---|
| | | *0 Tesla* | *1,5 Tesla* | *(%)* | *0 Tesla* | *1,5 Tesla* | *0 Tesla* | *1,5Tesla* |
| | $CO_2$ | 117,9±4,2 | 124,1±5,1 | 5,2 | | | | |
| $[P_{66614}][CoCl_4]$ | $N_2$ | 4,9±0,2 | 5,3±0,2 | 5,6 | 23,7 | 23,6 | 14,1 | 14,2 |
| | Aire | 8,4±0,3 | 8,7±0,4 | 4,1 | | | | |
| | $CO_2$ | 161,3±4,1 | 177,8±4,3 | 10,2 | | | | |
| $[P_{66614}][MnCl_4]$ | $N_2$ | 4,1±0,1 | 4,7±0,2 | 13,6 | 39,2 | 38,1 | 26,5 | 26,4 |
| | Aire | 6,1±0,3 | 6,7±0,3 | 10,7 | | | | |
| | $CO_2$ | 198,4±3,9 | 232,2±3,6 | 17,0 | | | | |
| $[P_{66614}][FeCl_4]$ | $N_2$ | 8,0±0,2 | 9,3±0,2 | 15,9 | 24,8 | 25,0 | 20,2 | 19,9 |
| | Aire | 9,8±0,4 | 11,6±0,3 | 18,8 | | | | |
| | $CO_2$ | 198,8±3,5 | 241,8±3,2 | 21,6 | | | | |
| $[P_{66614}][GdCl_6]$ | $N_2$ | 5,7±0,2 | 6,9±0,2 | 21,2 | 34,6 | 34,7 | 19,1 | 19,3 |
| | Aire | 10,4±0,3 | 12,5±0,4 | 20,5 | | | | |

Con el objetivo de evaluar el rendimiento en la separación $CO_2/N_2$ se ha utilizado como referencia el *límite máximo* establecido por Robeson (Robeson, 2008) para membranas poliméricas a partir de datos disponibles en la bibliografía. De modo que, los resultados por encima del *límite máximo* se pueden considerar una mejora sobre el estado actual del arte. Los resultados experimentales obtenidos en este trabajo mostrados en la Figura 2.8 están por debajo del *límite máximo*, debido a que, a pesar de existir una mejora en el rendimiento de la separación como consecuencia del aumento de la permeabilidad en presencia de un campo magnético externo, la selectividad ideal no se ve afectada.

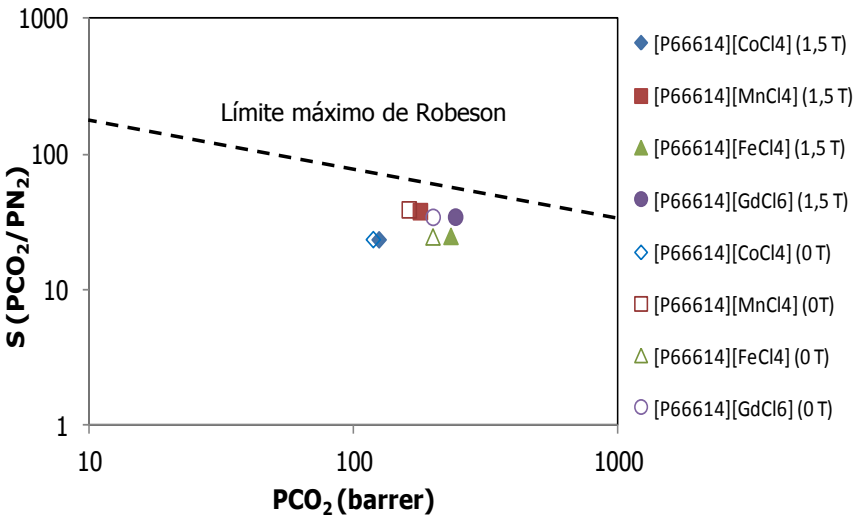


**Figura 2.8.** Límite máximo de Robeson para la separación $CO_2/N_2$ (1 Barrer = $10^{-10}$ $cm^3$ (STP).cm.$cm^{-2}$ $s^{-1}$.$cmHg^{-1}$).

*a. Permeabilidad-viscosidad en ausencia de campo magnético*

Scovazzo (Scovazzo et al., 2009) propuso una relación entre la permeabilidad de $CO_2$ y la viscosidad de los LIs utilizando los datos de la bibliografía recogidos en la Tabla 2.17. Estudió un rango de viscosidades entre 25 y 3000 cP, obteniendo una pendiente de -0,388. El presente trabajo, extiende esta correlación incluyendo los LIMs con valores de viscosidad entre 749 y 110060 cP a 298 K, obteniéndose una pendiente de -0,278 tal y como aparece en la Figura 2.9.

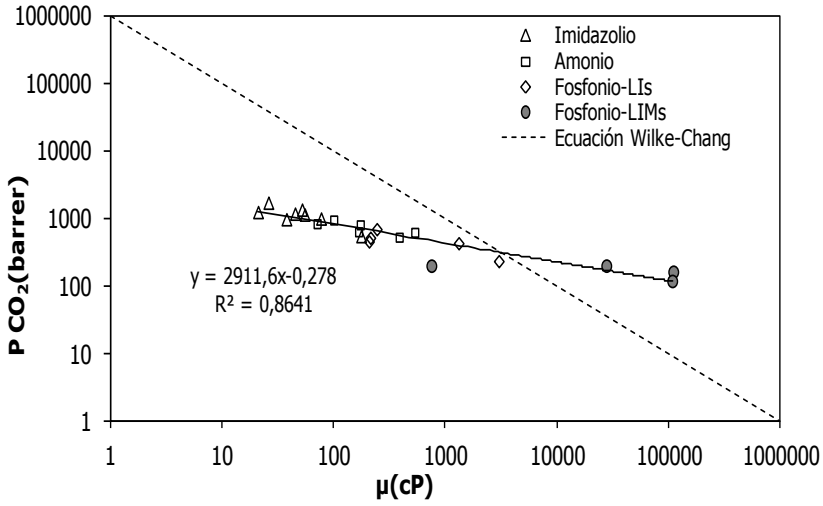


**Figura 2.9.** Correlación de la permeabilidad de $CO_2$ frente a la viscosidad.

**Tabla 2.17.** Valores de permeabilidad-viscosidad recogidos en bibliografía.

| *LIs* | *Permeabilidad $CO_2$ (barrers)* | *Viscosidad (cP)* |
|---|---|---|
| Imidazolio[a] | | |
| [Emim][$Bf_4$] | 968,5 | 37,7 |
| [Emim][$Tf_2N$] | 1702,4 | 26 |
| [Bmim][$Pf_6$] | 544,3 | 176 |
| [Emim][dca] | 1237,3 | 21 |
| [Bmim][$Tf_2N$] | 1344,3 | 52 |
| [Emim][TfO] | 1171,4 | 45 |
| [$C_6$mim][$Tf_2N$] | 1135,8 | 55 |
| [Bmim][BETI] | 991,4 | 77 |
| Amonio[b] | | |
| [$N_{1444}$][$Tf_2N$] | 523,9 | 386 |
| [$N_{4111}$][$Tf_2N$] | 830,5 | 71 |
| [$N_{6111}$][$Tf_2N$] | 943,2 | 100 |
| [$N_{10111}$][$Tf_2N$] | 800,4 | 173 |
| [$N_{1888}$][$Tf_2N$] | 619,4 | 532 |
| [$N_{6222}$][$Tf_2N$] | 630,3 | 167 |
| Fosfonio (LIs)[c] | | |
| [$P_{66614}$][Cl] | 426,6 | 1316 |
| [$P_{44414}$][DBS] | 231,7 | 3011 |
| [$P_{66614}$][$Tf_2N$] | 689,1 | 243 |
| [$P_{66614}$][dca] | 513,7 | 213 |
| [$P_{44414}$][DEP] | 453,4 | 207 |
| Fosfonio (LIMs)[d] | | |
| [$P_{66614}$][$GdCl_6$] | 198,8 | 27650 |
| [$P_{66614}$][$MnCl_4$] | 161,3 | 110060 |
| [$P_{66614}$][$FeCl_4$] | 198,4 | 749 |
| [$P_{66614}$[[$CoCl_4$] | 117,9 | 107700 |

[a]Scovazzo, 2009
[b]Condemarin y Scovazzo, 2009
[c]Ferguson y Scovazzo, 2007
[d]Santos et al., 2013a

*b. Influencia del campo magnético externo sobre la permeabilidad a través de MSLIMs*

La permeabilidad de gas se incrementa en presencia de un campo magnético externo en función de la susceptibilidad magnética de los LIMs, que varía de 2,10 a 6,51 emu.K.mol$^{-1}$, tal y como se muestra en la Figura 2.10. Se espera un aumento del 3,27% en la permeabilidad por

cada unidad de susceptibilidad magnética al aplicar un campo magnético máximo de 1,5 Tesla. Realizando un análisis comparativo a todos los LIMs se observa un mayor efecto en la permeabilidad en los LIMs de mayor susceptibilidad magnética como aparece reflejado en la Figura 2.11.

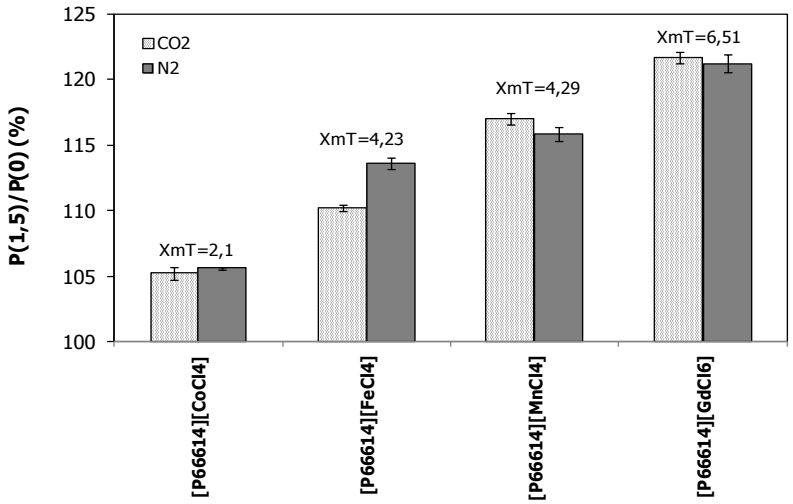


**Figura 2.10.** Dependencia de la permeabilidad con la susceptibilidad magnética.

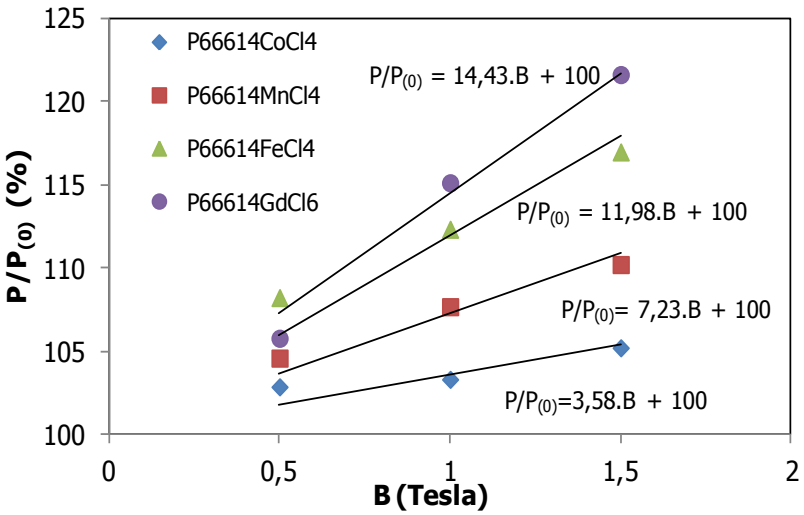


**Figura 2.11.** Permeabilidad de $CO_2$ a diferente intensidad de campo.

### *c. Correlación permeabilidad –viscosidad en presencia de campo magnético*

Para evaluar la influencia de la aplicación de un campo magnético externo sobre la viscosidad de los LIMs estudiados, se mide la viscosidad utilizando diferentes viscosímetros de vidrio capilar (Cannon-Ubbelohde, EEUU) de diferentes diámetros en función de la viscosidad de cada LIM (Modelos 9721-R95; 9721-R80 y 9721-R89). Los resultados de viscosidad en presencia de campo magnético entre 0 y 2 Tesla se recogen en la Tabla 2.18.

**Tabla 2.18.** Viscosidad de los LIMs a diferente intensidad de campo entre 0 y 2 Tesla.

| | *μ (cP)* | | | | |
|---|---|---|---|---|---|
| *LIMs* | *0 Tesla* | *0,5 Tesla* | *1Tesla* | *1,5 Tesla* | *2 Tesla* |
| $[P_{66614}][CoCl_4]$ | 107700 | 95230 | 94170 | 93510 | 88950 |
| $[P_{66614}][MnCl_4]$ | 110060 | 108360 | 107360 | 105730 | 100190 |
| $[P_{66614}][FeCl_4]$ | 749 | 719 | 702 | 693 | 672 |
| $[P_{66614}][GdCl_6]$ | 27650 | 27530 | 25600 | 24290 | 23550 |

Se ha representado la relación entre la permeabilidad y viscosidad a diferentes intensidades de campo de manera adimensional, referidas a los resultados en ausencia de campo magnético, tal y como muestra la Figura 2.12.

El ajuste lineal a los datos muestra un valor de la pendiente muy próximo a la unidad lo que sugiere una dependencia inversa según el modelo de Wilke Chan (Wilke y Chang, 1955). El producto de la permeabilidad y la viscosidad es una constante especifica para cada MSLIM e independiente del campo magnético aplicado. Los valores de estas constantes se recogen en la Tabla 2.19.

**Tabla 2.19.** Producto permeabilidad-viscosidad.

| *LIMs* | *$C.10^{10}$ (kg.m.$s^{-2}$)* |
|---|---|
| $[P_{66614}][CoCl_4]$ | 105 |
| $[P_{66614}][MnCl_4]$ | 147 |
| $[P_{66614}][FeCl_4]$ | 1,23 |
| $[P_{66614}][GdCl_6]$ | 45,6 |

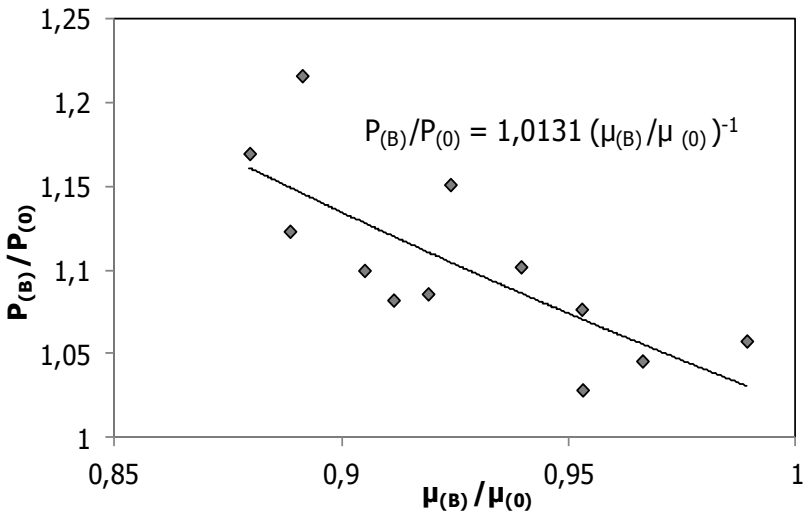


**Figura 2.12.** Correlación permeabilidad - viscosidad en presencia de campo.

La aplicación de un campo magnético externo provoca una variación en la viscosidad que causa una modulación de la permeabilidad de gas. Estos resultados innovadores abren la posibilidad a nuevas aplicaciones de separación en presencia de en campo magnético externo, como la modulación de la permeabilidad en MSLIMs.

## 2.4. Separación de $CO_2$ a través de membranas soportadas con líquidos iónicos basados en el anión acetato

Una vez evaluado el comportamiento de las MSLIMs en presencia de un campo magnético externo, se procede al estudio de la separación $CO_2/N_2$ a través de membranas soportadas con líquidos iónicos (MSLIs) basados en el anión acetato (Santos et al., 2014). La selección de estos LIs está motivada por la elevada solubilidad de $CO_2$ que presentan los LIs que contienen dicho anión (Shiflett et al., 2008; Yokozeki et al., 2008; Shiflett et al., 2009). Además, la utilización de LIs poliméricos se consiguen capacidades de absorción de $CO_2$ mayores que con los LIs monoméricos debido a una mayor velocidad de absorción y desorción (Supasitmongkol, 2010). Los valores de solubilidad más elevados han sido alcanzados en polímero iónico basado en el catión vinilbenzil trimetil amonio, [Vbtma], estudiado recientemente en la bibliografía en combinación con diferentes aniones (Supasitmongkol, 2010; Bhavsar, 2012). Por ello, con la utilización de dos LIs comerciales basados en el anión de acetato y otro líquido iónico polimérico que combine el anión acetato y el catión [Vbtma] se pretenden alcanzar los mayores valores posibles de permeabilidad y selectividad para la separación $CO_2/N_2$.

### 2.4.1. Estudio experimental

La viabilidad técnica de la separación de $CO_2$ a través de MSLIs basados en el anión acetato se ha llevado a cabo a través de un sistema experimental diseñado e instalado en el laboratorio 538 del *Departamento de Ingenierías Química y Biomolecular de la Universidad de Cantabria*.

*a. Materiales*

Los LIs 1-etil-3-metil imidazolio acetato [Emim][Ac] y 1-butil-3-metil imidazolio acetato [Bmim][Ac] han sido suministrados por Sigma Aldrich, mientras que el (vinilbenzil) trimetil amonio acetato [Vbtma][Ac] ha sido sintetizado en la *Faculdade de Farmácia, Universidade de Lisboa (Portugal)* (Santos et al., 2014).

Las propiedades térmicas de los LIs han sido evaluadas utilizando la termobalanza TG-DTA 60H Shimadzu (Japón) y atmósfera de nitrógeno en el rango de temperaturas desde temperatura ambiente hasta 873 K con una velocidad de calentamiento de 5 $K.min^{-1}$. La densidad de los LIs ha sido determinada utilizando un densímetro automático (Mettler Toledo DM40) a 298 K. Sus principales características están recogidas en la Tabla 2.20.

**Tabla 2.20.** Propiedades de los LIs estudiados.

| *LIs* | *Estructura* | *Peso molecular* *(g.mol$^{-1}$)* | *Densidad* *(g.cm$^{-3}$,298K)* | *Viscosidad* *(cP, 298K)* | *$T_{onset}$* *(K)* |
|---|---|---|---|---|---|
| [Emim][Ac] | 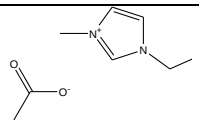 | 170,21 | 1,098 | 143,61[a] | 481,35 |
| [Bmim][Ac] | 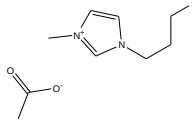 | 198,26 | 1,052 | 440[b] | 496,93 |
| [Vbtma][Ac] | 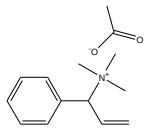 | 235,32 | 1,015 | - | 445,1 |

[a]Freire et al., 2011

[b]Maginn, 2005

Las MSLIs de acetato se han preparado utilizando un soporte polimérico comercial (Millipore Corporation). Se trata de un soporte hidrófobo de PVDF con un tamaño de poro de 0,22 μm y un espesor promedio de 125 μm. El procedimiento experimental de preparación es análogo descrito para las MSLIMs en el apartado 2.3.

*b. Sistema de permeación de gases*

La Figura 2.13 es una fotografía del sistema experimental instalado en laboratorio 538 del *Departamento de Ingenierías Química y Biomolecular de la Universidad de Cantabria* para llevar a cabo los estudios de permeación.

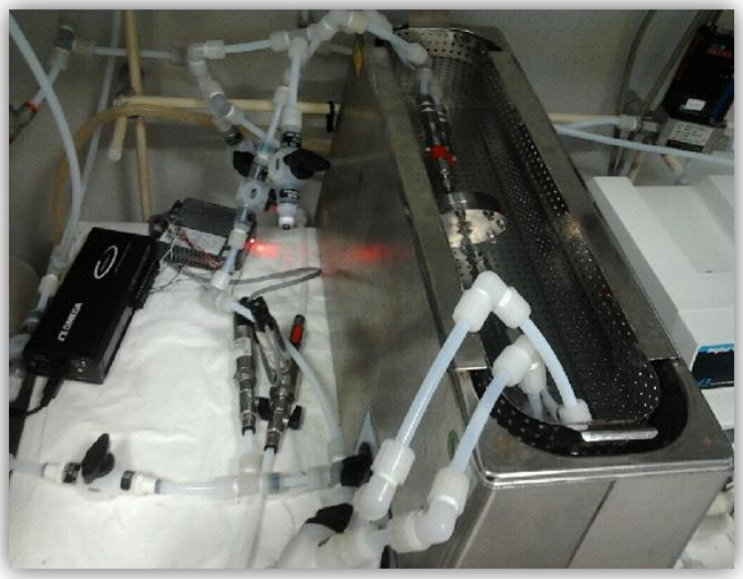

**Figura 2.13.** Imagen de la instalación experimental.

El sistema de permeación es análogo al descrito en el apartado 2.3.1., con tan solo dos diferencias significativas:

- La celda de permeación en este caso es de acero con un área efectiva de membrana de 14,05 $cm^2$ y un factor geométrico $\beta$=1188,9 $m^{-1}$.
- La temperatura se mantiene constante utilizando un baño termostatizado.

La metodología utilizada en el cálculo de la permeabilidad es la misma que se describe en el apartado 2.3.1.

*c. Medida de la solubilidad*

La medida de la solubilidad de $CO_2$ en los LIs se realiza por métodos termogravimétricos utilizando la termobalanza TG-DTA 60H Shimadzu (Japón). La temperatura de la muestra se mide con una precisión de ± 0,1 K, mientras que la sensibilidad de la TG es sobre 1 µg. Las condiciones de operación han sido un caudal de gas de 50 $mL.min^{-1}$ en un volumen de muestra de 30 µl en un crisol de alúmina durante 180 minutos. El rango de temperaturas en el que se ha trabajado es el comprendido entre 298 y 333 K.

*d. Cálculo de la difusividad*

Una vez determinada la permeabilidad de gas a través de la membrana y la solubilidad en el LI es posible calcular la difusividad efectiva, considerando que el transporte tiene lugar a través del mecanismo solución-difusión descrito en la ecuación 2.11:

$$P_{SILM} = S \cdot D_{eff} \tag{2.11}$$

donde $P_{SILM}$ es la permeabilidad a través de la membrana en barrers; $S$ la solubilidad de gas en $cm^3$(STP).$cmHg^{-1}$ y $D_{eff}$ el coeficiente de difusividad efectiva en $cm^2.s^{-1}$. Consecuentemente, se obtiene una difusividad efectiva dependiente del soporte utilizado (porosidad y tortuosidad).

### 2.4.2. Resultados

*a. Permeabilidad*

Se ha estudiado el efecto de la temperatura en el rango de 298 a 333 K en la permeabilidad de $CO_2$ y $N_2$, así como en la selectividad ideal $CO_2/N_2$. Tal y como se encuentra recogido en la Tabla 2.21, los valores de permeabilidad obtenidos varían de 852 a 2114 barrers, mientras que las selectividades varían de 26 a 39. Se observa un incremento en la permeabilidad de gas al aumentar la temperatura, mientras que la selectividad disminuye con la temperatura, tal y como se muestra en la Figura 2.14. Las MSLIs estudiadas basadas en el anión de acetato exhiben valores de permeabilidad elevados en comparación con los valores de permeabilidad recopilados de la bibliografía en membranas poliméricas generalmente por debajo de los 1000 barrers (Scovazo et al., 2004; Scovazzo et al., 2009; Bara et al., 2009; Cserjési et al., 2010; Neves et al., 2010; Jindaratsamee et al., 2011). Los resultados están en concordancia con los reportados en bibliografía (Shi et al., 2012) para MSLIs soportadas con el LI [Emim][Ac] para la separación $CO_2/H_2$, variando la permeabilidad de $CO_2$ entre 1325 y 3701 barrers en un rango de temperaturas de 310 a 373 K.

**Tabla 2.21.** Permeabilidad de $CO_2$ y $N_2$ a través de MSLIs.

| *LIs* | *T (K)* | *298,15* | *303,15* | *313,15* | *323,15* | *333,15* |
|---|---|---|---|---|---|---|
| [Emim][Ac] | $P_{CO2}$ (barrer) | 878,8 | 1118,1 | 1329,0 | 1721,3 | 2064,9 |
| | $P_{N2}$ (barrer) | 26,1 | 32,5 | 41,3 | 58,3 | 78,1 |
| | $P_{CO2}/P_{N2}$ | 33,7 | 34,4 | 32,2 | 29,5 | 26,4 |
| [Bmim][Ac] | $P_{CO2}$ (barrer) | 851,9 | 1005,3 | 1269,2 | 1601,5 | 1940,9 |
| | $P_{N2}$ (barrer) | 24,6 | 29,5 | 37,8 | 50,7 | 65,3 |
| | $P_{CO2}/P_{N2}$ | 34,6 | 34,1 | 33,6 | 31,6 | 29,7 |
| [Vbtma][Ac] | $P_{CO2}$ (barrer) | 1100 | 1305,6 | 1536,2 | 1828,3 | 2114,2 |
| | $P_{N2}$ (barrer) | 28,2 | 36,1 | 48,3 | 61,8 | 77,5 |
| | $P_{CO2}/P_{N2}$ | 39,0 | 36,2 | 31,8 | 29,6 | 27,3 |

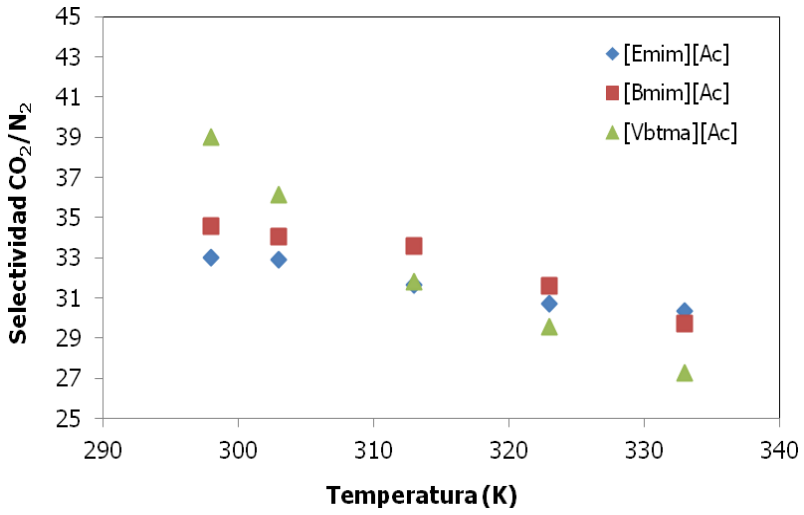


**Figura 2.14.** Influencia de la temperatura en la selectividad $CO_2/N_2$.

Se ha comparado el comportamiento en la separación $CO_2/N_2$ de las MSLIs conteniendo el anión de acetato con las membranas poliméricas utilizando como referencia el *límite máximo* de Robeson (Robeson, 2008). Los resultados experimentales sitúan estas MSLIs muy cerca del *límite máximo*, lo que supone que exhiben un mejor rendimiento que muchas membranas poliméricas estudiadas previamente tal y como aparece en la Figura 2.15.

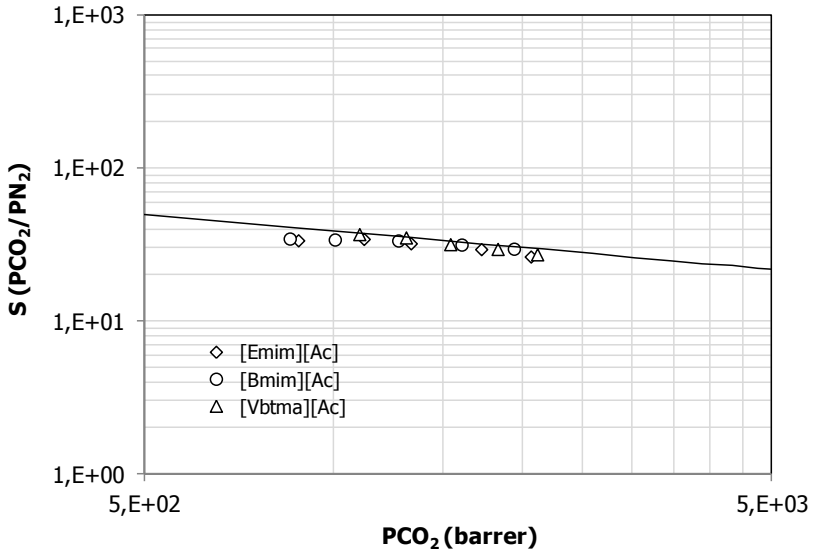


**Figura 2.15.** Límite máximo de Robeson para la separación $CO_2/N_2$.

Las energías de activación para la permeabilidad de $CO_2$ y $N_2$ pueden calcularse describiendo la influencia de la temperatura en la permeabilidad de gas a través de una ecuación tipo Arrhenius, tal y como se muestra en la Figura 2.16:

$$P = P_0 \exp\left(-E_p / RT\right) \tag{2.12}$$

donde $P_0$ es el factor pre-exponencial y $E_P$ la energía de activación para la permeabilidad.

Las energías de activación han sido recogidas en la Tabla 2.22 siendo mayores para el $N_2$ que para el $CO_2$, lo que está justificado por la influencia negativa de la temperatura en la selectividad. Los valores de energías de activación obtenidos están en concordancia con los valores de la bibliografía (Ilconich et al., 2007; Adibi et al., 2011; Iarikov et al., 2011; Shi et al., 2012), siendo las principales diferencias atribuibles a la porosidad del tipo de material del soporte (75-80% en materiales poliméricos frente al 25-50% en soportes inorgánicos).

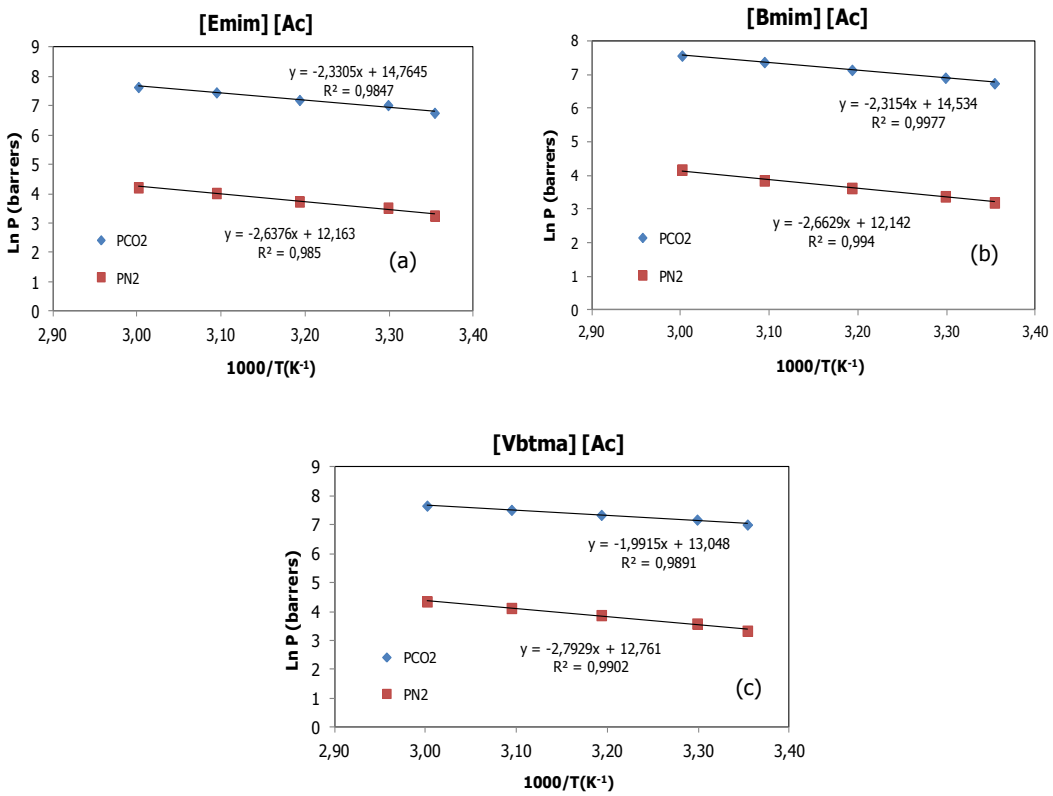


**Figura 2.16.** Logaritmo de la permeabilidad de $CO_2$ y $N_2$ a través de [Emim][Ac] (a), [Bmim][Ac] (b) y [Vbtma][Ac] (c) frente a la inversa de la temperatura. La linea continua se corresponde con la regresión lineal de los datos.

**Tabla 2.22.** Energías de activación para la permeabilidad, $E_P$.

| *Soporte* | *Gas* | *LIs* | *$E_p$(kJ.mol$^{-1}$)* | *Referencia* |
|---|---|---|---|---|
| Fluoruro de polivinilideno (PVDF) | $CO_2$ | [Emim][Ac] | 19,37 | Santos et al., 2014 |
| Fluoruro de polivinilideno (PVDF) | $N_2$ | [Emim][Ac] | 25,32 | Santos et al., 2014 |
| Fluoruro de polivinilideno (PVDF) | $CO_2$ | [Bmim][Ac] | 19,25 | Santos et al., 2014 |
| Fluoruro de polivinilideno (PVDF) | $N_2$ | [Bmim][Ac] | 22,13 | Santos et al., 2014 |
| Fluoruro de polivinilideno (PVDF) | $CO_2$ | [Vbtma][Ac] | 16,55 | Santos et al., 2014 |
| Fluoruro de polivinilideno (PVDF) | $N_2$ | [Vbtma][Ac] | 23,22 | Santos et al., 2014 |
| Polisulfona (PSF) | $CO_2$ | [Hmim][$Tf_2N$] | 17,38 | Ilconich et al., 2007 |
| Polisulfona (PSF) | He | [Hmim][$Tf_2N$] | 5,35 | Ilconich et al., 2007 |
| alumina | $CO_2$ | [Hmim][$Tf_2N$] | 8,03 | Adibi et al.,2011 |
| alumina | $CH_4$ | [Hmim][$Tf_2N$] | 29,35 | Adibi et al.,2011 |
| Polisulfona (PSF) | $CO_2$ | [Emim][Ac] | 25,47 | Shi et al., 2012 |
| Polisulfona (PSF) | $H_2$ | [Emim][Ac] | 16,02 | Shi et al., 2012 |
| α-alumina | $CO_2$ | [Bmim][$Bf_4$] | 7,5 | Iarikov et al.,2011 |
| α-alumina | $CH_4$ | [Bmim][$Bf_4$] | 20 | Iarikov et al.,2011 |

*b. Solubilidad*

Se ha evaluado la solubilidad de $CO_2$ en los tres LIs basados en el anión de acetato. Los resultados experimentales se muestran en la Tabla 2.23. Los valores de solubilidad están en concordancia con los reportados en bibliografía para [Emim][Ac] y [Bmim][Ac] en las mismas condiciones experimentales (Shiflett et al., 2008; Yokozeki et al., 2008; Shiflett et al., 2009).

**Tabla 2.23.** Solubilidad de $CO_2$ en los LIs de acetato en fracción molar.

| *T(K)* | *LIs* | | |
|---|---|---|---|
| | *[Emim][Ac]* | *[Bmim][Ac]* | *[Vbtma][Ac]* |
| 298,15 | 0,267 | 0,273 | 0,351 |
| 303,15 | 0,257 | 0,255 | 0,325 |
| 313,15 | 0,231 | 0,225 | 0,283 |
| 323,15 | 0,212 | 0,195 | 0,241 |
| 333,15 | 0,189 | 0,171 | 0,210 |

La dependencia de la solubilidad con la temperatura se describe mediante la ecuación de van´t Hoff :

$$S = S_0 \exp\left(-\Delta H_s / RT\right) \tag{2.13}$$

donde $S_0$ es el factor pre-exponencial y $\Delta H_s$ la entalpía molar parcial de absorción.

A partir de la Figura 2.17, donde se representa el logaritmo de la solubilidad de $CO_2$ frente a la inversa de la temperatura, se calcula la entalpía molar parcial de absorción que se recoge en la Tabla 2.24. Los valores negativos de la entalpía se corresponden con el comportamiento exotérmico del proceso.

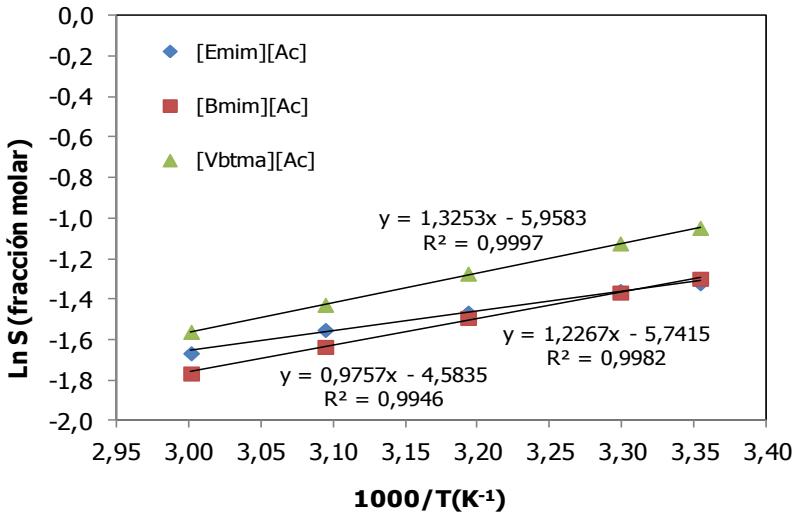


**Figura 2.17.** Logaritmo de la solubilidad de $CO_2$ frente a la inversa de la temperatura. La linea continua se corresponde con la regresión lineal de los datos.

**Tabla 2.24.** Entalpías de absorción para la solubilidad, $\Delta H_s$.

| *LIs* | *ΔHs (kJ.mol$^{-1}$)* | *Referencia* |
|---|---|---|
| [Emim][Ac] | -8,29 | Santos et al., 2014 |
| [Bmim][Ac] | -10,19 | Santos et al., 2014 |
| [Vbtma][Ac] | -11,02 | Santos et al., 2014 |
| [Hmim][$Tf_2N$] | -11,19 | Ilconich et al., 2007 |
| [Bmim][$Pf_6$] | -14,30 | Anthony et al., 2005 |
| [Bmim][$Pf_4$] | -13,90 | Anthony et al., 2005 |
| [Bmim][$Tf_2N$] | -12,50 | Anthony et al., 2005 |
| [MeBuPyrr][$Tf_2N$] | -11,90 | Anthony et al., 2005 |
| [Bmim][$Pf_6$] | -16,10 | Cadena et al., 2004 |
| [Bmmim][$Pf_6$] | -13,00 | Cadena et al., 2004 |
| [Bmim][$Pf_4$] | -15,90 | Cadena et al., 2004 |
| [Bmmim][$Bf_4$] | -14,50 | Cadena et al., 2004 |
| [Emim][$Tf_2N$] | -14,20 | Cadena et al., 2004 |
| [Emmim][$Tf_2N$] | -14,70 | Cadena et al., 2004 |

### *c. Difusividad*

La Tabla 2.25, muestra la permeabilidad en $cm^2.s^{-1}$ y la solubilidad adimensional calculadas como se indica en el Apéndice B, así como los coefcientes de difusión para el $CO_2$ en $cm^2.s^{-1}$ para cada uno de los tres LIs de acetato estudiados.

**Tabla 2.25.** Valores calculados de difusividad

| *LIs* | *T (K)* | *298,15* | *303,15* | *313,15* | *323,15* | *333,15* |
|---|---|---|---|---|---|---|
| [Emim][Ac] | $10^5$P ($cm^2.s^{-1}$) | 0,73 | 0,94 | 1,16 | 1,55 | 1,91 |
| | H(-) | 0,0237 | 0,0244 | 0,0263 | 0,0288 | 0,0306 |
| | $10^7$D ($cm^2.s^{-1}$) | 1,73 | 2,3 | 3,05 | 4,33 | 5,86 |
| [Bmim][Ac] | $10^5$P ($cm^2.s^{-1}$) | 0,71 | 0,85 | 1,11 | 1,44 | 1,80 |
| | H(-) | 0,0282 | 0,0299 | 0,0329 | 0,037 | 0,0412 |
| | $10^7$D ($cm^2.s^{-1}$) | 1,99 | 2,53 | 3,64 | 5,33 | 7,41 |
| [Vbtma][Ac] | $10^5$P ($cm^2.s^{-1}$) | 0,91 | 1,10 | 1,34 | 1,64 | 1,96 |
| | H(-) | 0,027 | 0,0287 | 0,0319 | 0,0365 | 0,0407 |
| | $10^7$D ($cm^2.s^{-1}$) | 2,46 | 3,17 | 4,28 | 6,01 | 7,99 |

De nuevo, la relación de la difusividad del gas con la temperatura se describe de acuerdo a la ecuación de Arrhenius:

$$D = D_0 \exp\left(-E_D / RT\right) \tag{2.14}$$

donde $D_0$ es el factor pre-exponencial y $E_D$ es la energía de activación para la difusión.

A partir de la Figura 2.18, donde se representa el logaritmo de la difusividad de $CO_2$ frente a la inversa de la temperatura, se calcula la energía de activación recogida en la Tabla 2.26. Los resultados experimentales son consistentes con los reportados en la bibliografía.

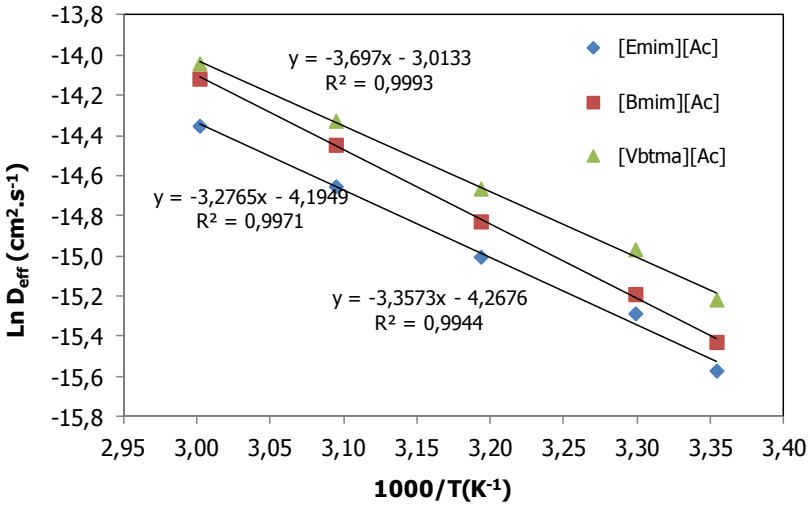


**Figura 2.18.** Logaritmo de la difusividad de $CO_2$ efectiva frente a la inversa de la temperatura. La linea continua se corresponde con la regresión lineal de los datos.

**Tabla 2.26.** Energías de activacion para la difusividad, $E_D$.

| *Gas* | *LIs* | *$E_D$ (kJ.mol$^{-1}$)* | *Referencia* |
|---|---|---|---|
| $CO_2$ | [Emim][Ac] | 27,91 | Santos et al., 2014 |
| $CO_2$ | [Bmim][Ac] | 30,74 | Santos et al., 2014 |
| $CO_2$ | [Vbtma][Ac] | 27,24 | Santos et al., 2014 |
| $CO_2$ | [Hmim][$Tf_2N$] | 16,42 | Ilconich et al., 2007 |
| $CO_2$ | [Bmpy][$Bf_4$] | 21 | Morganty and Baltus, 2010 |
| $CO_2$ | [Omim][$Bf_4$] | 18 | Morganty and Baltus, 2010 |
| $CO_2$ | [Hmim][$Bf_4$] | 22 | Morganty and Baltus, 2010 |
| $CO_2$ | [Hmim][$Tf_2N$] | 14 | Morganty and Baltus, 2010 |
| $CO_2$ | [Emim][$Tf_2N$] | 8 | Morganty and Baltus, 2010 |
| $CO_2$ | [Emim][Beti] | 14 | Morganty and Baltus, 2010 |
| $CO_2$ | [Emim][Tfa] | 11 | Morganty and Baltus, 2010 |
| $CO_2$ | [Emim][TfO] | 14 | Morganty and Baltus, 2010 |
| $CO_2$ | [Bmim][$Tf_2N$] | 10 | Morganty and Baltus, 2010 |
| $CO_2$ | [Pmmim][$Tf_2N$] | 15 | Morganty and Baltus, 2010 |
| $CO_2$ | [Bmpy][$Tf_2N$] | 12 | Morganty and Baltus, 2010 |
| $CO_2$ | [Bmim][$Bf_4$] | 6 | Morganty and Baltus, 2010 |
| $CO_2$ | [Bmim][$Pf_6$] | 27,2 | Shiflett and Yokozeki, 2005 |
| $CO_2$ | [Bmim][$Bf_4$] | 24,3 | Shiflett and Yokozeki, 2005 |
| $CO_2$ | [Bmim][$Pf_6$] | 47,72 | Barghi et al., 2010 |
| $CO_2$ | [Hmim][$Tf_2N$] | 21,50 | Adibi et al., 2011 |
| $CO_2$ | [Emim][$Tf_2N$] | 16,9 | Morgan et al., 2005 |
| $CO_2$ | [Bmim][Beti] | 22,3 | Morgan et al., 2005 |
| $CH_4$ | [hmim][$Tf_2N$] | 33,29 | Adibi et al., 2011 |
| $CH_4$ | [Bmim][$Pf_6$] | 61,11 | Barghi et al., 2010 |

Teniendo en cuenta los resultados experimentales obtenidos, la energía de activación para la permeabilidad es la suma algebraica de la energía de activación para la difusión y la entalpía molar de absorción. La influencia de la temperatura en la permeabilidad se describe mediante una ecuación de tipo Arrhenius con un valor de energía de activación que incluye la influencia de la temperatura en los valores efectivos de difusividad y solubilidad. Se recomienda la

utilización de LIs con una absorción endotérmica ya que permiten aumentar la energía de activación para la permeabilidad y así conseguir una mayor influencia de la temperatura sobre la permeabilidad.

## 2.5. Apéndices del Capítulo 2

Apéndice A

Diseño de la celda utilizada para los experimentos de permeación:

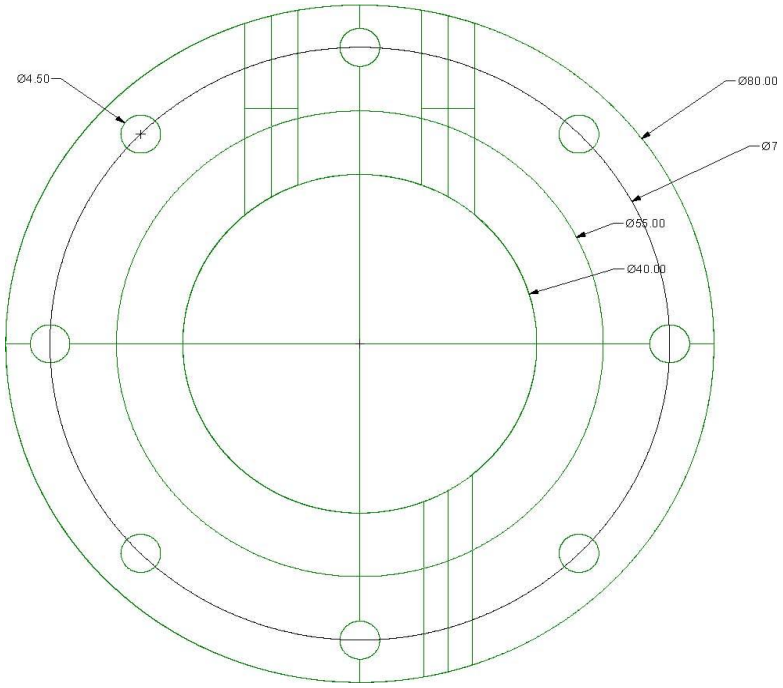


**Figura A.1.** Vista de planta de la celda de permeación.

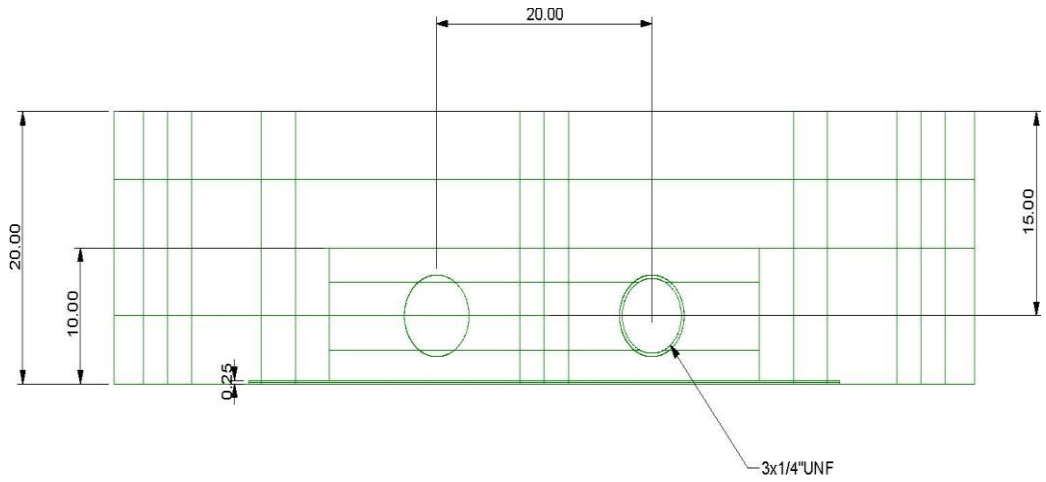


**Figura A.2.** Vista de perfil de la celda de permeación.

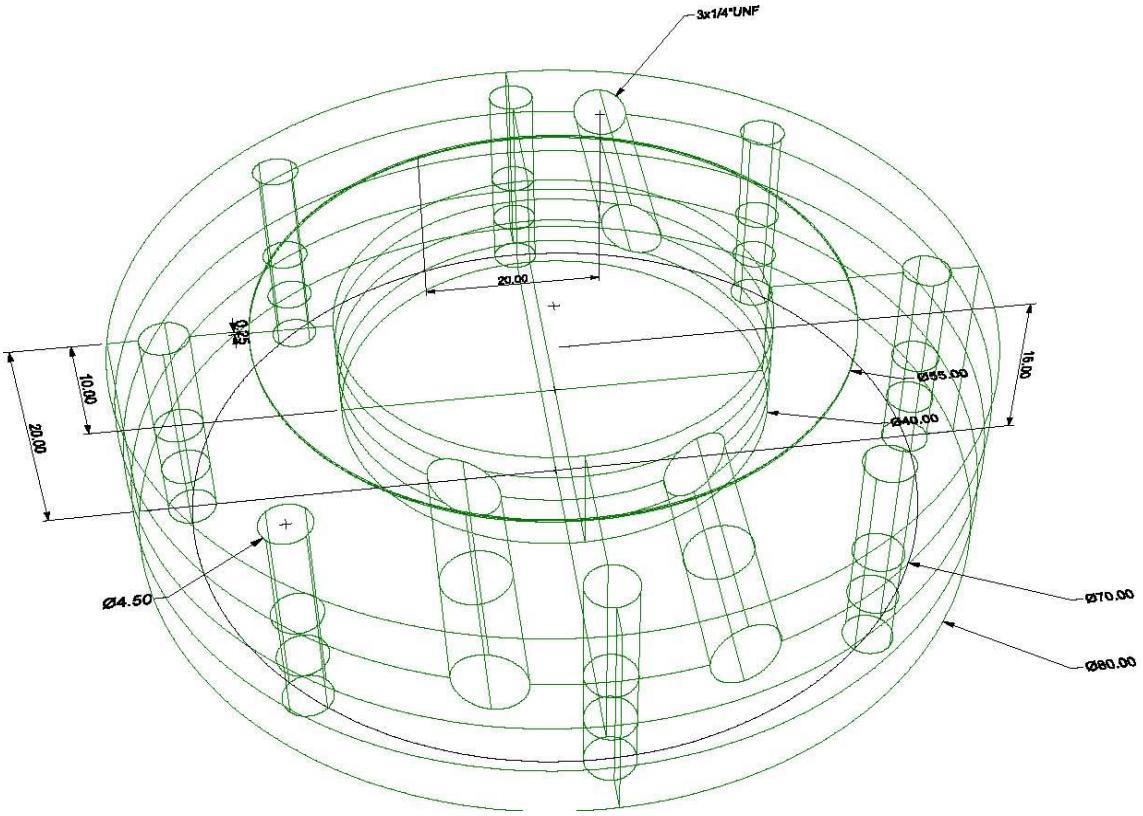


**Figura A.3.** Perspectiva de la celda de permeación.

Apéndice B

Los datos de permeabilidad se expresan habitualmente en barrer cuya definición es:

$$1barrer = \frac{10^{-10} cm^3 gas(STP)(cm\_espesor)}{(cm^2\_areamembrana)(cmHg\_presión).s} \quad \text{(B.1)}$$

(STP= 273,15 K y 1,01325 x $10^5$ Pa)

En el S.I. ($cm^2.s^{-1}$):

$$1barrer = \frac{10^{-10} cm^3(STP)cm}{cm^2.cmHg.\sec}.\left[\frac{mol(STP)}{22,4.10^3 cm^3}\right].\left[62,36367\,\frac{L.mmHg}{mol.K}.\frac{10^3 cm^3}{1L}.\frac{1cmHg}{10mmHg}\right].298,15K =$$

$$= 8,296.10^{-9} cm^2.s^{-1} \quad \text{(B.2)}$$

La constante de Henry ha sido calculada siguiendo la siguiente expressión (Sander,1999):

$$H = \frac{C_g^*}{C_l^*} = \frac{y^*.\rho_g}{x^*.\rho_l} = \frac{y^*}{x^*.\rho_l}.\frac{P_T}{R.T} = \frac{1}{S} \quad \text{(B.3)}$$

donde *y** y *x** son las fracciones molares en las fases gas y líquida, respectivamente, estando en equilibrio con ellas mismas; $\rho_l$es la densidad molar del líquido y $P_T$ la presión total.

## 2.6. Nomenclatura del Capítulo 2

*Símbolos*

| | |
|---|---|
| *A, B* | parámetros del modelo Orrick-Erbar |
| $A^+$, $B^+$ | parámetros de contribución de grupos para el catión |
| $A^-$, $B^-$ | parámetros de contribución de grupos para el anión |
| *A*,B** | parámetros normalizados del modelo Orrick-Erbar |
| *a,b,c* | coeficients de ajuste para la densidad |
| *B* | campo magnético (Tesla) |
| $D_0$ | factor pre-exponencial para la difusividad ($cm^2.s^{-1}$) |
| $D_{eff}$ | difusividad efectiva ($cm^2.s^{-1}$) |
| $E_D$ | energía de activación para la difusividad ($kJ.mol^{-1}$) |
| $E_P$ | energía de activación para la permeabilidad ($kJ.mol^{-1}$) |
| *H* | coeficiente de partición (-) |
| *M* | peso molecular ($g.mol^{-1}$) |

| | |
|---|---|
| $N$ | número de Avogadro ($mol^{-1}$) |
| $N_p$ | número de datos experimentales |
| $n$ | longitud de la cadena del catión |
| $P$ | permeabilidad (barrer) |
| $P_0$ | factor pre-exponencial para la permeabilidad (barrer) |
| $P_{MSLI}$ | permeabilidad a través de la membrana soportada con líquido iónico |
| $P_T$ | presión total (bar) |
| $p_{feed}$ | presión en el compartimento de alimentación (Pa) |
| $p_{perm}$ | presión en el compartimento de permeado (Pa) |
| $R$ | constante de los gases ideales ($bar.L.mol^{-1}.K^{-1}$) |
| $S$ | solubilidad de gas (fracción molar) |
| $S_0$ | factor pre-exponencial para la solubilidad (barrer) |
| $S_{A/B}$ | selectividad ideal (-) |
| $T$ | temperatura (K) |
| $t$ | tiempo (s) |
| $V$ | volumen molar ($Å^3$) |
| X*,Y* | variables normalizadas |
| x* | fracción molar de la fase líquida |
| y* | fracción molar de la fase gas en equilibrio con la fase líquida |

*Letras griegas*

| | |
|---|---|
| $\beta$ | factor geométrico ($m^{-1}$) |
| $\delta$ | espesor de membrana (m) |
| $\mu$ | viscosidad (cP) |
| $\Delta Hs$ | entalpía molar parcial de absorción ($kJ.mol^{-1}$) |
| $\rho$ | densidad ($g.cm^{-3}$) |
| $\rho l$ | densidad molar del líquido ($mol.L^{-1}$) |
| $\chi mT$ | susceptibilidad magnética ($emu.K.mol^{-1}$) |

*Subíndices*

| | |
|---|---|
| *0* | ausencia de campo magnético |
| *B* | presencia de campo magnético |
| *cal* | propiedad calculada (densidad y viscosidad) |
| *exp* | experimental (densidad y viscosidad) |
| *max* | valor máximo de las variables |
| *min* | valor mínimo de las variables |

*Acrónimos*

| | |
|---|---|
| *LIs* | líquidos iónicos |
| *LIMs* | líquidos iónicos magnéticos |
| *MSLIs* | membranas soportadas con líquidos iónicos |
| *MSLIMs* | membranas soportadas con líquidos iónicos magnéticos |

## 2.7. Referencias del Capítulo 2

Adibi M., Barghi S.H., Rashtchian D. Predictive models for permeability and diffusivity of $CH_4$ through imidazolium-based supported ionic liquid membranes. *J. Membr. Sci.* **2011**, 371, 127-133.

Albo J. Desarrollo de una tecnología innovadora para la mitigación del cambio climático: Absorción no dispersiva con líquidos iónicos, Tesis Doctoral, Universidad de Cantabria, Santander, **2012**.

Albo J., Santos E., Neves L.A., Simeonov S.P., Afonso C.A.M., Crespo J.G., Irabien A. Separation performance of $CO_2$ through Supported Magnetic Ionic Liquid Membranes (SMILMs). *Sep. Pur. Technol.* **2012**, 97, 26-33.

Anderson T.M., Ingersoll D., Rose A.J., Staiger C.L., Leonard J.C. Synthesis of an ionic liquid with an iron coordination cation. *Dalton Trans.* **2010**, 39, 8609-8612.

Andrade N.A Theory of the Viscosity of Liquids. *Phil. Mag.* **1934**,17, 698-732.

Anthony J.L., Anderson J.L., Maginn E.J., Brennecke J.F. Anion effects on gas solubility in ionic liquids. *J. Phys. Chem. B* **2005**, 109, 6366-6374.

Backer T., Breunig O., Valldor M., Merz K., Vasylyeva V., Mudring A-V. In-situ crystal growth and properties of the magnetic ionic liquid $[C_2mim][FeCl_4]$. *CrystGrowth Des.* **2011**, 11, 2564-2571.

Bara J.E., Carlisle T.K., Gabriel C.J., Camper D., Finotello A., Gin D.L., Noble R.D. Guide to $CO_2$ separations in imidazolium-based room-temperature ionic liquids. *Ind. Eng. Chem. Res.* **2009**, 48 , 2739-2751.

Barghi S.H., Adibi M., Rashtchian D. An experimental study on permeability, diffusivity, and selectivity of $CO_2$ and $CH_4$ through [bmim][$Pf_6$] ionic liquid supported on an alumina membrane: investigation of temperature fluctuations effects. *J. Membr. Sci.* **2010**, 362, 346-352.

Bhavsar R.S., Kumbharkar S.C., Kharul U.K. Polymeric ionic liquids (PILs): Effect of anion variation on their $CO_2$ sorption. *J. Membr. Sci.* **2012**, 389, 305-315.

Cadena C., Anthony J.L., Shah J.K., Morrow T.I., Brennecke J.F., Maginn E.J. Why is $CO_2$ so soluble in imidazolium-based ionic liquids?. *J. Am. Chem. Soc.* **2004**, 126, 5300-5308.

Condemarin R. y Scovazzo P. Gas permeabilities, solubilities, diffusivities, and diffusivity correlations for ammonium-based room temperature ionic liquids with comparison to imidazolium and phosphonium RTILs data. *Chem. Eng. J.* **2009**,147,1369-1374.

Cserjési P., Nemestóthy N., Bélafi-Bakó K. Gas separation properties of supported liquid membranes prepared with unconventional ionic liquids. *J. Membr. Sci.* **2010**, 349 6-11.

Cussler E.L., Diffusion. Mass Transfer in Fluid Systems, 2nd ed., Cambridge University Press, USA, **1997**, pp. 21-23, 434-435, 438-439.

Daniel C.I., Albo J., Santos E., Portugal C.A.M., Crespo J.G., Irabien A. A group contribution method for the influence of the temperature in the viscosity of magnetic ionic liquids. *Fluid Phase Equilib.* **2013**, 360, 29-35.

De Pedro I., Rojas D.P., Albo J., Luis P., Irabien A., Blanco J., Rodriguez J. Long-range magnetic ordering in magnetic ionic liquid: Emim[$FeCl_4$]. *J. Phys. Condens. Matter.* **2010**, 22, 296-306.

Del Sesto R.E., McCleskey T.M., Burrel A.K, Baker G.A., Thompson J.D., Scott B.L., Wilkes J.S., Williams P. Structure and magnetic behaviour of transition metal based ionic liquids. *Chem. Commun*. **2008**, 447-449.

Deng N., Lin M., Zhao L., Liu C., de Rooy S.L., Warner I.M. Highly efficient extraction of phenolic compounds by use of magnetic room temperature ionic liquids for environmental remediation. *J. Hazard. Mater.* **2011**, 192, 1350-1357.

Ferguson L. y Scovazzo P. Solubility, diffusivity and permeability of gases in phosphonium-based room temperature ionic liquids: data and correlations. *Ind. Eng. Chem. Res.* **2007**, 46, 1369-1374.

Freire M.G., Teles A.R.R., Rocha M.A.A., Schroder B., Neves C.M.S.S., Carvalho P.J., Evtuguin D.V., Santos L.M.N.B.F., Coutinho J.A.P. Thermophysical characterization of ionic liquids able to dissolve biomass. *J. Chem. Eng. Data* **2011**, 56, 4813-4822.

Fulcher G. Analysis of Recent Measurements of the Viscosity of Glasses. *J. Am. Ceram. Soc.* **1925**, 8, 339-355.

Gardas R.L. y Coutinho J.A.P. A group contribution method for viscosity estimation of ionic liquids. *Fluid Phase Equilib*. **2008**, 266, 195-201.

Gastonbonhomme Y., Petrino P., Chevalier J.L. UNIFAC visco group-contribution method for predicting kinematic viscosity - extension and temperature-dependence. *Chem. Eng. Sci.* **1994**, 49, 1799-1806.

Hayashi S., Saha S., Hamaguchi H.A. A new class of magnetic fluids: bmim[$FeCl_4$] and n-bmim [$FeCl_4$] ionic liquids. *IEEE Trans. Magn.* **2006**, 42, 12-14.

Iarikov D.D., Hacarlioglu P., Oyama S.T. Supported room temperature ionic liquid membranes for $CO_2/CH_4$ separation. *Chem. Eng. J*. **2011**, 166 401-406.

Ilconich J., Meyers C., Pennline H., Luebke D. Experimental investigation of the permeability and selectivity of supported ionic liquid membranes for $CO_2$/He separation at temperatures up to 125ºC. *J. Membr. Sci.* **2007**, 298, 41-47.

Jiang Y., Guo C., Liu H. Magnetically rotational reactor for absorbing benzene emissions by ionic Liquids. *China Part*. **2006**, 5, 130-133.

Jindaratsamee P., Shimoyama Y., Morizaki H., Ito A. Effects of temperature and anion species on $CO_2$ permeability and $CO_2/N_2$ separation coefficient through ionic liquid membranes. *J. Chem. Thermodyn.* **2011**, 43, 311-314.

Lee S., Ha S., Jin H., You C., Koo Y. Magnetic behavior of mixture of magnetic ionic liquid bmim[$FeCl_4$] and water. *J. Applied. Physics* **2007**, 101, 09J102.

Litovitz A. Temperature Dependence of the Viscosity of Associated Liquids. *J. Chem. Phys*. **1952**, 20, 1088-1089.

Luis P., Ortiz I., Aldaco R., Irabien A. A novel group contribution method in the development of a QSAR for predicting the toxicity (Vibrio fischeri EC50) of ionic liquids. *Ecotox. Environ. Safe.* **2007**, 67, 423-429.

Maginn E.J. Design and Evaluation of Ionic Liquids as Novel $CO_2$ Absorbents, 427 Quarterly Technical Report, January **2005** (DE-FG26-04NT42122).

Morgan D., Ferguson L., Scovazzo P. Diffusivities of gases in room temperature ionic liquids: data and correlations obtained using a lag-time technique. *Ind. Eng. Chem. Res*. **2005**, 44 4815-4823.

Morganty S.S. y Baltus R.E. Diffusivity of carbon dioxide in room temperature ionic liquids. *Ind. Eng. Chem. Res.* **2010**, 49, 9370-9376.

Neves L.A., Crespo J.G., Coelhoso I.M. Gas permeation studies in supported ionic liquid membranes. *J. Membr. Sci.* **2010**, 357, 160-170.

Reid R.C., Prausnitz J.M. , Sherwood T.K. The Properties of Gases and Liquids. 4th ed. McGraw-Hill. New York. **1987**.

Robeson L.M. The upper bound revisited. *J. Membr. Sci.* **2008**, 320, 390-400.

Sander R. Modeling atmospheric chemistry: interactions between bas-phase species and liquid cloud/aerosol particles. *Surv. Geophys.* **1999**, 20, 1-31.

Santos E., Albo J., Daniel C.I., Portugal C.A.M., Crespo J.G., Irabien A. Permeability modulation of Supported Magnetic Ionic Liquid Membranes (SMILMs) by an external magnetic field. *J. Membr. Sci.* **2013a**, 430, 56-61.

Santos E., Albo J., Rosatella A., Afonso C.A.M., Irabien A. Synthesis and characterization of Magnetic Ionic Liquids (MILs) for $CO_2$ separation. *J. Chem. Tech. Biotechnol.* Aceptado. **2013b**

Santos E., Albo J., Irabien A. Acetate based Supported Ionic Liquid Membranes (SILMs) for $CO_2$ separation: Influence of the temperature. *J. Membr. Sci.* **2014**, 452, 277-283.

Sastry S.R.S., Rao K.K. A new method for predicting saturated liquid viscosity at temperatures above the normal boiling point. *Fluid Phase Equilib.* **2000**, 175, 311-323.

Scovazzo P., Kieft J., Finan D.A., Koval C., DuBois D., Noble R. Gas separations using non-hexafluorophosphate [$PF_6$]− anion supported ionic liquid membranes. *J. Membr. Sci.* **2004**, 238, 57-63.

Scovazzo P. Determination of the upper limits, benchmarks, and critical properties for gas separations using stabilized room temperature ionic liquid membranes (SILMs) for the purpose of guiding future research. *J. Membr. Sci.* **2009**,343,199-211.

Scovazzo P., Havard D., McShea M., Mixon S., Morgan D. Long-term, continuous mixed-gas dry fed $CO_2/CH_4$ and $CO_2/N_2$ separation performance and selectivities for room temperature ionic liquid membranes. *J. Membr. Sci.* **2009**, 327 41-48.

Shi W., Myers C.R, Luebke D.R., Steckel J.A., Sorescu D.C. Theoretical and experimental studies of $CO_2$ and $H_2$ separation using the 1-ethyl-3 methylimidazolium acetate ([emim][$CH_3COO$]) ionic liquid. *J. Phys. Chem. B* **2012**, 116, 283-295.

Shifflet M.B. y Yokozeki A. Solubilities and diffusivities of carbon dioxide in ionic liquids: [bmim][$PF_6$] and [bmim][$BF_4$]. *Ind. Eng. Chem. Res.* **2005**, 44, 4453-4464.

Shiflett M.B., Kasprzak D.J., Yokozeki A. Phase behavior of {carbon dioxide + [bmim][Ac]} mixtures. *J. Chem. Thermodyn.* **2008**, 40, 25-31.

Shiflett M.B. y Yokozeki A. Phase behavior of carbon dioxide in ionic liquids: [emim][Acetate], [emim][Trifluoroacetate], and [emim][Acetate] + [emim][Trifluoroacetate] mixtures. *J. Chem. Eng. Data* **2009**, 54, 108-114.

Supasitmongkol S., Styrring P. High $CO_2$ solubility in ionic liquids and a tetraalkylammonium-based poly(ionic liquid). *Energy Environ. Sci.* **2010**, 3, 1961-1972.

Vogel H. The Law of the Relation Between the Viscosity of Liquids and the Temperature. *Phys. Z.* **1921**, 22, 645-646.

Wang M., Li B., Zhao C., Quian X., Xu Y., Chen G. Recovery of [BMIM]$FeCl_4$ from homogeneous mixture using a simple chemical method. *J. Chem. Eng.* **2010**, 27, 1275-1277.

Wang J., Yao H., Nie Y., Bai L., Zhang X., Li J. Application of iron-containing magnetic ionic liquids in extraction process of coal direct liquefaction residues. *Ind. Eng. Chem. Res.* **2012**, 51, 3776-3782.

Wilke C.R. y Chang P. Correlation of diffusion coefficients in dilute solutions. *AIChE J.* **1955**, 264-270.

Yokozeki A., Shiflett M.B., Grieco L.M., Foo T. Physical and chemical absorptions of carbon dioxide in room-temperature ionic liquids. *J. Phys. Chem. B* **2008**, 112, 16654-16663.

# 3 Conclusiones

# Conclusions

«Nada puedes enseñar a un hombre;

sólo ayudarle a encontrarlo por sí mismo»

Galileo Galilei (1564-1642)

Físico, astrónomo y filósofo italiano

## 3.1. Conclusiones y progreso de la investigación

### 3.1.1. Conclusiones

Las conclusiones obtenidas a lo largo de la presente Tesis Doctoral han sido difundidas en revistas científicas incluidas en el *Journal of Citation Reports-Science Edition (JCR).* Las publicaciones se listan a continuación indicando el índice de impacto para 2012, el cuartil de la revista dentro la categoría de Ingeniería Química, la posición relativa de la revista en dicha categoría y la posición relativa en el *Essential Science Indicators-Citations*, disponible en la plataforma *ISI Web of Knowledge*.

1. **Santos E.,** Albo J., Daniel C.I., Portugal C.A.M., Crespo J.G., Irabien A. Permeability modulation of Supported Magnetic Ionic Liquid Membranes (SMILMs) by an external magnetic field. *Journal of Membrane Science* 430:56-61 (**2013**). Índice de impacto: 4,093 // Cuartil Q1 // Posición relativa en la categoría Ingeniería Química: 7/133 // Posición relativa según *Essential Science Indicators-Citations*: 832/8471.

2. **Santos E.,** Albo J., Rosatella A., Afonso C.A.M., Irabien A. Synthesis and characterization of Magnetic Ionic Liquids (MILs) for $CO_2$ separation. *Journal of Chemical Technology and Biotechnology*. **Aceptado**. Índice de impacto: 2,504 // Cuartil Q1 // Posición relativa en la categoría Ingeniería Química: 23/133 // Posición relativa según *Essential Science Indicators-Citations*: 2066/8471.

3. **Santos E.**, Albo J., Irabien A. Acetate based Supported Ionic Liquid Membranes (SILMs) for $CO_2$ separation: Influence of the temperature. *Journal of Membrane Science* 452: 277-283 (**2014**). Índice de impacto: 4,093 // Cuartil Q1 // Posición relativa en la categoría Ingeniería Química: 7/133 // Posición relativa según *Essential Science Indicators-Citations*: 832/8471.

4. Albo J., **Santos E**., Neves L.A., Simeonov S.P., Afonso C.A.M., Crespo J.G., Irabien A. Separation performance of $CO_2$ through Supported Magnetic Ionic Liquid Membranes (SMILMs). *Separation and Purification Technology* 97:26-33 (**2012**). Índice de impacto: 2,894 // Cuartil Q1 // Posición relativa en la categoría Ingeniería Química: 15/133 // Posición relativa según *Essential Science Indicators-Citations*: 1598/8471.

5. Daniel C.I., Albo J., **Santos E.,** Portugal C.A.M., Crespo J.G., Irabien A. A group contribution method for the influence of the temperature in the viscosity of magnetic ionic liquids. *Fluid Phase Equilibria* 360:29-35 (**2013**). Índice de impacto: 2,379 //

Cuartil Q1 // Posición relativa en la categoría Ingeniería Química: 27/133 // Posición relativa según *Essential Science Indicators-Citations*: 2228/8471.

Las principales conclusiones extraídas del conjunto de este trabajo son las siguientes:

**1)** **Se ha caracterizado cuatro líquidos iónicos magnéticos** conteniendo el catión trihexil tetradecil fosfonio y diferentes aniones metálicos, $[P_{66614}][CoCl_4]$, $[P_{66614}][FeCl_4]$, $[P_{66614}][MnCl_4]$ y $[P_{66614}][GdCl_6]$. Se ha evaluado la susceptibilidad magnética, densidad, viscosidad, propiedades térmicas y solubilidad de $CO_2$ **obteniéndose información básica para el desarrollo de aplicaciones**.

Las medidas de susceptibilidad magnética indican un comportamiento paramagnético de todos los líquidos iónicos magnéticos estudiados situándose el momento magnético entre 2,10-6,51 $emu \cdot K \cdot mol^{-1}$. Los líquidos iónicos magnéticos presentan una muy buena estabilidad térmica siendo estables hasta 619 K. Finalmente, los valores de solubilidad de $CO_2$ encontrados son bajos si se comparan bajo las mismas condiciones de operación con otros líquidos iónicos específicos para captura de $CO_2$.

**2)** Con el objetivo de **estimar la viscosidad de los líquidos iónicos magnéticos a diferentes temperaturas** se ha aplicado un **método de contribución de grupos** basado en la ecuación de Orrick-Erbar que permita determinar la influencia del catión y el anión en la viscosidad del líquido iónico.

Se observa una contribución negativa del anión sobre la viscosidad contrarrestándose con el efecto positivo del catión. En términos absolutos, existe una contribución mayor por parte del anión con respecto al catión. Con respecto a la influencia de la temperatura, puede concluirse que la influencia del catión en la viscosidad es menor que la observada en el anión. Los resultados predichos utilizando el modelo están validan los resultados experimentales. Por lo tanto, puede concluirse que **este modelo es aplicable para la predicción de la viscosidad de los líquidos iónicos magnéticos a diferentes temperaturas** pudiendo ser extendido incluyendo nuevas combinaciones anión-catión.

**3)** Se ha demostrado la **influencia de la aplicación de un campo magnético externo en la modulación de la permeabilidad y selectividad $CO_2/N_2$ a través de membranas soportadas con líquidos iónicos magnéticos** en un rango de 0-1,5 Tesla.

La permeabilidad del gas se incrementa en función del campo magnético aplicado debido a una disminución en la viscosidad de los líquidos iónicos magnéticos en presencia de un campo magnético externo, mientras que la selectividad ideal permanece constante. El líquido iónico magnético $[P_{66614}][GdCl_6]$ muestra el máximo incremento de permeabilidad (21,64%) con respecto al valor en ausencia de campo magnético. Los resultados describen el efecto de **modulación de la permeabilidad mediante la regulación de la intensidad de campo**. **Estos resultados innovadores abren la posibilidad a nuevas aplicaciones de separación en presencia de un campo magnético externo.**

**4)** Se ha estudiado la **separación $CO_2/N_2$ a través de membranas soportadas con líquidos iónicos conteniendo el anión acetato**.

**La influencia de la temperatura** sobre la permeabilidad, solubilidad y difusividad ha sido **descrita utilizando una ecuación tipo Arrhenius** calculándose las energías de activación. Los **resultados experimentales** obtenidos se sitúan **sobre el límite máximo** establecido por **Robeson** para membranas poliméricas. **Se recomienda** la utilización de líquidos iónicos con una **absorción endotérmica que permite aumentar la energía de activación a fin de conseguir una mayor influencia de la temperatura en la permeabilidad.**

### 3.1.2. Progreso de la investigación

En relación con los resultados de esta Tesis Doctoral, se consideran relevantes las siguientes líneas para el progreso científico-técnico futuro:

- **Desarrollo de nuevas aplicaciones** basadas en la respuesta obtenida ante la aplicación de un campo magnético externo sobre la viscosidad de los líquidos iónicos magnéticos y la modulación de la permeabilidad mediante la regulación de la intensidad de campo. Del mismo modo, se propone el posible estudio de la **influencia de la aplicación de un campo magnético sobre la solubilidad y difusividad de los líquidos iónicos magnéticos.**

- Se propone el **estudio de la viabilidad de obtener nuevas membranas basadas en líquidos iónicos** que permitan superar el límite de Robeson para la separación $CO_2/N_2$, lo que supondría un avance importante hacia la implementación de la tecnología de membranas poliméricas selectivas que pudiera competir de manera eficiente con los procesos de separación convencionales. Se propone partir de

membranas poliméricas de elevado volumen libre disponibles comercialmente que se encuentren sobre el límite de Robeson e intentar mejorar la selectividad sin perjudicar la permeabilidad mediante la introducción de materiales de probada solubilidad tales como líquidos iónicos o polímeros iónicos. Por otra parte, también se plantea la **mejora de la estabilidad de las membranas** mediante la polimerización de los líquidos iónicos seleccionados para obtener películas poliméricas delgadas, soportadas o no en un substrato poroso que confiera resistencia mecánica.

## *3.1. Conclusions and on-going research*

### *3.1.1. Conclusions*

The conclusions obtained in this PhD Thesis have been communicated fundamentally in scientific journals included in *Journal of Citation Reports-Science Edition (JCR).* The publications are listed below, showing the impact factor for 2012, the quartile in the category of Chemical Engineering, the relative position of the journal in that category and the relative position in the *Essential Science Indicators-Citations* in *ISI Web of Knowledge* platform.

1. **Santos E.,** Albo J., Daniel C.I., Portugal C.A.M., Crespo J.G., Irabien A. Permeability modulation of Supported Magnetic Ionic Liquid Membranes (SMILMs) by an external magnetic field. *Journal of Membrane Science* 430:56-61 (**2013**). Impact factor: 4.093 // Quartile Q1 // Relative position in the category of Chemical Engineering 7/133 // Relative position according to *Essential Science Indicators-Citations*: 832/8471.

2. **Santos E.,** Albo J., Rosatella A., Afonso C.A.M., Irabien A. Synthesis and characterization of Magnetic Ionic Liquids (MILs) for $CO_2$ separation. *Journal of Chemical Technology and Biotechnology*. **Accepted**. Impact factor: 2.540 // Quartile Q1 // Relative position in the category of Chemical Engineering 23/133 // Relative position according to *Essential Science Indicators-Citations*: 2066/8471.

3. **Santos E.**, Albo J., Irabien A. Acetate based Supported Ionic Liquid Membranes (SILMs) for $CO_2$ separation: Influence of the temperature. *Journal of Membrane Science* 452: 277-283 (**2014**). Impact factor: 4.093 // Quartile Q1 // Relative position in the category of Chemical Engineering 7/133 // Relative position according to *Essential Science Indicators-Citations*: 832/8471.

4. Albo J., **Santos E**., Neves L.A., Simeonov S.P., Afonso C.A.M., Crespo J.G., Irabien A. Separation performance of $CO_2$ through Supported Magnetic Ionic Liquid Membranes (SMILMs). Separation and Purification Technology 97:26-33 (**2012**). Impact factor: 2.379 // Quartile Q1 // Relative position in the category of Chemical Engineering 15/133 // Relative position according to *Essential Science Indicators-Citations*: 1598/8471.

5. Daniel C.I., Albo J., **Santos E.,** Portugal C.A.M., Crespo J.G., Irabien A. A group contribution method for the influence of the temperature in the viscosity of magnetic ionic liquids. *Fluid Phase Equilibria* 360:29-35 (**2013**). Impact factor: 2.379 // Quartile Q1 // Relative position in the category of Chemical Engineering 27/133 // Relative position according to *Essential Science Indicators-Citations*: 2228/8471.

The main conclusions of this work are:

1) **Four magnetic ionic liquids** containing the trihexyl(tetradecyl)phosphonium cation and different magnetic anions, $[P_{66614}][CoCl_4]$, $[P_{66614}][FeCl_4]$, $[P_{66614}][MnCl_4]$ and $[P_{66614}][GdCl_6]$, **have been characterized.** The magnetic susceptibility, density, viscosity, thermal properties and $CO_2$ solubility have been evaluated **obtaining basic information for the development of applications.**

   The magnetic susceptibility measurements show a paramagnetic behavior in all the tested magnetic ionic liquids with the magnetic moment between 2.10-6.51 $emu \cdot K \cdot mol^{-1}$. Magnetic ionic liquids show a very good thermal stability since they are thermally stable up to 619 K. Finally, $CO_2$ solubility is low when compared with other specific ionic liquids for $CO_2$ capture under the same operating conditions.

2) With the aim of **estimating the magnetic ionic liquids viscosity at different temperatures a group contribution method based on the Orrick–Erbar equation has been applied which allows determining the influence of the cation and the anion in the viscosity**.

   A negative anion contribution to the viscosity is observed counteracting the positive cation effect. Considering the absolute parameters, there is a higher anion contribution for the viscosity than for the cation. Regarding the temperature influence, it can be concluded that the influence of the cation to the viscosity of magnetic ionic liquids is less relevant than that observed for the contribution of the anions. The predicted results using this model are in good agreement with the experimental values. Therefore, it can be concluded that **this model is applicable for the prediction of magnetic ionic liquids viscosities at different temperatures** and may be extended to include other anion-cation combinations.

3) **The influence of the external magnetic field application on $CO_2/N_2$ permeability and selectivity modulation through supported magnetic ionic liquid membranes has been shown** in the range of 0-1.5 Tesla.

   Gas permeability increases as a function of the applied magnetic field due to magnetic ionic liquids viscosity decrease in the presence of the external magnetic field, while the ideal selectivity remains constant. The magnetic ionic liquid $[P_{66614}][GdCl_6]$ shows the maximum $CO_2$ permeability increase (21.64%) in comparison with the result when no magnetic field is applied. The results describe the modulation effect of permeability by tuning the magnetic field intensity. These innovative results open the possibility of new separation applications in the presence of an external magnetic field.

4) **$CO_2/N_2$ separation through supported ionic liquid membranes containing the acetate anion** has been studied.

   **The influence of temperature** on the permeability, solubility and diffusivity has been **described using an Arrhenius type equation** which allowed the calculation of the activation energies. The **experimental results** are **above the Robeson upper bound** for polymeric membranes. The use of ionic liquids with **an endothermic absorption is recommended, which may increase the permeability activation energy in order to get a higher influence of the temperature.**

### *3.1.2. On-going research*

Based on the results presented on this PhD Thesis, the following relevant lines are considered for the future scientific-technical progress:

- **Development of new applications** based on the response to the application of an external magnetic field on the magnetic ionic liquids viscosity and the permeability modulation by tuning the magnetic field strength. In the same way, it is proposed to **study the influence of the application of a magnetic field on magnetic ionic liquids solubility and diffusivity.**

- It is proposed to **study the feasibility of obtaining new membrane based on ionic liquids** to overcome the Robeson upper bound for $CO_2/N_2$ separation, which would be an important step towards the implementation of selective polymeric membrane technology that could compete effectively with conventional separation processes. It will start from commercially available polymers or polymer membranes of high free volume that fall on the upper bound established by Robeson and try to improve the selectivity introducing materials that are proved good absorbents for $CO_2$ such as ionic liquids or polymerizable ionic liquids. Moreover, the **membrane stability improvement may be attempted** by the polymerization of selected ionic liquids in order to obtained thin polymeric films supported or not on a porous substrate to confer higher mechanical resistance.

# 4 Artículos científicos

# Scientific articles

«La ciencia es el alma de la prosperidad de las naciones

y la fuente de vida de todo progreso»

Luois Pasteur (1822-1895)

Químico y biólogo francés

## 4.1. Santos E., Albo J., Daniel C.I., Portugal C.A.M., Crespo J.G., Irabien A. Permeability modulation of Supported Magnetic Ionic Liquid Membranes (SMILMs) by an external magnetic field. *J. Membr. Sci.* 2013, 430, 56-61.

Resumen

Este trabajo se centra en la modulación de la permeabilidad de Membranas Soportadas con Líquidos Iónicos Magnéticos (MSLIMs) para separación de $CO_2$ cuando se aplica un campo magnético externo. Se han estudiado cuatro Líquidos Iónicos Magnéticos (LIMs) ($[P_{66614}][CoCl_4]$, $[P_{66614}][FeCl_4]$, $[P_{66614}][MnCl_4]$ y $[P_{66614}][GdCl_6]$) en combinación con un soporte poroso comercial hidrófobo de PVDF. Se ha llevado a cabo una evaluación experimental de la permeabilidad para el $CO_2$, $N_2$ y aire. Se ha estudiado también la influencia del campo magnético sobre la viscosidad de los LIMs, lo que permite establecer la relación entre la permeabilidad y de la viscosidad en función del campo magnético externo.

Un campo magnético externo entre 0 y 2 Tesla aumenta la permeabilidad de $CO_2$, $N_2$ y aire sin cambiar la relación de permeabilidades y disminuyendo la viscosidad de los LIMs, dependiendo de la susceptibilidad magnética. El LIM $[P_{66614}]$ $[GdCl_6]$ muestra el aumento de permeabilidad de $CO_2$ máximo (21,64 %) respecto al resultado en ausencia de campo magnético. El producto de la permeabilidad y viscosidad es una constante con un valor diferente para cada MSLIM estudiada. Los resultados experimentales confirman el potencial para la modulación de la permeabilidad de gas a través de las membranas líquidas soportadas mediante el ajuste de la intensidad del campo magnético externo.

*Original abstract*

This work is focused on the permeability modulation of Supported Magnetic Ionic Liquid Membranes (SMILMs) for $CO_2$ separation, when applying an external magnetic field. Four Magnetic Ionic Liquids (MILs) have been studied ($[P_{66614}][CoCl_4]$, $[P_{66614}][FeCl_4]$, $[P_{66614}][MnCl_4]$ and $[P_{66614}][GdCl_6]$) in combination with a commercial hydrophobic PVDF porous support. An experimental evaluation of the membrane permeability was carried out for $CO_2$, $N_2$ and air. The influence of the magnetic field on MILs viscosity was also studied, allowing to establish the relationship between permeability and viscosity depending on the external magnetic field.

An external magnetic field between 0 and 2 Tesla increases the gas permeability for $CO_2$, $N_2$ and air without changing the permeability ratio and decreases MILs viscosity, depending on the MILs magnetic susceptibility. The MIL $[P_{66614}][GdCl_6]$ shows the maximum $CO_2$ permeability increase (21.64%) in comparison with the result when no magnetic field is applied.The permeability and viscosity product is a constant with a different value for each SMILM studied.

Experimental results confirm the potential for gas permeability modulation through supported liquid membranes by tuning the external magnetic field intensity.

Journal of Membrane Science 430 (2013) 56–61

Contents lists available at SciVerse ScienceDirect

Journal of Membrane Science

journal homepage: www.elsevier.com/locate/memsci

# Permeability modulation of Supported Magnetic Ionic Liquid Membranes (SMILMs) by an external magnetic field

E. Santos [a,*], J. Albo [a], C.I. Daniel [b], C.A.M. Portugal [b], J.G. Crespo [b], A. Irabien [a]

[a] Departamento Ingeniería Química y Química Inorgánica, E.T.S. de Ingenieros Industriales y Telecomunicación, Universidad de Cantabria, 39005, Santander, Spain
[b] REQUIMTE-CQFB, Departamento de Química, Faculdade de Ciências e Tecnologia, Universidade Nova de Lisboa 2829-516 Caparica, Portugal

ARTICLE INFO

*Article history:*
Received 12 July 2012
Received in revised form
1 December 2012
Accepted 7 December 2012
Available online 20 December 2012

*Keywords:*
$CO_2/N_2$ permeability
Magnetic Ionic Liquids (MILs)
Supported Magnetic Ionic Liquid Membranes (SMILMs)
Gas permeability modulation
External magnetic field

ABSTRACT

This work is focused on the permeability modulation of Supported Magnetic Ionic Liquid Membranes (SMILMs) for $CO_2$ separation, when applying an external magnetic field. Four magnetic ionic liquids (MILs) have been studied ($[P_{66614}][CoCl_4]$, $[P_{66614}][FeCl_4]$, $[P_{66614}][MnCl_4]$ and $[P_{66614}][GdCl_6]$) in combination with a commercial hydrophobic PVDF porous support. An experimental evaluation of the membrane permeability was carried out for $CO_2$, $N_2$ and air. The influence of the magnetic field on MILs viscosity was also studied, allowing to establish the relationship between permeability and viscosity depending on the external magnetic field.

An external magnetic field between 0 and 2 T increases the gas permeability for $CO_2$, $N_2$ and air without changing the permeability ratio and decreases MILs viscosity, depending on the MILs magnetic susceptibility. The MIL $[P_{66614}][GdCl_6]$ shows the maximum $CO_2$ permeability increase (21.64%) in comparison with the result when no magnetic field is applied. The permeability and viscosity product is a constant with a different value for each SMILM studied. Experimental results confirm the potential for gas permeability modulation through supported liquid membranes by tuning the external magnetic field intensity.



## 1. Introduction

The permeability of $CO_2$ and $N_2$ through Supported Ionic Liquid Membranes (SILMs) has been studied by immobilising selected ionic liquids in polymeric porous commercial supports [1–3]. The influence of pore size, the stability evaluation regarding its hydrophobic or hydrophilic nature and the effect of water vapour in the gas stream has been reported in literature [4,5], however, there is not yet a clear understanding of this process [6]. Although SILMs present advantages due to room temperature ionic liquids (RTILs) properties, their applications are still limited mainly associated to problems in their stability and long-term behaviour [5]. Gas permeability and selectivity are the fundamental parameters characterising membrane gas separation. There is a general trade-off between both parameters; for polymeric materials this relationship is identified by the "upper bound" limit observed for different materials in gas separation [7,8]. The development of new materials exceeding this trade-off line represents a main challenge in $CO_2/N_2$ separation.

The magnetic behaviour of a new generation of RTILs containing metal ions is recently under study in the literature. The combination of general RTILs features (e.g. chemical and thermal stability, non-volatile character and non-flammability) with new properties due to the incorporation of a metal ion, has opened a new research area which is starting to attract a wide interest. Some applications for MILs have been shown in the literature including catalysts [9,10] or electrochromic devices [11]. The innovative character of the study comes from the unique combination of the use of membranes incorporating MILs based on different magnetic anions for selective and tunable transport of gases by applying an external magnetic field, which allows the development of a new generation of novel stimuli-responsive membrane separation processes. The possibility of permeability modulation might offer the development of new applications for MILs.

The MILs 1-butyl-3-methylimidazolium tetrachloroferrate ([bmim][$FeCl_4$]) and 1-butyronitrile-3-methylimidazolium tetrachloroferrate ([n-bmim][$FeCl_4$]) were the first reported MILs to respond to an external neodymium magnet of about 0.55 T due to changes of its organisation structure [12,13]. Del Sesto et al. [14] reported MILs based on different transition metal ions such as iron, cobalt, manganese or gadolinium showing a very interesting magnetic response with potential applications for magnetic and electrochromic switching. Okuno and Hamaguchi [15] demonstrated the possibility of magnetic transport of a gas in MILs, illustrated by the change in $N_2$ bubbles trajectory in the presence of a magnetic field.

The application of an external magnetic field may modify the physico-chemical properties, such as solubility or surface

* Corresponding author. Tel.: +34 942 206749; fax: +34 942 201591.
*E-mail address:* santosse@unican.es (E. Santos).

0376-7388/$ - see front matter © 2012 Elsevier B.V. All rights reserved.
http://dx.doi.org/10.1016/j.memsci.2012.12.009

tension, by tuning the magnetic conditions. The dependence between the magnetic field intensity and the binary MIL/water equilibrium has been also observed, showing the increase of solubility of MILs in aqueous medium [16], which could improve the process efficiency. Other recent applications, have shown a benzene solubility increase in the paramagnetic MIL [bmim][$FeCl_4$] when applying a rotational magnetic field [17] or the improvement of phenolic compounds extraction in the MIL [$3C_6PC1_4$][$FeCl_4$] in the presence of a neodymium magnet [18].

In a previous work [19], MILs with different magnetic susceptibility based on phosphonium cation were incorporated to hydrophobic and hydrophilic PVDF porous supports obtaining stable SMILMs for $CO_2$ permeation. An evaluation of the membrane stability was carried out and $CO_2$, $N_2$ and air permeabilites for SMILMs were experimentally determined. Pure gas permeation results demonstrated that these SMILMs showed much higher $CO_2$ permeabilities (147–259 barrers) when comparing with $N_2$ (5–7 barrers) or air (7–12 barrers).

This work shows the influence of an external magnetic field in gas permeability ($CO_2$, $N_2$, air) of SMILMs containing phosphonium based MILs due to the paramagnetic nature of the anion leading to modulate the gas permeability.

## 2. Experimental

### 2.1. Materials

The gases used in the experiments were nitrogen (99.99% purity), carbon dioxide (high-purity grade (99.998%)) and air (20% $O_2$, $CO_2 \leq 1$ ppm, $CO \leq 1$ ppm, $H_2O \leq 3$ ppm and $N_2$ rest to balance (99.999% purity)) all of them obtained from Praxair (USA).

The MILs based in the phosphonium cation studied in the present work are:

- Trihexyl(tetradecyl)phosphonium tretrachlorocobalt ([$P_{66614}$][$CoCl_4$]);
- Trihexyl(tetradecyl)phosphonium tretrachloroferrate ([$P_{66614}$][$FeCl_4$]);
- Trihexyl(tetradecyl)phosphonium tretrachloromanganese ([$P_{66614}$][$MnCl_4$]);
- Trihexyl(tetradecyl)phosphonium hexachlorogadolinium ([$P_{66614}$][$GdCl_6$]).

All the ionic liquids used were prepared in *Faculdade de Farmácia*, *Universidade de Lisboa* (*Portugal*), by the group of Prof. Carlos Afonso, according to published procedures [14,19]. Their molecular weight, density, solubility and magnetic susceptibility are listed in Table 1. MILs density was evaluated gravimetrically with a pycnometer, $CO_2$ solubility was experimentally obtained by a thermogravimetric system at room temperature and atmospheric pressure while the magnetic moment measurement procedure was previously described [19,20]. MILs water content was previously reported [19] and experiments were carried out under the same conditions (water content and humidity).

**Table 1**
Main properties of the magnetic ionic liquids (MILs) studied.

| MIL | Molecular weight (g mol$^{-1}$) | Density (g cm$^{-3}$) | $CO_2$ solubility (wt.%) | Magnetic Susceptibility (emu K mol$^{-1}$) |
|---|---|---|---|---|
| [$P_{66614}$][$CoCl_4$] | 1112 | 0.965 | 0.40 | 2.10 |
| [$P_{66614}$][$FeCl_4$] | 681.51 | 1.012 | 0.50 | 4.29 |
| [$P_{66614}$][$MnCl_4$] | 1103 | 0.956 | 0.36 | 4.23 |
| [$P_{66614}$][$GdCl_6$] | 1821.54 | 0.982 | 0.25 | 6.51 |

### 2.2. Gas permeation experiments in Supported Magnetic Ionic Liquid Membranes (SMILMs)

The SMILMs were prepared using commercial microporous membranes from Millipore Corporation (USA). These supports are hydrophobic polyvinylidene fluoride (PVDF) membranes with a pore diameter of 0.22 μm and an average thickness of 125 μm. The immobilisation procedure has been previously described [19]. To immobilise the MILs, the polymeric microporous membrane was introduced into a vacuum chamber for 1 h in order to facilitate the wetting. Afterwards, drops of MILs were spread out at the membrane surface using a syringe keeping the vacuum inside the chamber and, finally, the liquid excess on the membrane surface was wiped up softly with a tissue. The increase of weight and thickness was measured before and after the immobilisation procedure.

The experimental setup used for the gas permeation measurements has been previously described elsewhere [19]. Basically, it is composed by a polyvinylidene fluoride (PVDF) cell supplied by Micrux Technologies (Spain) divided by a membrane with an effective area of about 12.6 cm$^2$ into two compartments. A driving force of around 0.45 bar was established between both compartments leading to a flux across the membrane. The pressure change in both compartments over time was followed using two pressure transducers (Omega, UK). The temperature was controlled at 293.15 K during the experiments using a water electromagnet chiller.

The influence of the application of an external magnetic field in the separation performance was evaluated using a GMW Dipole Electromagnet (Model 3473-70, USA) which provides magnetic fields up to 2.5 T accepting pole gaps ranging from 0 to 100 mm. Permeation experiments were carried out in a vertical cell disposition with membrane pores perpendicularly positioned towards the electromagnet poles. A uniform magnetic field was applied along the membrane surface as shown in Fig. 1.

The gas permeation through SILMs follows three different steps: (i) the solute molecule sorption into the feed/membrane interface, (ii) gas diffusion across the membrane, and (iii) desorption at the opposite side of the membrane. The sorption/desorption equilibria depends on the solubility while the $CO_2$ permeability is also connected with the gas diffusion through the membrane. In general, gas permeability ($P$) is related to gas partition coefficient ($H$) and diffusivity ($D$) following the

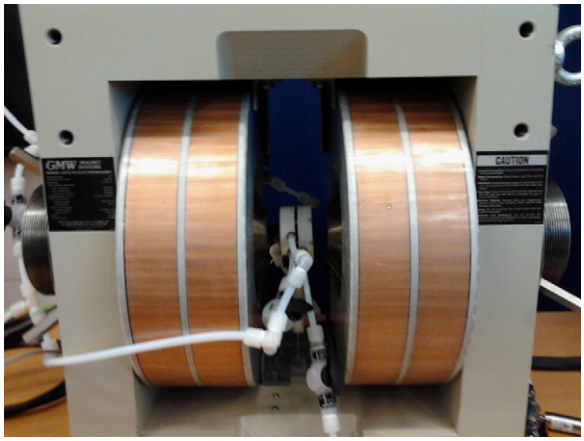


**Fig. 1.** Experimental setup for $CO_2$ separation in the presence of an external magnetic field.

solution-diffusion mechanism [21]:

$$P \propto H \cdot D \tag{1}$$

Gas permeability, $P$ (barrer), was calculated under room temperature and atmospheric pressure from the feed and permeate compartments pressure data as previously described [19] according to:

$$\ln\left(\frac{\left[p_{feed}-p_{perm}\right]_0}{\left[p_{feed}-p_{perm}\right]}\right) = \ln\left(\frac{\Delta p_0}{\Delta p}\right) = \frac{DH\beta}{\delta}.t \tag{2}$$

where $p_{feed}$ and $p_{perm}$ are the pressure in the feed and permeate compartments respectively (Pa), $D$ the diffusivity ($m^2\,s^{-1}$), $H$ the partition coefficient ($-$), $\beta$ the geometric factor ($m^{-1}$), $t$ the time (s) and $\delta$ the membrane thickness (m). Permeability, $P$ (barrer), is obtained from the product of diffusivity and partition coefficient [21] while ideal selectivity can be calculated by the ratio between the permeabilities of two pure different gases.

### 2.3. Experimental viscosity determination

The influence of the application of an external magnetic field in the MILs viscosity is measured using Cannon-Ubbelohde glass capillary viscometers size 5 (9721-R95), 3C (9721-R80) and 4C (9721-R89) depending on each MIL viscosity. These capillaries were manufactured and calibrated by Cannon Instrument Company (USA) having deviations from the mean smaller than $\pm 0.2\%$. Sets of six measurements each were performed. The influence of the application of an external magnetic field in MILs viscosity was also evaluated using the GMW Dipole Electromagnet applying magnetic field intensities from 0 to 2 T.

## 3. Results and discussion

### 3.1. Permeability–viscosity data in the absence of a magnetic field

Gas permeability through SMILMs and MILs viscosity has been measured in the absence of a magnetic field [19]. $CO_2$ permeability was measured using hydrophobic PVDF membranes as supporting material obtaining permeabilities between 117 and 198 barrers. MILs based on the phosphonium cation studied in the current work present viscosity values ranging from 749 to 110,060 cP which are, except the iron based MIL, higher than the phosphonium based RTILs reported in the literature [22].

Fig. 2 shows $CO_2$ permeability versus RTILs viscosity in a log–log plot assuming a constant partition coefficient ($H$). The Wilke–Chang equation [23] considers a strong diffusivity dependence on viscosity of dilute solutions $\left(PH^{-1} \propto D \propto \mu^{-1}\right)$. Additionally, Scovazzo [7] proposed a model where the relationship between $CO_2$ permeability and ionic liquid viscosity in a log–log plot is a line with slope equal to $-0.388$, showing lower viscosity dominance in determining $CO_2$ permeability in SILMs for viscosity values in the range of 25–3000 cP. Present work extends this correlation by including MILs with higher viscosity obtaining a slope of $-0.278$ including the literature data reported in Table 2.

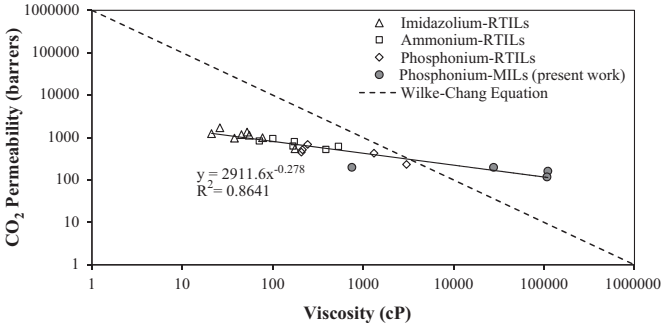


**Fig. 2.** Correlation of $CO_2$ permeability versus viscosity.

### 3.2. Separation performance of SMILMs in the presence of an external magnetic field

The influence of the external magnetic field on membrane permeability was studied for $CO_2$, $N_2$ and air. Permeability was calculated as the linear relationship between the driving force versus time according to Eq. (2) at different magnetic field intensities ranging from 0 to 1.5 T at 298.15 K.

Table 3 shows the $CO_2$, $N_2$ and air permeability, the maximum gas permeability increase ($\Delta P$) at 1.5 T magnetic field intensity, and the gas permeability ratio. The permeation ratio shows that SMILMs are highly selective for $CO_2$ when comparing with $N_2$ and air. The magnetic field leads to slight increase of the gas permeability but it does not show any influence on $CO_2/N_2$ and $CO_2$/air permeability ratio. An increase in gas permeability will decrease the effective membrane area required to perform the gas separation performance while the constant permeability ratio hinders the achievement of the target purity. It is important to note that the presence of an external magnetic field increases the individual gas permeability without changing their permeability ratio.

The Robeson upper bound correlation for $CO_2$ permeability versus ideal $CO_2/N_2$ selectivity [8] was used in order to evaluate the $CO_2/N_2$ separation performance of these systems. Experimental results obtained on this work are below this limit, although the separation performance is enhanced since gas permeability increases in the presence of an external magnetic field. This behaviour may be related to physical properties or molecular structure changes of the ionic liquid immobilised inside the membrane pores in the presence of a magnetic field. Fig. 3 presents $CO_2/N_2$ and $CO_2$/air separation performance enhancement for all the researched systems when a 1.5 T magnetic field is applied.

### 3.3. Permeability dependence on magnetic susceptibility

Gas permeability increases as a function of the applied magnetic field depending on the MILs magnetic susceptibility, ranging from 2.10 to 6.51 emu K $mol^{-1}$. Fig. 4 shows the influence of the permeability increase at 1.5 T for different MILs, depending on their magnetic susceptibility. An increase of 3.27% in permeability can be expected per unit of magnetic susceptibility under 1.5 T of magnetic field applied.

Therefore, the dependence of gas permeability with MILs magnetic behaviour when applying an external magnetic field, confirms the potential to modify gas transport of different species through SMILMs allowing the permeability modulation by tuning the magnetic field.

### 3.4. Influence of the magnetic field on MILs viscosity and $CO_2$ permeability of SMILMs

Fig. 5 shows the behaviour of $CO_2$ permeability ratio, $P_{(B)}/P_{(0)}$, with different magnetic field intensities ranging from 0 to 1.5 T. Again, a magnetic field intensity increase reveals an increase in the gas permeability depending on the MIL magnetic susceptibility. The comparative analysis between all the studied MILs shows a higher effect of the application of an external magnetic field in $CO_2$ permeability for MILs with higher magnetic susceptibility values.

Table 4 presents MILs viscosity in the presence of a magnetic field intensity ranging from 0 to 2 T. Note that viscosity values are two orders of magnitude higher for $[P_{66614}][GdCl_6]$ and three

**Table 2**
Literature data used for the permeability–viscosity correlation shown in Fig. 2.

| Abbreviation | Ionic liquid | $CO_2$ permeability (barrers) | Viscosity (cP) |
|---|---|---|---|
| *Imidazolium-RTILs* [7] | | | |
| [emim][$Bf_4$] | 1-Ethyl-3-methylimidazolium tetrafluoroborate | 968.5 | 37.7 |
| [emim][$Tf_2N$] | 1-Ethyl-3-methylimidazolium bis(trifluoromethanesulfonyl)imide | 1702.4 | 26 |
| [bmim][$Pf_6$] | 1-Ethyl-3-methylimidazolium hexafluorophosphate | 544.3 | 176 |
| [emim][dca] | 1-Ethyl-3-methylimidazolium dicyanamide | 1237.3 | 21 |
| [bmim][$Tf_2N$] | 1-Butyl-3-methylimidazolium bis(trifluoromethanesulfonyl)imide | 1344.3 | 52 |
| [emim][TfO] | 1-Ethyl-3-methylimidazolium trifluoromethanesulfone | 1171.4 | 45 |
| [$C_6$mim][$Tf_2N$] | 1-Hexyl-3-methylimidazolium bis(trifluoromethanesulfonyl)imide | 1135.8 | 55 |
| [bmim][BETI] | 1-Butyl-3-methylimidazolium bis(perfluoroethylesulfonyl)imide | 991.4 | 77 |
| *Ammonium-RTILs* [24] | | | |
| [$N_{1444}$][$Tf_2N$] | Trimethyl(butyl)ammonium bis((trifluoromethyl)sulfonyl)imide | 523.9 | 386 |
| [$N_{4111}$][$Tf_2N$] | Tributhyl(methyl)ammonium bis((trifluoromethyl)sulfonyl)imide | 830.5 | 71 |
| [$N_{6111}$][$Tf_2N$] | Trimethyl(hexyl)ammonium bis((trifluoromethyl)sulfonyl)imide | 943.2 | 100 |
| [$N_{10111}$][$Tf_2N$] | Trimethyl(decyl)ammonium bis((trifluoromethyl)sulfonyl)imide | 800.4 | 173 |
| [$N_{1888}$][$Tf_2N$] | Trioctyl(methyl)ammonium bis((trifluoromethyl)sulfonyl)imide | 619.4 | 532 |
| [$N_{6222}$][$Tf_2N$] | Triethyl(hexyl)ammonium bis((trifluoromethyl)sulfonyl)imide | 630.3 | 167 |
| *Phosphonium-RTILs* [22] | | | |
| [$P_{66614}$][Cl] | Trihexyl(tetradecyl)phosphonium chloride | 426.6 | 1316 |
| [$P_{44414}$][DBS] | Tributyl(tetradecyl)phosphonium dodecylbenzenesulfonate | 231.7 | 3011 |
| [$P_{66614}$][$Tf_2N$] | Trihexyl(tetradecyl)phosphonium bis((trifluoromethyl)sulfonyl)imide | 689.1 | 243 |
| [$P_{66614}$][dca] | Trihexyl(tetradecyl)phosphonium dicyanamide | 513.7 | 213 |
| [$P_{44414}$][DEP] | Tributyl(ethyl)phosphonium diethylphosphate | 453.4 | 207 |
| *Phosphonium-MILs* [b] | | | |
| [$P_{66614}$][$GdCl_6$][a] | Trihexyl(tetradecyl)phosphonium hexachlorogadolinium | 198.8 | 27,650 |
| [$P_{66614}$][$MnCl_4$][a] | Trihexyl(tetradecyl)phosphonium tretrachloromanganese | 161.3 | 110,060 |
| [$P_{66614}$][$FeCl_4$][a] | Trihexyl(tetradecyl)phosphonium tretrachloroferrate | 198.4 | 749 |
| [$P_{66614}$][[$CoCl_4$][a] | Trihexyl(tetradecyl)phosphonium tretrachlorocobalt | 117.9 | 107,700 |

Data for 30 °C otherwise noted.
[a] Data at 20 °C.
[b] Present work.

**Table 3**
Gas permeability (P) increase at 1.5 T intensity magnetic field and gas permeability ratio.

| SMILM | Gas | *P* (barrers) | | ΔP (%) | $P_{CO_2}/P_{N_2}$ | | $P_{CO_2}/P_{air}$ | |
|---|---|---|---|---|---|---|---|---|
| | | 0 T | 1.5 T | | 0 T | 1.5 T | 0 T | 1.5 T |
| [$P_{66614}$][$CoCl_4$] | $CO_2$ | 117.9 ± 4.2 | 124.1 ± 5.1 | 5.2 | 23.7 | 23.6 | 14.1 | 14.2 |
| | $N_2$ | 4.9 ± 0.2 | 5.3 ± 0.2 | 5.6 | | | | |
| | Air | 8.4 ± 0.3 | 8.7 ± 0.4 | 4.1 | | | | |
| [$P_{66614}$][$MnCl_4$] | $CO_2$ | 161.3 ± 4.1 | 177.8 ± 4.3 | 10.2 | 39. | 38.1 | 26.5 | 26.4 |
| | $N_2$ | 4.1 ± 0.1 | 4.7 ± 0.2 | 13.6 | | | | |
| | Air | 6.1 ± 0.3 | 6.7 ± 0.3 | 10.7 | | | | |
| [$P_{66614}$][$FeCl_4$] | $CO_2$ | 198.4 ± 3.9 | 232.2 ± 3.6 | 17.0 | 24.8 | 25.0 | 20.2 | 19.9 |
| | $N_2$ | 8.0 ± 0.2 | 9.3 ± 0.2 | 15.9 | | | | |
| | Air | 9.8 ± 0.4 | 11.6 ± 0.3 | 18.8 | | | | |
| [$P_{66614}$][$GdCl_6$] | $CO_2$ | 198.8 ± 3.5 | 241.8 ± 3.2 | 21.6 | 34.6 | 34.7 | 19.1 | 19.3 |
| | $N_2$ | 5.7 ± 0.2 | 6.9 ± 0.2 | 21.2 | | | | |
| | Air | 10.4 ± 0.3 | 12.5 ± 0.4 | 20.5 | | | | |

for [$P_{66614}$][$CoCl_4$] and [$P_{66614}$][$MnCl_4$] when comparing with [$P_{66614}$][$FeCl_4$].

### 3.5. Permeability–viscosity correlation in the presence of a magnetic field

Fig. 6 shows the relationship between the permeability and viscosity under the magnetic field intensities tested in a dimensionless form referred to the result in the absence of magnetic field. The fitting for all data shows a value close to unity from the slope and therefore, an inverse dependence for all the studied MILs is found following the Wilke–Chang model ($D \propto \mu^{-1}$) [23] This result suggests that the product of permeability and viscosity is a specific constant ($C$) for each SMILM tested and independent of the applied magnetic field according to:

$$P_B \mu_B = P_0 \mu_0 = C(SMILMs) \quad (3)$$

The constant ($C$) obtained from Eq. (3) are reported in Table 5. These numbers describe the constant behaviour of the product permeability–viscosity at different magnetic fields or without magnetic field for each SMILM.

This work has shown the permeability modulation in membranes including MILs in their porous structure. The external magnetic field produces a viscosity variation leading to tunable gas permeability. These innovative results open up the possibility for new developments based on the external magnetic field and permeability modulation in SMILMs.

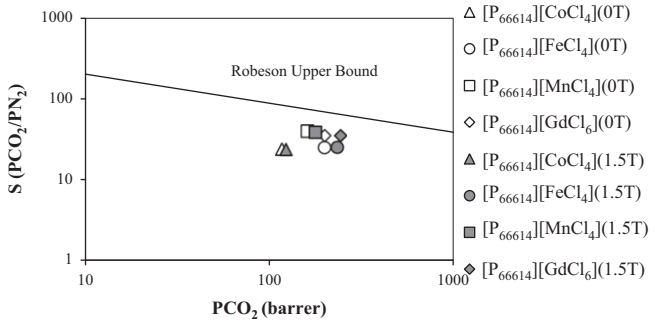


**Fig. 3.** Upper bound correlation for $CO_2/N_2$ separation (1 barrer = $10^{-10}$ cm$^3$ (STP) cm cm$^{-2}$ s$^{-1}$ cm Hg$^{-1}$).

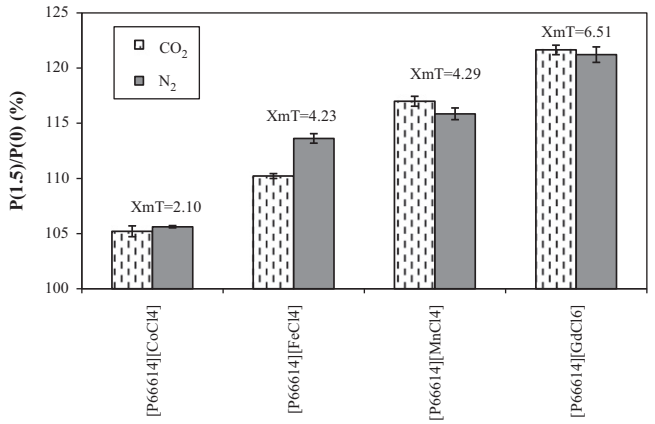


**Fig. 4.** Gas permeability behaviour depending on MILs magnetic susceptibility.

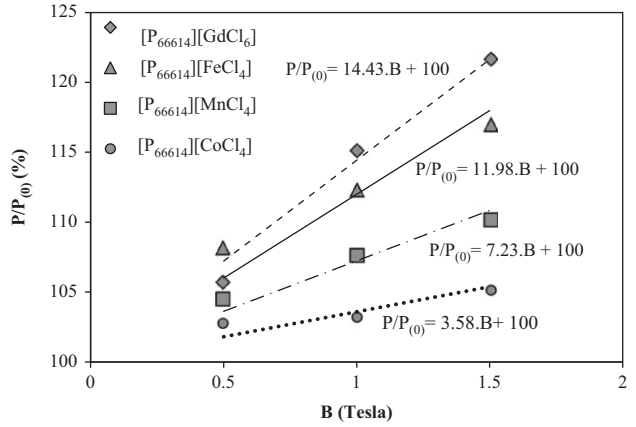


**Fig. 5.** $CO_2$ permeability ratio ($P_{(B)}/P_{(0)}$) at different magnetic field intensities.

In the present study, the permeability modulation by an external magnetic field has been experimentally shown in the $CO_2$, $N_2$ and air permeation through SMILMs.

## 4. Conclusions

This work has been able to show the influence of the external magnetic field application on gas permeability ($CO_2$, $N_2$ and air) through SMILMs in the range of 0–1.5 T. The gas permeability variation is related to the MILs viscosity change. Experimental results show that gas permeability increases as a function of the applied magnetic field depending on the magnetic ionic liquid,

**Table 4**
MILs viscosity at different magnetic field intensities from 0 to 2 T.

| μ (cP) | | | | | |
|---|---|---|---|---|---|
| MILs | 0 T | 0.5 T | 1 T | 1.5 T | 2 T |
| $[P_{66614}][CoCl_4]$ | 107,700 | 95,230 | 94,170 | 93,510 | 88,950 |
| $[P_{66614}][MnCl_4]$ | 110,060 | 108,360 | 107,360 | 105,730 | 100,190 |
| $[P_{66614}][FeCl_4]$ | 749 | 719 | 702 | 693 | 672 |
| $[P_{66614}][GdCl_6]$ | 27,650 | 27,530 | 25,600 | 24,290 | 23,550 |

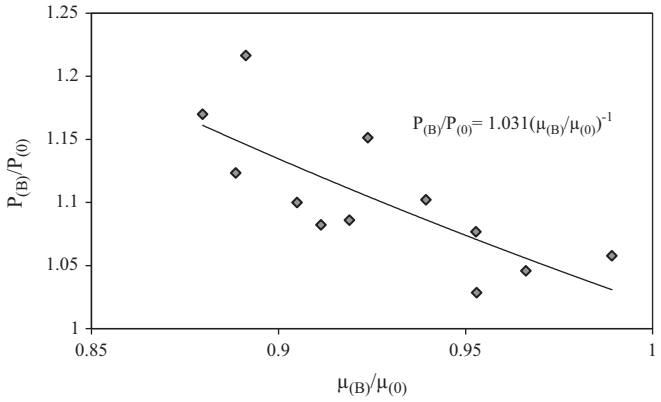


**Fig. 6.** $CO_2$ permeability vs. MILs viscosity ratio.

**Table 5**
Gas permeability–viscosity product for the different SMILMs studied.

| MIL | $C10^{10}$ (kg m s$^{-2}$)=$P_0\mu_0$ |
|---|---|
| $[P_{66614}][CoCl_4]$ | 105 |
| $[P_{66614}][MnCl_4]$ | 147 |
| $[P_{66614}][FeCl_4]$ | 1.23 |
| $[P_{66614}][GdCl_6]$ | 45.6 |

while the permeability ratio $(P_{CO_2}/P_{N_2})$ remains constant. An influence of the magnetic field in MILs viscosity, decreasing as a function of the magnetic field intensity, has been shown. The permeability and viscosity product is a specific constant for each SMILM and independent of the applied magnetic field. The change on gas permeability and MILs viscosity when applying an external magnetic field describes the modulation effect of permeability by tuning the magnetic field intensity.

## Nomenclature

| | |
|---|---|
| $B$ | magnetic field (T) |
| $D$ | diffusivity (m$^2$ s$^{-1}$) |
| $H$ | partition coefficient (−) |

$P$ permeability (barrer)
$p_{feed}$ pressure in the feed compartment (Pa)
$p_{perm}$ pressure in the permeate compartment (Pa)
$t$ time (s)

*Subscripts*

0 absence of magnetic field
$B$ presence of magnetic field

*Greek letters*

$\beta$ geometric factor ($m^{-1}$)
$\delta$ membrane thickness (m)
$\mu$ viscosity (cP)
$\mu_{eff}$ effective magnetic moment (emu K $mol^{-1}$)
$\chi_{mT}$ magnetic susceptibility (emu K $mol^{-1}$)

## Acknowledgements

The authors gratefully acknowledge the financial support from the European Research Action Network—ERANET Projects EUI2008-03857(Spain) and ERA-CHEM/0001/20008(Portugal).

## References

[1] J.E. Bara, C.J. Gabriel, T.K. Carlisle, D.E. Camper, A. Finotello, D.L. Gin, R.D. Noble, Gas separations in fluoroalkyl-functionalized room-temperature ionic liquids using supported liquid membranes, Chem. Eng. J. 147 (2009) 43–50.
[2] P. Luis, L.A. Neves, C.A.M. Afonso, I.M. Coelhoso, J.G. Crespo, A. Garea, A. Irabien, Facilitated transport of $CO_2$ and $SO_2$ through supported ionic liquid membranes (SILMs), Desalination 245 (2009) 485–493.
[3] P. Scovazzo, D. Havard, M. McShea, S. Mixon, D. Morgan, Long-term, continuous mixed gas dry fed $CO_2/CH_4$ and $CO_2/N_2$ separation performance and selectivities for room temperature ionic liquid membranes, J. Membr. Sci. 327 (2009) 41–48.
[4] P. Cserjési, N. Nemestóthy, K. Bélafi-Bakó, Gas separation properties of supported liquid membranes prepared with unconventional ionic liquids, J. Membr. Sci. 349 (1–2) (2010) 6–11.
[5] L.A. Neves, J.G. Crespo, I.M. Coelhoso, Gas permeation studies in supported ionic liquid membranes, J. Membr. Sci. 357 (2010) 160–170.
[6] A. Criscuoli, E. Drioli, Membrane contactors for gaseous streams treatments, in: A.K. Pabby, S.S.H. Rizvi, A.M. Sastre (Eds.), Handbook of Membrane Separations: Chemical, Pharmaceutical, Food, and Biotechnological Applications, CRC Press, Taylor & Francis Group Boca Raton, 2008, pp. 1041–1055.
[7] P. Scovazzo, Determination of the upper limits, benchmarks, and critical properties for gas separations using stabilized room temperature ionic liquid membranes (SILMs) for the purpose of guiding future research, J. Membr. Sci. 343 (2009) 199–211.
[8] L.M. Robeson, The upper bound revisited, J. Membr. Sci. 320 (2008) 390–400.
[9] M.D. Ngugen, L.V. Ngugen, E.H. Jeon, J.H. Kim, M. Cheong, H.S. Kim, J.S. Li, Fe-containing ionic liquids as catalysts for the dimerization of bicycle [2.21] hepta-2,5-diene, J. Catal. 258 (2008) 5–13.
[10] H. Wang, R.Y. Yan, Z.X. Li, X.P. Zhang, S.J. Zhang, Fe-containing magnetic ionic liquid as an effective catalyst for the glycolysis of poly(ethylene terephthalate), Catal. Commun. 11 (2010) 763–767.
[11] A. Branco, L.C. Branco, F. Pina, Electrochromic and magnetic ionic liquids, Chem. Commun. 47 (2011) 2300–2302.
[12] S. Hayashi, H.A. Hamaguchi, Discovery of a magnetic ionic liquid bmim [$FeCl_4$], Chem. Lett. 33 (2004) 1590–1591.
[13] S. Hayashi, S. Saha, H.A. Hamaguchi, A new class of magnetic fluids: bmim[$FeCl_4$] n-bmim[$FeCl_4$] ionic liquids, IEEE Trans. Magn. 42 (2006) 12–14.
[14] R.E. Del Sesto, T.M. McCleskey, A.K. Burrel, G.A. Baker, J.D. Thompson, B.L. Scott., J.S. Wilkes, P. Williams, Structure and magnetic behaviour of transition metal based ionic liquids, Chem. Commun. (2008) 447–449.
[15] M. Okuno, H. Hamaguchi, Magnetic manipulation of materials in a magnetic ionic liquid, Appl. Phys. Lett. 89 (2006) 132506.
[16] S.H. Lee, S.H. Ha, H.B. Jin, C.Y. You, Y. Koo, Magnetic behaviour of mixture of magnetic ionic liquid [bmim][$FeCl_4$] and water, J. Appl. Phys. 101 (2007) 09J102.
[17] Y. Jiang, C. Gou, H. Liu, Magnetically rotational reactor for absorbing benzene emissions by ionic liquids, China Particuology 5 (1–2) (2006) 130–133.
[18] N. Deng, M. Lin, L. Zhao, C. Liu, S. de Rooy, I.M. Warner, Highly efficient extraction of phenolic compounds by use of magnetic room temperature ionic liquids for environmental remediation, J. Hazard. Mater. 192 (3) (2011) 1350–1357.
[19] J. Albo, E. Santos, L.A. Neves, S.P. Simeonov, C.A.M. Afonso, J.G. Crespo, A. Irabien, Separation performance study of $CO_2$ through Supported Magnetic Ionic Liquid Membranes (SMILMs), Sep. Purif. Technol. 98 (2012) 432–440.
[20] I. de Pedro, D.P. Rojas, J. Albo, P. Luis, A. Irabien, J. Blanco, J. Rodriguez, Long-range magnetic ordering in magnetic ionic liquid: emim[$FeCl_4$], J. Phys. Condens. Matter. 22 (2010) 296–306.
[21] E.L. Cussler, Diffusion. Mass Transfer in Fluid Systems, 2nd ed., Cambridge University Press, USA, 1997, pp. 21–23, 434–435, 438–439.
[22] L. Ferguson, P. Scovazzo, Solubility, diffusivity and permeability of gases in phosphonium-based room temperature ionic liquids: data and correlations, Ind. Eng. Chem. Res. 46 (2007) 1369–1374.
[23] C.R. Wilke, P. Chang, Correlation of diffusion coefficients in dilute solutions, AIChE J. (1955) 264–270.
[24] R. Condemarin, P. Scovazzo, Gas permeabilities, solubilities, diffusivities, and diffusivity correlations for ammonium-based room temperature ionic liquids with comparison to imidazolium and phosphonium RTILs data, Chem. Eng. J. 147 (2009) 1369–1374.

## 4.2. Santos E., Albo J., Rosatella A., Afonso C.A.M., Irabien A. Synthesis and characterization of Magnetic Ionic Liquids (MILs) for $CO_2$ separation. *J. Chem. Technol. Biotechnol.* Aceptado.

Resumen

**ANTECEDENTES:** El comportamiento de una nueva generación de líquidos iónicos (LIs) que contienen metales de transición, líquidos iónicos magnéticos (LIMs), está siendo estudiada en la bibliografía. Debido a la etapa inicial de desarrollo de los LIMs, es necesario evaluar sus características con el fin de desarrollar nuevas aplicaciones. En este trabajo, cuatro LIMs basados en el catión trihexil (tetradecil) y diferentes aniones magnéticos ($[P_{66614}]_2[CoCl_4]$, $[P_{66614}][FeCl_4]$, $[P_{66614}]_2[MnCl_4]$ y $[P_{66614}]_3[GdCl_6]$ ) fueron sintetizados y caracterizados mediante la medida de la susceptibilidad magnética, densidad, viscosidad, propiedades térmicas y la solubilidad del dióxido de carbono para la separación de $CO_2$ .

**RESULTADOS:** La susceptibilidad magnética mostró un comportamiento paramagnético en todos los LIMs probados y eran consistentes con otros LIMs reportados en la bibliografía. La densidad y viscosidad fueron obtenidas experimentalmente y se correlacionaron utilizando el software Fitteia. Todos los LIMs estudiados mostraron una muy buena estabilidad térmica, ya que sus temperaturas de descomposición eran superiores a 619 K. La solubilidad de $CO_2$ en los LIMs era inferior al de otros líquidos iónicos estudiados en la bibliografía para la captura de $CO_2$ bajo las mismas condiciones de operación.

**CONCLUSIONES:** Este trabajo proporciona información relacionada con la síntesis y caracterización de LIMs basados en fosfonio y ofrece oportunidades para el desarrollo de nuevas aplicaciones.

*Original abstract*

**BACKGROUND:** The behaviour of a new generation of Ionic Liquids (ILs) containing transition metals, Magnetic Ionic Liquids (MILs), is recently under study in the literature. Due to the early stage of development of MILs, it is necessary to evaluate their characteristics in order to develop new applications. In this work, four MILs based in the trihexyl(tetradecyl)phosphonium cation and different magnetic anions ($[P_{66614}]_2[CoCl_4]$, $[P_{66614}][FeCl_4]$, $[P_{66614}]_2[MnCl_4]$ and $[P_{66614}]_3[GdCl_6]$) were synthesized and characterized by measuring magnetic susceptibility, density, viscosity, thermal properties and carbon dioxide solubility for $CO_2$ separation.

**RESULTS:** The magnetic susceptibility showed a paramagnetic behaviour in all the tested MILs and they were in good agreement with other MILs reported in the literature. MILs density and viscosity were experimentally obtained and correlated using *Fitteia* software. All the studied

MILs showed a very good thermal stability since their decomposition temperatures were higher than 619 K. $CO_2$ solubility in the MILs was lower than other ILs studied in literature for $CO_2$ capture at the same operational conditions.

**CONCLUSIONS:** This work provides further information related to synthesis and characterization of phosphonium-based MILs and offers potential chances in the development of new practical applications.

# Synthesis and characterization of Magnetic Ionic Liquids (MILs) for $CO_2$ separation

Esther Santos[a,*], Jonathan Albo[a], Andreia Rosatella[b], Carlos A.M. Afonso [b,c], Ángel Irabien[a]

[a]*Departamento Ingeniería Química y Química Inorgánica. E.T.S. de Ingenieros Industriales y Telecomunicación. Universidad de Cantabria, 39005. Santander, Spain*

[b] *Research Institute for Medicines and Pharmaceuticals Sciences, Faculdade de Farmácia. Universidade de Lisboa, 1649-003, Lisboa, Portugal.*

[c] *CQFM, Centro de Química-Física Molecular and IN–Institute of Nanosciences and Nanotechnology, Instituto Superior Técnico, 1049-001, Lisboa, Portugal.*

*Corresponding author: Tel: +34 942 206749, Fax: +34 942 201591, email: santosse@unican.es

## Abstract

**BACKGROUND:** The behaviour of a new generation of Ionic Liquids (ILs) containing transition metals, Magnetic Ionic Liquids (MILs), is recently under study in the literature. Due to the early stage of development of MILs, it is necessary to evaluate their characteristics in order to develop new applications. In this work, four MILs based in the trihexyl(tetradecyl)phosphonium cation and different magnetic anions ($[P_{66614}]_2[CoCl_4]$, $[P_{66614}][FeCl_4]$, $[P_{66614}]_2[MnCl_4]$ and $[P_{66614}]_3[GdCl_6]$) were synthesized and characterized by measuring magnetic susceptibility, density, viscosity, thermal properties and carbon dioxide solubility for $CO_2$ separation.

**RESULTS:** The magnetic susceptibility showed a paramagnetic behaviour in all the tested MILs and they were in good agreement with other MILs reported in the literature. MILs density and viscosity were experimentally obtained and correlated using *Fitteia* software. All the studied MILs showed a very good thermal stability since their decomposition temperatures were higher than 619 K. $CO_2$ solubility in the MILs was lower than other ILs studied in literature for $CO_2$ capture at the same operational conditions.

**CONCLUSIONS:** This work provides further information related to synthesis and characterization of phosphonium-based MILs and offers potential chances in the development of new practical applications.

**Keywords:** Magnetic Ionic Liquids (MILs); Synthesis; Characterization; $CO_2$ separation

## INTRODUCTION

Ionic Liquids (ILs) are defined as molten salts, liquid over a wide range of temperature, typically comprised of bulky organic cations and organic or inorganic anions.[1] They

exhibit very interesting physicochemical properties including negligible vapor pressure, non-flammability, high thermal and chemical stability, high conductivity and widely tunable properties by the appropriate selection of the cation or anion in their structure.[2] ILs have received increasing interest in applications in the fields of electrochemistry,[3,4] catalysis[5,6] or separation processes.[7,8] Magnetic Ionic Liquids (MILs) combine the general properties of ILs with magnetic properties associated with the incorporation of a metal ion in their structure, such as a strong response to an external magnetic field.

Until now, few applications for MILs have been shown in the literature. One of the main potential applications of MILs is in the field of the catalytic reactions.[9-13] Efforts have recently been made to obtain stable dispersions of magnetic nanoparticles in ILs.[14-18] MILs have been also investigated as new electrochromic materials for the manufacturing of different electronic devices [19] or as flow battery systems.[20] MILs with poor color contrast upon switching can find applications as contrast agents in Magnetic resonance Image (MRI) for medical diagnostics although this application is limited due to the ionic liquids toxicity.[21]

MILs are starting to attract a wide interest in the field of separation processes. [22-27] Jiang et al. in 2006 [22] showed a benzene solubility increase in the paramagnetic MIL [bmim][$FeCl_4$] when applying a rotational magnetic field. Okuno et al. in 2006 [23] demonstrated the possibility of magnetic transport of a gas in MILs, illustrated by the change in $N_2$ bubbles trajectory of in the presence of a magnetic field. Lee et al. in 2007 [24] as well as Wang at al. in 2010 [25] investigated the recovery of [bmim][$FeCl_4$] from its mixture with water. Deng et al. in 2011 [26] studied the use of the MIL [$3C_6PC1_4$][$FeCl_4$] as an extraction solvent for the separation of phenolic compounds from aqueous solution in the presence of a neodymium magnet. Wang et al. in 2012 [27] investigated the use of [bPy][$FeCl_4$] as an effective extractant for extracting asphaltene fractions from coal direct liquefaction residues (CDLR). In a previous work, [28] they were prepared a new class of supported liquid membranes based on magnetic ionic liquids: Supported Magnetic Ionic Liquids Membranes (SMILMs) for $CO_2$ separation. The influence of the application of an external magnetic field on $CO_2/N_2$ and $CO_2$/air permeability through SMILMs in the range of 0-1.5 Tesla was evaluated. [29] An increase in the gas permeability was observed due to MILs viscosity decrease depending on the MILs magnetic susceptibility. Experimental results confirmed the potential for a gas permeability modulation through supported liquid membranes by tuning the magnetic field intensity.

In the present work, four MILs containing the trihexyl (tetradecyl) phosphonium cation and different magnetic anions were synthesized and characterized in order to treat flue gas streams in post-combustion $CO_2$ capture processes at high temperatures. The following properties were evaluated: (1) *Magnetic susceptibility* in order to determine the influence of the application of an external magnetic field to MILs containing different transition metals in their structure; (2) MILs *viscosity* since this property is modified in the presence of an external magnetic field; (3) the influence of temperature by the evaluation of MILs *thermal properties* due to different membrane behavior at

increasing temperature; (4) the *carbon dioxide solubility* to assess the use of these MILs for $CO_2$ capture.

## MATERIALS AND METHODS

### Materials

All solvents used in MILs synthesis were distilled prior use. Trihexyl(tetradecyl)phosphonium chloride was kindly donated by CYTEC. Cobalt (II) chloride, iron (III) chloride, manganese (II) chloride and gadolinium (III) chloride were purchased from Sigma-Aldrich and used without further purification. A series of ionic liquids based in the trihexyl(tetradecyl)phosphonium cation and containing different paramagnetic anions were synthesized in *Faculdade de Farmácia, Universidade de Lisboa (Portugal)* and studied in the present work. Their main characteristics are listed in Table 1.

**Table 1.** Characteristics of the studied MILs.

| Name | Abbreviation | Appearance | Molecular weight/ g.mol$^{-1}$ | Structure |
|---|---|---|---|---|
| Trihexyl(tetradecyl) phosphonium tetrachlorocobalt | $[P_{66614}][CoCl_4]$ |  | 1112 | 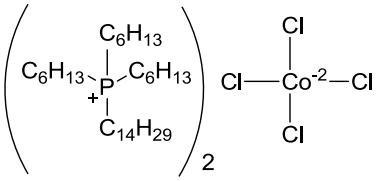 |
| Trihexyl(tetradecyl) phosphonium tetrachloroferrate | $[P_{66614}][FeCl_4]$ | 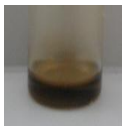 | 681.51 | 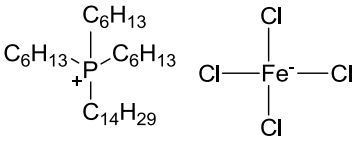 |
| Trihexyl(tetradecyl) phosphonium tetrachloromanganese | $[P_{66614}][MnCl_4]$ |  | 1103 | 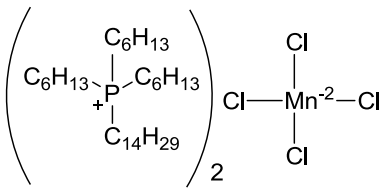 |
| Trihexyl(tetradecyl) phosphonium hexachlorogadolinium | $[P_{66614}][GdCl_6]$ | 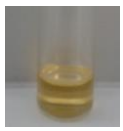 | 1821.54 | 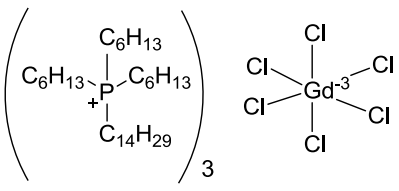 |

The ionic liquids were prepared according to published procedures.[30] To a solution of $[P_{66614}][Cl]$ (50 g, 0.096 mol) in dichloromethane was added cobalt (II) chloride (11.45 g, 0.5 equiv.), iron (III) chloride (26.02 g, 1 equiv.), manganese chloride (26.02 g, 0.5 equiv.) or gadolinium (III) chloride hexahydrate (11.92 g, 0.3 equiv.). The solution was stirred at room temperature for 24h. After that, two layers were formed, and the aqueous phase was decanted. The organic phase was dried over $MgSO_4$ and filtered. The solvent was removed under vacuum, and the IL stirred under vacuum (<1 mmHg) at 60°C overnight.

**$[P_{66614}]_2[CoCl_4]$** was obtained as a blue viscous oil, yield 52.87g (94%) (Elemental analysis for $C_{64}H_{140}Cl_4CoO_2P_2$. Calcd: C, 63.82; H, 11.74; %; found: C, 63.70; H, 11.62 %.);

**$[P_{66614}][FeCl_4]$** was obtained as brown viscous oil, yield 64.30g (98%), (Elemental analysis for $C_{32}H_{68}Cl_4FeP$. Calcd: C, 56.40; H, 10.06; %; found: C, 56.76; H, 10.28 %.);

**$[P_{66614}]_2[MnCl_4]$** was obtained as a green viscous oil, yield 53.8g (96%), (Elemental analysis for $C_{64}H_{136}Cl_4MnP_2$. Calcd: C, 66.01; H, 11.77; %; found: C, 66.31; H, 11.82 %.);

**$[P_{66614}]_3[GdCl_6]$** was obtained as a colourless viscous oil, yield 56.12g (96%), (Elemental analysis for $C_{96}H_{204}Cl_6GdP_3$. Calcd: C, 63.30; H, 11.29; %; found: C, 63.21; H, 11.40 %.).

The water content of the MILs measured by Karl–Fisher titration method were 0.00051 %wt for $[P_{66614}]_2[CoCl_4]$, 0.35 %wt $[P_{66614}]_2[MnCl_4]$ and 0.2 %wt $[P_{66614}]_3[GdCl_6]$. In the case of $[P_{66614}][FeCl_4]$ the water content was determined gravimetrically weighting 1 mL before and after 48 hours of vacuum and heating obtaining 1.02 %wt.

## Characterization of MILs

Magnetic susceptibility measurements were provided by *Magnetism in Matter group* at *CITIMAC (Universidad de Cantabria)* using a Quantum Design MPMS (SQUID) magnetometer. The magnetic susceptibilities were measured at 300 K in the magnetic field range of -85 to 85 kOe. Additionally, the temperature dependence of the magnetization was tested from 2 to 300 K under an applied magnetic field of 1 kOe.

The density of MILs was measured gravimetrically with a 10 mL pycnometer at temperatures ranging from 293.15 to 323.15 K using distilled water as working liquid. The experimental viscosities were measured using a rheometer (Haake RS75) from *Instituto Superior de Agronomia (ISA) (Universidade Técnica Lisboa)* covering the range of temperature 293.15-373.15 K.

TGA analyses were carried out using a TGA-60H Shimazdu thermobalance in a nitrogen ($N_2$) atmosphere at temperatures ranging from room temperature to 873.15 K with a heating rate of 5 $K \cdot min^{-1}$. Differential Scanning Calorimetry analyses (DSC)

were performed using a DSC SETARAM Setsys Evolution by heating from 300.15 to 3123.15 K under $N_2$ atmosphere at 5 $K \cdot min^{-1}$.

$CO_2$ solubility in the MILs was evaluated using a TGA-60H Shimazdu thermobalance where simultaneous thermogravimetry/differential thermal (TG/DTA) analyses were performed. A molecular sieve trap was installed to remove trace amount of water from the feed gas. The sample temperature was measured with an accuracy of ± 0.1 K and the TG sensivity was about 1 µg. The experimental conditions were a $CO_2$ flow rate of 50 $ml \cdot min^{-1}$, room temperature and atmospheric pressure.

## RESULTS AND DISCUSSION

### Magnetic susceptibility

The magnetic susceptibility measurements were considered to quantify the degree of magnetization of MILs containing different transition metals in their structure in response to an applied external magnetic field. The magnetic susceptibility of the studied MILs was measured at 300 K in the magnetic field range of -85 to 85 kOe. The results are shown in Fig. 1. The straight line obtained between the magnetic susceptibility and the applied magnetic field indicates the paramagnetic behaviour of the four studied MILs. From the slope of the linear fit to the data the magnetic susceptibilities of $[P_{66614}]_2[CoCl_4]$, $[P_{66614}][FeCl_4]$, $[P_{66614}]_2[MnCl_4]$ and $[P_{66614}]_3[GdCl_6]$ were determined and presented in Table 2. Moreover, the temperature dependence of the magnetization from 2 to 300 K at 1 kOe was determined. The four tested MILs followed the Curie-Weiss law as shown in Fig. 2. [31]

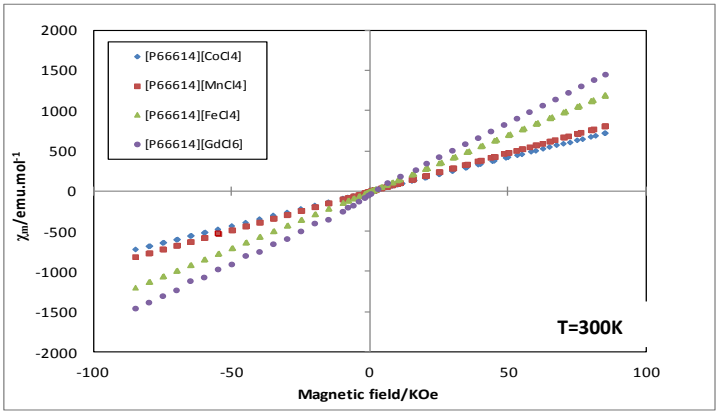


**Fig. 1.** Magnetization of MILs as a function of applied magnetic field at 300 K.

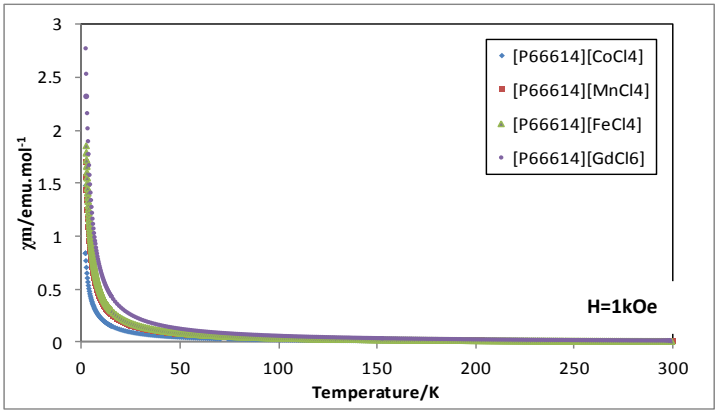


**Fig. 2.** Magnetization of MILs as a function of temperature under an applied magnetic field of 1kOe.

**Table 2.** Magnetic susceptibility of the studied MILs.

| Anion | Cation | χmT /emu K·mol$^{-1}$ | Reference |
|---|---|---|---|
| $[CoCl_4]$ | $[P_{66614}]$ | 2.10 | Present work |
| | $[PR_4]$ | 2.48 | Del Sesto et al. 2008 [30] |
| $[Co(NCS)_4]$ | $[PR_4]$ | 2.06 | Del Sesto et al. 2008 [30] |
| $[MnCl_4]$ | $[P_{66614}]$ | 4.23 | Present work |
| | $[PR_4]$ | 4.22 | Del Sesto et al. 2008 [30] |
| $[FeCl_4]$ | $[P_{66614}]$ | 4.29 | Present work |
| | [Bmim] | 4.11 | Hayashi et al. 2006 [32] |
| | $[C_{10}mim]$ | 4.01 | Del Sesto et al. 2008 [30] |
| | $[PR_4]$ | 4.34 | Del Sesto et al. 2008 [30] |
| | [Nbmim] | 4.34 | Hayashi et al. 2006 [32] |
| $[GdCl_6]$ | $[P_{66614}]$ | 6.51 | Present work |
| | $[PR_4]$ | 7.72 | Del Sesto et al. 2008 [30] |
| $[Dy\text{-}(SCN)_6(H_2O)_2]$ | $[C_6mim]_3$ | 13.41 | Mallick et al. 2008 [33] |
| $[Dy\text{-}(SCN)_7(H_2O)]$ | $[C_6mim]_4$ | 14.00 | Mallick et al. 2008 [33] |
| $[Dy\text{-}(SCN)_8]$ | $[C_6mim]_5$ | 14.00 | Mallick et al. 2008 [33] |

The experimental results are in good agreement with magnetic moments (χmT) reported in the literature for [$CoCl_4$] (2.06-2.48 emu K·$mol^{-1}$), [$FeCl_4$] (4.01-4.34 emu K·$mol^{-1}$), [$MnCl_4$] (4.22 emu K·$mol^{-1}$) and [$GdCl_6$] (7.72 emu K·$mol^{-1}$) .[30-32] Hayashi et al. in 2006 [32] reported for the first time the response of 1-butyl-3-methylimidazolium tetrachloroferrate ([bmim][$FeCl_4$]) and 1-butyronitrile-3-methylimidazolium tetrachloroferrate ([n-bmim][$FeCl_4$]) to an external neodymium magnet of about 0.55 Tesla founding a new class of IL with an unexpectedly strong response to a magnet at room temperature . Del Sesto et al. in 2008 [30] studied MILs based on different transition metals such as iron, cobalt, manganese or gadolinium resulting in a paramagnetic response with potential applications for magnetic and electrochromic switching. Additionally, Mallick et al. in 2008 [33] synthesized dysprosium-based MILs with an effective magnetic moment which approximately doubled the value of iron (III). The incorporation of these lanthanide ions provides the basis for the development of new MILs with improved magnetic properties which exhibits better response to an external magnetic field.

## Density and viscosity

Density and viscosity are fundamental physical properties of ILs. The information on the thermophysical properties of ILs and their temperature dependence is essential for most industrial applications. In the case of viscosity, is higher for most ILs when comparing with common organic solvents. Additionally, this property may be adjusted by the appropriate selection of the cation-anion combination leading to ILs with lower or higher viscosity depending on the application requirements.

The experimental results of density and viscosity for the MILs at different temperatures are presented in Table 3. As expected, both physical properties decreased with an increase in temperature.

**Table 3.** Experimental density (ρ) and viscosity (μ) of MILs at different temperatures.

| T/K | $[P_{66614}]_2[CoCl_4]$ | | $[P_{66614}][FeCl_4]$ | | $[P_{66614}]_2[MnCl_4]$ | | $[P_{66614}]_3[GdCl_6]$ | |
|---|---|---|---|---|---|---|---|---|
| | ρ/g.$cm^{-3}$ | μ/cP | ρ/g.$cm^{-3}$ | μ/cP | ρ/g.$cm^{-3}$ | μ/cP | ρ/g.$cm^{-3}$ | μ/cP |
| 293.15 | 0.965 | 123500 | 1.012 | 790 | 0.956 | 112300 | 0.983 | 28230 |
| 298.15 | 0.962 | 83450 | 1.008 | 650 | 0.949 | 75230 | 0.981 | 18390 |
| 303.15 | 0.959 | 40250 | 1.004 | 520 | 0.943 | 41560 | 0.979 | 13010 |
| 323.15 | - | 15360 | - | 230 | - | 13970 | - | 2890 |
| 373.15 | - | 11050 | - | 44 | - | 920 | - | 290 |

The experimental density data at different temperatures was correlated according to equation (1): [34]

$$\rho = \frac{M}{NV(a+bT+cP)} \quad (1)$$

where $\rho$ is the density in g.cm$^{-3}$, $M$ the molecular weight in g.mol$^{-1}$, $N$ the Avogadro constant in mol$^{-1}$, $V$ the molar volume in A$^3$, $T$ the temperature in K, $P$ the pressure in MPa and $a$, $b$ and $c$ the estimated coefficients.

Equation 1 can be simplified considering atmospheric pressure and can be rewritten including the parameters α and β as follows:

$$\rho = \frac{1}{\alpha+\beta T} \quad (2)$$

where $\alpha = \frac{NV(a+cP)}{M}$ in A.Kg$^{-1}$ and $\beta = \frac{NVb}{M}$ in A.K$^{-1}$.Kg$^{-1}$.

Table 4 presents the α and β values estimated within a 95% confidence range using *Fitteia* software for equation 2. The overall mean percentage deviation (MPD) of calculated densities is 0.22% which is consistent with the reported values in literature for a similar study (0.29%).[34]

**Table 4.** Fitting parameters of equation 2 to correlate MILs density.

| MILs | **α** | **β** | **MPD /%** |
|---|---|---|---|
| $[P_{66614}]_3[GdCl_6]$ | 9.3x10$^{-4}$ | 3.1x10$^{-7}$ | 0.25 |
| $[P_{66614}]_2$ $[MnCl_4]$ | 5.8x10$^{-4}$ | 1.6x10$^{-6}$ | 0.28 |
| $[P_{66614}]$ $[FeCl_4]$ | 7.6x10$^{-4}$ | 7.7 x10$^{-7}$ | 0.21 |
| $[P_{66614}]_2$ $[CoCl_4]$ | 8.2x10$^{-4}$ | 7.4x10$^{-7}$ | 0.14 |
| Overall MPD | | | 0.22 |

The viscosity of MILs is estimated using the Orrick-Erbar model[35] described by equation 3:

$$\ln\left(\frac{\mu}{\rho * M}\right) = A + \frac{B}{T} \quad (3)$$

where $\mu$ is the viscosity in cP, $\rho$ is the density in g.cm$^{-3}$, $M$ is the molecular weight in g.mol$^{-1}$, T is the temperature in K and A and $B$ are the Orrick-Erbar parameters.

Table 5 presents the A and B values estimated within a 95% confidence range using *Fitteia* software for equation 3. The overall MDP of calculated viscosities is 7.64% which is similar to the 7.78% obtained for a similar study of ILs from the literature.[34]

**Table 5.** Fitting parameters of equation 3 to correlate MILs viscosity.

| MILs | **A** | **B** | **MPD/%** |
|---|---|---|---|
| $[P_{66614}]_3[GdCl_6]$ | -18.39 | 6172.05 | 8.13 |
| $[P_{66614}]_2$ $[MnCl_4]$ | -16.98 | 6328.50 | 4.04 |
| $[P_{66614}]$ $[FeCl_4]$ | -12.78 | 3745.09 | 1.47 |
| $[P_{66614}]_2$ $[CoCl_4]$ | -4.58 | 2530.10 | 16.93 |
| Overall MPD | | | 7.64 |

## Thermal properties

The thermal properties of MILs were investigated by use of thermogravimetric analysis (TGA) and differential scanning calorimetry (DSC) in $N_2$ atmosphere. Experimental results are shown in Fig. 3. From TGA curve it can be concluded that MILs are thermally stable up to temperatures ranging from 619-655 K under $N_2$ atmosphere which suggests that all of these MILs have good thermal stabilities. A one-stage thermal decomposition process was observed for all the MILs studied. The onset temperature ($T_{onset}$) calculated as the intersection of the baseline weight from the beginning of the experiment and the tangent of the weight vs temperature curve as decomposition occurs was determined for each MIL and is reported in Table 6.

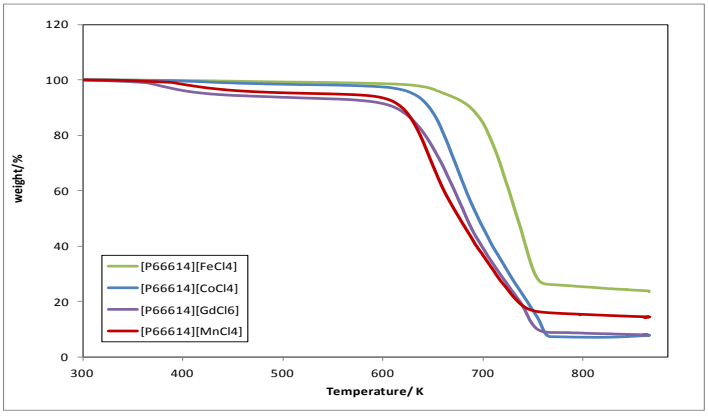


**Fig. 3.** TGA plot for MILs in the temperature range ambient to 873.15K at a scan rate of 5 $K.min^{-1}$.

**Table 6.** Decomposition temperatures of the studied MILs.

| MILs | $T_{onset}$ /K | Reference |
|---|---|---|
| $[P_{66614}]_2[CoCl_4]$ | 646 | Present work |
| $[P_{66614}][FeCl_4]$ | 655 | Present work |
| $Fe((OHCH_2CH_2)_2NH)_6(CF_3SO_3)_3$ | 533 | Anderson et al. 2010 [36] |
| $[3C_6PC1_4]$ $[FeCl_4]$ | 623 | Deng et al. 2011 [26] |
| $[C_2mim][FeCl_4]$ | 623 | Bäcker et al. 2011 [37] |
| $[P_{66614}]_2[MnCl_4]$ | 619 | Present work |
| $[P_{66614}]_3[GdCl_6]$ | 625 | Present work |

The experimental results are in good agreement with those reported in literature. [26, 36-37] From the DSC plot (not shown) an initial loss of water at 300 and 308 K was observed for $[P_{66614}]_2[CoCl_4]$ and $[P_{66614}]_3[GdCl_6]$ respectively. No melting points of the MILs were found in the temperature range studied. A different behavior was shown for the $[P_{66614}]$ $[FeCl_4]$ when comparing with the rest of the studied MILs. Above 600K an exothermic peak for the $[P_{66614}]$ $[FeCl_4]$ was observed possible related to the formation of chlorine compounds while endothermic peaks were found for the rest of studied MILs. All the studied MILs showed a very good thermal stability since their decomposition temperatures were higher than 619 K, which makes them resistant materials for the treatment of hot flue gas streams.

## $CO_2$ solubility

Carbon dioxide solubility was determined to evaluate the use of these MILs for $CO_2$ capture as an alternative to traditional solvents. Whether employed in conventional absorbers or in supported liquid membrane systems, the use of MILs as gas separation medium requires the knowledge of $CO_2$ solubility in these solvents. For the development of $CO_2$ solubility measurements, a sample of the MIL (30 µl) was placed in an open alumina pan programmed to hold at 298.15 K for 180 minutes when applying a $CO_2$ gas flow rate of 50 ml·min$^{-1}$. To release $CO_2$ from the liquid, $N_2$ was used as a sweep gas at 100 ml·min$^{-1}$ flow rate. Each experiment was performed three times and results were determined within a 95% confidence range. Experimental results are shown in Table 7. It is worth mentioning that $CO_2$ solubility in the MILs was very low when comparing with other ILs studied in literature for $CO_2$ capture at the same operational conditions (T=298K, P=1atm), [38,39] but they may show an influence under the application of an external magnetic field.

**Table 7.** $CO_2$ solubility in MILs at 298.15K.

| MIL | $CO_2$ solubility /%wt. |
|---|---|
| $[P_{66614}]_2[CoCl_4]$ | 0.40 |
| $[P_{66614}][FeCl_4]$ | 0.50 |
| $[P_{66614}]_2[MnCl_4]$ | 0.36 |
| $[P_{66614}]_3[GdCl_6]$ | 0.25 |

## CONCLUSIONS

Four types of MILs containing the trihexyl(tetradecyl)phosphonium cation and different magnetic anions were synthesized and characterized by means of magnetic susceptibility, density, viscosity, thermal properties and carbon dioxide solubility for $CO_2$ separation. Magnetic susceptibilities were measured at 300K and different magnetic field intensities obtaining a paramagnetic behavior for all the studied MILs. The magnetization dependence with temperature was also investigated between 2 to 300 K at 1 kOe. All the tested MILs showed very good thermal stability with decomposition temperatures ranging from 619-655 K. $CO_2$ solubility in the MILs was lower than other ILs studied in literature for $CO_2$ capture at the same operational conditions. Therefore, this work supplies useful information of MILs synthesis and characterization for future MILs practical applications.

## NOMENCLATURE

| | |
|---|---|
| A, B | parameters of Orrick-Erbar model |
| T | temperature (K) |
| M | molecular weight ($g.mol^{-1}$) |
| N | Avogadro number ($mol^{-1}$) |
| V | molar volume ($A^3$) |
| P | pressure (MPa) |
| a,b,c | coefficients of density equation |

*Greek letters*

| | |
|---|---|
| $\chi mT$ | magnetic susceptibility (emu K $mol^{-1}$) |
| $\mu$ | viscosity (cP) |
| $\rho$ | density ($g.cm^{-3}$) |

$\alpha$ , $\beta$ fitted parameters density correlation

## ACKNOWLEDGEMENTS

The authors gratefully acknowledge the financial support from the European Research Action Network- ERANET Project EUI2008-03857 (Spain) and ERA-CHEM/0001/2008 (Portugal) and the Spanish Ministry of Economy and Competiveness Project ENE2010-14828. The authors would like to thank Dr. Vitor Alves from Instituto Superior de Agronomia (ISA) - Universidade Técnica Lisboa for the assistance with the MILs viscosity measurements.

## REFERENCES

1 Seddon KR, Ionic liquids for clean technology. *J Chem Tech Biotechnol* **68**: 351-356 (1997).

2 Earle MJ, Esperança JMSS, Gilea MA, Canongia Lopes JN, Rebelo LPN, Magee JW, Seddon KR, Widegren JA, The distillation and volatility of ionic liquids. *Nature* **439:** 831-834 (2006).

3 Buzzeo MC, Evans RG, Compton RG, Non-haloaluminate room-temperature ionic liquids in electrochemistry-A review. *Chem Phys Chem* **5:** 1106-1120 (2004).

4 MacFarlane DR, Forsyth M, Howlett PC, Pringle JM, Sun J, Annat G, Neil W, Izgorodina EI, Ionic liquids in electrochemical devices and processes: managing interfacial electrochemistry. *Acc Chem Res* **40:** 1165-1173 (2007).

5 Pârvulescu VI, Hardacre C, Catalysis in ionic liquids. *Chem Rev* **107:** 2615-2665 (2007).

6 Hallett JP, Welton T, Room-temperature ionic liquids: solvents for synthesis and catalysis. 2. *Chem Rev* **111:** 3508-3576 (2011).

7 Han X, Armstrong DW, Ionic liquids in separations. *Acc Chem Res* **40:** 1079-1086 (2007).

8 Baltus RE, Counce RM, Culbertson BH, Luo H, DePaoli DW, Dai S, Duckworth DC, Examination of the potential of ionic liquids for gas separations. *Sep Sci Technol* **40:** 525-541 (2005).

9 Valkenberg MH, De Castro C, Hölderich WF, Friedel-Crafts acylation of aromatics catalysed by supported ionic liquids. *Appl Catal A* **215:** 185-190 (2001).

10 Tilve RD, Alexander MV, Khandekar AC, Samant SD, Kanetkar VR, Synthesis of 2, 3-unsaturated glycopyranosides by Ferrier rearrangement in $FeCl_3$ based ionic liquid. *J Mol Catal A* 223**:** 237-240 (2004).

11 Nguyen MD, Nguyen LV, Jeon EH, Kim JH, Cheong M, Kim HS, Lee JS, Fe-containing ionic liquids as catalysts for the dimerization of bicyclo [2.2.1] hepta-2,5-diene. *J Catal* **258:** 5-13 (2008).

12 Wang H, Yan R, Li Z, Zhang X, Zhang S, Fe-containing magnetic ionic liquid as an effective catalyst for the glycolysis of poly (ethylene terephthalate). *Catal Commun* **11:** 763-767 (2010).

13 Misuka V, Breuch D, Löwe H, Paramagnetic ionic liquids as "liquid fixed-bed" catays ts in flow applications. *Chem Eng J* **173:**536-540 (2011).

14 Oliveira FCC, Rossi LM, Jardin RF, Rubim JC, Magnetic fluids based on $\gamma$-$Fe_2O_3$ and $CoFe_2O_4$ nanoparticles dispersed in ionic liquids. *J Phys Chem C* **113:** 8566-8572 (2009).

15 Jain N, Zhang X, Hawkett BS, Warr GG, Stable and water-tolerant ionic liquid ferrofluids. *Appl Mater Interfaces* **3:** 662-667 (2011).

16 Rodriguez-Arco L, Lopez-Lopez MT, Gonzalez-Caballero F, Duran JDG, Steric repulsion as a way to achieve the required stability for the preparation of ionic liquid-based ferrofluids. *J Colloid Interface Sci* **357:** 252-254 (2011).

17 Rodriguez-Arco L, Lopez-Lopez MT, Duran JDG, Zubarev A, Chirikov DJ, Stability and magnetorheological behaviour of magnetic fluids based on ionic liquids. *J Phys: Condens Matter* **23:** 455101-455116 (2011).

18 Medeiros AMMS, Parize AL, Oliveira VM, Neto BAD, Bakuzis AF, Sousa MH, Rossi LM, Rubim JC, Magnetic ionic liquids produced by the dispersion of magnetic nanoparticles in 1 - n - Butyl-3-methylimidazolium bis(trifluoromethanesulfonyl)imide ($BMI.NTf_2$). *Appl Mater Interfaces* **4:** 5458-5465 (2012).

19 Branco A, Branco LC, Pina F, Electrochromic and magnetic ionic liquids. *Chem Commun* **47:** 2300-2302 (2011).

20 Arora P, Zhang Z, Battery separators. *Chem Rev* **104:** 4419-4462 (2004).

21 Lowe MP, Activated MR contrast agents. *Curr Pharm Biotechnol* **5:** 519-528 (2004).

22 Jiang Y, Gou C, Liu H, Magnetically rotational reactor for absorbing benzene emissions by ionic liquids. *China Particuology* **5:** 130-133 (2007).

23 Okuno M, Hamaguchi H, Hayashi S, Magnetic manipulation of materials in a magnetic ionic liquid. *Appl Phys Lett* **89:** 132506-132508 (2006).

24 Lee SH, Ha SH, You CY, Koo YM, Recovery of magnetic ionic liquid $[bmim]FeCl_4$ using electromagnet. *Korean J Chem Eng* **24:** 436-437 (2007).

25 Wang M, Li B, Zhao C, Quian X, Xu Y, Chen G, Recovery of $[BMIM]FeCl_4$ from homogeneous mixture using a simple chemical method. *J Chem Eng* **27:** 1275-1277 (2010).

26 Deng N, Lin M, Zhao L, Liu C, de Rooy SL, Warner IM, Highly efficient extraction of phenolic compounds by use of magnetic room temperature ionic liquids for environmental remediation. *J Hazard Mater* **192:** 1350-1357 (2011).

27 Wang J, Yao H, Nie Y, Bai L, Zhang X, Li J, Application of iron-containing magnetic ionic liquids in extraction process of coal direct liquefaction residues. *Ind Eng Chem Res* **51:** 3776-3782 (2012).

28 Albo J, Santos E, Neves LA, Simeonov SP, Afonso CAM, Crespo JG, Irabien A, Separation performance study of $CO_2$ through Supported Magnetic Ionic Liquid Membranes (SMILMs). *Sep Pur Technol* **97:** 26:33 (2012).

29 Santos E, Albo J, Daniel CI, Portugal CAM, Crespo JG, Irabien A, Permeability modulation of Supported Magnetic Ionic Liquid Membranes (SMILMs) by an external magnetic field. *J Membr Sci* **430:** 56-61 (2013).

30 Del Sesto RE, McCleskey TM, Burrel AK, Baker GA, Thompson JD, Scott BL, Wilkes JS, Williams P, Structure and magnetic behaviour of transition metal based ionic liquids. *Chem Commun* 447-449 (2008).

31 De Pedro I, Rojas DP, Albo J, Luis P, Irabien A, Blanco J, Rodriguez J, Long-range magnetic ordering in magnetic ionic liquid: Emim[$FeCl_4$]. *J Phys: Condens Matter* **22:** 296-306 (2010).

32 Hayashi S, Saha S, Hamaguchi HA, A new class of magnetic fluids: bmim[$FeCl_4$] n-bmim [$FeCl_4$] ionic liquids. *IEEE Trans Magn* **42:** 12-14 (2006).

33 Mallick B, Balke B, Felser C, Mudring A-V, Dysprosium room temperature ionic liquids with strong luminescence and response to magnetic fields. *Angew Chem Int Ed* **47:** 7635-7638 (2008).

34 Gardas RL, Coutinho JAP, A group contribution method for viscosity estimation of ionic liquids. *Fluid Phase Equilib* **266:** 195-201 (2008).

35 Reid RC, Prausnitz JM, Sherwood TK, The Properties of Gases and Liquids, ed McGraw-Hill: New York (1987).

36 Anderson TM, Ingersoll D, Rose AJ, Staiger CL, Leonard JC, Synthesis of an ionic liquid with an iron coordination cation. *Dalton Trans* **39:** 8609-8612 (2010).

37 Bäcker T, Breunig O, Valldor M, Merz K, Vasylyeva V, Mudring A-V, In-situ crystal growth and properties of the magnetic ionic liquid [$C_2$mim][$FeCl_4$]. *Cryst Growth Des* **11:** 2564-2571 (2011).

38 Shiflett MB, Yokozeki A, Phase behavior of carbon dioxide in ionic liquids: [emim][Acetate], [emim][Trifluoroacetate], and [emim][Acetate] + [emim][Trifluoroacetate] mixtures. *J Chem Eng Data* **54:** 108-114 (2009).

39 Shiflett MB, Kasprzak DJ, Junk CP, Yokozeki A, Phase behavior of {carbon dioxide + [bmim][Ac]} mixtures. *J Chem Therm* **40:** 25-31 (2008).

## 4.3. Santos E., Albo J., Irabien A. Acetate based Supported Ionic Liquid Membranes (SILMs) for $CO_2$ separation: Influence of the temperature. *J. Membr. Sci.* 2014, 452, 277-283.

Resumen

Se prepararon membranas soportadas con líquidos iónicos (MSLIs) utilizando los líquidos iónicos basados en el anión acetato 1-etil-3-metil imidazolio acetato ([Emim][Ac]), 1-butil-3-metil imidazolio acetato ([Bmim][Ac]) y el monómero vinilbencil trimetilamonio ([Vbtma][Ac]) con el fin de realizar la separación selectiva de dióxido de carbono ($CO_2$) de nitrógeno ($N_2$). Los LIs fueron soportados en en una membrana porosa de fluoruro de polivinilideno y se relaizaron los experimentos de permeación en el rango de temperatura de 298 a 333 K. La permeabilidad de gas aumenta con la temperatura, mientras que un aumento de la temperatura conduce a una disminución en la selectividad $CO_2/N_2$ para todos los LIs estudiados. Se evaluó la solubilidad del $CO_2$ en el rango de 298 a 333 K y presión atmosférica utilizando técnicas termogravimétricas. Los coeficientes de difusividad se calculan en base a la teoría de solución-difusión a partir de los datos de permeabilidad y solubilidad. La influencia de la temperatura en la permeabilidad, solubilidad y difusividad están bien descritas en términos de las relaciones exponenciales Arrhenius-van't Hoff.

*Original abstract*

Supported Ionic Liquid Membranes (SILMs) were prepared with the acetate based Room Temperature Ionic Liquids (RTILs) 1-ethyl-3-methylimidazolium acetate ([Emim][Ac]) ,1-butyl-3-methylimidazolium acetate ([Bmim][Ac]) and the monomer vinylbenzyl trimethylammonium acetate ([Vbtma][Ac]) in order to perform the selective separation of carbon dioxide ($CO_2$) from nitrogen ($N_2$). The RTILs were supported in a polyvinylidene fluoride porous membrane and permeation experiments were performed in the temperature range 298-333 K. Gas permeability increases with temperature while an increase in temperature leads to a decrease in the $CO_2/N_2$ selectivity for all the studied RTILs. $CO_2$ solubility was evaluated in the range 298-333 K and atmospheric pressure using thermogravimetric techniques. Diffusion coefficients were calculated based on the solution-diffusion theory using gas permeability and solubility data.The temperature influence on the gas permeability, solubility and diffusivity are well described in terms of the Arrhenius–van't Hoff exponential relationships.

Journal of Membrane Science 452 (2014) 277–283

Contents lists available at ScienceDirect

Journal of Membrane Science

journal homepage: www.elsevier.com/locate/memsci

# Acetate based Supported Ionic Liquid Membranes (SILMs) for $CO_2$ separation: Influence of the temperature

E. Santos *, J. Albo, A. Irabien

*Departamento de Ingeniería Química y Química Inorgánica, Universidad de Cantabria, Avda. de los Castros s/n., 39005 Santander, Spain*

ARTICLE INFO

*Article history:*
Received 4 August 2013
Received in revised form
8 October 2013
Accepted 12 October 2013
Available online 21 October 2013

*Keywords:*
$CO_2/N_2$ separation
Room Temperature Ionic Liquids
Supported Ionic Liquid Membranes
Gas permeation
Solution–diffusion

ABSTRACT

Supported Ionic Liquid Membranes (SILMs) were prepared with the acetate based Room Temperature Ionic Liquids (RTILs) 1-ethyl-3-methylimidazolium acetate ([Emim][Ac]), 1-butyl-3-methylimidazolium acetate ([Bmim][Ac]) and the monomer vinylbenzyl trimethylammonium acetate ([Vbtma][Ac]) in order to perform the selective separation of carbon dioxide ($CO_2$) from nitrogen ($N_2$). The RTILs were supported in a polyvinylidene fluoride porous membrane and permeation experiments were performed in the temperature range 298–333 K. Gas permeability increases with temperature while an increase in temperature leads to a decrease in the $CO_2/N_2$ selectivity for all the studied RTILs. $CO_2$ solubility was evaluated in the range 298–333 K and atmospheric pressure using thermogravimetric techniques. Diffusion coefficients were calculated based on the solution–diffusion theory using gas permeability and solubility data. The temperature influence on the gas permeability, solubility and diffusivity are well described in terms of the Arrhenius–van't Hoff exponential relationships.



## 1. Introduction

The use of Supported Ionic Liquid Membranes (SILMs) for the selective separation of gases has received growing attention during recent years. In a SILM system, Room Temperature Ionic Liquids (RTILs) are immobilized inside the porous matrix of a polymeric or inorganic support. RTILs are organic salts liquid at room temperature showing a large variety of properties such as negligible vapor pressure, thermal stability at high temperatures or non-flammability [1], making them very attractive as immobilized phase in SILMs. The use of RTILs reduces the problem of solvent evaporation that may occur in conventional Supported Liquid Membranes (SLMs), allowing for obtaining liquid membranes with a higher stability [2]. Additionally, RTILs can be synthesized as task-specific solvents by the appropriate selection of the cation or anion in their structure [3] resulting in enhanced properties such as the gas solubility. The possibility of synthesize new RTILs with desired properties provides the opportunity for creating an ideal solvent for each potential application.

RTILs have received interest in $CO_2$ selective separations where the separation of $CO_2$ from mixtures containing $N_2$ is of great interest in power generation applications associated with the purification of flue gas streams. $CO_2$ permeability and $CO_2/N_2$ selectivity are the fundamental parameters characterizing the gas separation using membrane based technologies. There is a general trade-off between both parameters identified by the "upper bound" limit observed for different polymeric materials in gas separation [4,5]. The development of new materials exceeding this line is a challenge in $CO_2/N_2$ separation.

There are several works available in the literature where SILMs were studied for $CO_2/N_2$ separation. Scovazzo et al. [6] report the gas permeability at 303 K of $CO_2$ and $N_2$ and the corresponding selectivities through a porous hydrophilic polyethersulfone (PES) support with different immobilized RTILs. They reported $CO_2$ permeabilities in the range of 350–920 barrers and $CO_2/N_2$ ideal selectivity ranged from 15 to 61. Bara et al. [7] obtained $CO_2$ permeabilities varying from 210 to 320 barrers and $CO_2/N_2$ separation factors between 16 and 26. Mixed-gas permeabilities and selectivities for $CO_2/N_2$ were also reported by Scovazzo et al. [8]. Cserjési et al. [9] investigated the use of SILMs prepared with 12 different types of RTILs immobilized in a hydrophilic polyvinylidene fluoride (PVDF) support. $CO_2$ permeabilities varied in the range of 94–750 barrers while $CO_2/N_2$ ideal selectivity ranged from 10.9 to 52.6. Neves et al. [10] studied the effect of the different cation alkyl chain length on the gas permeability. Gas permeability increases approximately by a factor of 2 with an increase in the cation alkyl chain length and the $CO_2/N_2$ ideal selectivity ranged from 22 to 39. Finally, Jindaratsamee et al. [11] studied the permeability of $CO_2$ through imidazolium based ionic liquid membranes supported with a polyvinylidene fluoride (PVDF) porous membrane. They reported $CO_2$ permeabilities in 303–343 K temperature range varied from 120 to 445 barrers, with an ideal $CO_2/N_2$ selectivies from 42 to 86.

The selection of a suitable solvent is essential for the technical and economical viability of the $CO_2$ absorption where the solubility is the property of interest and the main selection criteria which

* Corresponding author: Tel.: +34 942 206749; fax: +34 942 201591.
*E-mail address:* santosse@unican.es (E. Santos).

0376-7388/$ - see front matter © 2013 Elsevier B.V. All rights reserved.
http://dx.doi.org/10.1016/j.memsci.2013.10.024

has been the objective of many papers. The solubility of light gases such as $CO_2$ has been widely studied in RTILs. RTILs containing the acetate anion have been studied in the literature showing a strong absorption for $CO_2$. Maginn et al. [12] reported for the first time $CO_2$ solubility studies in the ionic liquid 1-butyl-3-methylimidazolium acetate ([Bmim][Ac]) showing very high $CO_2$ solubility. Chinn et al. [13] have proposed the $CO_2$/[Bmim][Ac]/water system for $CO_2$ capture. Shifflet et al. [14–18] have widely studied the phase behavior of $CO_2$ in 1-ethyl-3-methylimidazolium acetate [Emim][Ac] and 1-butyl-3-methylimidazolium acetate [Bmim][Ac] at temperatures ranging from 283 to 348 K and pressures up to 2 MPa. Bhargava et al. [19] and Steckel [20] performed ab initio calculations of the interaction between $CO_2$ and the acetate ion. Finally, Shi et al. [21] performed both simulation and experimental studies to separate mixtures of $CO_2$ and $H_2$ using [Emim][Ac] ionic liquid. Additionally, the use of polymeric ionic liquids (PILs) exhibits several times higher $CO_2$ absorption capacity than conventional monomeric Room Temperature Ionic Liquids (RTILs) due to faster $CO_2$ absorption and desorption rates [22]. The highest $CO_2$ solubility values and $CO_2/N_2$ selectivities can be achieved in the tetraalkylammonium poly(ionic liquid) p-[Vbtma] recently studied in the literature in combination with different anions [22,23].

In this work, the influence of the temperature on $CO_2$ and $N_2$ permeability and $CO_2$ solubility was investigated. SILMs including three acetate based RTILs were prepared in order to evaluate the $CO_2/N_2$ separation performance from 298 to 333 K. The $CO_2$ solubility was evaluated at 298–333 K and atmospheric pressure. The diffusion coefficients were calculated using gas permeability and solubility data applying the solution–diffusion hypothesis. The temperature dependence was described by using the Arrhenius or the van't Hoff equation in order to discuss the solubility and diffusivity contribution on the gas permeability through SILMs.

## 2. Experimental

### 2.1. Materials

The RTILs used in the present work were 1-ethyl-3-methylimidazolium acetate ([Emim][Ac]), 1-butyl-3-methylimidazolium acetate ([Bmim][Ac]) and (Vinylbenzyl)trimethylammonium acetate ([Vbtma][Ac]). [Emim][Ac] (assay $\geq$ 96.5%, $C_8H_{14}N_2O_2$ CAS no. 143314-17-4) and [Bmim][Ac] (assay $\geq$ 96%, $C_{10}H_{18}N_2O_2$ CAS no. 284049-75-8) they were supplied by Sigma Aldrich and used without further purification while [Vbtma][Ac] was synthesized in the *Faculdade de Farmácia*, *Universidade de Lisboa* (*Portugal*). A solution of [Vbtma][Cl] (5 g, 0.0236 mol) in methanol (10 mL) was passed through a column with Amberlite IRA-400 (OH) resin. A solution of acetic acid (1 equiv., 0.1418 g, 0.0236 mol) in methanol was slowly added to [Vbtma][OH] obtained from the column and the mixture was stirred at room temperature for 30 min. The solvent was removed under vacuum. The RTIL was stirred under vacuum ( $<$ 1 mmHg) at 60 °C overnight. (Vinylbenzyl)trimethylammonium acetate was obtained (5.4 g, 99.8%). Their molecular weight, density, viscosity and decomposition temperature are listed in Table 1. The density was determined using an automatic densimeter (Mettler Toledo DM40) at 298 K while viscosity data was obtained from the literature [24,25]. The density is in good agreement with the ones reported in the literature [24,25].

The thermal properties of the ionic liquids were determined by using thermogravimetric analysis (TGA). TGA analyses were carried out using a TGA-60H Shimazdu Thermobalance in a $N_2$ atmosphere at temperatures ranging from the room temperature to 873 K with a heating rate of 5 K $min^{-1}$. From the TGA curves shown in Fig. 1 it can be concluded that they are thermally stable up to 445 K under $N_2$ atmosphere which suggests that all of these RTILs have good thermal stabilities. A one-stage thermal decomposition process was observed for [Emim][Ac] and [Bmim][Ac] while a two-stage decomposition was observed for the monomer [Vbtma][Ac]. The onset temperature ($T_{onset}$) calculated as the intersection of the baseline weight from the beginning of the experiment and the tangent of the weight vs. temperature curve as decomposition occurs was determined for each RTIL and is reported in Table 1.

**Table 1**
Main characteristics of the studied RTILs.

| Ionic liquid | Molecular structure | Molecular weight (g $mol^{-1}$) | Density (g $cm^{-3}$, 298 K) | Viscosity (cP, 298 K) | $T_{onset}$ (K) |
|---|---|---|---|---|---|
| [Emim][Ac] | 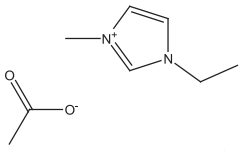 | 170.21 | 1.098 | 143.61 [24] | 481.35 |
| [Bmim][Ac] | 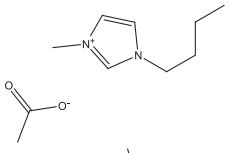 | 198.26 | 1.052 | 24.82 [25] | 496.93 |
| [Vbtma][Ac] | 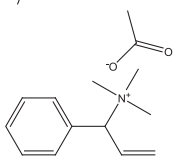 | 235.32 | 1.015 | – | 445.1 |

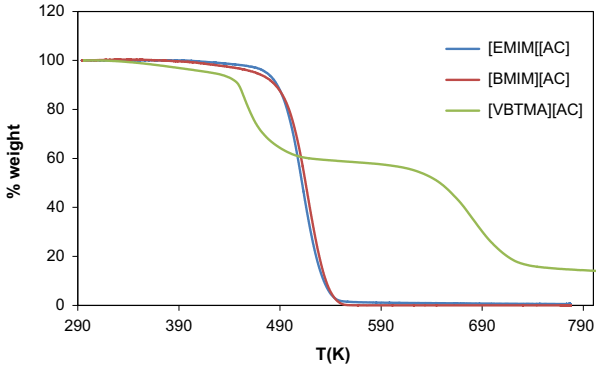


**Fig. 1.** TGA analyses for the for [Emim][Ac], [Bmim][Ac] and [Vbtma][Ac].

The polymeric membrane selected as support for the present study was purchased from Millipore Corporation (USA). It is a 75% porous hydrophobic polyvinylidene fluoride (PVDF) membrane with a nominal pore size of 0.22 μm and 47 mm in diameter. The PVDF membrane thickness was determined using a digital micrometer (Mitutoyo 369–250, ±0.001 mm accuracy), being the average value 125 μm. These membranes are characterized by their high chemical resistance, being previously used in other works as a supporting material for SILMs [10,26]. It is worth mentioning that the PVDF membranes used as supporting material have a maximum operating temperature of 358 K (manufacturer's data) so they are the limiting factor for the SILM high temperature performance. The gases used in the experiments were carbon dioxide (99.7 ± 0.01 vol%) and nitrogen (99.999 ± 0.001 vol%) provided by Air Liquide (Spain).

### 2.2. SILM preparation

The immobilization procedure has been previously described [27,28]. To immobilize the RTILs, the microporous PVDF membrane was introduced into a vacuum chamber for 1h in order to

remove the air from the pores and, therefore allowing an easier introduction of RTIL into their porous structure. Once the membrane was under vacuum for 1 h, drops of RTILs are spread out at the membrane surface using a syringe, while keeping the vacuum inside the chamber. Then the liquid excess on the membrane surface was wiped up softly with a tissue. The amount of liquid immobilized in the membrane was determined gravimetrically, and the increase of thickness was measured before and after the immobilization procedure.

### 2.3. Methods

The experimental setup used for the gas permeation experiments has been previously described elsewhere [27,28]. Basically, the SILM is placed over a stainless steel permeation cell leading to an effective membrane area about 14.05 $cm^2$. A driving force of around 0.45 bar was established and the pressure change was measured using two pressure transducers (Omega, UK). The temperature was maintained using a water bath.

Gas permeability through the SILM was determined according to Eq. (1):

$$\frac{1}{\beta}\ln\left(\frac{[p_{feed}-p_{perm}]_0}{[p_{feed}-p_{perm}]}\right)=\frac{1}{\beta}\ln\left(\frac{\Delta p_0}{\Delta p}\right)=P_{SILM}\frac{t}{\delta} \quad (1)$$

where $p_{feed}$ and $p_{perm}$ are the pressures in the feed and permeate compartments, respectively; $\beta$ a geometric parameter (1188.9 $m^{-1}$); $P_{SILM}$ the permeability through the membrane calculated under constant partial pressure difference; $t$ the time and $\delta$ is the membrane thickness. The ideal selectivity can be calculated by the ratio between the permeabilities of two pure different gases.

$CO_2$ solubility was evaluated using a TGA-60H Shimazdu Thermobalance where simultaneous thermogravimetric/differential (TG/DTA) analyses were performed. A molecular sieve trap was installed to remove traces of water from the feed gas. The sample temperature was measured with an accuracy of $\pm 0.1$ K and the TG sensitivity was about 1 μg. The experimental conditions were a $CO_2$ flow rate of 50 mL $min^{-1}$, temperatures from 298 to 333 K and atmospheric pressure.

Once determined the gas permeability through the membrane and $CO_2$ solubility in the RTIL, the effective diffusion coefficients can be calculated considering that gas transport occurs via solution–diffusion mechanism according to Eq. (2):

$$P_{SILM}=SD_{eff} \quad (2)$$

where $P_{SILM}$ is the permeability through the membrane; $S$ is the gas solubility and $D_{eff}$ the effective diffusion coefficient.

## 3. Results and discussion

### 3.1. Permeability

The experimental permeability results obtained in the present work are based on the following assumption: gas transport takes place entirely in the RTIL since the polyvinylidene fluoride (PVDF) support has very low permeabilities of 2.7 and 0.4 barrers for $CO_2$ and $N_2$ respectively. The SILMs permeabilities are between 325 barrers ($CO_2$) and 61.5 barrers ($N_2$) times greater in magnitude. Therefore, the assumption that the RTIL is the main contributor to gas permeability when comparing with the support is valid. The temperature effect on $CO_2$ and $N_2$ permeability as well as the $CO_2/N_2$ ideal selectivity was studied in the range of temperatures from 298 to 333 K. Table 2 shows the experimental $CO_2$ and $N_2$ permeability through the acetate based SILMs. The $CO_2$ permeance values for these membranes are in the order of 852–2114 barrers and $CO_2/N_2$ selectivity ranges between 26 and 39. According to the experimental research, the effect of the cation on gas permeability is negligible when comparing with the anion. The SILMs studied in this work displays higher permeability values when comparing to polymeric membranes reported in literature generally below 1000 barrers [6–11]. Moreover, the results are in good agreement with those reported by Shi et al. [21] for the separation $CO_2/H_2$ in [Emim][Ac] based SILMs showing $CO_2$ permeabilities from 1325 to 3701 barrers in the temperature range 310–373 K.

**Table 2**
Experimental $CO_2$ and $N_2$ permeability through SILMs.

| RTIL | T (K) | 298 | 303 | 313 | 323 | 333 |
|---|---|---|---|---|---|---|
| [Emim][Ac] | $P_{CO_2}$ (barrer) | 878.8 | 1118.1 | 1329.0 | 1721.3 | 2064.9 |
| | $P_{N_2}$ (barrer) | 26.1 | 32.5 | 41.3 | 58.3 | 78.1 |
| | $P_{CO_2}/P_{N_2}$ | 33.7 | 34.4 | 32.2 | 29.5 | 26.4 |
| [Bmim][Ac] | $P_{CO_2}$ (barrer) | 851.9 | 1005.3 | 1269.2 | 1601.5 | 1940.9 |
| | $P_{N_2}$ (barrer) | 24.6 | 29.5 | 37.8 | 50.7 | 65.3 |
| | $P_{CO_2}/P_{N_2}$ | 34.6 | 34.1 | 33.6 | 31.6 | 29.7 |
| [Vbtma][Ac] | $P_{CO_2}$ (barrer) | 1100 | 1305.6 | 1536.2 | 1828.3 | 2114.2 |
| | $P_{N_2}$ (barrer) | 28.2 | 36.1 | 48.3 | 61.8 | 77.5 |
| | $P_{CO_2}/P_{N_2}$ | 39.0 | 36.2 | 31.8 | 29.6 | 27.3 |

An increase in gas permeability is observed as a result of the temperature increase. The logarithm of the permeability follows a linear relationship with the inverse of the temperature as it is shown in Fig. 2; therefore, the temperature influence on the gas permeability is well described in terms of an Arrhenius type relationship by Eq. (3):

$$P=P_0\exp(-E_p/RT) \quad (3)$$

where $P_0$ is the pre-exponential factor and $E_p$ the activation energy of permeation.

The activation energies of permeation for $CO_2$ and $N_2$ are reported in Table 3. These results are in good agreement with the previous literature data [29–32].

The activation energies of $CO_2$ permeation is in the range of previous values reported in the literature using different commercial polymeric supports [21,29]. The differences in the $CO_2$ activation energies of permeation between the polymeric and the inorganic supports may be due to the greater porosity of the polymeric support (75–85%) compared to 25–50% for the alumina leading to a decrease in the membrane volume occupied by the RTILs. The activation energies of $N_2$ permeation are higher than those found for $CO_2$ as it is shown in Table 3, which justifies a negative influence of the temperature in the selectivity.

The $CO_2/N_2$ ideal selectivities in the SILMs are plotted in Fig. 3 as a function of the temperature. An increase in temperature leads to a decrease in the ideal $CO_2/N_2$ selectivity according with the activation energies.

Comparing the permeability results at increasing temperatures to the upper-bound values for the selectivity vs. permeability of polymer membranes for $CO_2/N_2$ separation given by Robeson [5] it can be concluded that most of these SILMs have better performance than many polymer membranes previously studied, being the experimental results near the upper bound as it is shown in Fig. 4.

### 3.2. Solubility

Table 4 shows the $CO_2$ solubility in molar fraction in the three studied ionic liquids. The solubility data are in good agreement

with values previously reported in the literature at the same experimental conditions for [Emim][Ac] and [Bmim][Ac] [14–16].

The solubility dependence with temperature is typically written in terms of the van't Hoff relationship according to Eq. (4):

$$S = S_0 \exp(-\Delta H_s/RT) \quad (4)$$

where $S_0$ is the pre-exponential factor and $\Delta H_s$ is the partial molar enthalpy of absorption. The natural logarithm of the solubility follows a linear relationship with the inverse of temperature as shown in Fig. 5. The $CO_2$ partial molar enthalpy of absorption, $\Delta H_s$, is reported in Table 5.The negative values of the absorption enthalpy corresponds to the exothermic behavior of the process. These values are in good agreement with the literature [29,32,33]. Taking into account the positive influence of the temperature in the diffusivity an endothermic absorption could be better in order to increase the permeability with the temperature.

### 3.3. Diffusivity

The calculation of $CO_2$ diffusivity from permeability and solubility, both measured and adjusted by linear fitting, it is possible considering that gas transport occurs via solution–diffusion mechanism where the permeability of a gas through the SILM ($P_{SILM}$) is the product of its solubility in the membrane ($S$) and effective diffusivity ($D_{eff}$) by applying Eq. (2) [34]. The permeability in $cm^2\ s^{-1}$, $P_{SILM}$, and the dimensionless solubility, $H$, are calculated according to Appendix A. The estimated diffusion coefficients $cm^2\ s^{-1}$ for $CO_2$ in the studied RTILs are presented in Table 6.

The Arrhenius equation describes well the relationship between gas diffusivity and temperature as it is shown in Fig. 6

$$D = D_0 \exp(-E_D/RT) \quad (5)$$

where $D_0$ is the pre-exponential factor and $E_D$ the activation energy of diffusion. The activation energies of diffusion, $E_D$, are

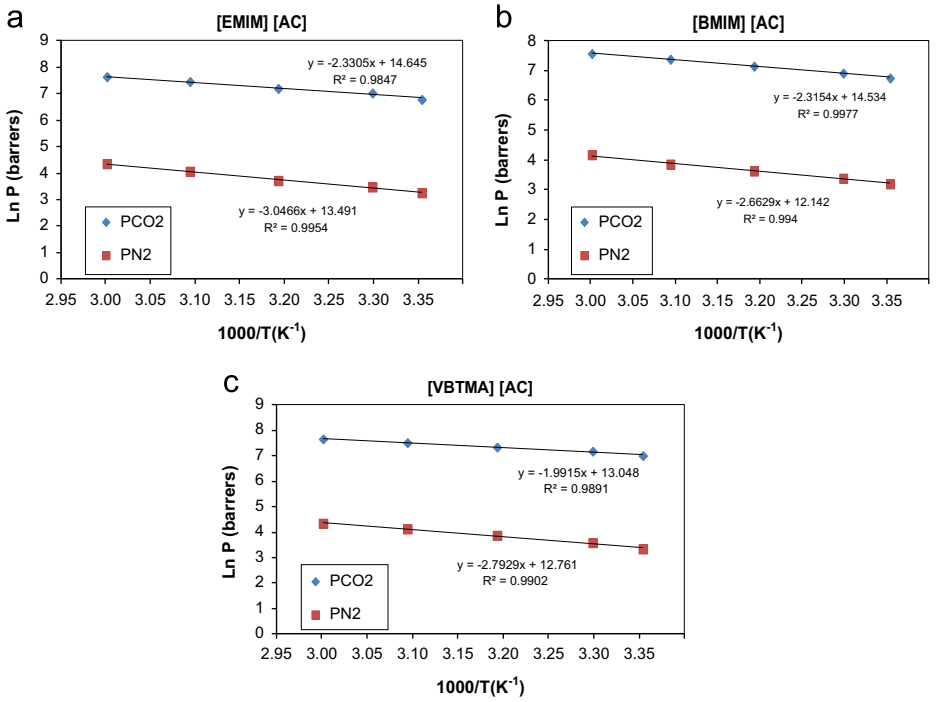


**Fig. 2.** Natural logarithm of $CO_2$ and $N_2$ permeability through [Emim][Ac] (a), [Bmim][Ac] (b) and [Vbtma][Ac] (c) plotted against the inverse of the temperature. Solid lines are the linear regression of the data.

**Table 3**
Experimental and literature activation energies of permeation, $E_p$.

| Support | Gas | RTIL | $E_p$ (kJ/mol) | Reference |
|---|---|---|---|---|
| Polyvinylidene fluoride (PVDF) | $CO_2$ | [Emim][Ac] | 19.37 | Present work |
| Polyvinylidene fluoride (PVDF) | $N_2$ | [Emim][Ac] | 25.32 | Present work |
| Polyvinylidene fluoride (PVDF) | $CO_2$ | [Bmim][Ac] | 19.25 | Present work |
| Polyvinylidene fluoride (PVDF) | $N_2$ | [Bmim][Ac] | 22.13 | Present work |
| Polyvinylidene fluoride (PVDF) | $CO_2$ | [Vbtma][Ac] | 16.55 | Present work |
| Polyvinylidene fluoride (PVDF) | $N_2$ | [Vbtma][Ac] | 23.22 | Present work |
| Polysulfone (PSF) | $CO_2$ | [Hmim][$Tf_2N$] | 17.38 | Ilconich et al. [29] |
| Polysulfone (PSF) | He | [Hmim][$Tf_2N$] | 5.35 | Ilconich et al. [29] |
| Alumina | $CO_2$ | [Hmim][$Tf_2N$] | 8.03 | Adibi et al. [30] |
| Alumina | $CH_4$ | [Hmim][$Tf_2N$] | 29.35 | Adibi et al. [30] |
| Polysulfone (PSF) | $CO_2$ | [Emim][Ac] | 25.47 | Shi et al. [21] |
| Polysulfone (PSF) | $H_2$ | [Emim][Ac] | 16.02 | Shi et al. [21] |
| α-Alumina | $CO_2$ | [Bmim][$Bf_4$] | 7.5 | Iarikov et al. [31] |
| α-Alumina | $CH_4$ | [Bmim][$Bf_4$] | 20 | Iarikov et al. [31] |

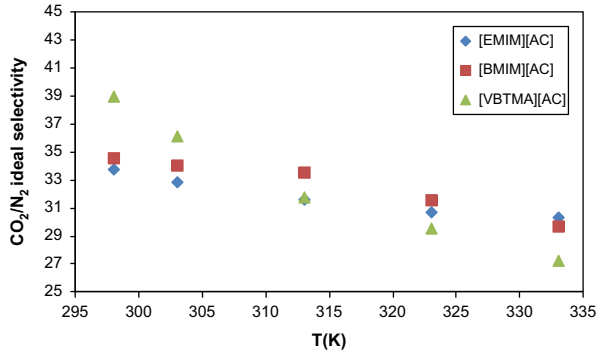


**Fig. 3.** Temperature influence on $CO_2/N_2$ selectivity.

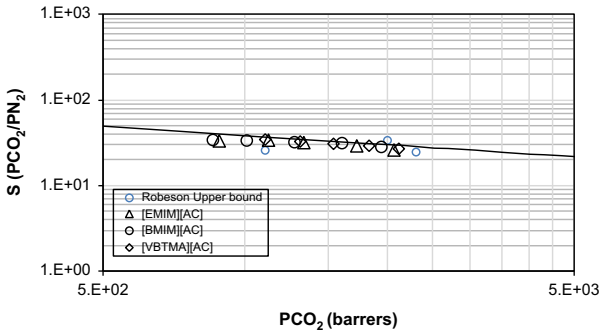


**Fig. 4.** Upper bound correlation for $CO_2/N_2$ separation.

**Table 4**
$CO_2$ solubility data in acetate based ionic liquids.

| *T* (K) | RTIL | | |
|---|---|---|---|
| | [EMIM][AC] | [BMIM][AC] | [VBTMA][AC] |
| 298.15 | 0.267 | 0.273 | 0.351 |
| 303.15 | 0.257 | 0.255 | 0.325 |
| 313.15 | 0.231 | 0.225 | 0.283 |
| 323.15 | 0.212 | 0.195 | 0.241 |
| 333.15 | 0.189 | 0.171 | 0.210 |

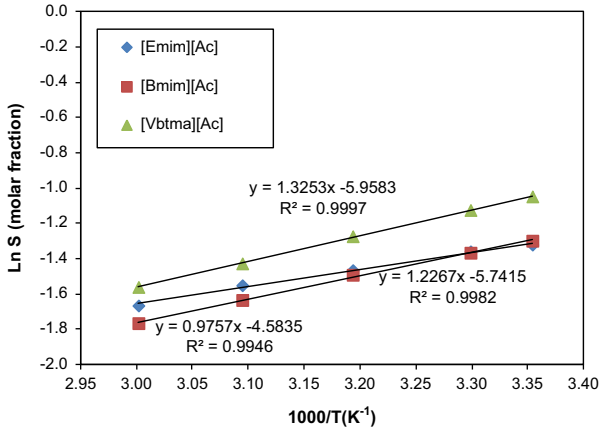


**Fig. 5.** Natural logarithm of $CO_2$ solubility plotted against the inverse of the temperature. Solid lines are the linear regression of the data.

reported in Table 7. These values are consistent with those values found in the literature [29,30,35–38].

According to our results, the activation energy for the permeability is the algebraic sum of the activation energy for the diffusivity and the partial molar enthalpy of absorption therefore, the influence of the temperature in the permeability is described by an exponential Arrhenius type equation, with an activation energy including the influence of the temperature in the effective diffusion and in the solubility.

**Table 5**
Experimental and literature $\Delta H_s$ data.

| RTIL | $\Delta H_s$ (kJ/mol) | Reference |
|---|---|---|
| [Emim][Ac] | −8.29 | Present work |
| [Bmim][Ac] | −10.19 | Present work |
| [Vbtma][Ac] | −11.02 | Present work |
| [Hmim][$Tf_2N$] | −11.19 | Ilconich et al. [29] |
| [Bmim][$Pf_6$] | −14.30 | Anthony et al. [32] |
| [Bmim][$Pf_4$] | −13.90 | Anthony et al. [32] |
| [Bmim][$Tf_2N$] | −12.50 | Anthony et al. [32] |
| [MeBuPyrr][$Tf_2N$] | −11.90 | Anthony et al. [32] |
| [Bmim][$Pf_6$] | −16.10 | Cadena et al. [33] |
| [Bmmim][$Pf_6$] | −13.00 | Cadena et al. [33] |
| [Bmim][$Pf_4$] | −15.90 | Cadena et al. [33] |
| [Bmmim][$Bf_4$] | −14.50 | Cadena et al. [33] |
| [Emim][$Tf_2N$] | −14.20 | Cadena et al. [33] |
| [Emmim][$Tf_2N$] | −14.70 | Cadena et al. [33] |

**Table 6**
Diffusivity calculated data.

| RTIL | *T* (K) | 298 | 303 | 313 | 323 | 333 |
|---|---|---|---|---|---|---|
| **[Emim][Ac]** | $10^5$ ***P*** **(cm²/s)** | 0.73 | 0.94 | 1.16 | 1.55 | 1.91 |
| | **H (–)** | 0.0237 | 0.0244 | 0.0263 | 0.02880 | 0.0306 |
| | $10^7$ ***D*** **(cm²/s)** | 1.73 | 2.30 | 3.05 | 4.33 | 5.86 |
| **[Bmim][Ac]** | $10^5$ ***P*** **(cm²/s)** | 0.71 | 0.85 | 1.11 | 1.44 | 1.80 |
| | ***H*** **(–)** | 0.0282 | 0.0299 | 0.0329 | 0.0370 | 0.0412 |
| | $10^7$ ***D*** **(cm²/s)** | 1.99 | 2.53 | 3.64 | 5.33 | 7.41 |
| **[Vbtma][Ac]** | $10^5$ ***P*** **(cm²/s)** | 0.91 | 1.10 | 1.34 | 1.64 | 1.96 |
| | **H (–)** | 0.027 | 0.0287 | 0.0319 | 0.0365 | 0.0407 |
| | $10^7$ ***D*** **(cm²/s)** | 2.46 | 3.17 | 4.28 | 6.01 | 7.99 |

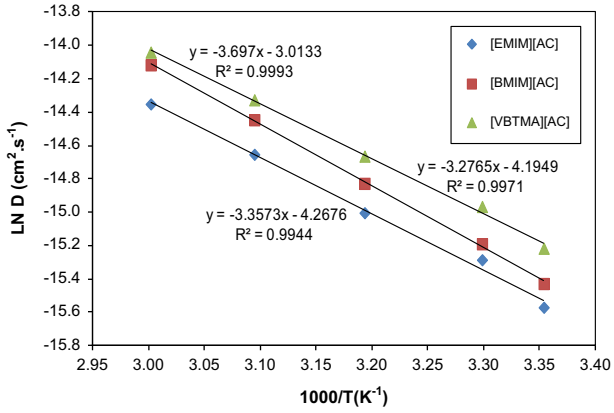


**Fig. 6.** Natural logarithm of $CO_2$ diffusivity vs. the inverse of the temperature for the studied RTILs. Solid lines are the linear regression of the data.

## 4. Conclusions

In this work, $CO_2$ and $N_2$ permeabilities through SILMs were determined at temperatures ranging from 298 to 333 K. Gas permeability increases with the temperature while $CO_2/N_2$ selectivity decreases with an increase in temperature for all the studied

**Table 7**
Calculated and literature $E_D$ data.

| Gas | RTIL | $E_D$ (kJ/mol) | Reference |
|---|---|---|---|
| $CO_2$ | [Emim][Ac] | 27.91 | Present work |
| $CO_2$ | [Bmim][Ac] | 30.74 | Present work |
| $CO_2$ | [Vbtma][Ac] | 27.24 | Present work |
| $CO_2$ | [Hmim][$Tf_2N$] | 16.42 | Ilconich et al. [29] |
| $CO_2$ | [Bmpy][$Bf_4$] | 21 | Morganty and Baltus [35] |
| $CO_2$ | [Omim][$Bf_4$] | 18 | Morganty and Baltus [35] |
| $CO_2$ | [Hmim][$Bf_4$] | 22 | Morganty and Baltus [35] |
| $CO_2$ | [Hmim][$Tf_2N$] | 14 | Morganty and Baltus [35] |
| $CO_2$ | [Emim][$Tf_2N$] | 8 | Morganty and Baltus [35] |
| $CO_2$ | [Emim][Beti] | 14 | Morganty and Baltus [35] |
| $CO_2$ | [Emim][Tfa] | 11 | Morganty and Baltus [35] |
| $CO_2$ | [Emim][TfO] | 14 | Morganty and Baltus [35] |
| $CO_2$ | [Bmim][$Tf_2N$] | 10 | Morganty and Baltus [35] |
| $CO_2$ | [Pmmim][$Tf_2N$] | 15 | Morganty and Baltus [35] |
| $CO_2$ | [Bmpy][$Tf_2N$] | 12 | Morganty and Baltus [35] |
| $CO_2$ | [Bmim][$Bf_4$] | 6 | Morganty and Baltus [35] |
| $CO_2$ | [Bmim][$Pf_6$] | 27.2 | Shiflett and Yokozeki [36] |
| $CO_2$ | [Bmim][$Bf_4$] | 24.3 | Shiflett and Yokozeki [36] |
| $CO_2$ | [Bmim][$Pf_6$] | 47.72 | Barghi et al. [37] |
| $CH_4$ | [Bmim][$Pf_6$] | 61.11 | Barghi et al. [37] |
| $CO_2$ | [Hmim][$Tf_2N$] | 21.50 | Adibi et al. [30] |
| $CH_4$ | [hmim][$Tf_2N$] | 33.29 | Adibi et al. [30] |
| $CO_2$ | [Emim][$Tf_2N$] | 16.9 | Morgan et al. [38] |
| $CO_2$ | [Bmim][Beti] | 22.3 | Morgan et al. [38] |

RTILs. The permeability activation energies are higher for nitrogen than for carbon dioxide.

Acetate based SILMs are useful for $CO_2/N_2$ separation since the results obtained in this work are near the Robeson upper bound corresponding to the best polymeric materials.

Gas diffusion coefficients were estimated assuming that gas permeation occurs via a solution–diffusion mechanism ($P=DS$) and the activation energies for the permeability, solubility and diffusivity were calculated. The experimental results of the activation energies and the absorption enthalpies agree well with the previous literature results.

In order to get a higher influence of the temperature in the permeability, it is recommended the introduction of RTILs with an endothermic absorption, which may increase the permeability activation energy.

## Acknowledgments

The authors gratefully acknowledge the financial support from the Spanish Ministry of Economy and Competiveness Project ENE 2010-14828 and Project CTQ2008-00690.

## Appendix A. Diffusivity

Permeability data is often expressed in barrer according to

$$1\ \text{barrer} = \frac{10^{-10}\ \text{cm}^3\ \text{gas (STP)}\ (\text{cm\_thickness})}{(\text{cm}^2\text{\_membrane area})\ (\text{cmHg\_pressure})\ \text{s}} \quad (A.1)$$

(STP = 273.15 K and $1.01325 \times 10^5$ Pa)

The equivalence in $\text{cm}^2\ \text{s}^{-1}$ is defined as

$$1\ \text{barrer} = \frac{10^{-10}\ \text{cm}^3\ (\text{STP})\ \text{cm}}{\text{cm}^2\ \text{cmHg s}} \left[\frac{\text{mol (STP)}}{22.4 \times 10^3\ \text{cm}^3}\right] \times \left[62.36367 \frac{\text{l mmHg}}{\text{mol K}} \frac{10^3\ \text{cm}^3}{1\ \text{L}} \frac{1\ \text{cmHg}}{10\ \text{mmHg}}\right] 298.15\ K = 8.296 \times 10^{-9}\ \frac{\text{cm}^2}{\text{s}} \quad (A.2)$$

The Henry's law constant has been calculated by means of the following equation [39]:

$$H = \frac{C_g^*}{C_l^*} = \frac{y^*\ \rho_g}{x^*\ \rho_l} = \frac{y^*}{x^*\ \rho_l} \frac{P_T}{RT} = \frac{1}{S} \quad (A.3)$$

where $y^*$ and $x^*$ are the molar fractions in the gas and liquid phases respectively, being in equilibrium with themselves; $\rho_l$ is the molar density of the liquid and $P_T$ the total pressure.

### Nomenclature

| | |
|---|---|
| $D_{eff}$ | effective diffusion coefficient ($\text{cm}^2\ \text{s}^{-1}$) |
| $D_0$ | pre-exponential factor of diffusion ($\text{cm}^2\ \text{s}^{-1}$) |
| $E_D$ | activation energy of diffusion ($\text{kJ mol}^{-1}$) |
| $E_p$ | activation energy of permeation ($\text{kJ mol}^{-1}$) |
| $H$ | Henry's law constant (–) |
| $P_0$ | pre-exponential factor of gas permeability (barrer) |
| $P_{SILM}$ | gas permeability through the membrane (barrer) |
| $P_T$ | total pressure (bar) |
| $p_{feed}$ | pressure in the feed compartment (Pa) |
| $p_{perm}$ | pressure in the permeate compartment (Pa) |
| $R$ | ideal gas constant ($\text{bar L mol}^{-1}\ \text{K}^{-1}$) |
| $S$ | gas solubility (molar fraction) |
| $S_0$ | pre-exponential factor of gas solubility (molar fraction) |
| $T$ | temperature (K) |
| $t$ | time (s) |
| $x^*$ | liquid molar fraction |
| $y^*$ | gas molar fraction in equilibrium with liquid |

*Greek letters*

| | |
|---|---|
| $\beta$ | geometric factor ($\text{m}^{-1}$) |
| $\delta$ | membrane thickness (m) |
| $\rho_l$ | molar density of the liquid ($\text{mol L}^{-1}$) |
| $\Delta H_s$ | partial molar enthalpy of absorption ($\text{kJ mol}^{-1}$) |

## References

[1] K.R. Seddon, Ionic liquids for clean technology, J. Chem. Technol. Biotechnol. 68 (1997) 351–356.
[2] F.J. Hernández-Fernandez, A.P. de los Ríos, F Tomás-Alonso, J.M Palacios, G. Víllora, Preparation of supported ionic liquid membranes: influence of the ionic liquid immobilization method on their operational stability, J. Membr. Sci. 341 (2009) 172–177.
[3] M.J. Earle, J.M.S.S. Esperança, M.A. Gilea, J.N Canongia Lopes, L.P.N. Rebelo, J. W. Magee, K.R. Seddon, J.A. Widegren, The distillation and volatility of ionic liquids, Nature 439 (2006) 831–834.
[4] P. Scovazzo, Determination of the upper limits, benchmarks, and critical properties for gas separations using stabilized room temperature ionic liquid membranes (SILMs) for the purpose of guiding future research, J. Membr. Sci. 343 (2009) 199–211.
[5] L.M. Robeson, The upper bound revisited, J. Membr. Sci. 320 (2008) 390–400.
[6] P. Scovazzo, J. Kieft, D.A. Finan, C. Koval, D. DuBois, R. Noble, Gas separations using non-hexafluorophosphate [PF6]$^-$ anion supported ionic liquid membranes, J. Membr. Sci. 238 (2004) 57–63.
[7] J.E. Bara, T.K. Carlisle, C.J. Gabriel, D. Camper, A. Finotello, D.L. Gin, R.D. Noble, Guide to $CO_2$ separations in imidazolium-based room-temperature ionic liquids, Ind. Eng. Chem. Res. 48 (2009) 2739–2751.
[8] P. Scovazzo, D. Havard, M. McShea, S. Mixon, D. Morgan, Long-term, continuous mixed-gas dry fed $CO_2/CH_4$ and $CO_2/N_2$ separation performance and selectivities for room temperature ionic liquid membranes, J. Membr. Sci. 327 (2009) 41–48.
[9] P. Cserjési, N. Nemestóthy, K. Bélafi-Bakó, Gas separation properties of supported liquid membranes prepared with unconventional ionic liquids, J. Membr. Sci. 349 (2010) 6–11.
[10] L.A. Neves, J.G. Crespo, I.M. Coelhoso, Gas permeation studies in supported ionic liquid membranes, J. Membr. Sci. 357 (2010) 160–170.

[11] P. Jindaratsamee, Y. Shimoyama, H. Morizaki, A. Ito, Effects of temperature and anion species on $CO_2$ permeability and $CO_2/N_2$ separation coefficient through ionic liquid membranes, J. Chem. Thermodyn. 43 (2011) 311–314.
[12] E.J. Maginn, Design and evaluation of ionic liquids as novel $CO_2$ absorbents, ⟨http://www.netl.doe.gov/technologies/coalpower/ewr/$CO_2$/pubs⟩, 2013 (accessed 24.01.13).
[13] D. Chinn, D.Q. Vu, M.S. Driver, L.C. Boudreau, $CO_2$ removal from gas using ionic liquid absorbents, US Patent US20,060,251,558A1, 2006, November 9; US20,050,129,598A1, 2005, June 16.
[14] M.B. Shiflett, D.J. Kasprzak, A. Yokozeki, Phase behavior of {carbon dioxide+[bmim][Ac]} mixtures, J. Chem. Thermodyn. 40 (2008) 25–31.
[15] A. Yokozeki, M.B. Shiflett, L.M. Grieco, T. Foo, Physical and chemical absorptions of carbon dioxide in room-temperature ionic liquids, J. Phys. Chem. B 112 (2008) 16654–16663.
[16] M.B. Shiflett, A. Yokozeki, Phase behavior of carbon dioxide in ionic liquids: [emim][Acetate], [emim][Trifluoroacetate], and [emim][Acetate]+[emim][Trifluoroacetate] mixtures, J. Chem. Eng. Data 54 (2009) 108–114.
[17] M.B. Shiflett, B.A. Elliott, A.M.S. Niehaus, A. Yokozeki, Separation of $N_2O$ and $CO_2$ using room-temperature ionic liquid [bmim][Ac], Sep. Sci. Technol. 47 (2012) 411–421.
[18] M.B. Shiflett, A.M.S. Niehaus, B.A. Elliott, A. Yokozeki, Phase behavior of $N_2O$ and $CO_2$ in room-temperature ionic liquids [bmim][$Tf_2N$], [bmim][$BF_4$], [bmim][$N(CN)_2$], [bmim][Ac], [eam][$NO_3$], and [bmim][SCN], Int. J. Thermophys. 33 (2012) 412–436.
[19] B.L. Bhargava, S. Balasubramanian, Probing anion–carbon dioxide interactions in room temperature ionic liquids: gas phase cluster calculations, Chem. Phys. Lett., 444, 2007, 2007; 242–246.
[20] J.A. Steckel, Ab initio calculations of the interaction between $CO_2$ and the acetate ion, J. Phys. Chem. A 116 (2012) 11643–11650.
[21] W. Shi, C.R. Myers, D.R. Luebke, J.A. Steckel, D.C. Sorescu, Theoretical and experimental studies of $CO_2$ and $H_2$ separation using the 1-ethyl-3 methylimidazolium acetate ([emim][$CH_3COO$]) ionic liquid, J. Phys. Chem. B 116 (2012) 283–295.
[22] S. Supasitmongkol, P. Styrring, High $CO_2$ solubility in ionic liquids and a tetraalkylammonium-based poly(ionic liquid), Energy Environ. Sci. 3 (2010) 1961–1972.
[23] R.S. Bhavsar, S.C. Kumbharkar, U.K. Kharul, Polymeric ionic liquids (PILs): effect of anion variation on their $CO_2$ sorption, J. Membr. Sci. 389 (2012) 305–315.
[24] M.G. Freire, A.R.R. Teles, M.A.A. Rocha, B. Schroder, C.M.S.S. Neves, P. J. Carvalho, D.V. Evtuguin, L.M.N.B.F. Santos, J.A.P. Coutinho, Thermophysical characterization of ionic liquids able to dissolve biomass, J. Chem. Eng. Data 56 (2011) 4813–4822.
[25] E.J. Maginn, Design and evaluation of ionic liquids as novel $CO_2$ absorbents, , 2005. (Quarterly Technical Report, January 2005 (DE-FG26-04NT42122).
[26] R. Fortunato, L.C. Branco, C.A.M. Afonso, J. Benavente, J.G. Crespo, Electrical impedance spectroscopy characterisation of supported ionic liquid membranes, J. Membr. Sci. 270 (2006) 42–49.
[27] J. Albo, E. Santos, L.A. Neves, S.P. Simeonov, C.A.M. Afonso, J.G. Crespo, A. Irabien, Separation performance study of $CO_2$ through Supported Magnetic Ionic Liquid Membranes (SMILMs), Sep. Purif. Technol. 97 (2012) 26–33.
[28] E. Santos, J. Albo, C.I. Daniel, C.A.M. Portugal, J.G. Crespo, A. Irabien, Permeability modulation of Supported Magnetic Ionic Liquid Membranes (SMILMs) by an external magnetic field, J. Membr. Sci. 430 (2013) 56–61.
[29] J. Ilconich, C. Meyers, H. Pennline, D. Luebke, Experimental investigation of the permeability and selectivity of supported ionic liquid membranes for $CO_2$/He separation at temperatures up to 125 °C, J. Membr. Sci. 298 (2007) 41–47.
[30] M. Adibi, S.H. Barghi, D. Rashtchian, Predictive models for permeability and diffusivity of $CH_4$ through imidazolium-based supported ionic liquid membranes, J. Membr. Sci. 371 (2011) 127–133.
[31] D.D. Iarikov, P. Hacarlioglu, S.T. Oyama, Supported room temperature ionic liquid membranes for $CO_2/CH_4$ separation, Chem. Eng. J. 166 (2011) 401–406.
[32] J.L. Anthony, J.L. Anderson, E.J. Maginn, J.F. Brennecke, Anion effects on gas solubility in ionic liquids, J. Phys. Chem. B 109 (2005) 6366–6374.
[33] C. Cadena, J.L. Anthony, J.K. Shah, T.I. Morrow, J.F. Brennecke, E.J. Maginn, Why is $CO_2$ so soluble in imidazolium-based ionic liquids? J. Am. Chem. Soc. 126 (2004) 5300–5308.
[34] R.C. Reid, J.M. Prausnitz, B.E. Poling, The Properties of Gases and Liquids, 4th ed., Mc Graw-HillNew York, 1987.
[35] S.S. Morganty, R.E. Baltus, Diffusivity of carbon dioxide in room temperature ionic liquids, Ind. Eng. Chem. Res. 49 (2010) 9370–9376.
[36] M.B. Shifflet, A. Yokozeki, Solubilities and diffusivities of carbon dioxide in ionic liquids: [bmim][$PF_6$] and [bmim][$BF_4$], Ind. Eng. Chem. Res. 44 (2005) 4453–4464.
[37] S.H. Barghi, M. Adibi, D. Rashtchian, An experimental study on permeability, diffusivity, and selectivity of $CO_2$ and $CH_4$ through [bmim][$Pf_6$] ionic liquid supported on an alumina membrane: investigation of temperature fluctuations effects, J. Membr. Sci. 362 (2010) 346–352.
[38] D. Morgan, L. Ferguson, P. Scovazzo, Diffusivities of gases in room temperature ionic liquids: data and correlations obtained using a lag-time technique, Ind. Eng. Chem. Res. 44 (2005) 4815–4823.
[39] R. Sander, Modeling atmospheric chemistry: interactions between bas-phase species and liquid cloud/aerosol particles, Surv. Geophys. 20 (1999) 1–31.

## 4.4. Albo J., Santos E., Neves L.A., Simeonov S.P., Afonso C.A.M., Crespo J.G., Irabien A. Separation performance of $CO_2$ through Supported Magnetic Ionic Liquid Membranes (SMILMs). *Sep. Pur. Technol.* 2012, 97, 26-33.

Resumen

Debido a propiedades únicas, como son la despreciable presión de vapor y selectividad, los líquidos iónicos (LIs) han alcanzando un gran interés como disolventes de $CO_2$, y por tanto su aplicación resulta interesante para la obtención de membranas líquidas soportadas. Los líquidos iónicos que contiene metales en su anión se conocen como Líquidos Iónicos Magnéticos (LIMs) y muestran diferente comportamiento en presencia de un campo magnético externo.

En este trabajo se evalúa la preparación y uso de una nueva clase de membranas líquidas soportadas basadas en Líquidos Iónicos Magnéticos: Membranas Soportadas con Líquidos Iónicos Magnéticos (MSLIMs) para la separación/concentración de $CO_2$. Se estudian cuatro líquidos iónicos paramagnéticos: $[P_{6,6,6,14}]^{2+}[CoCl_4]^{2-}$, $[P_{6,6,6,14}]^{+}[FeCl_4]^{-}$,$[P_{6,6,6,14}]^{2+}[MnCl_4]^{2-}$ y $[P_{6,6,6,14}]^{3+}[GdCl_6]^{3}$; impregnados en soportes porosos hidrofóbicos e hidrofílicos de PVDF. Se evalúa experimentalmente la estabilidad de las membranas y las permeabilidades de $CO_2$, $N_2$ y aire en las MSLIMs estables. Se calculan las selectividades $CO_2/N_2$ y $CO_2$/aire y se introducen en el diagrama de Robeson para su comparación. A través de los resultados con gases puros se observa que la permeabilidad de $CO_2$ en las MSLIMs es mayor a las permeabilidades de $N_2$ y aire. Esta selectividad podría indicar la aplicación potencial de las MSLIMs para la eliminación/recuperación de $CO_2$ de corrientes de gases. En trabajos futuros se evaluará la separación al aplicar un campo magnético externo.

*Original abstract*

Ionic liquids (ILs) have reached an enormous interest as $CO_2$ solvents due to their unique properties such as negligible vapour pressure and selectivity, making them very attractive in order to obtain stable supported liquid membranes. ILs containing magnetic metals in their anion are known as Magnetic Ionic Liquids (MILs) and they may show different behaviour in the presence of an external magnetic field.

This work evaluates the preparation and use of a new class of supported liquid membranes based on Magnetic Ionic Liquids: Supported Magnetic Ionic Liquid Membranes (SMILMs) for $CO_2$ separation/concentration. Four paramagnetic ionic liquids have been studied: $[P_{6,6,6,14}]^{2+}[CoCl_4]^{2-}$, $[P_{6,6,6,14}]^{+}[FeCl_4]^{-}$,$[P_{6,6,6,14}]^{2+}[MnCl_4]^{2-}$ and $[P_{6,6,6,14}]^{3+}[GdCl_6]^{3}$; in combination with a hydrophobic or a hydrophilic PVDF porous support. An evaluation of the membrane stability was carried out and $CO_2$, $N_2$ and air permeabilites for stable SMILMs were experimentally determined. $CO_2/N_2$ and $CO_2$/air selectivities were estimated and introduced in

the Robeson diagram for a comparison with previous reported materials. Pure gas permeation results demonstrate that these SMILMs show much higher $CO_2$ permeabilities when comparing with $N_2$ and air. This selectivity may indicate a potential application of using SMILMs for the selective removal/recovery of $CO_2$ from a gas stream and further work will perform the evaluation of an external magnetic field in the separation behaviour.

Separation and Purification Technology 97 (2012) 26–33

Contents lists available at SciVerse ScienceDirect

Separation and Purification Technology

journal homepage: www.elsevier.com/locate/seppur

# Separation performance of $CO_2$ through Supported Magnetic Ionic Liquid Membranes (SMILMs)

J. Albo [a,*], E. Santos [a], L.A. Neves [b], S.P. Simeonov [c], C.A.M. Afonso [c,d], J.G. Crespo [b], A. Irabien [a]

[a] Departamento Ingeniería Química y Química Inorgánica, E.T.S. de Ingenieros Industriales y Telecomunicación, Universidad de Cantabria, 39005, Avda. Los Castros s/n, Santander, Spain
[b] REQUIMTE-CQFB, Departamento de Quimica, Faculdade de Ciencias e Tecnologia, Universidade Nova de Lisboa, 2829-516 Caparica, Portugal
[c] iMed.UL, Faculdade de Farmácia, Universidade de Lisboa, 1649-003 Lisboa, Portugal
[d] CQFM, Centro de Química-Física Molecular and IN–Institute of Nanosciences and Nanotechnology, Instituto Superior Técnico, 1049-001 Lisboa, Portugal

ARTICLE INFO

*Article history:*
Available online 24 January 2012

*Keywords:*
Carbon dioxide separation
Magnetic Ionic Liquids
Supported Magnetic Ionic Liquid Membranes (SMILMs)
$CO_2/N_2$ membrane separation

ABSTRACT

Ionic liquids (ILs) have reached an enormous interest as $CO_2$ solvents due to their unique properties such as negligible vapour pressure and selectivity, making them very attractive in order to obtain stable supported liquid membranes. ILs containing magnetic metals in their anion are known as Magnetic Ionic Liquids (MILs) and they may show different behaviour in the presence of an external magnetic field.

This work evaluates the preparation and use of a new class of supported liquid membranes based on Magnetic Ionic Liquids: Supported Magnetic Ionic Liquid Membranes (SMILMs) for $CO_2$ separation/concentration. Four paramagnetic ionic liquids have been studied: $[P_{6,6,6,14}]_2^+[CoCl_4]^{2-}$, $[P_{6,6,6,14}]^+[FeCl_4]^-$, $[P_{6,6,6,14}]_2^+[MnCl_4]^{2-}$ and $[P_{6,6,6,14}]_3^+[GdCl_6]^3$; in combination with a hydrophobic or a hydrophilic PVDF porous support. An evaluation of the membrane stability was carried out and $CO_2$, $N_2$ and air permeabilites for stable SMILMs were experimentally determined. $CO_2/N_2$ and $CO_2$/air selectivities were estimated and introduced in the Robeson diagram for a comparison with previous reported materials. Pure gas permeation results demonstrate that these SMILMs show much higher $CO_2$ permeabilities when comparing with $N_2$ and air. This selectivity may indicate a potential application of using SMILMs for the selective removal/recovery of $CO_2$ from a gas stream and further work will perform the evaluation of an external magnetic field in the separation behaviour.



## 1. Introduction

Carbon dioxide ($CO_2$) absorption is an important separation process where efforts have to be applied in order to develop sustainable processes for greenhouse gases mitigation. The existing process for $CO_2$ capture uses a reversible absorption in amines. Typically, this process requires the application of high temperatures to a stripper re-boiler for solvent regeneration and $CO_2$ desorption, which poses as main drawbacks the energy consumption and the solvent losses.

As an alternative, gas separation using membrane technology offers numerous advantages over the absorption process, including their modular design, high surface area per unit volume and energy efficiency among others [1], but it remains with few technical applications due to the permeability and selectivity requirements of the process.

Some studies have applied the non-dispersive membrane-based technology for $CO_2$ absorption, such as hollow fibre membrane contactors, where gas and liquid flow on opposites sides of the membrane equipment and a fluid/fluid interface forms inside each membrane pore. Previous studies report different conditions for the carbon dioxide separation processes using membranes [2–4]. Specifically, recent works combine hollow membrane contactors with ionic liquids (ILs) for $CO_2$ absorption [5,6] since they can have an extraordinary affinity to this gas [7,8].

Microporous and/or dense membranes are very attractive but it is still possible to improve the selectivity and permeability of the gas separation process by using supported ionic liquid membranes (SILMs) [9–19]. In a supported ionic liquid membrane, an ionic liquid is immobilized inside the pores of a polymeric or a ceramic support. In this configuration, the solute molecule dissolves into the membrane at the feed/membrane interface, it diffuses through the membrane and desorbs at the opposite membrane surface. Although the combination of ionic liquids (ILs) with SLMs present advantages due to the high stability and non-volatile character of these liquids, these membranes still present limited mechanical stability, which restrict membrane flux needed for industrial application. As an alternative, polymerized ILs have been developed as dense membranes. These polymerized membranes present higher

* Corresponding author. Tel.: +34 942 206749; fax: +34 942 201591.
*E-mail address:* alboj@unican.es (J. Albo).

1383-5866/$ - see front matter © 2012 Elsevier B.V. All rights reserved.
doi:10.1016/j.seppur.2012.01.034

mechanical stability and can be easily fabricated into thin-layer films [20–23]. However, a decrease in permeability has been reported due to lower gas diffusivity [24]. Even though, supported ionic liquid membranes (SILMs) and (poly-ILMs) showed promising permeability/selectivity results that are among the best results presented in literature using other materials represented by the Robeson plot upper bound [14,15,20,22,24] for the $CO_2/N_2$ separation.

One of the most interesting properties of ionic liquids is the fact that their physical and chemical properties are tuneable, depending on the cation and anion present in their structure, making them to be considered as 'designer solvents'. This property has made possible the substitution of common anions for others with a metal ion, such us $FeCl_4^-$, conferring them a magnetic response. These Magnetic Ionic Liquids (MILs) are an interesting approach in selective separation processes, since the molecule to be separated, may have higher or lower permeability depending on the magnetic field strength applied to a SMILM [25]. An example described in literature using Magnetic Ionic Liquids has shown that the extraction of some organics increases using MILs in the presence of a magnetic field [26].

In this work, Supported Magnetic Ionic Liquid Membranes (SMILMs) including a number of new different phosphonium based MILs: $[P_{6,6,6,14}]_2^+[CoCl_4]^{2-}$, $[P_{6,6,6,14}]^+[FeCl_4]^-$, $[P_{6,6,6,14}]_2^+[MnCl_4]^{2-}$ and $[P_{6,6,6,14}]_3^+[GdCl_6]^3$ were studied. Two different microporous membranes (hydrophilic and hydrophobic) made of PVDF were used as support to evaluate the following properties: (1) immobilisation of MIL in polymeric membranes; (2) stability of these systems and characterisation of the ionic liquid support interaction; (3) gas permeability and selectivity towards $CO_2$ and (4) behaviour of the prepared membranes in the separation of $CO_2/N_2$ mixtures in comparison with the Robeson upper bound. Based in these results, future work will be focused on the influence of an external magnetic field in the SMILMs behaviour.

## 2. Materials and methods

### 2.1. Polymeric microporous membranes

The supported ionic liquid membranes were prepared using commercial microporous membranes made of polyvinylidene fluoride (PVDF) as supporting material. The membranes present similar pore size but different chemical nature: one is hydrophobic (from Millipore Corporation) and the other one hydrophilic (provided by Pall Corporation). They are characterized by their high chemical resistance and usefulness for a wide range of applications. The nominal pore size and thickness are included in Table 1.

### 2.2. Magnetic Ionic Liquids (MILs)

The following MILs based in the phosphonium cation were first synthesized in *Faculdade de Farmácia*, *Universidade de Lisboa* (*Portugal*) and studied in the present work:

- Phosphonium tretrachlorocobalt ($[P_{6,6,6,14}][CoCl_4]$).
- Phosphonium tretrachloroferrate ($[P_{6,6,6,14}][FeCl_4]$).
- Phosphonium tretrachloromanganese ($[P_{6,6,6,14}][MnCl_4]$).
- Phosphonium hexachlorogadolinium ($[P_{6,6,6,14}][GdCl_6]$).

**Table 1**
Commercial membranes used as the support of MILs.

| | Material | Pore size (μm) | Thickness (μm) |
|---|---|---|---|
| Pall corporation | Hydrophilic PVDF | 0.20 | 129 |
| Millipore | Hydrophobic PVDF | 0.22 | 125 |

All are based in the phosphonium cation, due to the relatively high $CO_2$ solubility reported in phosphonium-based MILs [27]. In addition, different metals presenting different magnetic response [28] are included in the anion, in order to study the stability and gas transport properties when MILs are immobilized in a polymeric porous support.

The ionic liquids were prepared according to the following procedures [28]. To a solution of $[P_{6,6,6,14}][Cl]$ (50 g, 0.096 mol) in dichloromethane was added cobalt chloride (11.45 g, 0.5 equiv.), iron (III) chloride hexahydrate (26.02 g, 1 equiv.), manganese chloride (26.02 g, 0.5 equiv.) or gadolinium (III) chloride hexahydrate (11.92 g, 0.3 equiv.). The solution was stirred at room temperature for 24 h. After that, two layers were formed, and the aqueous phase was decanted. The organic phase was dried over $MgSO_4$ and filtered. The solvent was removed under vacuum, and the IL stirred under vacuum (<1 mmHg) at 60 °C overnight. $[P_{6,6,6,14}]_2^+[CoCl_4]^{2-}$ was obtained as a blue viscous oil, yield 52.87 g (94%); $[P_{6,6,6,14}]^+[FeCl_4]^-$ brown viscous oil, yield 64.30 g (98%); $[P_{6,6,6,14}]_2^+[MnCl_4]^{2-}$ as a green viscous oil, yield 53.8 g (96%) and $[P_{6,6,6,14}]_3^+[GdCl_6]^{3-}$ colourless viscous oil, yield 56.12 g (96%).

The water content was determined by Karl–Fisher titration method, while in the case of $[P_{6,6,6,14}]^+[FeCl_4]^-$ was determined gravimetrically weighting 1 mL before and after 48 h of vacuum and heating. The $CO_2$ solubility was experimentally obtained by a thermogravimetric system at room temperature and atmospheric pressure in the absence of magnetic field [27]. Values are listed in Table 2.

The magnetic moment measurement procedure was described previously [29]. Results were provided by *Magnetism in Matter* group at CITIMAC, University of Cantabria, and they are shown in Table 3.

The results are in good agreement with the literature reported magnetic moments ($\chi_m T$) for $[CoCl_4]^{2-}$ (2.01–2.48 emu K/mol), $[FeCl_4]^-$ (3.74–4.46 emu K/mol), and $[MnCl_4]^{2-}$ (4.14–4.76 emu K/mol) but it does not agree well with the expected value for the gadolinium anion (7.72 emu K/ mol) reported in the literature [28–30].

### 2.3. Preparation of Supported Magnetic Ionic Liquid Membranes (SMILMs)

To immobilize the MILs, the microporous PVDF membrane was introduced into a vacuum chamber for 1 h in order to remove the air from the pores and, therefore allowing an easier introduction of MIL into their porous structure. Once the membrane was under vacuum for 1 h, drops of MILs are spread out at the membrane surface using a syringe, while keeping the vacuum inside the chamber. Then the liquid excess on the membrane surface was wiped up softly with a tissue. The amount of liquid immobilized in the membrane was determined gravimetrically, and the increase of thickness was measured using a micrometer before and after the immobilization procedure.

After soaking the membrane, their weight and thickness increased, depending on the hydrophilic or hydrophobic character of the liquid and the membrane. Table 4 shows that the increase is higher when using the more hydrophilic PVDF membrane. This difference may be due only to differences in the membrane porosity and thickness.

These results show an increase of 52.3–63.4% and 6.9–20% for weight and thickness respectively, depending on the MIL-microporous membrane combination.

### 2.4. Stability of SMILMs

The experimental set-up used for evaluation of membrane stability has been described elsewhere [9]. Basically, the SMILMs were placed in a dead-end filtration cell, with an effective membrane

**Table 2**
Magnetic Ionic Liquids (MILs).

| Molecular formula | Structure | Molecular weight (g mol$^{-1}$) | Water content (% wt.) | $CO_2$ solubility (% wt.) |
|---|---|---|---|---|
| $[P_{6,6,6,14}]_2^+[CoCl_4]^{2-}$ | 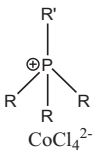 R= hexyl R'= tetradecyl $CoCl_4^{2-}$ | 1112 | $5.1 \times 10^{-4}$ | 0.405 |
| $[P_{6,6,6,14}]^+[FeCl_4]^-$ | 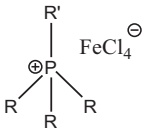 $FeCl_4^{\ominus}$ R=hexyl R'=tetradecyl | 681.51 | 1.02 | 0.499 |
| $[P_{6,6,6,14}]_2^+[MnCl_4]^{2-}$ | 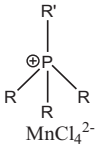 R=hexyl R'= tetradecyl $MnCl_4^{2-}$ | 1103 | 0.35 | 0.363 |
| $[P_{6,6,6,14}]_3^+[GdCl_6]^{3-}$ | 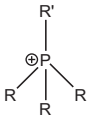 R=hexyl R'=tetradecyl $GdCl_6^{3-}$ | 1821.54 | 0.2 | 0.251 |

**Table 3**
Magnetic properties of selected transition metal based MILs.

| MILs | $\chi_m T$ (emu K/mol) | $\mu_{eff}$ ($\mu_B$/ion) | $\theta_p$ (K) |
|---|---|---|---|
| $[P_{6,6,6,14}]_2^+[CoCl_4]^{2-}$ | 2.10 | 4.00 | 3 |
| $[P_{6,6,6,14}]^+[FeCl_4]^-$ | 4.29 | 5.89 | −0.5 |
| $[P_{6,6,6,14}]_2^+[MnCl_4]^{2-}$ | 4.23 | 5.40 | −1.6 |
| $[P_{6,6,6,14}]_3^+[GdCl_6]^{3-}$ | 6.51 | 6.32 | 1.29 |

**Table 4**
Weight increase and thickness after immobilization.

| MIL | Membrane | Weight increase (% wt.) | Thickness increase (% thk.) |
|---|---|---|---|
| $[P_{6,6,6,14}]_2^+[CoCl_4]^{2-}$ | Hydrophobic PVDF | 53.1 | 11.1 |
| | Hydrophilic PVDF | 63.4 | 20 |
| $[P_{6,6,6,14}]^+[FeCl_4]^-$ | Hydrophobic PVDF | 52.9 | 6.9 |
| | Hydrophilic PVDF | 59.7 | 14.3 |
| $[P_{6,6,6,14}]_2^+[MnCl_4]^{2-}$ | Hydrophobic PVDF | 52.2 | 6.9 |
| | Hydrophilic PVDF | 60.6 | 11.1 |
| $[P_{6,6,6,14}]_3^+[GdCl_6]^{3-}$ | Hydrophobic PVDF | 54.3 | 11.1 |
| | Hydrophilic PVDF | 61.2 | 17.2 |

area of 3.46 cm$^2$. A pressure up to 2 bar was applied using a nitrogen flux. To determine their stability, the membranes were weighed using an analytical balance (Sartorius A.G. Göttingen CP225D, Germany) at regular periods of time in order to determine the weight decrease, which is assumed to be related to the loss of MIL along time. In addition, the flux of $N_2$ through the membrane was measured using a gas flowmeter (J&W Scientific) connected to the cell permeate outlet, in order to evaluate the stability of SMILMs by following the increase of flow with the applied pressure.

### 2.5. Gas permeation experiments

The gases used in the experiments were nitrogen (industrial grade (99.99%), Praxair, USA), carbon dioxide (high-purity grade (99.998%), Praxair, USA) and air (20% $O_2$, $CO_2 \leqslant 1$ ppm, $CO \leqslant 1$ ppm, $H_2O \leqslant 3$ ppm and $N_2$ rest to balance (99.999%), Praxair, USA).

The experimental setup used for the gas permeation measurements is shown in Fig. 1. The effective membrane area was about 12.6 cm$^2$. The feed gas ($CO_2$, $N_2$ or air) is introduced in the compartments and after opening the permeate outlet, a driving force of around 0.45 bar between the feed and the permeate is established. This pressure difference leads to a flux across the membrane. Two pressure transducers measure the pressure in both compartments during the experimented time. The temperature is maintained at 25 °C in a water bath.

The permeability of the pure gas through the membrane is calculated from the pressure data from the feed and permeate compartments, according to the following equation:

$$\ln\left(\frac{[p_{feed} - p_{perm}]_0}{[p_{feed} - p_{perm}]}\right) = \ln\left(\frac{\Delta p_0}{\Delta p}\right) = \frac{D \cdot H \cdot \beta}{\delta} \cdot t \quad (1)$$

where $p_{feed}$ and $p_{perm}$ are the pressures in the feed and permeate compartments respectively; $D$ (m$^2$ s$^{-1}$) is the diffusivity, $H$ is the partition coefficient, $t$ is the time (s) and $\delta$ is the membrane thickness (m). The geometric parameter $\beta$ (m$^{-1}$) is:

$$\beta = A_m\left(\frac{1}{V_{feed}} + \frac{1}{V_{perm}}\right) \quad (2)$$

where $A_m$ is the membrane area (m$^2$) and $V_{feed}$ and $V_{permeate}$ are the volume of the feed and permeate compartments (m$^3$), respectively, and this take a value of 118.96 m$^{-1}$. The pressure data can be plotted as $\ln(\Delta p_0/\Delta p)$ versus $t$, and the gas permeability is obtained from the slope.

The permeability referred to a pressure gradient, $P$ (barrer), is calculated under room temperature conditions, atmospheric pressure and the standard molar volume, according to:

$$D \cdot H = P \cdot R \cdot T \quad (3)$$

$$P(barrer) = 8.3 \times 10^{-13}\ (\text{m}^2\ \text{s}^{-1}) \quad (4)$$

The ideal selectivity ($S_{A/B}$) can be determined by dividing the permeabilities of two different gases ($A$ and $B$). The selectivity can be also expressed by the solubility ($S$) and diffusion ($D$) contribution of each gas:

$$S_{A/B} = \frac{P_A}{P_B} = \frac{S_A \cdot D_A}{S_B \cdot D_B} \quad (5)$$

## 3. Results and discussion

### 3.1. Stability of SMILMs

The membrane weight as a function of time is represented in Fig. 2(a), for the different MILs immobilised in the hydrophobic and hydrophilic membranes, respectively, for a $N_2$ applied pressure of 1 bar. It is observed from the figure, an initial membrane weight loss below 10% in all cases, and after this decrease, a stabilisation in the amount of MILs within the membrane pores occurs, with the exception of the ionic liquid $[P_{6,6,6,14}]_2^+[CoCl_4]^{2-}$, probably related to a poorer impregnation into the pores due to its high viscosity. In hydrophilic supports, the membrane weight loss never reaches a stable value for the experimental time period (~13 h) at 1 bar pressure difference, providing a higher MILs looses (5.6–7.2%) than that observed for a hydrophobic support (3–5.5%), in accordance with literature results [9].

The use of an hydrophobic support impregnated with $[P_{6,6,6,14}]_3^+[GdCl_6]^{3-}$ ionic liquid exhibits the lowest weight losses value (3% wt.) from all the combinations studied. In order to further explore the stability of this gadolinium based membrane Fig. 2(b) represents the weight loss as a function of time for increasing applied pressures (up to 2 bar), in comparison with this liquid immobilised in hydrophilic supports.

According to the figure, when using the hydrophobic support, the main decrease in the membrane weight is observed in the first hour, reaching a stable value even if pressure differences up to 1.5 bar are applied. However, at 2 bar, a severe decrease in the membrane weight was observed in all cases. This pressure value probably exceeds the breakthrough pressure associated to the surface tension of the MIL within the membrane pores. In the case of the hydrophilic support, a decrease in membrane weight is produced for all applied pressure differences. Similar results were obtained for the other three SMILMs studied. All results indicate that the membranes based on the more hydrophobic support are more stable than those based on the hydrophilic support making possible a stable operation up to 1.5 bar pressure difference.

### 3.2. Gas permeation and ideal selectivities results

Gas permeability results are shown in Table 5. Permeability has been calculated as the linear relationship between the driving force

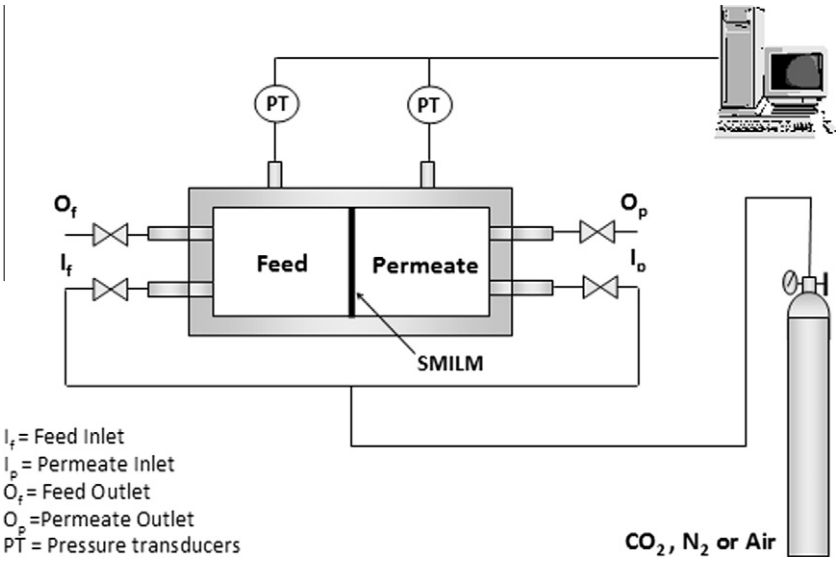


**Fig. 1.** Experimental set-up for gas permeation tests.

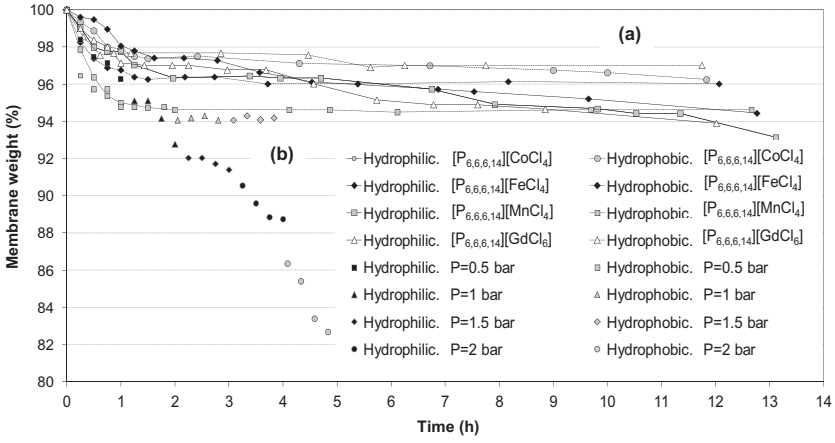


**Fig. 2.** (a) Relative membrane weight in hydrophobic and hydrophilic membranes immobilised with MILs as a function of time. Applied pressure difference 1 bar. (b) Relative membrane weight in hydrophobic and hydrophilic membranes immobilised with $[P_{6,6,6,14}]_3^+[GdCl_6]^{3-}$ as a function of time for different applied pressures.

**Table 5**
Permeability and selectivity for the SMILMs tested.

| MIL | Support | Gas | Permeability (barrer) | $CO_2/N_2$ selectivity | $CO_2$/air selectivity |
|---|---|---|---|---|---|
| $[P_{6,6,6,14}]_2^+[CoCl_4]^{2-}$ | Hydrophobic PVDF | $CO_2$ | 147.06 | 23.24 | 14.24 |
| | | $N_2$ | 6.33 | | |
| | | air | 10.33 | | |
| | Hydrophilic PVDF | $CO_2$ | 149.95 | 22.70 | 15.22 |
| | | $N_2$ | 6.61 | | |
| | | air | 9.85 | | |
| $[P_{6,6,6,14}]^+[FeCl_4]^-$ | Hydrophobic PVDF | $CO_2$ | 259.04 | 24.17 | 20.98 |
| | | $N_2$ | 10.72 | | |
| | | air | 12.34 | | |
| | Hydrophilic PVDF | $CO_2$ | 206.36 | 29.51 | 18.41 |
| | | $N_2$ | 6.99 | | |
| | | air | 11.21 | | |
| $[P_{6,6,6,14}]_2^+[MnCl_4]^{2-}$ | Hydrophobic PVDF | $CO_2$ | 202.63 | 41.20 | 26.90 |
| | | $N_2$ | 4.92 | | |
| | | air | 7.53 | | |
| | Hydrophilic PVDF | $CO_2$ | 155.01 | 21.08 | 18.42 |
| | | $N_2$ | 7.35 | | |
| | | air | 8.41 | | |
| $[P_{6,6,6,14}]_3^+[GdCl_6]^{3-}$ | Hydrophobic PVDF | $CO_2$ | 176.35 | 30.80 | 19.40 |
| | | $N_2$ | 5.73 | | |
| | | air | 9.09 | | |
| | Hydrophilic PVDF | $CO_2$ | 159.96 | 23.91 | 17.37 |
| | | $N_2$ | 6.69 | | |
| | | air | 9.21 | | |

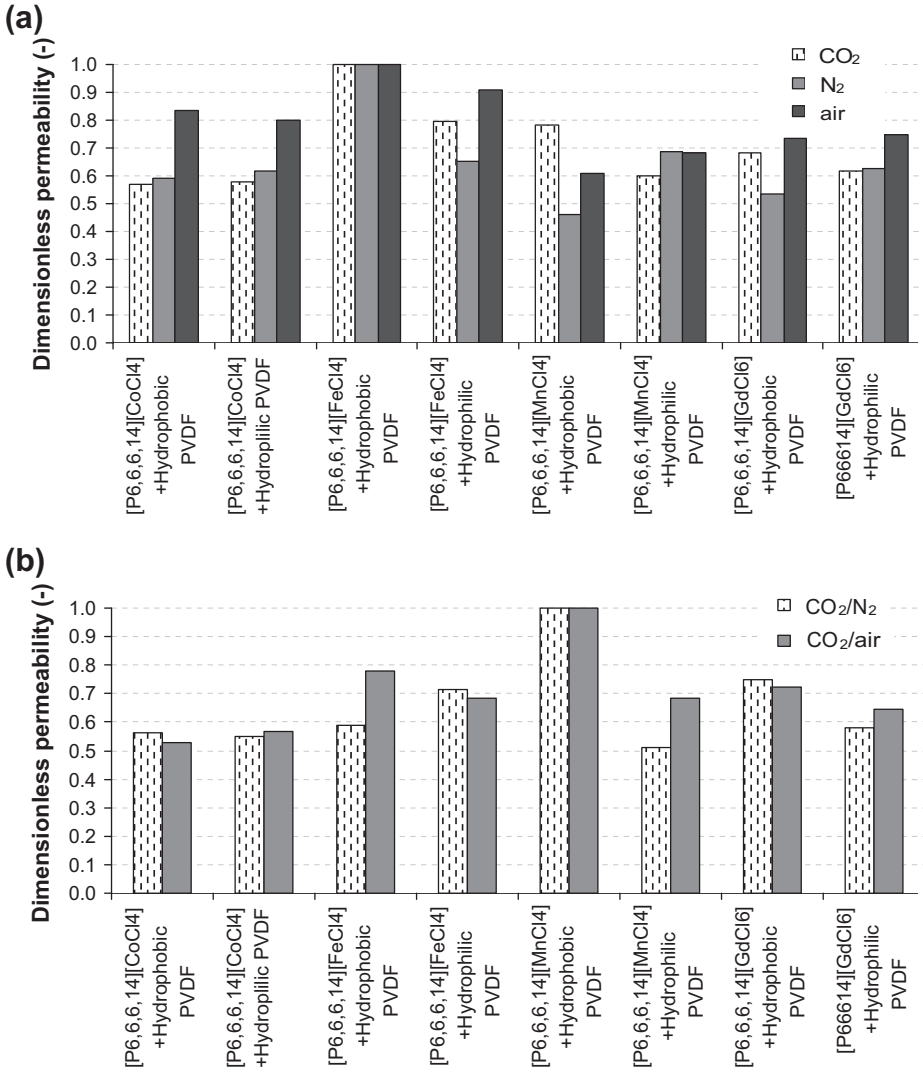


**Fig. 3.** Dimensionless (a) permeability (maximum $CO_2$ permeability = 259.04 barrer; maximum $N_2$ permeability = 10.72 barrer; maximum air permeability = 12.34 barrer. (b) selectivity (maximum selectivity $SCO_2/N_2$ = 41.2; maximum selectivity $SCO_2$/air = 26.9).

**Table 6**
Permeability of $CO_2$ through several SILMs.

| SILMs | | Permeability (barrer) | $CO_2$ solubility (% wt.) | $CO_2/N_2$ selectivity | $CO_2$/air selectivity | Reference |
|---|---|---|---|---|---|---|
| Membrane material | Ionic liquid | | | | | |
| Hydrophobic PVDF [a] | [mim][Ac] | 435.51 ± 0.48 | – | – | 27.5 | [17] |
| | [bim][Ac] | 1303.04 ± 2.41 | – | – | 27.7 | [17] |
| | [bmim][Ac] | 317.50 ± 0.72 | 7.70 | 25.1 | – | [27] |
| | [bmim][$BF_4$] | ~391.76 | 0.38 | 35 ± 0.2 | – | [9,31] |
| | [bmim][$BF_4$] [b] | 93.90 | 0.38 | 52.3 | – | [32,31] |
| | [bmim][$PF_6$] | ~168.76 | 0.30 | 23 ± 0.5 | – | [17,31] |
| | [emim][Ac] | 497.35 ± 0.96 | 8.60 | 32.66 | – | [27] |
| | [emim][$CF_3SO_3$] | 486.02 | – | 34 | – | [32] |
| | [$C_{10}$mim][$BF_4$] | ~512.30 | – | 22 ± 0.1 | – | [9] |
| | [$C_8$mim][$PF_6$] | ~361.62 | – | – | – | [9] |
| | Ammoeng 100 [b] | 93.90 | – | 52.6 | – | [32] |
| | Ecoeng 1111P [b] | 127.05 | – | 10.9 | – | [32] |
| | Cyphos 102 [b] | 637.05 | – | 41.5 | – | [32] |
| | Cyphos 103 [b] | 486.98 | – | 43.1 | – | [32] |
| | Cyphos 104 [b] | 642.00 | – | 31.6 | – | [32] |
| | [$Set_3$][$Tf_2N$] [b] | 746.99 | – | 26.3 | – | [32] |
| Hydrophilic PVDF [c] | [mim][Ac] | 529.41 ± 0.48 | – | – | 37 | [17] |
| | [bim][Ac] | 2460.22 ± 6.03 | – | – | 32.4 | [17] |
| | [bmim][Ac] | 369.33 ± 0.72 | 7.70 | 34.31 | – | [27] |
| | [emim][Ac] | 514.59 ± 2.65 | 8.60 | 42.43 | – | [27] |
| Polyethersulfone | [bmim][$BF_4$] | 460.22 ± 12.05 | 0.38 | – | – | [33][31] |
| | [bmim][$PF_6$] | 360.17 ± 15.07 | 0.30 | – | – | [33][31] |
| | [bmim][$TF_2N$] | 980.47 ± 23.02 | 0.90 | 17.76 | – | [33][34] |
| | [emim][$CF_3SO_3$] | 920.44 ± 30.01 | 0.24 | 35 | – | [14] |
| | [emim][Dca] | 610.29 ± 20.01 | 0.33 | 61 | – | [14] |
| | [emim][$TF_2N$][d] | 960.46 | 0.31 | 21 | – | [14] |
| | [emim][$TF_2N$][e] | 1050.51 | 0.30 | 20 | – | [14] |
| | [hmim][$BF_4$] | 520.25 ± 10.97 | 0.37 | – | – | [33][35] |
| | [thtdp][Cl] | 350.17 ± 20.01 | 0.30 | 15 | – | [14] |
| Polysulfone | [hmim][$TF_2N$] | 860.41 | 0.41 | – | – | [11][31] |

[a] Membrane thickness = 125 μm (applied in this work).
[b] Membrane thickness = 150 μm.
[c] Membrane thickness = 129 μm (applied in this work).
[d] 10% humidity.
[e] 85% humidity.

and time period according to Eq. (1), when temperature is maintained at 25 °C. It is worth mentioning that SMILMs act as a barrier for $N_2$ and air, since permeability of these gases is one order of magnitude lower than $CO_2$ permeability in all cases. According to these results stable SMILMs showing useful properties for the $CO_2/N_2$ separation can be prepared using PVDF microporous supports and MILs.

Fig. 3(a) shows a comparison between $CO_2$, $N_2$ and air permeability, in order to highlight the enhanced transport of $CO_2$. Permeabilities are shown in a dimensionless form referred to the maximum permeability. It can be observed that the ionic liquid $[P_{6,6,6,14}]^+[FeCl_4]^-$ reports the highest permeability in both membranes, being higher when combining with a PVDF hydrophobic support for $CO_2$ (259.04 barrer), $N_2$ (10.72 barrer), and air (12.34 barrer) gases.

Ideal selectivities $CO_2/N_2$ and $CO_2$/air have been calculated taking into account the ratio of pure gases permeability, following Eq. (5) and are presented in Fig. 3(b). It can be observed that all membranes tested present high selectivity towards $CO_2$ when compared with the gases $N_2$ and air. In this case, highest values of ideal selectivity are obtained with the SMILMs composed on $[P_{6,6,6,14}]_2^+[MnCl_4]^{2-}$ immobilised in the hydrophobic PVDF porous support.

A comparison of the permeabilities of $CO_2$ through several SILMs reported in literature is shown in Table 6. It can be observed that the SMILMs permeabilities reported in this work (ranging from $P_{CO_2}$ = 147.06–259.04 barrer and $P_{CO_2}$ = 149.47–206.36 barrer for PVDF hydrophobic and hydrophilic supports, respectively) are in the order of magnitude of the results reached in SILMs based in non-magnetic ILs, in which seems to be related to the higher $CO_2$ solubility in the acetate ionic liquids. The highest reported permeability towards $CO_2$ is observed using 1-butylimidazolium acetate [bim][Ac] ionic liquid in both, PVDF hydrophobic and hydrophilic supports.

In addition, the influence of the microporous support has been reported in $CO_2$ permeability results of SILMs based in 0.22 μm polyethersulfone support with the ionic liquid 1-butyl-3-methylimidazolium tetrafluoroborate [bmim][$BF_4$], which shows higher values than PVDF hydrophobic supports, although it is important to consider liquid immobilization on these supported membranes, compromising membrane mechanical stability.

### 3.3. Separation performance of SMILMs

An upper bound correlation for $CO_2/N_2$ separation in polymeric membranes was given by Robeson from data available in literature [36]. Therefore, results above this trend may be considered as an improvement over the current state of the art. Fig. 4 presents $CO_2/N_2$ selectivity as a function of $CO_2$ permeability, *P*. Results are compared with the separation performance when no liquid is impregnated and when highest $CO_2$ solubility commercial IL, [emim][Ac], [31] is immobilized inside the pores of these PVDF membranes.

From this figure it can be observed that the results obtained in this work for SMILMs are below the Robeson upper bound although, the separation performance is enhanced on these systems when comparing to non-impregnated membranes probably due to $CO_2$ solubility produced in the MILs. Hydrophobic PVDF supports in combination with $[P_{6,6,6,14}]_2^+[MnCl_4]^{2-}$ exhibit the best separation performance of the SMILMs researched systems.

Previous works have found a benzene solubility increase in MIL [bmim][$FeCl_4$], when applying a rotational magnetic field, due to its paramagnetic behaviour [25]. In addition higher phenolic

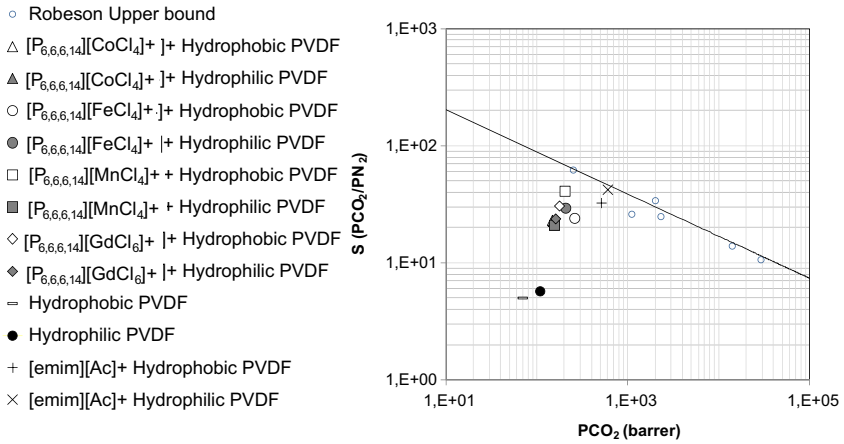


**Fig. 4.** $CO_2/N_2$ selectivity as a function of $CO_2$ permeability (1 barrer = $10^{-10}$ $cm^3$ (STP) cm $cm^{-2}$ $s^{-1}$ cm $Hg^{-1}$).

compounds extraction was observed by using $[3C_6PC_{14}][FeCl_4]$ at the presence of a neodymium magnet [26]. Once stable SMILMs have been prepared and characterized by first time in the literature, the application of an external magnetic field to SMILMs will be evaluated in order to understand the influence on the separation performance.

## 4. Conclusions

This work has been able to immobilize MILs, which were synthesised by first time, in microporous PVDF membranes obtaining stable SMILMs. It was observed that the hydrophobic Supported Magnetic Ionic Liquid Membranes (SMILMs) prepared are stable up to 1.5 bar pressure, possibly due to chemical affinity between the MILs and the supporting membrane. This pressure ensures their adequacy for operation under real process conditions.

The permeabilities of $CO_2$, $N_2$ and air have been determined using the different SMILMs prepared. For the combination of $[P_{6,6,6,14}]^+[FeCl_4]^-$ with a hydrophobic support, maximum values of permeability were obtained in the studied systems: $CO_2$ (259.04 barrer), $N_2$ (10.72 barrer), and air (12.34 barrer). However, $[P_{6,6,6,14}]_2^+[MnCl_4]^{2-}$ displays the best $CO_2/N_2$ separation performance in combination with hydrophobic PVDF since its result is closer to the Robeson upper bound correlation. The pure gas permeation results have also demonstrated that these systems are more selective to $CO_2$ when compared with $N_2$ and air, which indicates a potential application of using SMILMs for selective removal/recovery of $CO_2$ from gas streams.

The transition metals based MILs prepared containing phosphonium cations respond to a magnetic field due to the anion's paramagnetic nature. Further work is now ongoing on the use of an external magnetic field to SMILMs a technique for enhancing the separation performance for $CO_2$ recovery.

## Acknowledgements

The authors gratefully acknowledge the financial support from the European Research Action Network-ERANET Project EUI2008-03857 and CTM2006-0357. L.A. Neves would like to acknowledge the financial support of FCT-MCTES through the post-doc research Grant SFRH/BPD/64975/2009.

## References

[1] P. Bernardo, E. Drioli, G. Golemme, Membrane gas separation: a review/state of the art, Ind. Eng. Chem. Res. 48 (2009) 4638–4663.
[2] Y. Lee, R.D. Noble, B-Y. Yeom, Y-I. Park, K-H. Lee, Analysis of CO2 removal by hollow fiber membrane contactors, J. Memb. Sci. 194 (1) (2001) 57–67.
[3] M.H. Al-Marzouqi, M.H. El-Naas, S.A.M. Marzouk, M.A. Al-Zarooni, N. Abdullatif, R. Faiz, Modelling of $CO_2$ absorption in membrane contactors, Sep. Purif. Technol. 59 (2008) 286–293.
[4] R. Wang, H.Y. Zhang, P.H.M. Feron, D.T. Liang, Influence of membrane wetting on $CO_2$ capture in microporous hollow fiber membrane contactors, Sep. Purif. Technol. 46 (1–2) (2006) 33–40.
[5] J. Albo, P. Luis, A. Irabien, Carbon Dioxide Capture from Flue Gases Using a Cross-Flow Membrane Contactor and the Ionic Liquid 1-Ethyl-3-methylimidazolium Ethylsulfate, Ind. Eng. Chem. Res. 49 (2010) 11045–11051.
[6] J. Albo, P. Luis, A. Irabien, Absorption of coal combustion flue gases in ionic liquids using different membrane contactors, Desalin. Water Treat. 27 (2011) 54–59.
[7] R.E. Baltus, R.M. Counce, B.H. Culbertson, H. Luo, D.W. Depaoli, S. Dai, D.C. Duckworth, Examination of the Potential of Ionic Liquids for Gas Separations, Sep. Sci. Technol. 40 (2005) 525–541.
[8] R. Condermarin, P. Scovazzo, Gas Permeabilities, Solubilities, Diffusivities, and Diffusivity Correlations for Ammonium-based Room Temperature Ionic Liquids with Comparison to Imidazolium and Phosphonium RTIL Data, Chem. Eng. J. 147 (2009) 51–57.
[9] L.A. Neves, J.G. Crespo, I.M. Coelhoso, Gas permeation studies in supported ionic liquid membranes, J. Memb. Sci. 357 (2010) 160–170.
[10] R. Fortunato, C.A.M. Afonso, M.A.M. Reis, J.G. Crespo, Supported Liquid Membranes using Ionic Liquid: Study of Stability and Transport Mechanisms, J. Membr. Sci. 242 (2004) 197–209.
[11] J. Ilconich, C. Myers, H. Pennline, D. Luebke, Experimental Investigation of the Permeability and Selectivity of Supported Ionic Liquid Membranes for $CO_2$/He Separation at Temperatures up to 125 °C, J. Membr. Sci. 298 (2007) 41–47.
[12] L. Ferguson, P. Scovazzo, Solubility, Diffusivity, and Permeability of Gases in Phosphonium-based Room Temperature Ionic Liquids: Data and Correlations, Ind. Eng. Chem. Res 46 (2007) 1369–1374.
[13] A. Yokozeki, M.B. Shiflett, Hydrogen Purification using Room-Temperature Ionic Liquids, Appl. Energy. 84 (2007) 351–361.
[14] P. Scovazzo, J. Kieft, D.A. Finan, C. Koval, D. DuBois, R.D. Noble, Gas Separation using Non-Hexafluorophosphate [$PF_6$] anion Supported Ionic Liquid Membranes, J. Membr. Sci. 238 (2004) 57–63.
[15] P. Scovazzo, D. Havard, M. McShea, S. Mixon, D. Morgan, Long-Term, Continuous Mixed-gas Dry Fed $CO_2/CH_4$ and $CO_2/N_2$ Separation Performance and Selectivities for Room Temperature Ionic Liquid Membranes, J. Membr. Sci. 327 (2009) 41–48.
[16] J.E. Bara, C.J. Gabrel, T.K. Carlisle, D.E. Camper, A. Finotello, D.L. Gin, R.D. Noble, Gas Separation in Fluoroalkyl- Functionalized Room-Temperature Ionic Liquids Using Supported Liquid Membranes, Chem. Eng. J. 47 (2009) 43–50.
[17] P. Luis, L.A. Neves, C.A.M. Afonso, I.M. Coelhoso, J.G. Crespo, A. Garea, A. Irabien, Facilitated transport of $CO_2$ and $SO_2$ through Supported Ionic Liquid Membranes (SILMs), Desalination. 245 (2009) 485–493.
[18] Q. Gan, D. Rooney, M. Xue, G. Thompson, Y. Zou, An experimental study of gas transport and separation properties of ionic liquids supported on nanofiltration membranes, J. Membr. Sci. 280 (2006) 948–956.
[19] L.C. Branco, J.N. Rosa, J.J. Moura Ramos, C.A.M. Afonso, Preparation and characterization of new room temperature ionic liquids, Chem. Eur. J. 8 (2002) 3671–3677.
[20] J.E. Bara, S. Lessmann, C.J. Gabriel, E.S. Hatakeyama, R.D. Noble, D.L. Gin, Synthesis and performance of polymerizable room-temperature ionic liquids as gas separation membranes, J. Membrane Sci. 46 (2007) 5397–5404.
[21] J.E. Bara, C.J. Gabriel, E.S. Hatakeyama, T.K. Carlisle, S. Lessmann, R.D. Noble, D.L. Gin, Improving $CO_2$ selectivity in polymerized room-temperature ionic liquid gas separation membranes through incorporation of polar substituents, J. Memb. Sci. 321 (2008) 3–7.

[22] J.E. Bara, E.S. Hatakeyama, L.G. Douglas, R.D. Noble, Improving $CO_2$ permeability in polymerized room-temperature ionic liquid gas separation membranes through the formation of a solid composite with a room-temperature ionic liquid, Polym. Adv. Technol. 19 (2008) 1415–1420.
[23] T.K. Carlisle, J.E. Bara, A.L. Lafrateb, D.L. Gin, R.D. Noble, Main-chain imidazolium polymer membranes for $CO_2$ separations: An initial study of a new ionic liquid-inspired platform, J. Memb. Sci. 359 (2010) 37–43.
[24] P. Scovazzo, Determination of the Upper Limits, Benchmarks and Critical Properties for Gas Separations using Stabilized Room Temperature Ionic Liquid Membranes (SILMs) for the Purpose of Guiding Future Research, J. Membr. Sci. 343 (2009) 199–211.
[25] Y. Jiang, C. Gou, H. Liu, Magnetically rotational reactor for absorbing benzene emissions by ionic liquids, China Part. 5 (1–2) (2006) 130–133.
[26] N. Deng, M. Lin, L. Zhao, C. Liu, S. de Rooy, I.M. Warner, Highly efficient extraction of phenolic compounds by use of magnetic room temperature ionic liquids for environmental remediation, J. Hazard. Mater (2011), doi:10.1016/j.jhazmat.2011.06.053.
[27] J. Albo, E. Santos, A. Rosatella, C. Afonso, A. Irabien, Solubility of Carbon Dioxide in Magnetic Ionic Liquids, in: 2nd Iberian Meeting on Ionic Liquids, Santiago de Compostela, Spain, 2011.
[28] R.E. Del Sesto, T.M. McCleskey, A.K. Burrel, G.A. Baker, J.D. Thompson, B.L. Scott, J.S. Wilkes, P. Williams, Structure and magnetic behaviour of transition metal based ionic liquids, Chem. Commun. (2008) 447–449.
[29] I. de Pedro, D.P. Rojas, J. Albo, P. Luis, A. Irabien, J. Blanco, J. Rodriguez, Long-range magnetic ordering in magnetic ionic liquid: Emim[$FeCl_4$], J. Phys. Condens. Matter. 22 (2010) 296–306.
[30] S. Hayashi, S. Saha, H.A. Hamaguchi, A new class of magnetic fluids: bmim[FeCl4] nbmim [FeCl4] Ionic Liquids, IEEE Transaction on Magnetics. 42 (2006). Nª1 January.
[31] A. Yokozeki, M.B. Shiflett, C.P. Junk, L.M. Grieco, T. Foo, Physical and Chemical Absorptions of Carbon Dioxide in Room-Temperature Ionic Liquids, J. Phys. Chem. B. 112 (2008) 16654–16663.
[32] P. Cserjési, N. Nemestóthy, K. Bélafi-Bakó, Gas separation properties of supported liquids membranes prepared with unconventional ionic liquids, J. Membr. Sci. 349 (2010) 6–11.
[33] Y. Jiang, Z. Zhou, Z. Jiao, L. Li, Y. Wu, Z. Zhang, $SO_2$ gas separation using supported ionic liquid membranes, J. Phys. Chem. B. 111 (19) (2007) 5058–5061.
[34] S. Supasitmongkol, P. Styring, High $CO_2$ solubility in ionic liquids and a tetraalkylammonium-based poly(ionic liquid), Energy Environ. Sci. 3 (2010) 1961–1972.
[35] Y.S. Kim, W.Y. Choi, J.H. Jang, K.-P. Yoo, C.S. Lee, Solubility measurement and prediction of carbon dioxide in ionic liquids, Fluid Phase Equilibr. 228–229 (2005) 439–445.
[36] L.M. Robeson, The upper bound revisited, J. Memb. Sci. 320 (2008) 390–400.

## 4.5. Daniel C.I., Albo J., Santos E., Portugal C.A.M., Crespo J.G., Irabien A. A group contribution method for the influence of the temperature in the viscosity of magnetic ionic liquids. *Fluid Phase Equilibr.* 2013, 360, 29-35.

Resumen

Los líquidos iónicos están siendo ampliamente estudiados debido a sus potenciales propiedades como disolventes. La predicción de sus propiedades físico-químicas es una estrategia importante que permite lograr un mejor conocimiento para futuras aplicaciones.

El presente trabajo aplica un método de contribución de grupos para estimar la viscosidad a diferentes temperaturas de una nueva generación de líquidos iónicos, líquidos iónicos magnéticos (LIMs), que están compuestos por aniones que contienen metales de transición. Estas nuevas sustancias han recibido un gran interés debido a su respuesta a la presencia de un campo magnético. En este estudio, los líquidos iónicos magnéticos están basados en el catión fosfonio $[P_{66614}]^+$ con diferentes longitudes de cadena y en los aniones magnéticos: $[GdCl_6]^{3-}$ $[MnCl_4]^{2-}$ $[FeCl_4]^-$ y $[CoCl_4]^{2-}$. La base de datos abarca un amplio rango de temperaturas, 293,15- 373,15K y de viscosidades 44-123500 cP. Las estimaciones del modelo muestran una buena concordancia con los resultados experimentales con un porcentaje de desviación media de 7,64 %. Estos resultados confirman el interés de este modelo para la estimación de la viscosidad y la influencia de la temperatura, pudiendo ser extendido para una gran variedad de combinaciones de grupos en los líquidos iónicos magnéticos que conducen a diferentes aplicaciones.

*Original abstract*

Ionic liquids are widely under research due to their potential properties as solvents. The prediction of their physicochemical properties is an important strategy to achieve a better knowledge for further applications.

The present work applies a group contribution method to estimate the viscosity at different temperatures of a new generation of ionic liquids, magnetic ionic liquids (MILs), which are comprised by anions containing transition metal complexes. These new substances have received a high interest due to their response at the presence of a magnetic field. In this study the magnetic ionic liquids are based on the phosphonium cation $[P_{66614}]^+$ with different chain lengths and on the magnetic anions: $[GdCl_6]^{3-}$ $[MnCl_4]^{2-}$ $[FeCl_4]^-$ and $[CoCl_4]^{2-}$. The database covers a wide range of temperature, 293.15-373.15K, and viscosity 44-123500 cP. The modelling estimations show a good agreement with the experimental results, presenting a mean percentage deviation of 7.64%. These results confirm the interest of this model for the

estimation of viscosity and the influence of the temperature, which can be extended for a large variety of group combinations in magnetic ionic liquids leading to different applications.

Fluid Phase Equilibria 360 (2013) 29–35

Contents lists available at ScienceDirect

Fluid Phase Equilibria

journal homepage: www.elsevier.com/locate/fluid

# A group contribution method for the influence of the temperature in the viscosity of magnetic ionic liquids

C.I. Daniel[a,*], J. Albo[b], E. Santos[b], C.A.M. Portugal[a], J.G. Crespo[a], A. Irabien[b]

[a] REQUIMTE-CQFB, Departamento de Quimica, Faculdade de Ciências e Tecnologia, Universidade Nova de Lisboa, 2829-516 Caparica, Portugal
[b] Departamento Ingeniería Química y Química Inorgánica, E.T.S. de Ingenieros Industriales y Telecomunicación, Universidad de Cantabria, 39005 Santander, Spain

ARTICLE INFO

*Article history:*
Received 25 March 2013
Received in revised form 23 August 2013
Accepted 26 August 2013
Available online 10 September 2013

*Keywords:*
Magnetic ionic liquids
Viscosity
Temperature influence
Group contribution model

ABSTRACT

Ionic liquids are widely under research due to their potential properties as solvents. The prediction of their physicochemical properties is an important strategy to achieve a better knowledge for further applications.

The present work applies a group contribution method to estimate the viscosity at different temperatures of a new generation of ionic liquids, magnetic ionic liquids (MILs), which are comprised by anions containing transition metal complexes. These new substances have received a high interest due to their response at the presence of a magnetic field. In this study the magnetic ionic liquids are based on the phosphonium cation $[P_{66614}]^+$ with different chain lengths and on the magnetic anions: $[GdCl_6]^{3-}$, $[MnCl_4]^{2-}$, $[FeCl_4]^-$ and $[CoCl_4]^{2-}$. The database covers a wide range of temperature, 293.15–373.15 K, and viscosity 44–123 500 cP. The modelling estimations show a good agreement with the experimental results, presenting a mean percentage deviation of 7.64%. These results confirm the interest of this model for the estimation of viscosity and the influence of the temperature, which can be extended for a large variety of group combinations in magnetic ionic liquids leading to different applications.



## 1. Introduction

Ionic liquids (ILs) have been receiving a high interest for their unique physicochemical properties. They may be regarded as organic solvents comprised entirely by ions in the liquid state over a wide temperature range including room temperature (RTILs – room temperature ionic liquids). These ILs show a low melting point, high thermal stability and thermal capacities, non-measurable vapour pressure and they are non-flammable, and reusable. Additionally, their physicochemical properties can be modified by changing their cationic and anionic composition according to their specific task, being recognized as "green and designer solvents" [1].

A new generation of magnetic sensitive ionic liquids – magnetic ionic liquids (MILs), exhibiting a response to the magnetic field has been developed [2–4]. MILs are comprised by anions containing transition metal complexes, having properties (solubility, viscosity, surface tension and molecular orientation), that may be influenced by the presence of an applied magnetic field [2–5]. Actually, magnetically induced changes of IL solubility were confirmed by the dependence found between the concentration of binary MIL/water mixtures and the applied magnetic field strength [2].

A deeper knowledge about the fundamental properties of ILs is required, including: density, viscosity, solubility, surface tension, refractive index and speed of sound, in order to better understand their structure–properties relationships [6]. One of the important physical properties of ILs is viscosity [7], which is higher for most ILs than for common organic solvents. The viscosity of ILs may be adjusted by a judicious cation–anion combination leading to ILs with lower or higher viscosity depending on the requirements.

ILs estimation models for the temperature influence in the viscosity are available in the literature supported in different assumptions. The widely used are: Arrhenius-like law [8], Vogel–Fulcher–Tamman (VFT) [9–11], modified Vogel–Fulcher–Tamman (mVFT) [12], Litovitz, fluidity equation [13] and Orrick–Erbar equation [14]. The group contribution methods are common to estimate the viscosity of complex molecules, such as Orrick–Erbar equation [14], Sastry–Rao method [15] and the UNIFAC–VISCO method [16]. In this method it is assumed that the physicochemical properties of the molecules are the

*Abbreviations:* MIL, magnetic ionic liquid; IL, ionic liquid; RTILs, room temperature ionic liquids; VFT, Vogel–Fulcher–Tamman equation; mVFT, modified Vogel–Fulcher–Tamman equation; $[P_{66614}]^+$, phosphonium cation; $[GdCl_6]^{3-}$, hexachlorogadolinium anion; $[MnCl_4]^{2-}$, tetrachloromanganese anion; $[FeCl_4]^-$, tetrachloroferrate anion; $[CoCl_4]^{2-}$, tetrachlorocobalt anion; $[P_{66614}]_3[GdCl_6]$, phosphonium hexachlorogadolinium; $[P_{66614}]_2[MnCl_4]$, phosphonium tetrachloromanganese; $[P_{66614}][FeCl_4]$, phosphonium tetrachloroferrate; $[P_{66614}]_2[CoCl_4]$, phosphonium tetrachlorocobalt; MPD, mean percentage deviation.

* Corresponding author. Tel.: +351 212948300.
*E-mail address:* cid17734@campus.fct.unl.pt (C.I. Daniel).

0378-3812/$ – see front matter © 2013 Published by Elsevier B.V.
http://dx.doi.org/10.1016/j.fluid.2013.08.031

**Table 1**
Properties of the magnetic ionic liquids.

| MILs | Structure | Molecular weight (g mol$^{-1}$) | Density (g cm$^{-3}$) | Water content (%wt.) |
|---|---|---|---|---|
| $[P_{66614}]_3[GdCl_6]$ | 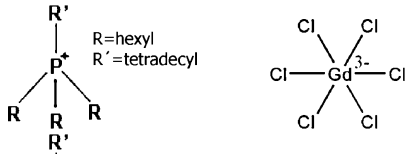  | 1821.5 | 0.982 | 0.2 |
| $[P_{66614}]_2[MnCl_4]$ | 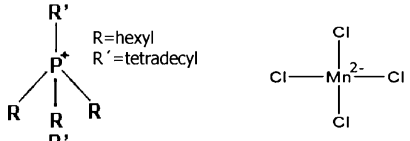  | 1103.0 | 0.956 | 0.35 |
| $[P_{66614}][FeCl_4]$ | 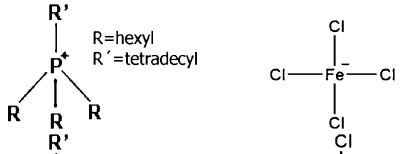  | 681.5 | 1.012 | 1.02 |
| $[P_{66614}]_2[CoCl_4]$ | 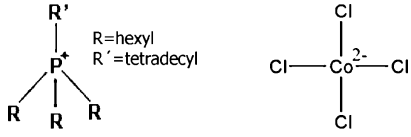  | 1112.0 | 0.965 | $5.1 \times 10^{-4}$ |

summation of the contribution of their atoms and/or fragments [17].

The Vogel–Fulcher–Tamman (VFT) has been used recently, [18] as a new correlation based on the group contribution model to predict the viscosity, electrical conductivity, thermal conductivity, refractive index, isobaric expansivity and isothermal compressibility of ILs. This correlation has been applied instead of the Orrick–Erbar equation to overcome the limitation of density data.

The density is a fundamental property of the compounds and recent works are focused on energetic ILs/salts, since ionic compounds present many advantages over molecular species such as low vapour pressure and high density values [19]. The correlation of the IL density may be based on different models [6], [19]. Jenkins proposed an equation based on the contribution of the cation and anion volumes, where the molar volume of the molecule is the summation of the two contributions [20]. The Ye and Shreeve method has followed this theory for RTILs and salts [19] and its extension from Gardas et al. [21] is based on the same assumptions, but including others parameters to estimate densities accurately.

The aim of the present work is the estimation of the viscosity at different temperatures of MILs using the Orrick–Erbar equation [14,22] with the contribution of the MILs structure, considering the phosphonium cation $[P_{66614}]^+$ with different chain lengths and the magnetic anions: $[CoCl_4]^{2-}$, $[FeCl_4]^-$, $[MnCl_4]^{2-}$ and $[GdCl_6]^{3-}$ density is correlated using the model proposed by Gardas et al. [21] which is currently applied to describe the influence of the temperature in the viscosity of different compounds.

## 2. Materials and methods

The selected MILs based on the phosphonium cation were:

- Phosphonium hexachlorogadolinium: $[P_{66614}]_3[GdCl_6]$.
- Phosphonium tretrachloromanganese: $[P_{66614}]_2[MnCl_4]$.
- Phosphonium tretrachloroferrate: $[P_{66614}][FeCl_4]$.
- Phosphonium tretrachlorocobalt: $[P_{66614}]_2[CoCl_4]$.

The MILs were prepared in the Faculdade de Farmácia, Universidade de Lisboa according to the experimental procedure reported elsewhere [23,24]. Their properties, molecular weight, density and water content at room temperature are listed in Table 1. The density of MILs was determined gravimetrically with a pycnometer and their water content was measured using Karl–Fisher technique [24].

The experimental viscosities and densities were measured using a rheometer (Haake RS75), covering the range of temperature, 293.15–373.15 K as presented in Table 2.

Table 2 shows the experimental results of viscosity with the temperature, which includes 20 experimental data points for MILs based on the same phosphonium cation and four magnetic anions. Comparing the present data with the literature [17], this study covers a wide range of viscosities, 44–123 500 cP.

## 3. Results and discussion

The group contribution method based on the Orrick–Erbar model [14], described by Eq. (1), was applied to estimate the viscosity for different temperatures of these MILs. For the ionic liquids, the group contribution is due to the presence of cations and anions. In the present case the contribution is divided in the phosphonium cation $[P_{66614}]^+$ with different chain lengths and

**Table 2**
Experimental viscosities and densities of the MILs at different temperatures.

| Phosphonium-MILs | $T$ (K) | $\eta$ (cP) | $\rho$ (g cm$^{-3}$) |
|---|---|---|---|
| $[P_{66614}]_3[GdCl_6]$ | 293.15 | 28 230 | 0.983 |
| | 298.15 | 18 390 | 0.981 |
| | 303.15 | 13 010 | 0.979 |
| | 323.15 | 2980 | |
| | 373.15 | 290 | |
| $[P_{66614}]_2[MnCl_4]$ | 293.15 | 112 300 | 0.956 |
| | 298.15 | 75 230 | 0.949 |
| | 303.15 | 41 560 | 0.943 |
| | 323.15 | 13 970 | |
| | 373.15 | 920 | |
| $[P_{66614}][FeCl_4]$ | 293.15 | 790 | 1.012 |
| | 298.15 | 650 | 1.008 |
| | 303.15 | 520 | 1.004 |
| | 323.15 | 230 | |
| | 373.15 | 44 | |
| $[P_{66614}][CoCl_4]$ | 293.15 | 123 500 | 0.965 |
| | 298.15 | 83 450 | 0.962 |
| | 303.15 | 40 250 | 0.959 |
| | 323.15 | 15 360 | |
| | 373.15 | 11 050 | |

**Table 3**
Fitted parameters for the prediction of the density of the studied MILs.

| Phosphonium-MILs | $\alpha$ (Å$^3$ kg$^{-1}$ MPa) | $\beta$ (Å$^3$ K$^{-1}$ kg$^{-1}$) | MPD (%) (95%) | $\chi^2$ |
|---|---|---|---|---|
| $[P_{66614}]_3[GdCl_6]$ | $9.3 \times 10^{-4}$ | $3.1 \times 10^{-7}$ | 0.25 | 0.02 |
| $[P_{66614}]_2$ $[MnCl_4]$ | $5.8 \times 10^{-4}$ | $1.6 \times 10^{-6}$ | 0.28 | 1.9 |
| $[P_{66614}]$ $[FeCl_4]$ | $7.6 \times 10^{-4}$ | $7.7 \times 10^{-7}$ | 0.21 | 0.2 |
| $[P_{66614}]_2$ $[CoCl_4]$ | $8.2 \times 10^{-4}$ | $7.4 \times 10^{-7}$ | 0.14 | 0.4 |
| Global fit | | | 0.22 | |

in the four magnetic anions: $[GdCl_6]^{3-}$, $[MnCl_4]^{2-}$, $[FeCl_4]^{-}$ and $[CoCl_4]^{2-}$.

$$\ln\left(\frac{\eta}{\rho * M}\right) = A + \frac{B}{T} \tag{1}$$

Eq. (1) can be decomposed in the two contributions of the ionic liquids:

$$\ln\left(\frac{\eta}{\rho * M}\right) = n \cdot \left(A^+ + \frac{B^+}{T}\right) + \left(A^- + \frac{B^-}{T}\right) \tag{2}$$

where $\eta$ is the viscosity (cP), $\rho$ is the density (g cm$^{-3}$), $M$ is the molecular weight (g mol$^{-1}$). $T$ is the absolute temperature (K), $A$ and $B$ are the Orrick–Erbar parameters, $n$ stands for the chain length of the cation, $A^+$ and $B^+$ are the parameters of cation contribution, and $A^-$ and $B^-$ are the parameters of anion contribution for the viscosity.

The phosphonium cation is common for all the MILs, although the chain length is different, as well as the magnetic anion. Therefore, the global equation of the model can be written as follows:

$$\ln\left(\frac{\eta}{\rho * M}\right) = n_i \cdot \left(A + B \cdot \frac{1}{T}\right) + \Sigma_i \left(A_i + B_i \cdot \frac{1}{T}\right) \tag{3}$$

where $n_i$ is each chain length of the cation, $A$ and $B$ are the parameters of cation contribution and $A_i$ and $B_i$ are the parameters of anions contribution.

The dependent variable $\ln(\eta/\rho * M)$ includes the density. The model of Orrick and Erbar uses only the density at 293 K [14], however, other recent studies [21] using an extension of the Ye and Shreeve method [19], proposed a predictive method for ILs, using the density as a function of temperature.

The experimental densities are reported in Table 2, and the density dependency with temperature is estimated according with the following equation [22]:

$$\rho = \frac{M}{NV(a + bT + cP)} \tag{4}$$

where, $\rho$ is the density (g cm$^{-3}$), $M$ is the molecular weight (g mol$^{-1}$), $N$ is the Avogadro constant (mol$^{-1}$), $V$ is the molecular volume (Å$^3$), $T$ is the temperature (K), $P$ is the pressure (MPa) and $a$, $b$ and $c$ are the coefficients to be estimated by fitting.

The behaviour of the density with temperature was described by Eq. (4), following the same modelling procedure for the ILs group contribution model. This model includes the contribution of the density for the final viscosity estimation [21,22].

The density of MILs in this temperature range was estimated by the model following Eq. (4), all the experiments were performed at constant pressure (atmospheric pressure), $P$ is constant, and Eq. (4) can be simplified to Eq. (5):

$$\rho = \frac{1}{\alpha + \beta T} \tag{5}$$

where

$$\alpha = \frac{NV}{M}(a + cP) \quad (\text{Å}^3\,\text{kg}^{-1}\,\text{MPa})$$

$$\beta = \frac{NVb}{M} \quad (\text{Å}^3\,\text{K}^{-1}\,\text{kg}^{-1})$$

Eq. (5) includes the parameters $\alpha$ and $\beta$ as parameters and the estimation of the parameters has been carried out using *Fitteia* software. Results are shown in Table 3.

The MPD values obtained are between 0.14 and 0.28%, with 0.22% for the global fit when all MILs are included, in agreement with the 0.29% value previously obtained in a similar study for ILs from literature [22].

**Table 4**
Absolute and normalized variables for MILs viscosity and temperature.

| Phosphonium-MILs | $T$ (K) | $1/T$ (K$^{-1}$) | $\ln\left(\frac{\eta}{\rho * M}\right)$ | Normalized $1/T$ | Normalized $\ln\left(\frac{\eta}{\rho * M}\right)$ |
|---|---|---|---|---|---|
| $[P_{66614}]_3[GdCl_6]$ | 293.15 | 0.00341 | 2.76 | −1.00 | −0.48 |
| | 298.15 | 0.00335 | 2.33 | −0.84 | −0.37 |
| | 303.15 | 0.00330 | 1.99 | −0.69 | −0.28 |
| | 323.15 | 0.00309 | 0.52 | −0.13 | 0.11 |
| | 373.15 | 0.00268 | −1.79 | 1.00 | 0.72 |
| $[P_{66614}]_2[MnCl_4]$ | 293.15 | 0.00341 | 4.67 | −1.00 | −0.98 |
| | 298.15 | 0.00335 | 4.28 | −0.84 | −0.88 |
| | 303.15 | 0.00330 | 3.69 | −0.69 | −0.72 |
| | 323.15 | 0.00309 | 2.63 | −0.13 | −0.44 |
| | 373.15 | 0.00268 | −0.02 | 1.00 | 0.25 |
| $[P_{66614}][FeCl_4]$ | 293.15 | 0.00341 | −0.01 | −1.00 | 0.25 |
| | 298.15 | 0.00335 | −0.21 | −0.84 | 0.30 |
| | 303.15 | 0.00330 | −0.43 | −0.69 | 0.36 |
| | 323.15 | 0.00309 | −1.24 | −0.13 | 0.57 |
| | 373.15 | 0.00268 | −2.87 | 1.00 | 1.00 |
| $[P_{66614}]_2[CoCl_4]$ | 293.15 | 0.00341 | 4.75 | −1.00 | −1.00 |
| | 298.15 | 0.00335 | 4.36 | −0.84 | −0.90 |
| | 303.15 | 0.00330 | 3.63 | −0.69 | −0.71 |
| | 323.15 | 0.00309 | 2.68 | −0.13 | −0.46 |
| | 373.15 | 0.00268 | 2.39 | 1.00 | −0.38 |

**Table 5**
Group contribution to the dimensionless viscosity.

| Group | Molecular descriptor |
|---|---|
| Cation | |
| $n$ | Influence of the number of cations chains (1, 2 or 3) |
| $A^*$ and $B^*$ | Influence of the phosphonium cation: ($P_{66614}$). 1 if it exists and 0 if not exists. |
| Anion | |
| $A_1{}^*$ and $B_1{}^*$ | Influence of the anion: $GdCl_6$, 1 if it exists and 0 if not exists |
| $A_2{}^*$ and $B_2{}^*$ | Influence of the anion: $MnCl_4$, 1 if it exists and 0 if not exists |
| $A_3{}^*$ and $B_3{}^*$ | Influence of the anion: $FeCl_4$, 1 if it exists and 0 if not exists |
| $A_4{}^*$ and $B_4{}^*$ | Influence of the anion: $CoCl_4$, 1 if it exists and 0 if not exists |
| Number of descriptors | 11 |

Normalized variables were used instead of their absolute values in order to avoid the influence of the absolute value on the parameter estimation. Dimensionless viscosity and $1/T$, $Y^*$ and $X^*$, respectively, take the values between +1 and −1 as calculated by Eqs. (6) and (7):

$$Y^* = \frac{-Y + ((Y_{MAX} + Y_{MIN})/2)}{((Y_{MAX} - Y_{MIN})/2)} \quad (6)$$

$$X^* = \frac{-X + ((X_{MAX} + X_{MIN})/2)}{((X_{MAX} - X_{MIN})/2)} \quad (7)$$

The $Y_{MAX}$ and $X_{MAX}$ are the maximum values of $\ln(\mu/(\rho * M))$ and $1/T$. The $Y_{MIN}$ and $X_{MIN}$ are the minimum values. The values are showed in Table 4.

To determine the dependence of the contribution of each group (cation and anion), it is necessary to define the descriptors for the MILs, shown in Tables 5 and 6.

The dimensionless viscosity can be calculated by this group contribution model, following Eq. (2), rewritten in this context:

$$Y^* = n_i \cdot (A^* + B^* \cdot X^*) + \Sigma_i (A_i^* + B_i^* \cdot X^*) \quad (8)$$

**Table 7**
Group contribution parameters fitted by Orrick–Erbar correlation (Eq. (2)) for the normalized viscosity and temperature of the MILs.

| Phosphonium-MILs | Contribution | | |
|---|---|---|---|
| | $A^*$ | $B^*$ (K) | $\chi^2$ |
| Cation | | | 28.8 |
| $[P_{66614}]^+$ | 0.8 ± 0.03 | 0.07 ± 0.06 | |
| Anion | | | |
| $[GdCl_6]^{-3}$ | −2.3 ± 0.09 | 0.45 ± 0.19 | |
| $[MnCl_4]^{-3}$ | −2.0 ± 0.06 | 0.47 ± 0.13 | |
| $[FeCl_4]^-$ | −0.21 ± 0.07 | 0.31 ± 0.07 | |
| $[CoCl_4]^{-2}$ | −2.2 ± 0.06 | 0.088 ± 0.05 | |

From the results shown in Table 7 and Fig. 1, it can be observed that there is a negative anion contribution to the viscosity in the following order: $[GdCl_6]^{-3} < [CoCl_4]^{-2} < [MnCl_4]^{-2} < [FeCl_4]^-$, counteracting to the positive cation effect. Considering the absolute parameters values, a higher anion contribution for the viscosity has been found when comparing with the cation.

The temperature influence of the cation to the viscosity of MILs is less relevant than that observed for the contribution of the anions, as is shown by the negligible $B^*$ value ($B^*$ (K) = 0.07 ± 0.06). Actually, the influence of temperature on the contribution of the anions to viscosity of MILs is considerable and increases according to the following order (as it shown in Table 7): $[CoCl_4]^{-2} < [FeCl_4]^- < [GdCl_6]^{-3} < [MnCl_4]^{-2}$. For the $[CoCl_4]^{-2}$ magnetic anion, the temperature has the lowest influence ($B^*$ (K) = 0.088 ± 0.05).

The experimental and calculated viscosities are shown in Fig. 2, which shows the parity plot.

The mean percentage deviation (MPD) obtained was 7.64% (similar to the 7.78% value obtained for a similar study of ILs from the literature [22]).

Table 8 presents a resume of the main statistic parameters of the group contribution model of this work, with a good agreement between experimental and calculated viscosity, described with a $R^2 = 0.98$.

In order to compare the group contribution parameters with those described in the literature [22], the absolute values have to be fitted to obtain the absolute parameters, $A$ and $B$, which are represented in Table 9.

**Table 6**
MILs viscosity, dimensionless viscosity ($Y^*$) and group contribution descriptors.

| Phosphonium-MILs | $1/T$ ($K^{-1}$) | $\ln\left(\frac{\eta}{\rho * M}\right)$ | $Y^*$ | $n$ | $A^*$ | $B^*$ | $A_1{}^*$ | $A_2{}^*$ | $A_3{}^*$ | $A_4{}^*$ | $B_1{}^*$ | $B_2{}^*$ | $B_3{}^*$ | $B_4{}^*$ |
|---|---|---|---|---|---|---|---|---|---|---|---|---|---|---|
| $[P_{66614}]_3$ $[GdCl_6]$ | | | | 3 | 1 | 1 | 1 | 0 | 0 | 0 | 1 | 0 | 0 | 0 |
| | 0.00341 | 2.76 | −0.48 | | | | | | | | | | | |
| | 0.00335 | 2.33 | −0.37 | | | | | | | | | | | |
| | 0.00330 | 1.99 | −0.28 | | | | | | | | | | | |
| | 0.00309 | 0.52 | 0.11 | | | | | | | | | | | |
| | 0.00268 | −1.79 | 0.72 | | | | | | | | | | | |
| $[P_{66614}]_2$ $[MnCl_4]$ | | | | 2 | 1 | 1 | 0 | 1 | 0 | 0 | 0 | 1 | 0 | 0 |
| | 0.00341 | 4.67 | −0.98 | | | | | | | | | | | |
| | 0.00335 | 4.28 | −0.88 | | | | | | | | | | | |
| | 0.00330 | 3.69 | −0.72 | | | | | | | | | | | |
| | 0.00309 | 2.63 | −0.44 | | | | | | | | | | | |
| | 0.00268 | −0.02 | 0.25 | | | | | | | | | | | |
| $[P_{66614}]$ $[FeCl_4]$ | | | | 1 | 1 | 1 | 0 | 0 | 1 | 0 | 0 | 0 | 1 | 0 |
| | 0.00341 | −0.01 | 0.25 | | | | | | | | | | | |
| | 0.00335 | −0.21 | 0.30 | | | | | | | | | | | |
| | 0.00330 | −0.43 | 0.36 | | | | | | | | | | | |
| | 0.00309 | −1.24 | 0.57 | | | | | | | | | | | |
| | 0.00268 | −2.87 | 1.00 | | | | | | | | | | | |
| $[P_{66614}]_2$ $[CoCl_4]$ | | | | 2 | 1 | 1 | 0 | 0 | 0 | 1 | 0 | 0 | 0 | 1 |
| | 0.00341 | 4.75 | −1.00 | | | | | | | | | | | |
| | 0.00335 | 4.36 | −0.90 | | | | | | | | | | | |
| | 0.00330 | 3.63 | −0.71 | | | | | | | | | | | |
| | 0.00309 | 2.68 | −0.46 | | | | | | | | | | | |
| | 0.00268 | 2.39 | −0.38 | | | | | | | | | | | |

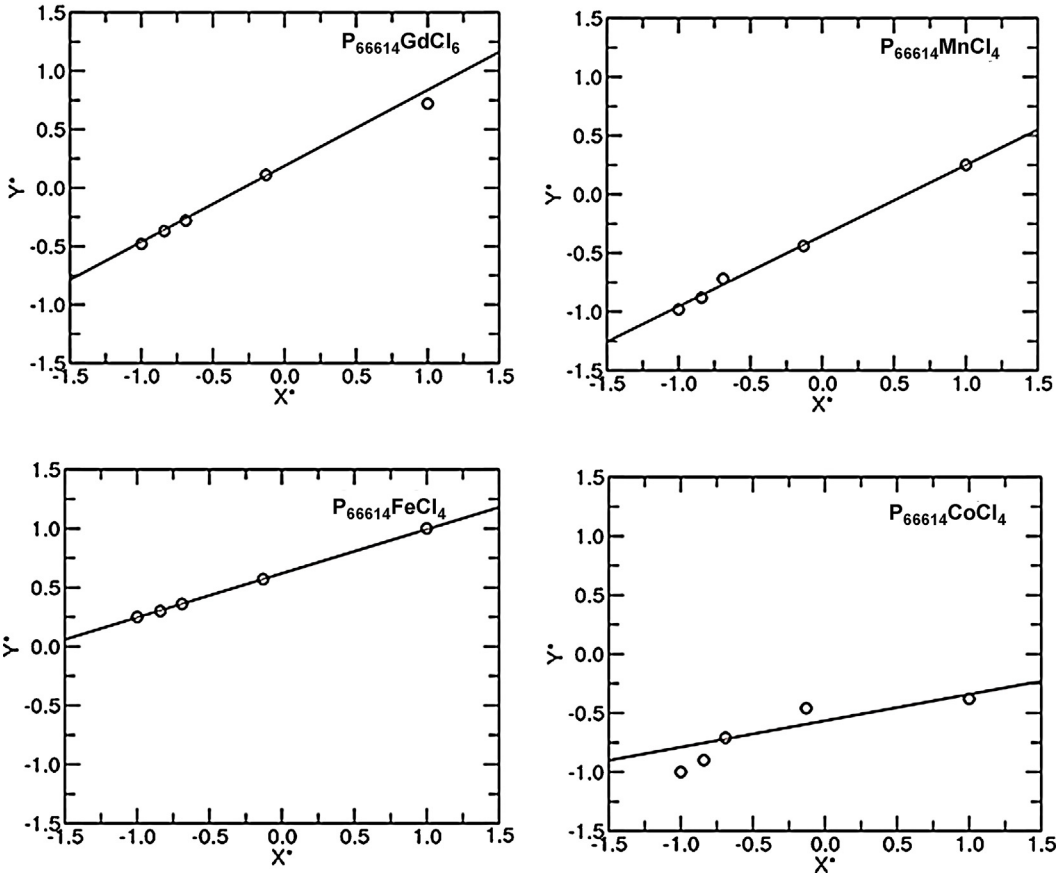


**Fig. 1.** Normalized viscosity fitted for all the MILs by Orrick–Erbar correlation using *Fitteia* software.

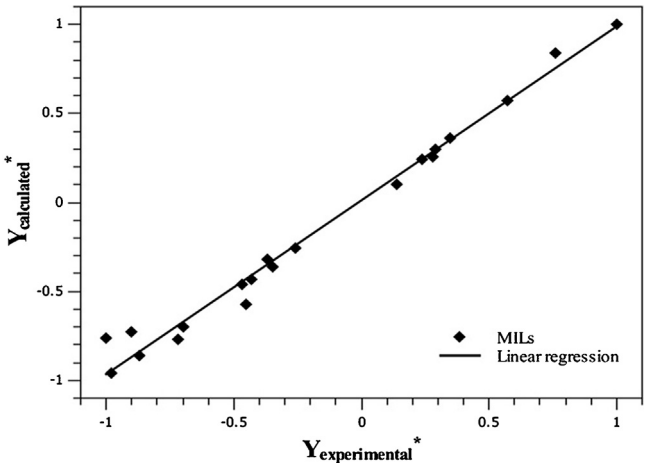


**Fig. 2.** Experimental and calculated dimensionless MILs viscosity results using Orrick–Erbar correlation.

Comparing the absolute values with the literature [22], there is a positive cation contribution and a negative anion contribution for the ILs and MILs viscosity.

**Table 8**
Statistic parameters of the datasheet.

| | |
|---|---|
| Data number | 20 |
| Maximum value (*Y*) | 4.75 |
| Minimum value (*Y*) | −2.87 |
| Average (*Y*) | 1.71 |
| Median | 2.36 |
| Standard deviation | 2.30 |

**Table 9**
Absolute values of the parameters of Orrick–Erbar correlation for viscosity of the MILs.

| Phosphonium-MILs | Contribution | | |
|---|---|---|---|
| | *A* | *B* (K) | $\chi^2$ |
| Cation | | | 18.3 |
| $[P_{66614}]^+$ | 1.48 ± 0.08 | 975 ± 2.7 | |
| Anion | | | |
| $[GdCl_6]^{-3}$ | −22.9 ± 0.4 | 3426 ± 129.3 | |
| $[MnCl_4]^{-2}$ | −19.8 ± 0.02 | 4333 ± 7.9 | |
| $[FeCl_4]^-$ | −14.3 ± 0.01 | 2772 ± 3.2 | |
| $[CoCl_4]^{-2}$ | −7.56 ± 0.95 | 581 ± 312.23 | |

Table 10 shows the cations contribution in the present work and in a previous literature study [22].

From these comparisons it can be concluded that the phosphonium cation has a lower contribution (A values) comparing with imidazolium, pyridinium and pyrrolidinium cations, and temperature (B values) has a lower influence in the viscosity for the phosphonium than the others cations.

**Table 10**
Comparison of the *A* and *B* parameters of Orrick–Erbar correlation for different cations of MILs and ILs.

| ILs and MILs cations | Contribution | |
|---|---|---|
| | *A* | *B* (K) |
| Cations | | |
| Phosphonium[a] | 1.48 | 975 |
| Imidazolium[b] | 6.56 | 1757 |
| Pyridinium[b] | 6.87 | 1704 |
| Pyrrolidinium[b] | 5.43 | 2233 |

[a]Present work.
[b]Literature [22].

**Table 11**
Comparison of the $A$ and $B$ parameters of Orrick–Erbar correlation for different anions of MILs and ILs.

| ILs and MILs anions | Contribution | |
|---|---|---|
| | $A$ | $B$ (K) |
| Anions | | |
| $[GdCl_6]^{3-}$ [a] | −22.9 | 3426 |
| $[MnCl_4]^{2-}$ [a] | −19.8 | 4333 |
| $[FeCl_4]^{-}$ [a] | −14.3 | 2772 |
| $[CoCl_4]^{2-}$ [a] | −7.56 | 581 |
| $[PF_6]^{-}$ [b] | −20.49 | 2099 |
| $[BF_4]^{-}$ [b] | −18.1 | 1192 |
| $[Tf_2N]^{-}$ [b] | −17.4 | 510 |
| $[Cl]^{-}$ [b] | −27.6 | 5458 |
| $[CH_3COO]^{-}$ [b] | −21.3 | 2742 |
| $[MeSO_4]^{-}$ [b] | −19.5 | 1733 |
| $[EtSO_4]^{-}$ [b] | −19.1 | 1587 |
| $[CF_3SO_3]^{-}$ [b] | −17.7 | 906 |

[a] Present work.
[b] Literature [22].

Table 11 shows the comparison of the anions contribution in the present work and in a previous literature study [22].

In the anions contribution of MILs, the values of parameter $A$ for the $[FeCl_4]^-$ and $[CoCl_4]^-$ have the lowest contribution, compared to other MILs and ILs for the reduction of ILs viscosity. The temperature, parameter $B$, has the lowest influence in the $[CoCl_4]^{2-}$ and $[Tf_2N]^-$ anions and the larger influence in $[MnCl_4]^{2-}$ and $[Cl]^-$ anions.

## 4. Conclusion

This work shows a group contribution method based on the Orrick–Erbar equation for the estimation of the influence of the temperature in the viscosity for a new class of ionic liquids, the magnetic ionic liquids, based on the phosphonium cation with different chain lengths and distinct magnetic anions, which are: $[P_{66614}]_3[GdCl_6]$, $[P_{66614}]_2[MnCl_4]$, $[P_{66614}][FeCl_4]$ and $[P_{66614}]_2[CoCl_4]$. The model assumes the summation of group contribution from cations and anions.

A database with 20 points for a wide range of temperature 293.15–373.15 K and viscosity 44–123 500 cP was used. The results obtained are comparable with a previous study and show a 7.64% of mean percentage deviation (MPD) and $R^2 = 0.98$. This result means that the calculated viscosities based on this model are in a good agreement with the experimental values and, therefore this model is applicable for the prediction of MIL viscosities. In this work the cations with different chain lengths have a positive contribution for the MILs viscosity and the anions a negative one. Further work will expand this study in order to include new magnetic ionic liquids with other cations and anions. Results agree well with previous literature data.

*List of symbols*

| | |
|---|---|
| $A, B$ | parameters of Orrick–Erbar model |
| $A^+, B^+$ | parameters of cation contribution |
| $A^-, B^-$ | parameters of anion contribution |
| $n$ | chain length of the phosphonium cation |
| $T$ | temperature |
| $M$ | molecular weight |
| $N$ | Avogadro number |
| $V$ | molar volume |
| $P$ | pressure |
| $a,b,c$ | coefficients of density equation |
| $N_p$ | number of experimental data |
| $Y^*, X^*$ | normalized variables |
| $A^*, B^*$ | normalized parameters of Orrick–Erbar model |

**Greek letters**

| | |
|---|---|
| $\eta$ | viscosity |
| $\rho$ | density |
| $\alpha, \beta$ | fitted parameters of the density correlation |

**Subscripts**

| | |
|---|---|
| cal | calculated property (density and viscosity) |
| exp | experimental (density and viscosity) |
| max | maximum value of the variables |
| min | minimum value of the variables |

## Acknowledgments

The authors gratefully acknowledge the financial support from the European Research Action Network-ERANET, ERA-CHEM/0001/2008 Project (Portugal) and Project EUI 2008-03857 (Spain). C.I. Daniel would like to acknowledge the financial support of FCT-MCTES through the Doctoral fellowship SFRH/BD/81552/2011. We are grateful to Dr. Vitor Alves from Instituto Superior de Agronomia – Universidade Técnica Lisboa, for the contribution in the viscosity measurements and to Professor Carlos Afonso from Faculdade de Farmácia – Universidade de Lisboa, for the work on MILs synthesis.

## References

[1] Y. Hu, Ch. Xu, Effect of the structures of ionic liquids on their physical–chemical properties and the phase behavior of mixtures involving ionic liquids, Am. Chem. Soc. (2006).
[2] S. Lee, S. Ha, H. Jin, C. You, Y. Koo, Magnetic behavior of mixture of magnetic ionic liquid bmim[$FeCl_4$] and water, J. Appl. Phys. 101 (2007) 102.
[3] I. de Pedro, D.P. Rojas, J.A. Blanco, J.R. Férnandez, Antiferromagnetic ordering in magnetic ionic liquid Emim[$FeCl_4$], J. Magn. Magn. Mater. 323 (2011) 1254–1257.
[4] I. de Pedro, D.P. Rojas, J. Albo, P. Luis, A. Irabien, J.A. Blanco, J.R. Fernandez, Long-range magnetic ordering in magnetic ionic liquid: Emim[$FeCl_4$], J. Phys.: Condens. Matter 22 (2010) 296006.
[5] S. Hayashi, S. Saha, H. Hamaguchi, A new class of magnetic fluids: bmim[$FeCl_4$] and nbmim[$FeCl_4$] Ionic Liquids, IEEE Trans. Magn. 42 (2006) 12.
[6] R.G. Seoane, S. Corderí, E. Gomez, N. Calvar, E.J. González, E.A. Macedo, A. Domínguez, Temperature dependence and structural influence on the thermophysical properties of eleven commercial ionic liquids, Ind. Eng. Chem. Res. 51 (2012) 2492–2504.
[7] S. Aparicio, M. Atilhan, F. Karadas, Thermophysical properties of pure ionic liquids: review of present situation, Ind. Eng. Chem. Res. 49 (2010) 9580–9595.
[8] N. Andrade, A theory of the viscosity of liquids, Phil. Mag. 17 (1934) 698–732.
[9] H. Vogel, The law of the relation between the viscosity of liquids and the temperature, Phys. Z. 22 (1921) 645–646.
[10] G. Fulcher, Analysis of recent measurements of the viscosity of glasses, J. Am. Ceram. Soc. 8 (1925) 339–355.
[11] G. Tammann, Z. Hesse, The dependence of viscosity upon the temperature of supercooled liquids, Anorg. Allg. Chem. 156 (1926) 245–257.
[12] A. Litovitz, Temperature dependence of the viscosity of associated liquids, J. Chem. Phys. 20 (1952) 1088–1089.
[13] H. Ghatee, M. Zare, R. Zolghadr, Temperature-dependent density and viscosity of the ionic liquids 1-alkyl-3-methylimidazolium iodides: experiment and molecular dynamics simulation, J. Chem. Eng. Data 55 (2010) 3084–3088.
[14] R.C. Reid, J.M. Prausnitz, T.K. Sherwood, The Properties of Gases and Liquids, fourth ed., McGraw-Hill, New York, 1987.
[15] S.R.S. Sastry, K.K. Rao, A new method for predicting saturated liquid viscosity at temperatures above the normal boiling point, Fluid Phase Equilib. 175 (2000) 311–323.
[16] Y. Gastonbonhomme, P. Petrino, J.L. Chevalier, UNIFAC VISCO group-contribution method for predicting kinematic viscosity – extension and temperature-dependence, Chem. Eng. Sci. 49 (1994) 1799–1806.
[17] P. Luis, I. Ortiz, R. Aldaco, A. Irabien, A novel group contribution method in the development of a QSAR for predicting the toxicity (*Vibrio fischeri* $EC_{50}$) of ionic liquids, Ecotoxicol. Environ Saf. 67 (2007) 423–429.
[18] R. Gardas, J. Coutinho, Group contribution methods for the prediction of thermophysical and transport properties ionic liquids, Am. Inst. Chem. Eng. 55 (2009) 1274–1290.
[19] C. Ye, J.M. Shreeve, Rapid and accurate estimation of densities of room-temperature ionic liquids and salts, J. Phys. Chem. A 111 (2007) 1456–1461.

[20] H.D.B. Jenkins, H.K. Roobottom, Relationships among ionic lattice energies, molecular (formula unit) volumes, and thermochemical radii, Inorg. Chem. 38 (1999) 3609–3620.
[21] R.L. Gardas, J.A.P. Coutinho, Extension of the Ye and Shreeve group contribution method for density estimation of ionic liquids in a wide range of temperatures and pressures, Fluid Phase Equilib. 263 (2008) 26–32.
[22] R. Gardas, J. Coutinho, A group contribution method for viscosity estimation of ionic liquids, Fluid Phase Equilib. 266 (2008) 195–201.
[23] R.E. Del Sesto, T.M. McCleskey, A.K. Burrel, G.A. Baker, J.D. Thompson, B.L. Scott, J.S. Wilkes, P. Williams, Structure and magnetic behaviour of transition metal based ionic liquids, Chem. Commun. (2008) 447–449.
[24] J. Albo, E. Santos, L.A. Neves, S.P. Simeonov, C.A.M. Afonso, J.G. Crespo, A. Irabien, Separation performance study of $CO_2$ through supported magnetic ionic liquid membranes (SMILMs), Sep. Pur. Technol. 97 (2012) 26–33.

# Anexo

# Difusión de resultados

«En principio la investigación necesita más cabezas que medios»

Severo Ochoa (1905 -1993)

Científico español

## Anexo. Difusión de resultados

| Revista | Título y autores |
|---|---|
|  <br>Índice de impacto: 4,093 | **Santos E.,** Albo J., Daniel C.I., Portugal C.A.M., Crespo J.G., Irabien A. Permeability modulation of Supported Magnetic Ionic Liquid Membranes (SMILMs) by an external magnetic field. *Journal of Membrane Science* 430:56-61 (**2013**) |
| | **Santos E.**, Albo J., Irabien A. Acetate based Supported Ionic Liquid Membranes (SILMs) for $CO_2$ separation: Influence of the temperature. *Journal of Membrane Science* 452:277-283 (**2014**) |
|  <br>Índice de impacto: 2,504 | **Santos E.,** Albo J., Rosatella A., Afonso C.A.M., Irabien A. Synthesis and characterization of Magnetic Ionic Liquids (MILs) for $CO_2$ separation. *Journal of Chemical Technology and Biotechnology*. **Aceptado**. |
|  <br>Índice de impacto: 2,894 | Albo J., **Santos E**., Neves L.A., Simeonov S.P., Afonso C.A.M., Crespo J.G., Irabien A. Separation performance of $CO_2$ through Supported Magnetic Ionic Liquid Membranes (SMILMs). *Separation and Purification Technology* 97:26-33 (**2012**) |
|  <br>Índice de impacto: 2,379 | Daniel C.I., Albo J., **Santos E.,** Portugal C.A.M., Crespo J.G., Irabien A. A group contribution method for the influence of the temperature in the viscosity of magnetic ionic liquids. *Fluid Phase Equilibria* 360:29-35 (**2013**) |

| Congreso | Autores, título y tipo de comunicación |
|---|---|
| 21st International Congress of Chemical and Process Engineering (CHISA 2014) http://www.chisa.cz/2014/<br><br>23-27 agosto 2014 Praga (República Checa) | **Santos E.**, Casado-Coterillo C., Irabien A.<br><br>Composite poly[Vbtma][Ac]-CS membranes for $CO_2/N_2$ selective separation<br><br>Comunicación por determinar |
| 4th International Congress on Green Process Engineering http://www.gpe2014.org/<br><br>7-10 abril 2014<br><br>Sevilla (España) | Rodríguez-Fernández E., **Santos E.**, Casado-Coterillo C., Irabien A.<br><br>Hybrid chitosan-ionic liquid membranes for $CO_2$ separation: effect of temperature<br><br>Comunicación por determinar |
| XXXIV Reunión Bienal de la Real Sociedad Española de Química<br>http://rseq2013.unican.es/<br><br>15-18 septiembre 2013<br><br>Santander, Cantabria (España) | **Santos E.**, Albo J., Daniel C.I., Portugal C.A.M., Afonso C.A.M., Crespo J.G., Irabien A.<br><br>Síntesis y caracterización de líquidos iónicos magnéticos para captura de $CO_2$<br><br>Comunicación Poster |

| | |
|---|---|
| ,   9th World Congress of Chemical Engineering (WCCE9) http://www.wcce9.org/<br>18-23 agosto 2013<br>Seúl (República de Corea) | **Santos E.**, Albo J., Daniel C.I., Portugal C.A.M., Crespo J.G., Irabien A.<br>Gas permeation through Supported Magnetic Ionic Liquid Membranes (SMILMs) Temperature Influence.<br>Comunicación Poster |
|   Summer School of the Galician Network of Ionic Liquids (REGALIS) http://regalis.udc.es<br>9-12 junio 2013<br>O Grove, Pontevedra (España) | **Santos E.**, Irabien A.<br>Thermal properties of Magnetic Ionic Liquids (MILs)<br>Comunicación Poster |
| 23rd Annual Meeting North American Membrane Society (NAMS 2013) 8-12 junio 2013, Boise, ID (USA) http://www.membranes.org/2013/index.html   | Daniel C. I., **Santos E.**, Albo J., Afonso C.A.M., Vaca F., Sebastião P., Irabien A., Portugal C.A.M., Crespo J.G.<br>Impact of the Magnetic Ionic Liquids Properties On the Transport of Solutes Through Magnetic-Responsive Liquid Membranes<br>Comunicación oral |

| | |
|---|---|
| 9th European Congress of Chemical Engineering (ECCE9)<br>http://www.ecce2013.eu/<br><br>21-25 abril 2013<br><br>La Haya (Países Bajos) | **Santos E.**, Albo J., Daniel C.I., Portugal C.A.M., Crespo J.G., Irabien A.<br><br>Synthesis, characterization and potential applications of Magnetic Ionic Liquids (MILs)<br><br>Comunicación oral |
| ZeoForum "Foro de Innovación en Zeolitas y otros materiales porosos ordenados" 3-4 diciembre 2012, Valencia (España)<br>http://zeoforum.com/ | Casado-Coterillo C., **Santos E.**, Albo J., Irabien A.<br><br>Mixed matrix membranes from polymerizable ionic liquids<br><br>Comunicación Poster |
| 20th International Congress of Chemical and Process Engineering (CHISA 2012) http://www.chisa.cz/2012/<br><br>25-29 agosto 2012<br><br>Praga (República Checa) | **Santos E.**, Albo J., Irabien A.<br><br>$CO_2$ capture based on absorption/desorption with [Emim][Ac] ionic liquid<br><br>Comunicación oral |
| | Casado-Coterillo C., **Santos E.**, Albo J., Irabien A.<br><br>Mixed matrix membranes from polymerizable ionic liquids<br><br>Comunicación Poster |

| | |
|---|---|
| 12th International Conference on Inorganic Membranes (ICIM 2012) 9-13 julio 2012 Enschede (Países Bajos) http://www.icimconference.com/   | Casado-Coterillo C., Albo J., **Santos E.**, Irabien A.<br>Poly[VTBMA][Ac] based mixed matrix membrane for $CO_2$ separation from a gas stream<br>Comunicación Poster |
| International Congress of Chemical Engineering (ANQUE-ICCE 2012) http://anqueicce2012.org/ 24-27 junio 2012 Sevilla (España)   | **Santos E.**, Albo J., Irabien A.<br>High $CO_2$ solubility in task-specific ionic liquids containing the acetate anion<br>Comunicación oral |
| 12th Mediterranean Congress of Chemical Engineering (12MCC) 15-18 noviembre 2011 http://www.ub.edu/congmedit/ Barcelona (España)   | **Santos E.**, Albo J., Irabien A.<br>Carbon dioxide separation using supported ionic liquid membranes (SILMs)<br>Comunicación Poster |

| | |
|---|---|
| 2nd Iberian Meeting on Ionic Liquids (2nd IMIL)<br>http://www.usc.es/congresos/imil2/<br>20-22 julio 2011<br>Santiago de Compostela (España) | Albo J., **Santos E.**, Rosatella A., Afonso C. A.M., Irabien A.<br>Solubility of carbon dioxide in magnetic ionic liquids (MILs)<br>Comunicación oral |
| Trondheim CCS Conference (TCCS-6)<br>http://www.sintef.no/Projectweb/TCCS-6/<br>14-16 julio 2011<br>Trondheim (Noruega) | Albo J., **Santos E.**, Salazar M., Irabien A.<br>Ionic Liquids for Carbon Dioxide Capture: Absorbent selection<br>Comunicación Poster |
| Minilubes Scientific Fellows' Congress<br>http://regid.cesga.es<br>1-3 junio 2011<br>Vigo (España) | **Santos E.**, Albo J., Irabien A.<br>Experimental determination of $CO_2$ solubility in ionic liquids<br>Comunicación oral |